

2018 AAP / ASCI / APSA JOINT MEETING

Meeting Program & Abstracts



APSA
American Physician Scientists Association

THE PREMIER ANNUAL MEETING FOR PHYSICIAN-SCIENTISTS



This activity is jointly provided by Harvard Medical School.

APRIL 20 – 22, 2018
**FAIRMONT CHICAGO
MILLENNIUM PARK
CHICAGO, ILLINOIS**



www.jointmeeting.org

SPECIAL EVENTS AT THE 2018 AAP / ASCI / APSA JOINT MEETING

FRIDAY, APRIL 20

ASCI President's Reception in Honor of the 20th Anniversary of the Stanley J. Korsmeyer Award

6:00 p.m. – 7:15 p.m. Gold Room

ASCI Dinner & New Member Induction Ceremony *(Ticketed event)*

7:30 p.m. – 9:30 p.m. Rouge, Lobby Level

Invited Speaker: George Q. Daley, MD, PhD, *Harvard Medical School*

APSA Welcome Reception *(Ticketed event, ID required)*

9:00 p.m. – Midnight Mid-America Club, Aon Center *(Off-site)*

SATURDAY, APRIL 21

ASCI Food & Science Evening *(ID required)*

6:30 p.m. – 9:00 p.m. Mid-America Club, Aon Center *(Off-site)*

Featuring Poster Presentations by the ASCI's 2018 Young Physician-Scientist Awardees

AAP Member and New Member Induction Banquet *(Ticketed event, formal attire required)*

7:00 p.m. – 9:30 p.m. Imperial Ballroom, Level B2

Data Sharing in the Setting of Clinical Trials

Invited Speaker: Jeffrey M. Drazen, MD, *Editor-in-Chief, New England Journal of Medicine*

APSA Dinner & Founder's Award Presentation *(Ticketed event)*

7:30 p.m. – 9:00 p.m. Rouge, Lobby Level

Founder's Award Recipient: Dania Daye, MD, PhD, *Massachusetts General Hospital*

Charting Your Path as a Physician Scientist

Dinner Speaker: Juliane Bubeck-Wardenburg, MD, PhD, *Washington University School of Medicine*

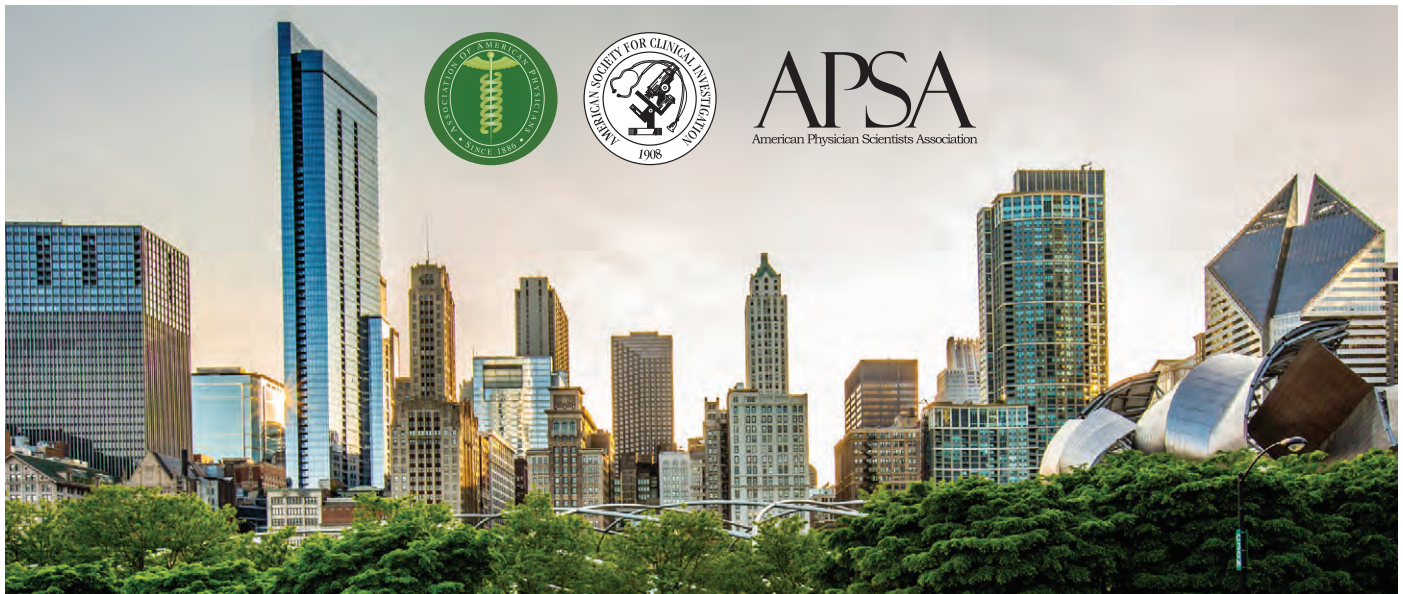
Dessert Reception & Best Poster Awards *(Open to all attendees)*

9:45 p.m. – 11:30 p.m. Imperial Lobby, Level B2

SUNDAY, APRIL 22

APSA Residency Luncheon

12:30 p.m. – 2:30 p.m. International Ballroom



PROGRAM CONTENTS

General Program Information	2
Continuing Medical Education Information	3
Joint Program Planning Committee & APSA Events Committee	4
Scientific Program Schedule	5
Speaker Biographies	13
Call for Nominations: 2019 Harrington Prize for Innovation in Medicine	19
2018 AAP/ASCI/APSA Leadership	20
Travel Award Recipients	21
Call for Nominations: George M. Kober Medal	23
Oral Presentations & Poster Abstracts	24
Oral Presentations & Poster Abstracts Author Index	137
Hotel Floor Plans	142
Joint Meeting Sponsors	Inside Back Cover
Future Joint Meeting Dates	Back Cover



GENERAL PROGRAM INFORMATION

Registration Desk Hours

Friday, April 20	7:00 a.m. – 6:30 p.m.
Saturday, April 21	7:00 a.m. – 5:00 p.m.
Sunday, April 22	7:30 a.m. – 10:00 a.m.

Americans with Disabilities Act

Event staff will be glad to assist you with any special needs (i.e., physical, dietary, etc.). Please contact the Registration Desk at the meeting if you require any special assistance.

Joint Meeting Evaluations

The AAP/ASCI/APSA Joint Meeting Planning Committee relies on your input to enhance its meetings. Following the Joint Meeting, an online meeting evaluation will be emailed to all attendees. APSA attendees will receive a separate survey to help its planning committee enhance APSA-sponsored events at future AAP/ASCI/APSA Joint Meetings. Your participation in this survey is greatly appreciated.

AAP/ASCI/APSA Joint Meeting Code of Conduct

We value your attendance. Our conference is dedicated to providing a harassment-free experience for everyone, regardless of gender, gender identity and expression, age, sexual orientation, disability, physical appearance, body size, race, ethnicity, or religious preference. AAP/ASCI/APSA do not tolerate harassment of conference participants in any form. A participant engaging in harassing behavior will be warned and may be asked to leave the conference with no refund. If you are being harassed, notice that someone else is being harassed, or have any other concerns, please contact a member of conference staff at the registration desk immediately. Conference staff and organizers are dedicated to making all participants feel safe for the duration of the conference.

Poster Session Schedule

Friday, April 20

10:00 a.m. – 3:00 p.m.	Poster Setup
6:15 p.m. – 9:30 p.m.	Informal Viewing: presenters do not need to be at poster

Saturday, April 21

TWO Poster Presentation Sessions

8:00 a.m. – 9:00 a.m.	Poster Session with Continental Breakfast ODD numbered posters presented
11:45 a.m. – 1:30 p.m.	Poster Session with Lunch EVEN numbered posters presented
1:30 p.m. – 2:00 p.m.	Poster Dismantle
9:45 p.m. – 11:30 p.m.	Best Poster Awards (during Dessert Reception in Imperial Foyer)

Poster presenters should plan to be available on Saturday for their appointed poster presentation session and the resulting awards program later in the evening.

Best Poster Awards

Best Poster Awards will be given in the amount of \$1,000 each. Members of the AAP, ASCI and APSA will judge posters on scientific novelty, quality and clarity of presentation. Awards will be presented on Saturday, April 21, from 9:45 p.m. – 11:30 p.m. Poster presenters should plan on attending for award presentation.

Continuing Medical Education (CME) Information

The AAP/ASCI/APSA Joint Meeting annually brings together physician-scientists of all backgrounds to highlight some of the best examples of translational biomedical research, to celebrate new members elected to the AAP and ASCI in recognition of their research and leadership contributions, and to recognize the careers of physician-scientists who have had major impact on their fields.

Meeting Learning Objectives

Upon completion of this activity, participants will be able to:

- Evaluate important recent advances in the scientific basis of disease and therapy.
- Consider novel strategies to address challenges to the physician-scientist.
- Determine the roles that improved understanding of these advances and strategies can play in the potential treatment of human disease.

Target Audience

This activity is targeted towards physician-scientists, trainees and students across a broad range of specialties including basic research, cardiology/cardiovascular research, cell and molecular biology, endocrine and metabolism, hematology, immunology, infectious diseases, nephrology, pulmonology, and others.

HMS Disclosure Policy

HMS adheres to all Accreditation Council for Continuing Medical Education (ACCME) Accreditation Criteria and Policies. It is HMS's policy that those who have influenced the content of a CME activity (e.g. planners, faculty, authors, reviewers and others) disclose all relevant financial relationships with commercial entities so that HMS may identify and resolve any conflicts of interest prior to the activity. These disclosures will be provided in the activity materials for the learners along with disclosure of any commercial support received for the activity prior to the beginning of the activity.

HMS strives to ensure that the content of all its accredited activities is independent from any commercial influence, presents a balance of therapeutic options, promotes improvements in healthcare and is in alignment with the ACCME Content Validation Policy. Additionally, faculty members have been instructed to disclose any limitations of data and unlabeled or investigational uses of products, pharmaceuticals or medical devices during their presentations.

Accreditation Statement

This activity has been planned and implemented in accordance with the accreditation requirements and policies of the Accreditation Council for Continuing Medical Education (ACCME) through the joint providership of Harvard Medical School and the Association of American Physicians, the American Society for Clinical Investigation, and the American Physician Scientists Association. The Harvard Medical School is accredited by the ACCME to provide continuing medical education for physicians.

AMA Credit Designation Statement

The Harvard Medical School designates this live activity for a maximum of 8 *AMA PRA Category 1 Credits*[™]. Physicians should claim only the credit commensurate with the extent of their participation in the activity.

Claiming CME Credit and Obtaining Certificates

Participants will be sent a link to the online evaluation before the start of the meeting and will be required to complete the online evaluation to receive CME credit. Once the evaluation is completed, participants may print, save, or email their CME certificates or certificates of attendance (for non-physicians). Questions related to this activity or on completing this online evaluation may be directed to ceprograms@hms.harvard.edu.

Disclaimer

CME activities sponsored by Harvard Medical School are offered solely for educational purposes and do not constitute any form of certification of competency. Practitioners should always consult additional sources of information and exercise their best professional judgment before making clinical decisions of any kind. The content of each presentation does not necessarily reflect the views of Harvard Medical School.

JOINT PROGRAM PLANNING COMMITTEE & APSA EVENTS COMMITTEE

Joint Program Planning Committee Members

From the AAP:

AAP President

Serpil Erzurum, MD
Cleveland Clinic

AAP Vice President

John Carethers, MD
University of Michigan

AAP Immediate Past President

Linda Fried, MD, MPH
*Columbia University,
Mailman School of Public Health*

From the ASCI:

ASCI President

Benjamin L. Ebert, MD, PhD
*Harvard Medical School,
Dana-Farber Cancer Institute*

ASCI President-Elect

Kieren Marr, MD
John Hopkins School of Medicine

ASCI Immediate Past President

Vivian G. Cheung, MD
*Howard Hughes Medical Institute;
University of Michigan Medical School*

From APSA:

APSA President

Jillian Liu
Ohio State University

Immediate Past President

Alexander Adami
University of Connecticut

APSA President-Elect

Audra Iness
VCU School of Medicine

APSA Events Co-Chair

Allyson Palmer
Mayo Clinic

APSA Events Co-Chair

Jason Siu
Ohio State University

APSA Events Committee

President

Jillian Liu (6th year MD/PhD)
Ohio State University

President-Elect

Audra Iness (5th year MD/PhD)
Virginia Commonwealth Univ. School of Medicine

Events Co-Chair

Allyson Palmer (8th year MD/PhD)
Mayo Clinic

Events Co-Chair

Jason Siu (6th year MD/PhD)
Ohio State University

Events Vice-Chair

Jeremie Lever (5th year MD/PhD)
University of Alabama at Birmingham

Events Vice-Chair

Lillian Zhang (4th year MD/PhD)
UC Davis School of Medicine

Events Committee Member

Seemaab Ali (4th year MD/PhD)
Ohio State University

Events Committee Member

Eileen Hu (4th year MD/PhD)
Ohio State University

Events Committee Member

Rachel Hurley (6th year MD/PhD)
Mayo Clinic

Events Committee Member

Jose Rodrigues (2nd year MD/PhD)
Michigan State



SCIENTIFIC PROGRAM SCHEDULE

Friday, April 20, 2018

Time	Event	Location
8:30 a.m. – 11:00 a.m.	APSA Business Meeting <i>(Open to all APSA members)</i>	Rouge
APSA Session I		
11:00 a.m. – 11:45 a.m.	 Selective Autophagy and Age-related Diseases: Making a Career out of Cellular Waste Managing Invited Speaker: Ana Maria Cuervo, MD, PhD <i>Albert Einstein College of Medicine</i>	International Ballroom
12:00 p.m. – 12:45 p.m.	 How Dreams Come True: Reflections on a Physician-Scientist Career Invited Speaker: Levi Garraway, MD, PhD <i>Eli Lilly</i>	International Ballroom
1:00 p.m. – 3:00 p.m.	Poster Setup	Imperial Ballroom
Plenary Session I: Aging and Health Living I		
Moderators: Vivian Cheung, Linda Fried, and Jillian Liu		
1:00 p.m. – 1:30 p.m.	 Catalyzing Innovation and Charting a Path for the Future of Healthy Longevity: The Role of the National Academy of Medicine Invited Speaker: Victor Dzau, MD <i>National Academy of Medicine</i>	International Ballroom
1:30 p.m. – 2:00 p.m.	 Searching for the Common Root of Multi Morbidity and Functional Decline in Aging: The Geroscience Initiative Invited Speaker: Luigi Ferrucci, MD, PhD <i>National Institutes of Health/National Institute on Aging</i>	International Ballroom
ASCI and AAP New Member Presentations		
2:00 p.m. – 2:15 p.m.	 Understanding and Targeting Mutations in RNA Splicing Factors in Cancer ASCI New Member: Omar Abdel-Wahab, MD, PhD <i>Memorial Sloan Kettering Cancer Center</i> <i>Recipient, 2017 Seldin-Smith Award</i>	International Ballroom
2:15 p.m. – 2:30 p.m.	 The Rising Incidence of IBD in Immigrants: Is it All in the Genes? AAP New Member: Maria T. Abreu, MD <i>University of Miami Miller School of Medicine</i>	International Ballroom
2:30 p.m. – 2:45 p.m.	 Our Red Queen's Race: The Conflict that Creates Genomes and its Roles in Disease ASCI New Member: Kathleen H. Burns, MD, PhD <i>John Hopkins University School of Medicine</i>	International Ballroom
2:45 p.m. – 3:00 p.m.	 Clonal Hematopoiesis, Aging, and Human Disease AAP New Member: Ross L. Levine, MD <i>Memorial Sloan Kettering Cancer Center</i>	International Ballroom
3:00 p.m. – 3:30 p.m.	Break	

SCIENTIFIC PROGRAM SCHEDULE

Friday, April 20, 2018 *(continued)*

Time	Event	Location
3:30 p.m. – 4:00 p.m.	<p>Moderators: Serpil Erzurum, Kieren Marr, and Allyson Palmer</p>  <p>ASCI Harrington Prize Lecture Recipient: Helen H. Hobbs, MD <i>University of Texas Southwestern Medical Center</i></p>	International Ballroom
4:00 p.m. – 4:30 p.m.	 <p>APSA Lasker Award Winner Lecture Elucidation of Cellular Oxygen Sensing Pathways: Implications for Medicine Sir Peter J. Ratcliffe, FRS <i>University of Oxford</i></p>	International Ballroom
4:30 p.m. – 5:00 p.m.	 <p>ASCI Presidential Address The Next Generation of Physician-Scientists Benjamin L. Ebert, MD, PhD <i>Dana-Farber Cancer Institute</i></p>	International Ballroom
5:00 p.m. – 5:30 p.m.	 <p>ASCI/Stamley J. Korsmeyer Award Lecture Natural Product Drug Targets are Conserved from Model and Pathogenic Yeasts to Humans Joseph Heitman, MD, PhD <i>Duke University Medical Center</i></p>	International Ballroom
5:30 p.m. – 5:45 p.m.	<p>Special Service Award for Physician Scientist Workforce Working Group: David Ginsburg, Sherry Mills, Susan Shurin Presented by Benjamin Ebert and Serpil Erzurum</p>	International Ballroom
5:45 p.m. – 7:00 p.m.	<p>APSA Diversity Working Group</p>	State Room
6:00 p.m. – 7:15 p.m.	<p>ASCI President's Reception in Honor of the 20th Anniversary of the Stanley J. Korsmeyer Award Featuring remarks from: Benjamin L. Ebert, MD, PhD Susan Korsmeyer Scott A. Armstrong, MD, PhD Timothy J. Ley, MD</p>	Gold Room
6:15 p.m. – 9:30 p.m.	<p>Poster Viewing Only</p>	Imperial Ballroom
7:00 p.m. – 9:00 p.m.	<p>AAP Offsite President's Dinner <i>(By invitation only and ID required)</i></p>	Mid-America Club
7:30 p.m. – 9:30 p.m.	 <p>ASCI Dinner & New Member Induction Ceremony Speaker: George Q. Daley, MD, PhD <i>Harvard Medical School</i> Attire: Business <i>(Ticketed event)</i></p>	Rouge
9:00 p.m. – Midnight	<p>APSA Welcome Reception <i>(Ticketed event, ID required)</i></p>	Mid-America Club

SCIENTIFIC PROGRAM SCHEDULE

Saturday, April 21, 2018

Time	Event	Location
7:00 a.m. – 8:00 a.m.	AAP Council Meeting	State Room, 2nd Level
7:00 a.m. – 8:00 a.m.	Mentoring Breakfast: Navigating the Physician Scientist Career <i>(Ticketed event)</i>	Rouge
8:00 a.m. – 9:00 a.m.	APSA Board of Directors Meeting	Embassy Room
8:00 a.m. – 9:00 a.m.	Poster Session and Continental Breakfast <i>ODD number posters will be presented/judged.</i>	Imperial Ballroom
9:00 a.m. – 9:30 a.m.	Plenary Session II: Aging and Health Living II Moderators: Serpil Erzurum, W. Kimryn Rathmell, and Jason Siu  Frailty and Resilience in Aging Invited Speaker: Linda Fried, MD, MPH <i>Columbia University, Mailman School of Public Health</i>	International Ballroom
9:30 a.m. – 9:45 a.m.	 APSA Trainee Oral Abstract Presentation: Using CLCA1 vWA Domain to Activate Alternate Anion Currents in Cystic Fibrosis Airway Invited Speaker: Kayla Berry <i>Washington University School of Medicine</i> <i>APSA Travel Awardee</i>	International Ballroom
9:45 a.m. – 10:15 a.m.	 Digitizing Healthspan Invited Speaker: Eric Topol, MD <i>Scripps Research Institute</i>	International Ballroom
10:15 a.m. – 10:30 a.m.	Break	
10:30 a.m. – 11:00 a.m.	Moderators: Hossein Ardehali, Mitchell Lazar, and Lillian Zhang  The Telomere Syndromes: A Paradigm for Molecular Medicine Invited Speaker: Mary Y. Armanios, MD <i>John Hopkins Medicine</i>	International Ballroom
11:00 a.m. – 11:30 a.m.	 Revisiting a Classic: NAD+ Metabolism and Aging APSA Invited Speaker: Eric M. Verdin, MD <i>The Buck Institute for Research on Aging</i>	International Ballroom
11:30 a.m. – 11:45 a.m.	ASCI Seldin-Smith Award for Pioneering Research Recognition of the 2018 Recipients:  Anna Greka, MD, PhD <i>Harvard Medical School</i>  Deepak Nijhawan, MD, PhD <i>UT Southwestern Medical Center</i>	International Ballroom

SCIENTIFIC PROGRAM SCHEDULE

Saturday, April 21, 2018 (continued)

Time	Event	Location
11:45 a.m. – 1:30 p.m.	Poster Session with Lunch <i>EVEN number posters will be presented/judged.</i>	Imperial Ballroom
12:45 p.m. – 1:30 p.m.	Poster Reviewer Meeting	Royal Room, Level B2
1:30 p.m. – 2:00 p.m.	Plenary Session III: Human Genetics and Healthy Longevity Moderators: Benjamin Ebert, Mary Klotman, and Jeremie Lever	International Ballroom
	 The Genome(s) and Epigenome(s) of Acute Myeloid Leukemia Invited Speaker: Timothy J. Ley, MD <i>Washington University School of Medicine</i>	
2:00 p.m. – 2:15 p.m.	 APSA Trainee Oral Abstract Presentation: Characterization and Metabolic Synthetic Lethal Testing in a New Model of SDH-Loss Familial Pheochromocytoma and Paraganglioma Invited Speaker: John Smestad <i>Mayo Clinic</i> <i>AAP/ASCI Travel Awardee</i>	International Ballroom
2:15 p.m. – 2:45 p.m.	 Normal and Neoplastic Stem Cells Invited Speaker: Irving L. Weissman, MD <i>Stanford University</i>	International Ballroom
2:45 p.m. – 3:15 p.m.	Break	
3:15 p.m. – 3:45 p.m.	Moderators: John Carethers, Benjamin Ebert, and Audra Iness  Genes, Genomes and Future of Medicine Invited Speaker: Richard P. Lifton, MD, PhD <i>Rockefeller University</i>	International Ballroom
3:45 p.m. – 4:15 p.m.	 Science, Serendipity and the Single Degree Kober Lecturer: Helen H. Hobbs, MD <i>University of Texas Southwestern Medical Center</i>	International Ballroom
4:15 p.m. – 4:45 p.m.	 AAP Presidential Address The American Physician-Scientist: 60 is the new 40 Serpil Erzurum, MD <i>Cleveland Clinic</i>	International Ballroom
4:45 p.m. – 5:15 p.m.	Kober Medal Presentation  Recipient: Stuart H. Orkin, MD <i>Dana Farber Cancer Institute</i>  Presenter: Leonard I. Zon, MD <i>Howard Hughes Medical Institute,</i> <i>Harvard Medical School, Boston Children's Hospital</i>	International Ballroom
5:15 p.m. – 5:30 p.m.	AAP Business Meeting	International Ballroom



SCIENTIFIC PROGRAM SCHEDULE

Saturday, April 21, 2018 *(continued)*

Time	Event	Location
5:45 p.m. – 7:00 p.m.	<p>APSA Panel: Policy and Advocacy Workshop Moderator: Samantha Spellicy Panelists:</p> <div style="display: flex; flex-direction: column; gap: 10px;"> <div style="display: flex; align-items: center;">  <div style="margin-left: 10px;"> <p>Michael Coburn <i>Research!America</i></p> </div> </div> <div style="display: flex; align-items: center;">  <div style="margin-left: 10px;"> <p>Ryan Murray, BS <i>American Society of Nephrology</i></p> </div> </div> <div style="display: flex; align-items: center;">  <div style="margin-left: 10px;"> <p>Benjamin Krinsky, PhD <i>Federation of American Societies for Experimental Biology</i></p> </div> </div> <div style="display: flex; align-items: center;">  <div style="margin-left: 10px;"> <p>Sharon K. Inouye, MD, MPH <i>Hebrew SeniorLife/Harvard Medical School</i></p> </div> </div> </div>	Crystal Room
5:45 p.m. – 7:00 p.m.	<p>APSA Panel: Critical and Social Perspectives on Aging Moderator: Josh Franklin Panelists:</p> <div style="display: flex; flex-direction: column; gap: 10px;"> <div style="display: flex; align-items: center;">  <div style="margin-left: 10px;"> <p>Janelle Taylor, PhD <i>University of Washington</i></p> </div> </div> <div style="display: flex; align-items: center;">  <div style="margin-left: 10px;"> <p>Greg A. Sachs, MD <i>Indiana University</i></p> </div> </div> <div style="display: flex; align-items: center;">  <div style="margin-left: 10px;"> <p>Carla Keirns, MD, PhD <i>Kansas University Medical Center</i></p> </div> </div> </div>	Ambassador Room
6:30 p.m. – 9:00 p.m.	<p>ASCI Food & Science Evening Featuring Poster Presentations by the ASCI's 2018 Young Physician-Scientist Awardees <i>(ID required)</i></p>	Mid-America Club
7:00 p.m. – 9:30 p.m.	<p>AAP Member and New Member Induction Banquet: Data Sharing in the Setting of Clinical Trials Invited Speaker: Jeffrey M. Drazen, MD <i>Editor-in-Chief, New England Journal of Medicine</i> Attire: Formal Required <i>(Ticketed event)</i></p>	Imperial Ballroom

SCIENTIFIC PROGRAM SCHEDULE

Saturday, April 21, 2018 *(continued)*

Time	Event	Location
7:30 p.m. – 9:00 p.m.	APSA Dinner & Founder's Award Presentation <i>(Ticketed event)</i>  Founder's Award Recipient: Dania Daye, MD, PhD <i>Massachusetts General Hospital</i>  Charting Your Path as a Physician Scientist Dinner Speaker: Juliane Bubeck-Wardenburg, MD, PhD <i>Washington University School of Medicine</i>	Rouge
9:45 p.m. – 11:30 p.m.	Dessert Reception and Best Poster Awards <i>(Open to all attendees)</i>	Imperial Lobby

Sunday, April 22, 2018

Time	Event	Location
8:00 a.m. – 12:00 p.m.	APSA Session II	
8:00 a.m. – 9:30 am	Mentoring Breakfast: Medical Specialty Exploration	International Ballroom
8:30 a.m. – 9:30 a.m.	Society Leadership Wrap Up Meeting	State Room
9:30 a.m. – 10:00 a.m.	 Delirium in Older Adults: My Investigative Journey Invited Speaker: Sharon Inouye, MD, MPH <i>Hebrew SeniorLife/Harvard Medical School</i>	Gold Room
10:00 a.m. – 11:00 a.m.	APSA Panel: Alternative Careers Moderator: Eileen Hu Panelists:  Daryll C. Dykes, PhD, MD, JD <i>Medical and Surgical Spine Consultants of Minnesota</i>  Anna Fisher, MD <i>University of Rochester School of Medicine & Dentistry</i>  Andrew Chan, MD, PhD <i>Genentech, Inc.</i>	Gold Room
10:00 a.m. – 12:00 p.m.	APSA Research Pathway Residency Program Directors Meeting	State Room

SCIENTIFIC PROGRAM SCHEDULE

Sunday, April 22, 2018 *(continued)*

Time	Event	Location
11:00 a.m. – 12:00 p.m.	<p>APSA Panel: Resilience Workshop Moderator: Audra Iness Panelists:</p> <div style="display: flex; align-items: flex-start; margin-bottom: 10px;">  <div style="margin-left: 10px;"> <p>Kay Lund, PhD <i>National Institutes of Health</i></p> </div> </div> <div style="display: flex; align-items: flex-start; margin-bottom: 10px;">  <div style="margin-left: 10px;"> <p>Dani Dumitriu, MD, PhD <i>Icahn School of Medicine at Mount Sinai</i></p> </div> </div> <div style="display: flex; align-items: flex-start;">  <div style="margin-left: 10px;"> <p>Michael Helmrath, MD, MS <i>Cincinnati Children's Hospital Medical Center</i></p> </div> </div>	Gold Room
11:00 a.m. – 12:00 p.m.	<p>APSA Panel: The Do's and Don'ts of MSTP Admissions Moderator: Jose Rodrigues Panelists:</p> <div style="display: flex; align-items: flex-start; margin-bottom: 10px;">  <div style="margin-left: 10px;"> <p>Andrea Amalfitano, DO, PhD <i>Michigan State University</i></p> </div> </div> <div style="display: flex; align-items: flex-start; margin-bottom: 10px;">  <div style="margin-left: 10px;"> <p>Dianna Milewicz, MD, PhD <i>University of Texas Medical School at Houston</i></p> </div> </div> <div style="display: flex; align-items: flex-start;">  <div style="margin-left: 10px;"> <p>Paul Utz, MD <i>Stanford University School of Medicine</i></p> </div> </div>	Ambassador Room
12:30 p.m. – 2:30 p.m.	<p>APSA Residency Luncheon</p> <ol style="list-style-type: none"> 1 Beth Israel Deaconess Medical Center Internal Medicine Physician Scientist Track <i>Director: Steven Freedman, MD, PhD</i> <hr/> 2 University of Pennsylvania Internal Medicine Physician Scientist Pathway Program <i>Director: Peter Klein, MD, PhD</i> <hr/> 3 Massachusetts General Hospital Internal Medicine Residency Program <i>Director: Jatin Vyas, MD, PhD. Associate Director: Caroline Sokol, MD, PhD</i> <hr/> 4 Cincinnati Children's Hospital Pediatric Scientist Development Program <i>Chair of Hematology Translational Research: Russell Ware, MD, PhD</i> <hr/> 5 Brigham and Women's Hospital Internal Medicine Residency Program <i>Director: Joel Katz, MD. Assoc. Program Director: Rebecca Baron, MD</i> <hr/> 6 Vanderbilt University School of Medicine Physician-Scientist Training Program <i>Director: Patrick Hu, MD, PhD</i> <hr/> 7 Ohio State University Physician Scientist Training Program <i>Director: Robert Baiocchi, MD, PhD</i> <hr/> 8 Baylor Pediatric Pediatrician-Scientist Training & Development Program <i>Assoc. Director: Audrea Burns, PhD</i> 	International Ballroom

SCIENTIFIC PROGRAM SCHEDULE

Sunday, April 22, 2018 (continued)

Time	Event	Location
12:30 p.m. – 2:30 p.m.	APSA Residency Luncheon (continued)	International Ballroom
	9 University of Alabama at Birmingham ABIM Research Pathway Program <i>Director: Sonya Heath, MD</i>	
	10 Children's Hospital of Los Angeles George Donnell Society for Pediatric Scientists <i>Director: Lee Helman, MD</i>	
	11 University of Minnesota Internal Medicine Physician Scientist Training Program <i>Director: Clifford Steer, MD</i>	
	12 University of Iowa Multidisciplinary Physician Scientist Training Program <i>Director: Joel Kline, MD</i>	
	13 University of Cincinnati Internal Medicine Physician Scientist Training Program <i>Director: Jack Rubinstein, MD, Dept. of Medicine. Research Manager: Yolanda Wess, MEd, BSN</i>	
	14 National Institutes of Health Clinical Center Residency and Fellowship Programs <i>Director: Robert Lembo, MD</i>	
	15 University of Rochester Medical Center ABIM Research Pathway <i>Director: Jason Mendler, MD, PhD</i>	
	16 University of Utah Physician Scientist Training Program <i>Associate Chair of Research: Guy Zimmerman, MD</i>	



SPEAKER BIOGRAPHIES

Omar I. Abdel-Wahab, MD

Dr. Abdel-Wahab is Associate Member in the Human Oncology and Pathogenesis Program and an Attending Physician on the Leukemia Service in the Department of Medicine at Memorial Sloan Kettering Cancer Center (MSK). He also serves as co-director of the Hematology/Medical Oncology fellowship program at MSK and co-director of the Center for Hematologic Malignancies. His research focuses on understanding the functional implications of somatic mutations found in patients with hematopoietic malignancies with the hopes of improving our understanding of disease biology and develop novel therapies. Currently, his laboratory is centered on the role of mutations affecting the transcriptional regulation in leukemias. This includes mutations in epigenetic modifiers in leukemia pathogenesis as well as mutations in components of the RNA splicing factor machinery. His laboratory has generated substantial reagents to study the role of mutated spliceosomal factors in hematopoietic malignancies and solid tumors, including several murine models of mutations in the gene *Srsf2*, *Sf3b1*, and *Zrsr2*. His laboratory utilizes these models to create novel murine models of myeloid malignancies for epigenomic, functional, and preclinical therapeutic studies. Finally, his laboratory is also interested in hematological malignancies driven by MAP kinase pathway alterations. His laboratory's research is supported by the NIH, National Cancer Institute, National Heart, Lung, and Blood Institutes, the Leukemia & Lymphoma Society, the Dept. of Defense, the American Society of Hematology, and numerous additional philanthropic organizations. Dr. Abdel-Wahab's work has been recognized by a 2017 ASCI Seldin-Smith Award for Pioneering Research and the 2016 Joanne Levy Memorial Award for Outstanding Achievement from the American Society of Hematology.

Maria T. Abreu, MD

Dr. Abreu is a physician-scientist in gastroenterology with a focus in inflammatory bowel disease (IBD). She completed her medical degree at the University of Miami, Miller School of Medicine, her residency in medicine at Brigham and Women's Hospital, and research fellowship in gastroenterology at the University of California, Los Angeles (UCLA). She is currently the Director of the Crohn's and Colitis Center at UM, Professor of Medicine and Professor of Microbiology and Immunology.

Dr. Abreu was elected to the American Society for Clinical Investigation in 2010. She is the current Chair of the American Gastroenterological Association (AGA) Institute Council. Her research has focused on innate immunity and its contribution to IBD. Dr. Abreu's laboratory-based NIH-funded research focuses on colitis-associated cancer, stem cells, and the microbiome. Since returning to Miami, Dr. Abreu's translational research focuses on the rising incidence of IBD in immigrants from Latin America and in Hispanic-Americans. She and her colleagues have described the phenotype and genotype of Hispanic patients in Miami developing IBD.

Mary Armanios, MD

Dr. Armanios is Professor of Oncology and Genetic Medicine at the Johns Hopkins University School of Medicine. Her research interests have focused on understanding the role of telomeres and

telomerase in disease. Dr. Armanios earned her medical degree at the Ohio State University, where she went on to complete a combined internal medicine and pediatrics residency. She then moved to Johns Hopkins to complete her medical oncology fellowship. She is currently the Clinical Director of the Telomere Center at Johns Hopkins and oversees the telomere diagnostics lab at Johns Hopkins Hospital. Dr. Armanios is a member of the American Society for Clinical Investigation and serves as Associate Editor of the *Journal of Clinical Investigation*.

Kathleen H. Burns, MD, PhD

Dr. Burns is a physician-scientist and practicing hematopathologist at the Johns Hopkins University School of Medicine. Her research laboratory studies roles mobile genetic elements play in human disease. Her lab was one of the first to develop a targeted method to amplify mobile DNA insertion sites in the human genome for comprehensive insertion mapping. Their studies have shown that mobile element insertions represent a significant source of inherited structural variation in human populations, and the group has identified numerous potentially functional insertion variants at loci associated with human disease risk. Her lab also studies the expression and activity of mobile DNAs in human cancers. The lab has developed reagents to detect proteins encoded by active retrotransposons, namely, Long INterspersed Element-1 (LINE-1) open reading frame 1p (ORF1p) and ORF2p. They have shown aberrant expression of ORF1p in a wide variety of human cancers. This activation of LINE-1 is associated with somatic activity, and the Burns lab has mapped insertions of LINE-1 sequences acquired during the clonal evolution of gastrointestinal and ovarian cancers. The lab has ongoing projects to discern the functional consequences of somatically-acquired mobile element insertions, as well as other effects of ORF1p and ORF2p expression in malignancy. Dr. Burns recently served as co-Chair of a strategic workshop at the National Cancer Institute on roles of mobile genetic elements in cancer, and as the Organizer for a FASEB meeting on Mobile DNAs in the Mammalian Genome. She has authored numerous primary articles and reviews on human transposons and their roles in disease. Dr. Burns also serves as Vice Chair for Research for the Department of Pathology at Johns Hopkins, and as the inaugural Director of the institution's Physician Scientist Training Program (PSTP).

Ana María Cuervo, MD, PhD

Dr. Cuervo is the R.R. Belfer Chair for Neurodegenerative Diseases, Professor in the Departments of Developmental and Molecular Biology and of Medicine of the Albert Einstein College of Medicine and co-director of the Einstein Institute for Aging Studies. She obtained her M.D. and a Ph.D. in Biochemistry and Molecular biology from the University of Valencia (Spain) and received postdoctoral training at Tufts University, Boston. In 2002, she started her laboratory at the Albert Einstein College of Medicine, where she continues her studies in the role of protein-degradation in neurodegenerative diseases and aging.

Dr. Cuervo has received prestigious awards such as the P. Benson and the Keith Porter in Cell Biology, the Nathan Shock Memorial Lecture, the Vincent Cristofalo and the Bennett J. Cohen in basic aging biology and the Marshall Horwitz and the Saul Korey Prize for

SPEAKER BIOGRAPHIES

excellence in research and in Translational Medicine. She delivered prominent lectures such as the Robert R. Konh, the NIH Director's, the Roy Walford, the Feodor Lynen, the Margaret Pittman, the IUBMB Award, the David H. Murdoxk, the Gerry Aurbach and the Harvey Society Lecture. She is currently co-Editor-in-Chief of Aging Cell and has been member of the NIA Scientific Council and of the NIH Council of Councils.

George Q. Daley, MD, PhD

Dr. Daley is dean of Harvard Medical School (HMS) and the Caroline Shields Walker Professor of Medicine at HMS. He has been professor of biological chemistry and molecular pharmacology at HMS since 2010 and an investigator of the Howard Hughes Medical Institute since 2008. In July 2016, he became the Robert A. Stranahan Professor of Pediatrics and Professor of Biological Chemistry and Molecular Pharmacology at HMS. He previously held, as its inaugural incumbent, the Samuel E. Lux, IV Chair in Hematology/Oncology at Boston Children's Hospital. A former chief resident in medicine at Massachusetts General Hospital (1994-95), Daley maintained an active clinical practice in hematology/oncology at Massachusetts General Hospital (MGH) and then at Boston Children's, until assuming his administrative role as director of the Pediatric Stem Cell Transplantation Program at Dana-Farber/Boston Children's Cancer and Blood Disorders Center, a post he held until Jan. 2017. Dr. Daley earned his PhD in biology (1989) at MIT, working in David Baltimore's laboratory at the MIT-affiliated Whitehead Institute for Biomedical Research, and his MD from HMS in 1991. He then pursued clinical training in internal medicine at MGH and was a clinical fellow at Brigham and Women's and Boston Children's hospitals. Dr. Daley was an inaugural winner of the National Institutes of Health Director's Pioneer Award for highly innovative research (2004). Other honors include the American Philosophical Society's Judson Daland Prize for achievement in patient-oriented research, the American Pediatric Society's E. Mead Johnson Award for contributions to stem cell research, the American Society of Hematology's E. Donnell Thomas Prize for advances in human-induced pluripotent stem cells and the International Chronic Myeloid Leukemia Foundation's Janet Rowley Prize for outstanding lifetime contributions to the understanding and/or treatment of the disease. He is an elected member of the National Academy of Medicine and the ASCI, among other professional societies.

Jeffrey M. Drazen, M.D.

Dr. Drazen was born and raised in Clayton, Missouri. Dr. Drazen majored in applied physics at Tufts University and graduated from Harvard Medical School in 1972. He currently holds the positions of senior physician at the Brigham and Women's Hospital, Distinguished Parker B. Francis Professor of Medicine at Harvard Medical School, professor of physiology at the Harvard School of Public Health and adjunct professor of medicine at the Boston University School of Medicine. He is the recipient of honorary degrees from the University of Ferrara, the University of Athens and the University of Modena.

Dr. Drazen is an elected member of the American Society for Clinical Investigation, the Association of American Physicians, the Interurban Clinical Club and the National Academy of Medicine.

He serves on the National Academy of Medicine's Forum on Drug Discovery, Development, and Translation.

An active researcher in the field of pulmonary medicine, Dr. Drazen defined the role of novel endogenous chemical agents in asthma, leading to four licensed pharmaceuticals for asthma, now used by tens of millions of people worldwide. He has published over 500 papers, editorials and review articles and has edited ten books, including *Goldman-Cecil Medicine* and *Asthma and COPD*.

In 2000, Dr. Drazen became editor-in-chief of the *New England Journal of Medicine*. Since then, the *Journal* has published major papers advancing the science of medicine, including the first descriptions of SARS, timely coverage of the Ebola and Zika virus epidemics, and advances in the treatment of cancer, heart disease and lung disease. It has been at the forefront of worldwide efforts to register all clinical trials and to share clinical trial data. The *Journal* now has over a half a million readers every week and the highest impact factor of any journal publishing original research.

Victor J. Dzau, MD

Dr. Dzau is the President of the National Academy of Medicine (NAM), formerly the Institute of Medicine (IOM). In addition, he serves as Vice Chair of the National Research Council. Dr. Dzau is Chancellor Emeritus and James B. Duke Professor of Medicine at Duke University and the past President and CEO of the Duke University Health System. Previously, Dr. Dzau was the Hersey Professor of Theory and Practice of Medicine and Chairman of Medicine at Harvard Medical School's Brigham and Women's Hospital, as well as Chairman of the Department of Medicine at Stanford University.

Dr. Dzau is an internationally acclaimed leader and scientist whose work has improved health care in the United States and globally. Since arriving at the National Academies, Dr. Dzau has led important initiatives such as the Commission on a Global Health Risk Framework; the Human Gene Editing Initiative; and Vital Directions for Health and Health Care, and the NAM Grand Challenges in Healthy Longevity. His own research laid the foundation for development of the class of lifesaving drugs known as ACE inhibitors, used globally to treat high blood pressure and congestive heart failure. He pioneered gene therapy and regenerative medicine for cardiovascular diseases.

In his role as a leader in health care, Dr. Dzau has led efforts in innovation to improve health, including the development of the Duke Translational Medicine Institute, the Duke Global Health Institute, the Duke-National University of Singapore Graduate Medical School, and the Duke Institute for Health Innovation. As one of the world's preeminent health leaders, Dr. Dzau advises governments, corporations, and universities worldwide. He has served as a member of the Advisory Committee to the Director of the National Institutes of Health (NIH) and as Chair of the NIH Cardiovascular Disease Advisory Committee. Currently he is a member of the Board of the Singapore Health System, member of the Health Biomedical Sciences the International Advisory Council of Singapore and Advisory Council of the Imperial College Health Partners, UK. He was on the Board of Health Governors of the World Economic Forum and chaired its Global Agenda Council on Personalized and Precision Medicine.

SPEAKER BIOGRAPHIES

Among his many honors and recognitions are the Gustav Nylin Medal from the Swedish Royal College of Medicine, the Distinguished Scientist Award from the American Heart Association, Ellis Island Medal of Honor, and the Henry Freisen International Prize. In 2014, he received the Public Service Medal from the President of Singapore. He is a member of the Institute of Medicine of the National Academy of Sciences, the American Academy of Arts and Sciences and the European Academy of Sciences and Arts.

Benjamin L. Ebert, MD, PhD

Dr. Ebert, 2017-2018 President of the American Society for Clinical Investigation, is chair of Medical Oncology at Dana-Farber Cancer Institute, is professor of Medicine at Harvard Medical School, an institute member of the Broad Institute, and leader of the Leukemia Program for the Dana-Farber/Harvard Cancer Center. His research focuses on the genetics, biology, and therapy of myeloid malignancies. This work has led to the characterization of clonal hematopoiesis as a pre-malignant state for hematologic malignancies, and elucidation of the mechanism of action of lenalidomide and related molecules that induce degradation of specific proteins. Dr. Ebert received a bachelor's degree from Williams College, a doctorate from Oxford University on a Rhodes Scholarship, and an MD from Harvard Medical School. He completed a residency in internal medicine at Massachusetts General Hospital and a fellowship in hematology/oncology at Dana-Farber.

Serpil Erzurum, MD

Dr. Erzurum is the Alfred Lerner Chair of the Lerner Research Institute and a staff physician at the Cleveland Clinic. Dr. Erzurum earned her medical degree from Northeastern Ohio Universities College of Medicine and completed residency training in Internal Medicine at Baylor College of Medicine where she was named the MacIntosh outstanding resident. Following completion of residency, she practiced in the Indian Health service in South Dakota, serving as TB officer for the western part of the state. Subsequently, she entered pulmonary and critical care fellowship training at the University of Colorado/National Jewish Center and then postdoctoral research training at the National Heart, Lung and Blood Institute. Dr. Erzurum's scientific accomplishments over the past 30 years have been broad and far-reaching in impact for respiratory medicine. Her scientific contributions and leadership in pulmonary research have led to diagnostic and therapeutic advances in asthma and lung vascular diseases, and helped to identify human physiologic adaptive responses to high-altitude hypoxia. She has published more than 250 peer-reviewed articles and her research is funded by a wide variety of grants from the National Institutes of Health. She has earned numerous awards, including the MERIT award from NHLBI, election to the American Society for Clinical Investigation (ASCI), election to the Association of American Physicians, election to the National Academy of Medicine, and the Elizabeth Rich Award from the American Thoracic Society for her work in advancing the careers of women in medicine and science. In addition to her leadership at Cleveland Clinic, Dr. Erzurum serves the profession as member of the Advisory Council to the NHLBI, Chair of the American Board of Internal Medicine Pulmonary Disease Subspecialty Board, and is currently the President of the Association of American Physicians.

Luigi Ferrucci, MD, PhD

Dr. Ferrucci is a geriatrician and an epidemiologist who conducts research on the causal pathways leading to progressive physical and cognitive decline in older persons. He has made major contributions in the design of many epidemiological studies conducted in the U.S. and in Europe, including the *European Longitudinal Study on Aging*, the *"ICare Dicomano Study,"* the AKEA study of Centenarians in Sardinia and the *Women's Health and Aging Study*. He was also the Principal Investigator of the *InCHIANTI* study, a longitudinal study conducted in the Chianti Geographical area (Tuscany, Italy) looking at risk factors for mobility disability in older persons. Dr. Ferrucci received a Medical Degree and Board Certification in 1980, Board Certification in Geriatrics in 1982 and Ph.D. in Biology and Pathophysiology of Aging in 1998 at the University of Florence, Italy. He spent a 2-year internship at the Intensive Care Unit of the Florence Institute of Gerontology and Geriatrics, and was for many years Associate Professor of Biology, Human Physiology and Statistics at the University of Florence. Between 1985 and 2002 he was Chief of Geriatric Rehabilitation at the Department of Geriatric Medicine and Director of the Laboratory of Clinical Epidemiology at the Italian National Institute of Aging. In September 2002, he became the Chief of the Longitudinal Studies Section at NIA. From 2002 to 2014 he was the Director of the Baltimore Longitudinal Study on Aging. Dr. Ferrucci is currently the Scientific Director of NIA, since May 2011.

Linda P. Fried, MD, MPH

Dr. Fried, Dean of the Mailman School of Public Health is a public health leader in the fields of epidemiology and geriatrics. She has dedicated her career to the science of healthy aging and defining how to transition to a world where greater longevity benefits people of all ages. An internationally renowned scientist, she has done seminal work in defining frailty as a clinical syndrome and illuminating both its causes and the potential for prevention as keys to optimizing health for older adults. Her scientific discoveries have transformed medical care and public health globally, and our understanding of how to build successful societies of longer lives. Under Fried's visionary leadership, the Mailman School continues to be a leader in transforming the health of populations and is one of the top five NIH-funded schools of public health. Fried led the School to build the nation's first program on climate and health and a multidisciplinary program that delivers economic evidence on the value of prevention. Fried opened the Columbia Center for Aging and elevated Columbia's leadership role in research, policy and programming to support healthy cities. As a leader in public health education, she initiated Columbia/Mailman's innovative interdisciplinary public health curriculum that emphasizes a life-course approach to prevention of disease and disability. Fried is an elected member of the U.S. National Academy of Medicine, as well as the President of the Association of American Physicians, the elected society of the U.S. leading physician scientists. She is the first Dean of a School of Public Health to be President of AAP. She is also Co-Chair of the World Economic Forum's Global Council on the Future of Human Enhancement and on the Steering Committee for their Council on Human Centric Health.

SPEAKER BIOGRAPHIES

Levi A. Garraway, MD, PhD

Dr. Garraway received his AB, MD, and PhD degrees from Harvard Medical School. Thereafter, he did an internship and residency in internal medicine at the Massachusetts General Hospital, where he also served as Medical Chief Resident in 2003. Garraway completed his fellowship training in medical oncology at the Dana-Farber Cancer Institute. He received board certification in internal medicine and medical oncology.

Prior to joining Eli Lilly and Company, Garraway served as an investigator of the Howard Hughes Medical Institute and an Associate Professor of Medicine at the Dana-Farber Cancer Institute, Harvard Medical School and an Institute Member of the Broad Institute. He was the inaugural Director of the Joint Center for Cancer Precision Medicine, which spans the Dana-Farber, Brigham and Women's Hospital, Boston Children's Hospital and the Broad Institute of MIT and Harvard. Garraway led a research group that studied cancer genomics, drug resistance, and cancer precision medicine. His research informed several gene targets and "druggable" pathways relevant to the genesis and therapeutic vulnerabilities of melanoma, prostate cancer, and other malignancies. Garraway has received numerous awards including the Paul Marks Prize for Cancer Research, the Jane Cooke Wright Award from AACR, the New Innovator Award from the NIH and an Outstanding Investigator Award from the National Cancer Institute.

Joseph Heitman, MD, PhD

Dr. Heitman is a James B. Duke Professor in the Departments of Molecular Genetics and Microbiology, Pharmacology and Cancer Biology, and Medicine at Duke University Medical Center and Chair of the Department of Molecular Biology and Director of the Duke Center for Microbial Pathogenesis. He served as director of the Duke University Program in Genetics and Genomics from 2002-2009. Dr. Heitman received his undergraduate training at the University of Chicago in chemistry and biochemistry, as an MD-PhD student at Cornell and Rockefeller Universities, where he worked with Peter Model and Norton Zinder on how restriction enzymes recognize specific DNA sequences and how bacteria respond to and repair DNA breaks and nicks. Dr. Heitman was an EMBO long-term fellow at the Biocenter in Basel, Switzerland prior to moving to Duke in 1992. Dr. Heitman and colleagues focus on the model yeast *Saccharomyces cerevisiae* and the pathogenic fungi *Cryptococcus neoformans* and *Candida albicans*. Their studies have revealed the conserved targets for immunosuppressive antifungal drugs and delineated calcineurin and Tor signaling pathways. Dr. Heitman is a recipient of the Burroughs Wellcome Scholar Award in Molecular Pathogenic Mycology, the 2002 ASBMB AMGEN award for significant contributions using molecular biology to our understanding of human disease, and the 2003 Squibb Award from the Infectious Diseases Society of America (IDSA) for outstanding contributions to infectious disease research. Dr. Heitman has been an instructor since 1998 at the Woods Hole Molecular Mycology Course, is an editor of *Eukaryotic Cell*, is a member of the ASCI (elected 2003), a fellow of the IDSA in 2003, a fellow of the American Academy of Microbiology in 2004, and a fellow of the American Association for the Advancement of Science (2005).

Helen Hobbs, MD

Dr. Hobbs received her undergraduate degree from Stanford University and her medical degree from Case Western Reserve University School of Medicine. After obtaining her clinical and post-doctoral training at Columbia-Presbyterian Hospital and University of Texas (UT) Southwestern Medical Center Dallas, she joined the faculty of UT Southwestern. She is currently Professor of Internal Medicine and Molecular Genetics, as well as Director of the McDermott Center for Human Growth and Development at UT Southwestern Medical Center in Dallas. Since 2002, she has been an Investigator of the Howard Hughes Medical Institute. In partnership with Jonathan Cohen, she has identified genes and sequence variations contributing to metabolic and cardiovascular disorders with a focus on lipids and lipoproteins. Together they showed that rare genetic variations contribute to complex traits in the general population. By concentrating on alleles of low frequency and large phenotypic effect size, they have discovered new therapeutic targets for the prevention and treatment of heart disease, including PCSK9. Most recently, they have identified genetic variants that contribute to the full spectrum of fatty liver disease, extending from hepatic steatosis to cirrhosis. Hobbs was elected to the Institute of Medicine, American Academy of Arts and Sciences, and the National Academy of Sciences. She has been awarded prizes for her work from the American Heart Association [the Clinical Research Prize (2005) and the Distinguished Scientist Award (2007)], the Inaugural International Society of Atherosclerosis Prize (2012), the Pasarow Foundation Award in Cardiovascular Research (2013), the Pearl Meister Greengard Prize (2015), the 2016 Breakthrough Prize in Life Sciences and the Passano Award (2016).

Sharon K. Inouye, MD, MPH

Dr. Inouye is an internationally recognized leader in geriatric medicine and aging research. She is an elected member of the National Academy of Medicine, chaired the Delirium Clinical Guidelines Panel for the American Geriatrics Society, and serves as an Associate Editor of the *Journal of the American Geriatrics Society*. Her research focuses on prevention of delirium and cognitive decline with aging, promoting healthy aging and independence follow acute illness, and improvement of healthcare systems through policy.

Continuously NIH-funded since 1989 with over 50 grants and over 250 publications, Dr. Inouye developed the Confusion Assessment Method (CAM)—the most widely used method for delirium identification, used in over 4000 publications and translated into 20 languages—along with the Hospital Elder Life Program (HELP) for delirium prevention, a cost-effective model of patient-centered care that has been disseminated to over 200 hospitals worldwide. She was recently awarded an R24 Delirium Network grant by the National Institutes of Health. She is committed to translating research into practice and policy changes.

Ross Levine, MD

Dr. Levine is a Member of the Human Oncology and Pathogenesis Program and an Attending Physician on the Leukemia Service, Department of Medicine. He is the Laurence Joseph Dineen Chair in Leukemia Research, a Professor of Medicine at Weill

SPEAKER BIOGRAPHIES

Cornell Medical College, and is the Director of the MSK Center for Hematologic Malignancies. Dr. Levine was born and raised in the New York area, and then received his AB from Harvard College and a M.D. from Johns Hopkins. Dr. Levine served as a Resident in Internal Medicine at the MGH and subsequently as a Hematology-Oncology Fellow at DFCI/Harvard. In September 2007, he was recruited to MSK to the Human Oncology and Pathogenesis Program, while he also sees patients on the MSK Leukemia Service.

Timothy J. Ley, MD

Dr. Ley received his BA from Drake University, his MD degree from Washington University Medical School, and performed his internal medicine residency at Massachusetts General Hospital. He completed fellowships in Hematology and Oncology at the NIH and at Washington University, and joined the faculty at Washington University in St. Louis in 1986. He now holds the Lewis T. and Rosalind B. Apple Chair in Oncology, is Professor of Medicine and of Genetics at Washington University, and serves as Director of the Stem Cell Biology Section in the Department of Medicine. Ley is a past president of the American Society for Clinical Investigation, past treasurer of the American Association of Physicians, a fellow of AAAS and the American Academy of Arts and Sciences, and a member of the National Academy of Medicine. He was appointed by President Obama to the National Cancer Advisory Board in 2015.

Ley has developed approaches to reactivate fetal hemoglobin synthesis for patients with hemoglobinopathies, defined the role of the perforin/granzyme system for the function of cytotoxic and regulatory T cells, and has performed pioneering studies that have precisely defined the genomics of acute myeloid leukemia. He has written extensively about the physician-scientist career path, and was an advocate for establishing the extramural Loan Repayment Programs at the NIH. He has mentored more than 50 pre- and post-doctoral fellows in his laboratory; most hold research positions in academic medicine or pharmaceutical companies.

Richard P. Lifton, MD, PhD

Dr. Lifton is President of The Rockefeller University where he is also head of the laboratory of Human Genetics and Genomics. He graduated *summa cum laude* from Dartmouth, and received MD and PhD degrees from Stanford. He then was Resident and Chief Resident in Medicine at Brigham and Women's Hospital, and continued on the Harvard Medical School faculty before being recruited to Yale in 1993, where he served as Sterling Professor and Chair of Genetics from 1998 to 2016 before moving to Rockefeller. At Yale, he was also Founder and Executive Director of the Yale Center for Genome Analysis.

Dr. Lifton has used human genetics and genomics to identify mutations that identify key genes and pathways underlying hypertension, myocardial infarction, osteoporosis, cerebral hemorrhage, congenital heart disease and neoplasia. His work on hypertension, which affects one billion people worldwide, has demonstrated the key roles of renal salt and potassium handling in blood pressure regulation, leading to new approaches to treatment and prevention that have been applied to the general population world-wide. In 2009, his group developed exome sequencing and performed the first clinical diagnosis by genome-

level sequencing.

He is a member of the National Academy of Sciences, the National Academy of Medicine and the American Academy of Arts and Sciences. He formerly served on the Governing Councils of the National Academy of Sciences and the Institute of Medicine, and is currently on the Advisory Council to the NIH Director, the Scientific Advisory Boards of Massachusetts General Hospital, the Whitehead Institute, the Broad Institute, the Simons Foundation for Autism Research, and the Board of Directors of Roche and Genentech. He recently served as Co-Chair of the Planning Committee for the President's Precision Medicine Initiative.

He has received the highest scientific awards of the American Heart Association, the American Society of Nephrology, the Council for High Blood Pressure Research, the American Society of Hypertension, the International Society of Hypertension, and the International Society of Nephrology. He received the 2008 Wiley Prize for Biomedical Sciences and the 2014 Breakthrough Prize in Life Sciences.

Dr. Stuart H Orkin, MD

Dr. Orkin is the David G. Nathan Distinguished Professor of Pediatrics at Harvard Medical School, and an Investigator of the Howard Hughes Medical Institute. Dr. Orkin's pioneering efforts defined the molecular basis of human blood disorders and mechanisms governing blood cell development. His early accomplishments led to the first comprehensive molecular dissection of an inherited disorder (the thalassemia syndromes). He characterized genes responsible for other human blood disorders, including X-linked chronic granulomatous disease (the first positional cloning). Dr. Orkin then transformed the study of blood stem cell development by identifying and characterizing the first hematopoietic transcription factors (the GATA family) and their critical co-activators. His recent landmark studies on BCL11A, a critical repressor of fetal hemoglobin (HbF), have illuminated regulation of the fetal-to-adult switch and improved prospects for HbF reactivation as genetic or pharmacological therapy of the thalassemias and sickle cell disease. These contributions to human genetics and medicine are unmatched for their breadth, focus, and broad impact. He is also an elected member of the National Academy of Sciences (NAS), Institute of Medicine, American Academy of Arts and Sciences, and the American Philosophical Society, and recipient of the E. Mead Johnson Award of the American Academy of Pediatrics, the Warren Alpert Prize, the Helmut Horten Foundation Prize, the Distinguished Research Award from the Association of American Medical Colleges (AAMC), the E. Donnall Thomas, Dameshek and Basic Science Mentor Awards of the American Society of Hematology (ASH), the Metcalf Award of the International Society of Experimental Hematology (ISEH), and the William A. Allan Award of the American Society of Human Genetics. In 2013, he received Jessie Stevenson Kovalenko Medal of the NAS for "important contributions to the medical sciences".

Sir Peter Ratcliffe, FRS

Dr. Ratcliffe is a physician scientist who trained in medicine at Gonville and Caius College, Cambridge and St. Bartholomew's Hospital, London, before moving to Oxford to specialize in renal medicine. His work on oxygen sensing has won a number of

SPEAKER BIOGRAPHIES

awards including the Louis-Jeantet Prize in Medicine, the Canada Gairdner International Award, and the Lasker Award for Basic Biomedical Research. Peter was elected to the Fellowship of the Royal Society and to the Academy of Medical Sciences in 2002. He is a member of EMBO and a foreign honorary member of the American Academy of Arts and Sciences. He was knighted for services to medicine in the New Year's Honours, 2014.

In 2004, he was appointed Nuffield Professor of Clinical Medicine at the University of Oxford and served as Head of the Nuffield Department of Clinical Medicine from 2004-2016. In May 2016 he was appointed Director of Clinical Research at the Francis Crick Institute, retaining a position at Oxford as member of the Ludwig Institute of Cancer Research and Director of Oxford's Target Discovery Institute.

Eric Topol, MD

Dr. Topol is the Founder and Director of the Scripps Translational Science Institute (STSI), Professor, Molecular Medicine, and Executive Vice-President of The Scripps Research Institute (TSRI). As a researcher, he has published over 1100 peer-reviewed articles, with more than 185,000 citations, elected to the National Academy of Medicine, and is one of the top 10 most cited researchers in medicine (Thomson Reuters ISI, "Doctor of the Decade"). His principal scientific focus has been on the genomic and digital tools to individualize medicine—and the power that brings to individuals to drive the future of medicine.

In 2016, Topol was awarded a \$207M grant from the NIH to lead a significant part of the Precision Medicine Initiative, a prospective research program that aims to enroll 1 million participants in the US. Prior to coming to lead Scripps STSI in 2007, for which he is the principal investigator of a flagship \$33M NIH grant, he led the Cleveland Clinic to become the #1 center for heart care and was the founder of a new medical school there. He has been voted as the #1 most Influential physician leader in the United States in a national poll conducted by *Modern Healthcare*. Besides editing several textbooks, he has published 2 bestseller books on the future of medicine: *The Creative Destruction of Medicine* and *The Patient Will See You Now*.

Eric Verdin, MD

Dr. Verdin is the President and CEO of the Buck Institute for Research on Aging. A native of Belgium, Dr. Verdin received his Doctorate of Medicine (MD) from the University of Liege and additional clinical and research training at Harvard Medical School. He has held faculty positions at the University of Brussels, the National Institutes of Health (NIH), the Picower Institute for Medical Research and the Gladstone Institutes. Dr. Verdin is also a Professor of Medicine at University of California, San Francisco. Dr. Verdin's laboratory focuses on the role of epigenetic regulators in the aging process. His laboratory was first to clone a family of enzymes, called HDACs, which regulate histone acetylation. Dr. Verdin studies how metabolism, diet and small molecules regulate the activity of HDACs and Sirtuins and thereby the aging process and its associated diseases, including Alzheimer's. He has published more than 210 scientific papers and holds more than 15 patents. He has been recognized for his research with a Glenn Award for Research in Biological Mechanisms of Aging and a senior scholarship from the Ellison Medical Foundation. He is a fellow of

the American Association for the Advancement of Science and an elected member of the American Society for Clinical Investigation and the Association of American Physicians. He also serves on the Advisory Council of NIDA at the National Institutes of Health.

Irving L. Weissman, MD

Dr. Weissman is the Director of the Stanford Institute for Stem Cell Biology and Regenerative Medicine and Director of the Stanford Ludwig Center for Cancer Stem Cell Research.

Dr. Weissman was a member of the founding Scientific Advisory Boards of Amgen (1981-1989), DNAX (1981-1992), and T-Cell Sciences (1988-1992). He co-founded, was a Director, and chaired the Scientific Advisory Board at SyStemix 1988-1996, StemCells in 1996-present, and Cellerant in 2001-9. He founded Forty Seven Inc. in 2015, and is a Director of the Company.

His research encompasses the biology and evolution of stem cells and progenitor cells, mainly blood-forming and brain-forming. He is also engaged in isolating and characterizing the rare cancer and leukemia stem cells as the only dangerous cells in these malignancies, especially with human cancers. He discovered that all cancer stem cells express CD47, the 'don't eat me' signal, to overcome phagocytic signals that arise during cancer development, and has shown that blocking antibodies to CD47 have therapeutic potential for all tested human cancers. Finally, he has a long-term research interest in the phylogeny and developmental biology of the cells that make up the blood-forming and immune systems. His laboratory was first to identify and isolate the blood-forming stem cell from mice, and has purified each progenitor in the stages of development between the stem cells and mature progeny (granulocytes, macro-phages, etc.). At SyStemix he co-discovered the human hematopoietic stem cell and at StemCells, he co-discovered a human central nervous system stem cell. In addition, the Weissman laboratory has pioneered the study of the genes and proteins involved in cell adhesion events required for lymphocyte homing to lymphoid organs *in vivo*, either as a normal function or as events involved in malignant leukemic metastases.

Professor Weissman is a member of the National Academy of Sciences, the Institute of Medicine at the National Academy, and the American Association of Arts and Sciences. He has received many awards, including the Kaiser Award for Excellence in Preclinical Teaching, the Pasarow Award in Cancer Research, the California Scientist of the Year, the De Villiers International Achievement Award of the Leukemia Society of America, the Robert Koch Award, the Rosenstiel Award, The max Delbruck Medal, and the Jessie Stevenson Kovalenko Award of the National Academy of Sciences. He is also the 2004 New York Academy of Medicine Award for distinguished contributions to biomedical research, and has several honorary doctorates.

Leonard I. Zon, MD

Dr. Zon is the Grousbeck Professor of Pediatric Medicine at Harvard Medical School, an Investigator at Howard Hughes Medical Institute, and the Director of the Stem Cell Program at Boston Children's Hospital. He is internationally-recognized for his pioneering work in stem cell biology and cancer genetics, and has been the preeminent figure in establishing zebrafish as an invaluable genetic model for the study of blood and hematopoietic development.

The Harrington Prize for Innovation in Medicine

NOW ACCEPTING NOMINATIONS FOR 2019

The Harrington Prize for Innovation in Medicine, presented by the American Society for Clinical Investigation (ASCI) and the Harrington Discovery Institute at University Hospitals in Cleveland, Ohio, honors a physician-scientist who has moved the field forward through innovation, creativity and potential to impact human health.

Applications are now being accepted for the 2019 Harrington Prize – an international award open to those holding an MD or equivalent degree.


This annual prize includes:

- An unrestricted \$20,000 honorarium
- The Harrington Prize Lecture, delivered at the 2019 AAP/ASCI/APSA Joint Meeting
- Participation at the annual Harrington Discovery Institute Symposium
- A personal essay, published in the Journal of Clinical Investigation

Nominations accepted through **August 28, 2018**.

To learn more or to apply, visit HarringtonDiscovery.org/ThePrize.

THE HARRINGTON PROJECT
FOR DISCOVERY & DEVELOPMENT

Harrington Discovery Institute
 University Hospitals | Cleveland, Ohio

**THE AMERICAN SOCIETY
FOR CLINICAL INVESTIGATION**
honoring the physician-scientist

**ACCELERATING BREAKTHROUGH
DISCOVERIES INTO MEDICINES**

2018 AAP/ASCI/APSA LEADERSHIP

AAP Council Officers

President

Serpil Erzurum, MD
Cleveland Clinic

Vice-President

John Carethers, MD
University of Michigan

Secretary

Mitchell Lazar, MD, PhD
*Perelman School of Medicine,
University of Pennsylvania*

Treasurer

Robert Brown, DPhil, MD
University of Mass. Medical School

AAP Councilors

Nancy Davidson, MD
Fred Hutchinson Cancer Research Center

Betty Diamond, MD
The Feinstein Institute for Medical Research

Maurizio Fava, MD
Massachusetts General Hospital

David Ginsburg, MD
Life Sciences Institute, Univ. of Michigan

Todd Golub, MD
*Broad Institute of MIT and Harvard,
Dana Farber Cancer Institute*

Peter Igarashi, MD
University of Minnesota Medical School

John Ioannidis, MD
Stanford University

Daniel Kelly, MD
*Perelman School of Medicine,
University of Pennsylvania*

Mary Klotman, MD
Duke University School of Medicine

Warren Leonard, MD
National Institutes of Health

Elizabeth McNally, MD, PhD
Northwestern Feinberg School of Medicine

David Thomas, MD, MPH
Johns Hopkins University

ASCI Council Officers

President

Benjamin L. Ebert, MD, PhD
*Harvard Medical School,
Dana-Farber Cancer Institute*

President-Elect

Kieren Marr, MD
Johns Hopkins School of Medicine

Vice President

W. Kimryn Rathmell, MD, PhD
Vanderbilt University

Secretary-Treasurer

Hossein Ardehali, MD, PhD
Northwestern University Medical Center

Editor, The Journal of Clinical Investigation

Gordon F. Tomaselli, MD
Johns Hopkins University

Editor, JCI Insight

Howard A. Rockman, MD
Duke University School of Medicine

Immediate Past President

Vivian G. Cheung, MD
*Howard Hughes Medical Institute;
University of Michigan Medical School*

ASCI Councilors

Clara Abraham, MD
Yale University School of Medicine

Andrew P. Fontenot, MD
University of Colorado Denver

Jay D. Horton, MD
UT Southwestern Medical Center

Donna M. Martin, MD, PhD
University of Michigan

Ben Z. Stanger, MD, PhD
University of Pennsylvania

Sohail F. Tavazoie, MD, PhD
Rockefeller University

APSA Board of Directors

Chair

Moshe Levi, MD
Georgetown University

Immediate Past-Chair

Jaimo Ahn, MD, PhD
University of Pennsylvania

Director

Lawrence (Skip) Brass, MD, PhD
University of Pennsylvania

Director

Dania Daye, MD, PhD
Massachusetts General Hospital

Director

Shwayta Kukreti, MD, PhD
UCLA

Director

Jillian Liu (6th-year MD/PhD)
Ohio State University

Director

Robin Lorenz, MD, PhD
University of Alabama at Birmingham

Director

David Markovitz, MD
University of Michigan

Director

Kofi Mensah, MD, PhD
Yale University

Director

Evan Noch, MD, PhD
New York Presbyterian Hospital-Cornell

Director

Kerry O'Banion, MD, PhD
University of Rochester

Director

Aylin Rodan, MD, PhD
University of Utah

APSA Executive Council

President

Jillian Liu (6th year MD/PhD)
Ohio State University

Immediate Past-President

Alexander Adami (8th year MD/PhD)
University of Connecticut

2018 AAP/ASCI/APSA LEADERSHIP

APSA Executive Council *(continued)*

President-Elect

Audra Iness (5th year MD/PhD)
Virginia Commonwealth University
School of Medicine

Vice-President

Hanna Erickson (5th year MD/PhD)
University of Illinois at Urbana-Champaign

Events Co-Chair

Allyson Palmer (8th year MD/PhD)
Mayo Clinic

Events Co-Chair

Jason Siu (6th year MD/PhD)
Ohio State University

Fundraising Co-Chair

Karen Doersch (8th year MD/PhD)
Texas A&M Health Science Center

Fundraising Co-Chair

Nadav Weinstock (6th-year MD/PhD)
SUNY Buffalo

Membership Chair

Abhik Banerjee (6th year MD/PhD)
USC/Caltech

Partnerships Chair

Daniel Barnett (7th year DO-PhD)
Michigan State University

Policy Co-Chair

Shinnyi "Cindy" Chou (PGY1 Psychiatry
Resident)
University of Pittsburgh

Policy Co-Chair

Mariam Bonyadi (5th year MD/PhD)
University of Illinois at Urbana-Champaign

Public Relations Chair

Vadim Yerokhin (5th year DO/PhD)
Oklahoma State University Center for
Health Sciences

Technology Chair

Tim Kennell (4th year MD/PhD)
University of Alabama at Birmingham

MAL MD/DO

Siyu Shi (1st year MD)
Stanford School of Medicine

MAL DO-MD/PhD

Teddy Mamo (7th year MD/PhD)
Mayo Clinic

Co-MAL SSH

Tyler Zahrli (7th year MD/PhD)
Saint Louis University

Co-MAL SSH

Joshua Franklin (5th year MD-PhD)
University of Pennsylvania

TRAVEL AWARD RECIPIENTS

2018 AAP/ASCI Travel Award Recipients

Amanda Garfinkel

Harvard Medical School

Meghan Green Haney

University of Kentucky

Lauren Harasymiw

University of Minnesota

Paishiun Hsieh

Case Western Reserve University

Eric Irons

University at Buffalo

Anjali Jacob

Boston University School of Medicine

Sunil Joshi

Knight Cancer Institute, Oregon Health &
Science University

Kunio Kawanishi

University of California, San Diego

Lindsay Kozek

Vanderbilt University

Daniel Leonard

Cleveland Clinic Lerner College of
Medicine at Case Western Reserve
University

Evan Lynch

University of Kentucky College of
Medicine

Beth Neilsen

University of Nebraska Medical Center

Anjan Saha

University of Michigan

John Smestad

Mayo Clinic

Jaelyn Souder

University of Alabama at Birmingham

Samantha Spellicy

Medical College of Georgia and the
University of Georgia

Alexander Tereshchenko

University of Iowa

Priya Umapathi

Johns Hopkins Medical Institutions

Natalie Vandeven

University of Washington

John Walker

Vanderbilt University

Lillian Zhang

University of California, Davis

TRAVEL AWARD RECIPIENTS

2018 APSA Travel Award Recipients

Adewunmi Adelaja
UCLA

Damian Almiron Bonnin
Geisel School of Medicine

Kayla Berry
Washington Univ. School of Medicine

Michelle Corkrum
University of Minnesota

Kow Essuman
Washington Univ. School of Medicine

Nicholas Eustace
University of Alabama at Birmingham

Guillermo Flores
*Michigan St. College of Human Medicine/
Van Andel Institute Graduate School*

Nelson Gil
Albert Einstein College of Medicine

Jose Grajales-Reyes
Washington Univ. School of Medicine

LeMoyné Habimana-Griffin
Washington University in Saint Louis

Jonathan Herrera
University of Michigan

Gabriel Heymann
University of Washington

Donovan Inniss
*Saint John's University/The College of
St. Benedict*

Bianca Islam
Augusta University

Samuel Jean-Baptiste
University of Pennsylvania

Jeremie Lever
University of Alabama at Birmingham

Rachel Levy
University of Florida

Aaron Gabriel Sandoval
University of Florida

Ashley Scott
Mayo Clinic

Emile Vieta Ferrer
San Juan Bautista School of Medicine

2018 American Association of Immunologists Travel Award Recipients

Joshua Alinger
Washington University in St. Louis

Aaron Fan
Augusta University

John Klement
Augusta University

Megan Maurano
University of Washington

Alfonso Tan Garcia
Duke-NUS Medical School

2018 American Society of Nephrology (ASN) Travel Award Recipients

Emily Groopman
Columbia University

Aaron Lim
Vanderbilt University School of Medicine

Hannah Turbeville
University of Mississippi Medical Center

2018 Society for Academic Emergency Medicine Travel Award Recipients

Anshul Dhingra
Case Western Reserve University

Uriel Kim
Case Western Reserve University

Monica Lieng
University of California, Davis

Mohamad Fadhli Masri
Duke-NUS Medical School

Meaghan Roy-O'Reilly
*University of Texas Health Sciences
Center at Houston*

2018 APSA Undergraduate Travel Award Recipients

Melanie Barbini
Northeastern University

Jordy Botello
University of Florida

Rochelle Hall
Brooklyn College-CUNY

Carlos Jeronimo
CUNY Lehman College

Jennifer Jung
Princeton University

Yifan Mao
The University of Chicago

Kimberly Meza
Barnard College/Columbia University

Nadine Ramirez
University of Denver

Valeria Rodriguez Alfaro
New York University

Sinibaldo Romero Arocha
*Mayo Clinic Graduate School of
Biomedical Sciences*

Caroline Haoud
Columbia University

Andy Tang
North Seattle College

Call for Nomination for the George M. Kober Medal

This is a Call for Nomination for the George M. Kober Medal Recipient for 2020.

He was active in the early days as a leader of several national organizations including the Association of American Physicians - an early organization founded in the 1885 by seven Physicians (including William Osler) an organization which promotes:

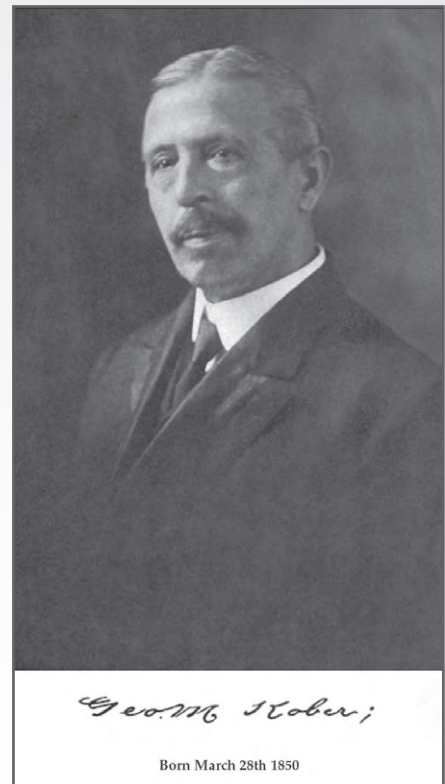
“the pursuit of medical knowledge, and the advancement through experimentation and discovery of basic and clinical science and their application to clinical medicine...”

Please provide a brief cover letter highlighting the major accomplishments of the nominee along with an updated CV and submit by December 1, 2018 to Lori Ennis at admin@aap-online.org

George M. Kober Medal

The Association of American Physicians honors Kober and continues to honor him by giving their highest award to an honoree every year. This award is given to an AAP member whose lifetime efforts have had an enormous impact on the field of Internal Medicine (or the specific member's discipline) through the scientific discipline they have brought to the field and the many outstanding scientists that they have trained.

To view a list of past recipients go to: <http://aap-online.org/kober>





ORAL PRESENTATIONS & POSTER ABSTRACTS



APSA
American Physician Scientists Association

www.jointmeeting.org

APSA Trainee Oral Presentations

1 Using CLCA1 vWA Domain to Activate Alternate Anion Currents in Cystic Fibrosis Airway

Kayla Berry

Washington University School of Medicine, St. Louis, USA

In the airway, proper activity of the anion channel CFTR contributes to innate immune defense by maintaining a hydrated and alkaline mucus layer. This allows potentially pathogenic microorganisms to be trapped, quickly killed, and cleared via mucociliary clearance, thus preventing microbial colonization of the lungs. In cystic fibrosis (CF), this activity is impaired, resulting in repeated pulmonary infections that damage the lung and, if severe and prolonged enough, lead to early death without lung transplantation. Available therapies remain focused on targeted rescue of the CFTR mutation. However, given the thousands of mutations found in this patient population, individualized rescue of each would be difficult. An alternative and potentially universal strategy may involve activation of a different chloride channel in lung epithelium to bypass CFTR dysfunction. Toward that end, we recently demonstrated that the vWA domain of CLCA1 (calcium activated chloride channel regulator 1) directly engages the calcium activated chloride channel TMEM16A and stabilizes its surface expression on the order of minutes, thereby increasing anion currents through the channel. Further supporting a trafficking mechanism, we find that CLCA1 rescues TMEM16A from a late endosomal fate. We are currently pursuing a structural model of this interaction, which would be used to inform future design of therapies based on the CLCA1/TMEM16A interaction. We have made significant progress by determining the structure of the CLCA1 vWA domain to 2.05 Å, the first structure of any part of CLCA1. Since CLCA1 directly engages TMEM16A, we hypothesized that this molecular recognition could be utilized to specifically activate anion currents in airway epithelia through TMEM16A to compensate for dysfunctional CFTR channels. In whole cell patch clamp experiments, we demonstrate that CLCA1, and in particular its vWA domain, is able to activate TMEM16A currents in primary CF airway epithelial cells from three distinct CF genotypes ($\Delta F508/2789+5G>A$, $\Delta F508/\Delta F508$ and $\Delta F508/2184insA$). We furthermore show that purified vWA domain is able to sustain currents through TMEM16A in polarized CF airway epithelia of another genotype ($\Delta F508/621+1G>T$) in Ussing chamber studies. Together, these studies highlight the exciting potential for universal CF treatment modeled after the CLCA1 vWA domain/TMEM16A interaction, and future work will examine the ability of the interaction to restore healthy mucous properties.

2 Characterization and metabolic synthetic lethal testing in a new model of SDH-loss familial pheochromocytoma and paraganglioma

John A. Smestad

Mayo Clinic, Rochester, USA

Succinate dehydrogenase (SDH)-loss pheochromocytoma and paraganglioma (PPGL) are tumors driven by tricarboxylic acid (TCA) cycle metabolic derangement. Bi-allelic loss of function in SDH subunits leads to accumulation of intracellular succinate, which competitively inhibits dioxygenase enzymes, causing activation of pseudohypoxic signaling and hypermethylation of histones and DNA. The mechanisms by which these alterations lead to tumorigenesis are unclear, however. In an effort to fundamentally understand how SDH loss reprograms cell biology, we developed an immortalized mouse embryonic fibroblast cell line with conditional genetic disruption of *Sdhc* for use in systematic multi-omic studies to examine how this specific perturbation affects biology at multiple levels. We first validate the derived model by tracking the kinetics of *Sdhc* gene rearrangement, SDHC protein loss, and subsequent intracellular succinate accumulation. We then perform global transcriptomic, epigenomic, and proteomic characterization of changes resulting from SDHC loss, identifying specific perturbations at multiple biological levels. In the transcriptome, we observe strong activation of antiviral response genes, along with increased expression of extracellular matrix genes that has been reported previously for other SDH loss systems. Examination of DNA methylation patterns via reversed representation bisulfite sequencing reveals that observed transcriptomic perturbations are weakly correlated with altered patterns of gene promoter methylation, although the top gene ontologies affected by transcriptional perturbations were not reflected in gene ontology analysis of promoter differential methylation. At the CpG site level, two distinctive patterns of methylation change were observed: hypermethylation of loci with initially low methylation values, and hypomethylation of loci with initially high methylation values. This observation challenges the simple model of succinate-mediated inhibition of TET DNA demethylases resulting in global DNA hypermethylation. Global proteomic analysis reveals general down-regulation of components of the cytosolic ribosome, and variable up- and down-regulation of specific mitochondrial proteins. In particular, observed changes include up-regulation of mitochondrial solute transport, antioxidant defense, fatty acid catabolism, and fermentation pathways, and down-regulation of complex I. Finally, we perform analysis of SDHC synthetic lethality with lactate dehydrogenase A (LDHA) and pyruvate carboxylase (PCX), which are believed to be important for regeneration of NAD⁺ and aspartate biosynthesis, respectively. Our data show that SDH-loss cells are selectively vulnerable to LDH genetic knock-down or chemical inhibition, suggesting that LDH inhibition may be an effective therapeutic strategy for SDH-loss PPGL.

1 Characterization of external globus pallidus neurons from the Dbx1 lineage

Zachary A. Abecassis
Northwestern University, USA

Parkinson's disease (PD) is a prevalent neurodegenerative disease that affects the central nervous system. Early stages of the disease include symptoms of resting tremor, muscle rigidity, bradykinesia, and gait instability that often lead to other complications, such as dementia or depression. Dysfunction within the basal ganglia, particularly the external globus pallidus (GPe), has been implicated in the motor manifestations of the disease. The GPe most notably projects to other areas within the basal ganglia circuit, primarily the dorsal striatum and subthalamic nucleus (STN). Its communication with other areas of the brain, such as the cortex and thalamus, remains largely unknown. We recently identified a subtype of GPe neurons that originate from progenitor cells expressing the protein-coding gene developing brain homeobox 1 (Dbx1+) during embryologic development. Contrary to the majority of the GPe that originates from the medial and lateral ganglionic eminences, these neurons originate from the preoptic area. The objective of this study was to comprehensively profile these neurons to determine whether they possess any unique qualities as compared to the known subtypes of GPe neurons, i.e., parvalbumin- (PV) and Npas1 transcription factor-expressing neurons. By crossing a Dbx1-Cre transgenic mouse with a floxed-stop tdTomato (Ai14) mouse, we have been able to identify neurons originating from the Dbx1 lineage (Dbx1+) with tdTomato fluorescence. Immunohistochemistry was performed for known GPe proteins, and intrinsic cell properties were captured using cell-attached and whole-cell patch-clamp recordings. Finally, retrograde tracers (fluorogold and cholera toxin subunit B) were injected into various brain regions, including the subthalamic nucleus, cortex, and parafascicular nucleus of the thalamus (PF), in order to evaluate potential projection sites of Dbx1+ GPe neurons. Immunohistochemistry revealed that Dbx1+ GPe neurons constitute 10 percent of GPe neurons. These neurons were heavily PV+ (~62%), with some expressing Npas1 (~10%). Contrary to two-thirds of Npas1 neurons, the Npas1+ Dbx1+ neurons did not express Foxp2, a subset of Npas1 neurons known to project exclusively to the striatum. Electrophysiological analysis revealed that Dbx1+ GPe neurons appear to match the results seen in the immunohistochemistry, representing a subset of both PV+ and Npas1+ neurons. Retrograde tracing revealed projections to both the STN and PF. Electrophysiology and immunohistochemistry reveal that GPe neurons of Dbx1 lineage appear to be representative of the greater neuronal population of the GPe. However, the projection to the PF represents a novel projection site of these neurons, not seen by any other biomarkers within the GPe. Therefore, the unique origin of these neurons presents an opportunity to leverage this transgenic mouse to further explore this anatomical projection.

2 Single-cell analysis of NFkB signaling in primary macrophages

Adewunmi O. Adelaja
UCLA, Los Angeles, USA

Macrophages are the primary initiators and coordinators of immune responses. They exhibit highly heterogeneous phenotypes to regulate innate defense, initiation and coordination of adaptive immunity and tissue repair. These phenotypes are a function of the tissue microenvironment, determined by cytokines. Inflammatory responses in macrophages are dependent on the activity of the transcription factor NFkB, which is regulated by stimulus-induced degradation

of IkBs, which also provide negative feedback. Several studies of examined NFkB signaling by exogenous expression of a fluorescent NFkB fusion protein reporter in cell lines, but how NFkB signaling is controlled in primary macrophages and how polarizing cytokines may affect NFkB control remains unknown.

Using bone-marrow-derived macrophage (BMDMs) derived from RelA-Venus knockin mice, single cell analysis of NFkB signaling in macrophages revealed oscillatory dynamics in response to cytokine stimuli such as TNF and largely non-oscillatory dynamics response to Myd88-mediated pathogen ligands. This fundamental distinction between friend vs foe signaling contributed to a large mutual information score of more than 2.1 bits.

Interestingly, IFN γ -polarized macrophages, modeling those found in inflammatory lesions, showed a dramatically reduced capacity to distinguish TNF from PAMP ligands in terms of NFkB dynamics. Frequency-domain analysis revealed that IFN γ enhances non-oscillatory NFkB dynamics, thus diminishing the mutual information generated by TNF or PAMP stimulation.

We are currently examining the molecular mechanism by which IFN γ alters the NFkB-IkB signaling module to diminish its ability to distinguish friend- vs foe-like ligands.

3 Dietary protein load, stone type and stone procedures predict albuminuria in kidney stone formers

Omar Al Dhaybi
University of Chicago, Chicago, USA

There is evidence that kidney stones may cause chronic kidney disease (CKD), and kidney stone patients develop end stage renal failure at rates higher than the general population. However, we do not yet know what aspects of stone disease give rise to the well known association between having stones and losing kidney function. Urine albumin is an accepted biomarker for progressive CKD, that may become evident prior to loss of glomerular filtration rate (GFR) and might identify patients who are at risk for progression.

We measured urine albumin in 466 patients evaluated by the Kidney Stone Prevention Program at the University of Chicago since 2008. Each patient collects three 24 hour urines with a matching blood, off medications that affect mineral metabolism, which are analyzed for stone risk factors prior to the first clinic visit. Only urines testing negative for blood with a standard dipstick were used in this analysis. All patients gave consent for use of their data, and the protocol was approved by the Institutional Review Board. Data analyzed included laboratory and demographic data, stone analyses, history of stone events and procedures, past medical history, and number of stones on radiographs. Our aim in this study was to determine whether specific stone types or associated conditions, number of stone episodes, or procedures for stone removal were associated with pathologic albuminuria. We also explored the effect of the excretion rate of various urine analytes on albuminuria in separate analyses.

In our sample of 347 kidney stone formers, cystinuria (least squares mean albuminuria difference of 175 mg/g, $p=0.002$) and urinary sulfate were strongly correlated with pathologic albuminuria. Calcium phosphate and uric acid stones were not associated with worsening albuminuria. Albuminuria was not affected by the number of stone episodes, or none of the procedures performed, except percutaneous nephrolithotomies (least squares mean albuminuria increase by 193 mg/g in patients who underwent three or more procedures, $p=0.007$). Albuminuria was greatly amplified in CKD IV/V patients with high protein intake (least squares mean albuminuria increase by >1,000 for interaction of CKD IV/V – protein catabolic rate, $p=0.002$). This

effect was not seen in patients with CKD III. In a matched CKD cohort, the slope of sulfate's effect on albuminuria was even steeper.

Our study suggests that cystine stone formers have increased urine albumin excretion compared to other stone formers. Higher dietary protein loads are also significantly related to higher risk of albuminuria progression in kidney stone formers with advanced CKD.

4 Sulfasalazine as a treatment for acquired epilepsy

Oscar B. Alcoreza

Virginia Tech Carilion School of Medicine and Research Institute, USA

Epilepsy affects approximately 2.2 million Americans, with 150,000 new cases being diagnosed each year. Despite some success managing epilepsy, current therapeutics offer no benefit to 1-in-3 patients. Previous studies from our lab revealed that primary brain tumors release glutamate and induce electroencephalographic (EEG)-confirmed behavioral seizures in adult mice implanted with human-derived glioma cells. These studies identified increased expression of system xc (SXC), a cysteine/glutamate exchanger, on glioma cells as a major contributor to elevated glutamate levels in tumor-implanted mice. Inhibition of SXC via sulfasalazine (SAS), an FDA-approved anti-inflammatory drug, decreased glutamate release and EEG-confirmed behavioral seizures.

SXC is normally expressed on glial cells and gliosis is a prominent feature of many forms of epilepsy. Additionally, recent studies revealed that astroglial dysfunction, leading to pathological changes in the extracellular environment and neuronal metabolism, may play a critical role in the initiation of seizures and development of epilepsy. We therefore hypothesize that gliosis may cause an increase in SXC expression leading to enhanced glutamate release in acquired epilepsies and that treatment with SAS can decrease seizure occurrence in mouse models of epilepsy. To test this, we used the kainic acid (KA)-induced model of acquired epilepsy, which present with gliosis, to characterize changes in the expression of SXC. Our preliminary data reveal that animals treated with KA showed increase protein expression of SXC in the hippocampus and that treatment with SAS decreases the expression of SXC. Using the beta-1 integrin knockout mouse model, which is characterized by widespread chronic astroglial dysfunction and spontaneous seizures, our preliminary results suggest that treatment with SAS decreases EEG-confirmed behavioral seizures.

These results suggest that SXC may play a role in the pathogenesis of acquired epilepsies and that further studies on SXC and the effects of SAS is warranted as a potential novel therapeutic modality. As most treatments for epilepsy involves modifying neuronal excitatory or inhibitory mechanisms, SXC provides an unexplored glial target for decreasing glutamate release in acquired epilepsies.

5 Human PLCG2 Haploinsufficiency Results in NK Cell Immunodeficiency and Herpesvirus Susceptibility

Joshua Alinger

Washington University in St. Louis, St. Louis, USA

Natural Killer (NK) cells are innate cytotoxic lymphocytes critical for the control of DNA viruses. NK cell deficiency (NKD) is a poorly understood disorder that results in severe or recurrent infections with Herpesviruses such as Herpes Simplex Virus 1 (HSV1) and Cytomegalovirus (CMV). However, the genetic causes of disease are unknown in most NKD patients. Herein, we investigate three patients from two kindreds presenting with severe or recurrent Herpesvirus infections and NKD using mass cytometry (CyTOF) and whole exome sequencing. Kindred A consisted of two patients

presenting with HSV1 susceptibility and autoimmunity. Kindred B consisted of one patient with severe CMV myocarditis and adenoviral hepatitis. Both kindreds were evaluated for NK cell function and showed reductions in target killing in spite of normal cytotoxic granule degranulation against the same target. Microscopy analysis suggested that granule mobility was reduced in at least one kindred. CyTOF revealed reductions in PLCG2 phosphorylation after receptor crosslinking in the NK cells of both kindreds. Kindred A also presented with a reduction in naïve B cells without perturbations in immunoglobulin output, B cell memory formation or class switching. Trio whole exome sequencing was performed and revealed rare heterozygous *PLCG2* mutations in both kindreds. Functional analysis, as well as mouse and CRISPR models, support a functional haploinsufficiency as a cause for NKD in these patients. Heterozygous loss-of-function point mutations in *PLCG2* have not been previously investigated as a cause of NK cell deficiency or recurrent Herpesvirus infection. Thus, these patients represent a novel immunodeficiency involving *PLCG2* haploinsufficiency, NK cell dysfunction, and Herpesvirus susceptibility.

6 Characterization of the heterogeneity in 5-aminolevulinic acid-induced fluorescence in GBM

Damian A. Almiron Bonnin

Geisel School of Medicine, Lebanon, USA

5-Aminolevulinic acid (5-ALA)-induced fluorescence is an innovative and effective surgical approach for the intraoperative identification of tumor tissue for resection. Fluorescence-guided neurosurgery using 5-ALA has recently been shown to improve glioblastoma (GBM) resection and, consequently, prolong survival in GBM, which is the most common and most aggressive primary brain tumor of adults. The effectiveness of this approach in GBM, however, has been compromised by the heterogeneity of 5-ALA-induced fluorescence observed during surgery. While some regions within GBM readily fluoresce after 5-ALA administration, other regions of the tumor, which are histologically indistinguishable from the fluorescent tissues, do not.

To understand this heterogeneity in 5-ALA-induced fluorescence, we collected both fluorescent and non-fluorescent GBM specimens from a total of fourteen surgical patients and examined their gene expression profiles. We examined approximately fifty thousand different genes in each specimen and found that fluorescent and non-fluorescent GBM tissues were characterized by distinct gene expression signatures. While non-fluorescent tumor tissue tended to resemble the neural subtype of GBM, fluorescent tumor tissue did not exhibit a prominent pattern corresponding to known subtypes of GBM. Consistent with this observation, neural GBM samples from the Cancer Genome Atlas database exhibited a significantly lower fluorescence score than non-neural GBM samples as determined by our fluorescence signature. We also discovered that non-fluorescent GBM tissue expressed a pattern of genes suggestive of high phospho-myo-inositol pathway activity. In our preliminary studies, treating GBM-derived cell lines with valproic acid, a well-known inhibitor of myo-inositol synthesis, significantly increased 5-ALA-induced tumor cell fluorescence. These findings characterize the molecular differences between fluorescent and non-fluorescent GBM tissues during fluorescence-guided surgery with 5-ALA, and they provide a rationale for the evaluation of myo-inositol synthesis inhibitors such as valproic acid in fluorescence-guided surgery with 5-ALA.

7 Alcohol Use Disorder Symptomatology is Related to Disrupted Reward Neuro-circuitry Responsiveness in Adolescents

Joseph Aloï

University of Nebraska Medical Center, Boys Town, USA

In 2014, 8.1% of adults in the US were diagnosed with a substance use disorder, including alcohol use disorder (AUD) and/or cannabis use disorder (CUD). Alcohol and/or cannabis use during adolescence is associated with increased risk of developing AUD and/or CUD during adulthood. Animal and neuroimaging studies have shown that AUD and CUD are related to dysfunction in reward processing neuro-circuitries. However, very few studies to date have examined differential effects of AUD versus CUD on reward processing in adolescents. This preliminary study uses a Monetary Incentive Delay (MID) task to investigate reward neurocircuitry dysfunction during reward outcomes in adolescents with a history of AUD and/or CUD symptomatology. One-hundred fifty youths aged 14-18 years recruited from a residential treatment facility and the surrounding community completed a MID task during functional magnetic resonance imaging (fMRI) scanning. The average age of participants was 16.1 (SD=1.08) and the average IQ was 100.5 (SD=12.29). AUD and CUD symptomatology was assessed using the Alcohol Use Disorder Identification Test (AUDIT) and the Cannabis Use Disorder Identification Test (CUDIT). The average score on the AUDIT was 4.0 (SD=6.77) and the average score on the CUDIT was 7.31 (SD=9.37). There was a negative relationship between AUDIT scores and BOLD response modulated by reward value in bilateral ventral striatum (r^2 's=-.330--.345, p 's<.001). However, there was no relationship between CUDIT scores and BOLD response modulated by reward value in the ventral striatum. These data suggest that impaired functioning of reward processing neuro-circuitry in adolescents is related to AUD symptomatology, but not CUD symptomatology. Future work should examine whether these altered neural responses are risk factors for, or outcomes of, AUD in adolescents. Additionally, since AUD and/or CUD in adolescents are often comorbid with Attention Deficit/Hyperactivity Disorder and/or Disruptive Behavior Disorders, future work should examine the neural relationships between these disorders and AUD and/or CUD symptomatology.

8 The congenital heart disease candidate gene myelin regulatory factor plays an unexpected role in left right patterning

Sarah K. Amalraj

Yale University School of Medicine, USA

Congenital heart disease (CHD) is the most common major birth defect, affecting nearly 3% of children. Although the causes of CHD are not well understood, abnormalities in left-right (LR) patterning (known as heterotaxy [Htx]) are associated with severe forms of CHD. A recent analysis of Htx/CHD patients identified numerous candidate genes, including the gene myelin regulatory factor (MYRF). The protein MYRF is known to be a transcription factor for the generation of myelin in the central nervous system during development; however, its role in LR patterning and heart development is undefined. Here, we show that depletion of myrf using CRISPR-based gene modification in *Xenopus tropicalis* causes midline heart looping defects phenocopying our patient. We then analyzed the LR patterning markers *pitx2* and *coco* and found abnormal bilateral expression of *pitx2*, but normal expression of *coco* in myrf-depleted embryos. Additionally, we depleted myrf in one cell of a two-cell embryo and found that left-sided injected embryos resulted in heart looping defects, abnormal bilateral *pitx2*

expression, and normal *coco* expression. Conversely, right-sided injected embryos had no LR patterning defects. Together, our data suggests MYRF plays a role in LR patterning, possibly by acting as a midline protein regulating transcription of nodal gene *xnr1*, as nodal signaling occurs between *coco* and *pitx2* expression in the LR patterning cascade. We conclude that patient-driven gene discovery from patients with congenital heart disease can provide new insights into the molecular mechanisms that drive cardiac patterning and LR axis formation.

9 IL-33/T regulatory cell axis triggers development of a cancer-promoting immune environment in chronic inflammation

Amir H. Ameri

Massachusetts General Hospital, Harvard Medical School, USA

Chronic inflammation is a well-characterized driver of cancer in the skin and other epithelial organs; however, the mechanism underlying the development of cancer-promoting chronic inflammation is unknown. We previously showed that chronic allergic contact dermatitis (ACD) is a type 2 inflammatory disease and potent inducer of squamous cell carcinoma in mice and humans. In contrast, acute ACD, a common skin inflammatory condition, is marked by type 1 inflammation, including T helper 1, cytotoxic T, and NK cells, which inhibit cancer development. The opposite effects of chronic versus acute ACD on cancer provide a unique paradigm to investigate how cancer-promoting chronic inflammation develops. To determine the mechanism underlying the transition from acute to chronic ACD, we examined the epithelium-derived cytokines IL-33, TSLP, and IL-25, which are master drivers of type 2 inflammation in barrier organs. IL-33 expression markedly increased during the transition from acute to chronic ACD, initiating tumor-promoting, type 2 inflammation in chronic ACD. Mice lacking IL-33 or IL-33 receptor (ST2) were protected from ACD-induced skin cancer compared with wild-type controls, and IL-33 was required for the progression of inflammatory bowel disease-induced colorectal cancer. Notably, IL-33's direct effect on T regulatory cells was required for the development of a cancer-promoting immune environment in the skin and colon. Our findings elucidate a mechanism underlying the formation of a tumor-initiating immune environment in chronic inflammatory diseases and yield novel targets for cancer treatment and prevention in chronic inflammatory contexts.

10 Personal neoantigen vaccine for glioblastoma stimulates neoepitope-specific intratumoral T cell responses

Annabelle J. Anandappa

Dana-Farber Cancer Institute, USA

Recent studies have demonstrated that therapies targeting neoantigens can elicit effective antitumor immunity. These antigens arise from somatic tumor mutations, and are attractive targets for immunotherapy given their exquisite tumor specificity and exemption from central tolerance. Personalized neoantigen vaccines have been shown to be feasible, safe, and immunogenic in highly mutated cancers, such as melanoma, but have not been tested in tumors with lower mutation rate.

A phase I/II trial of personal neoantigen vaccines for glioblastoma (GBM), a tumor with ten-fold-lower mutation burden than melanoma, was conducted. Following standard-of-care surgery and radiation, eight patients received vaccine consisting of up to 20 synthetic long peptides (median 12, range 7-20) that encode predicted neoepitopes, and poly-ICLC adjuvant. Changes in the tumor microenvironment were assessed in post-vaccination surgical resection specimens from five patients. Vaccination induced de novo circulating

polyfunctional neoantigen-specific CD4+ and CD8+ T cell responses and increased tumor-infiltrating lymphocytes (TILs) in two patients who did not receive dexamethasone during vaccine priming. In these patients, infiltrating CD8+ T cells increased significantly from a baseline of 28.9 to 100.4 cells/mm² (P = 0.006) after vaccination, with a significant increase in the CD8+PD-1+ subset. In contrast, all three patients who received dexamethasone during vaccine priming failed to generate circulating immune responses, with no significant change in T cell infiltrate.

We hypothesized that post-vaccination TILs were specific for immunizing neoantigens. Single-cell T cell receptor (TCR) analysis of CD3+ TILs and peripheral T cells in vitro expanded against immunizing peptides was performed from one patient with circulating neoantigen-specific T cells. Four CD4+ and two CD8+ T cell clonotypes in peripheral blood were identical to TILs. In order to probe their specificity, we applied a pipeline developed in our laboratory to clone and express TCR sequences of interest and screen them against candidate antigens. We identified a TCR shared in CD4+ T cells in peripheral blood and TILs specific for ARHGAP35, a neoantigen targeted by vaccination, and capable of discriminating between the mutant and wild-type peptide. The intratumoral TCR repertoire was probed further using an algorithm called grouping of lymphocyte interactions by paratope hotspots (GLIPH) to cluster TCRs by similarity. Representative TCRs from each cluster are being tested for neoantigen specificity and reactivity against autologous tumor.

Our observations demonstrate that neoantigen vaccines favorably alter the immune milieu of GBM and that neoepitope-specific T cells can traffic from the periphery into intracranial tumors. These results are particularly promising in a tumor with relatively low mutation burden and low immune infiltrates at baseline. However, there remain significant immunosuppressive factors to overcome for neoantigen-specific T cells to generate clinically significant antitumor activity. We anticipate that combination therapy with checkpoint blockade may be more effective in augmenting antitumor immunity and improving outcomes to therapy.

II Characterization of a polymorphic region of MSH3, a mismatch repair protein associated with colorectal cancer

Bianca Arao

University of California Davis, Davis, USA

Elevated Microsatellite Alterations at Selected Tetranucleotide repeats (EMAST) is a genetic signature associated with cancer metastasis and recurrence in colorectal cancers. It is caused by a deficiency in MSH3, a DNA mismatch repair (MMR) protein that contains a *bona fide* nuclear localization signal (NLS) and two nuclear export signals (NESs). The NLS and NESs allow for MSH3 shuttling between the nucleus and the cytosol under cellular stress. The pro-inflammatory cytokine Interleukin-6 (IL-6) alters MSH3 localization, causing defects in DNA mismatch repair. Shuttling of MSH3 appears to be affected by a polymorphism near the NLS that contains a deletion of 27 base pairs (MSH3Δ27bp), which increases the cytosolic presence of MSH3, thereby increasing EMAST. Our aim is to explore how specific sequences within the Δ27bp polymorphism affect MSH3 shuttling function. The polymorphic region has a poly-alanine tract (Poly-Ala) and a Proline-rich domain (Pro). We hypothesize that Poly-Ala and Pro regions are critical in regulating the NLS function and that they have different roles in this regulation. If this hypothesis is true, we predict that deletions in the peri-NLS region of MSH3 will lead to differences in localization of MSH3. To begin to test this prediction, we successfully generated reporter

constructs of the peri-NLS MSH3 region expressing three different deletions (ΔA₁₂, ΔPro, ΔPolyA) by PCR mutagenesis and molecular cloning. Continuing studies will examine the subcellular location of MSH3 for each construct, evaluated through immunofluorescence microscopy (IFM), using an MSH3-antibody in cells with and without IL-6 treatment. This approach may provide important details about the mechanisms of MSH3 shuttling, with potential implications for prevention and treatment of EMAST-associated colorectal cancer in patients.

I2 Circulating exosomal microRNA as a non-invasive biomarker for pediatric medulloblastoma

Sydney N. Ariagno

Weill Cornell Medicine, USA

Medulloblastoma (MB) is the most common malignant pediatric brain tumor, and over one-third of children with this cerebellar tumor die within five years of diagnosis. Clinicians are currently limited in their abilities to diagnose this tumor without surgical biopsy and identify metastatic or recurrent disease at early stages. The development of a noninvasive biomarker could help address these problems. Exosomes are microvesicles that are secreted from tumors constitutively and contain cell type-specific proteins and genetic material, including microRNAs (miRs). In addition, exosomes are easily isolated from plasma and provide an unexplored reserve for noninvasive biomarkers.

Using a sporadic Sonic Hedgehog (SHH)-driven mouse model of MB, we assessed exosomal profiles from tumor tissue explant cultures and plasma at early and late tumor stages. Exosomes from cerebellar tissue explants and plasma were similarly collected from age-matched control mice. Tissue explants were cultured for 24 hours in exosome-depleted media. Conditioned media from explants and plasma samples then underwent differential ultracentrifugation to isolate exosomes, and exosomal protein amount was quantified. Tissue- and plasma-derived exosomes then underwent miR sequencing. Exosomal protein amount and miR expression were compared between early-stage preneoplastic and late tumor stages, as well as between tissue and plasma samples at each stage.

We found that exosomal protein abundance from late-stage tumor tissue was significantly higher than early-stage preneoplastic tissue (0.246 vs. 0.114 μg/mg, ****P < 0.0001) after normalization for explant brain weight. Additionally, exosomal protein amount from late-stage tumor tissue was significantly higher than that of late-stage control cerebellum (0.246 vs. 0.126 μg/mg, ****P < 0.0001). A similar trend was seen with exosomal plasma samples, although statistical significance was not reached (0.04 vs. 0.0207 μg/mg, P = 0.232; 0.039 vs. 0.025 μg/mg, P = 0.136). With regard to tumor exosomal content, miR sequencing revealed the presence of the miR-17~92 cluster which is specifically associated with the human SHH-driven MB subtype. qPCR validation of miR expression in circulating exosomes confirmed that miR-17, -19b, -20a, and -92 (all members of the 17~92 cluster) were approximately twice as prevalent in exosomes from tumor mice as compared with control mice.

In conclusion, our data suggest that tumor exosomes may be a potential noninvasive biomarker for monitoring disease status in children with MB. Tumor tissue explant and plasma exosomal protein amount in our SHH-MB mouse model correlates with tumor stage. Exosomal miR sequencing shows upregulation of components of the miR-17~92 cluster that are specific for the SHH MB subgroup. Additional studies will be needed to validate these preclinical findings in human MB tissue and plasma samples.

13 An Unusual Etiology For Acute Fulminant Liver Failure

C. Edmond Awah

University of Illinois at Chicago, Urbana Campus, Champaign, USA

Introduction: Acute fulminant liver failure is a life-threatening condition characterized by elevated transaminases and prothrombin time/international normalized ratio (INR). The poor prognosis necessitates treatment in an intensive care unit capable of performing liver transplants. Wide ranges of etiologies from congenital to infections have been reported in the literature. Acute fulminant liver failure typically presents secondary to shock liver, acute hepatitis, and Tylenol toxicity. We present a case of a young female who presented with an unusual etiology for acute fulminant liver failure. Clinical Case Summary: A 29-year-old female with a history of non-ischemic heart failure secondary to methamphetamine abuse and COPD presented to an outside hospital with 5 days of emesis and diarrhea. Emesis is non-bloody and non-bilious. Stools are loose with no frank blood. She reports right upper quadrant abdominal pain, moderate in intensity, non-radiating, and no aggravating or relieving factors. She also reported worsening shortness of breath with orthopnea and paroxysmal nocturnal dyspnea. Urine drug screen was positive for amphetamines. She was tachycardiac on presentation with a heart rate of 117/minute and a blood pressure of 110/66. Physical exam showed icteric sclera, jugular venous distention, right upper quadrant tenderness, and hepatomegaly 2 cm below costal margin. Comprehensive metabolic panel showed an aspartate aminotransferase (AST) 939 U/L, alanine aminotransferase (ALT) 999 U/L, and INR 1.7. Right upper quadrant ultrasound showed non-homogenous hepatomegaly, pulsatile portal vein flow, and right pleural effusion. Breathing improved with diuresis but liver enzymes continued to rise with AST 1965 U/L and ALT 1718 U/L. Arterial blood gases revealed hypoxia and metabolic acidosis with respiratory compensation. Subsequent liver function tests showed no improvement and INR increased to 2.0. Patient was transferred to tertiary transplant facility for acute fulminant liver failure. Discussion: Basic science research in the animal model showing methamphetamine-induced acute liver injury has been well documented. No case reports have been published showing this relationship. Hyperthermia is the predominant mechanism causing liver injury. Researchers measured transaminase levels of rats receiving saline, methamphetamine, and methamphetamine with environmental cooling. The most notable results showed a significant increase in the ALT of rats receiving methamphetamine versus saline control and no significant difference in the ALT of rats receiving methamphetamine with environmental cooling versus saline control. Conclusion: It is important for clinicians to be aware of the range of sequela from methamphetamine abuse and to provide appropriate counseling recommendations as well as detoxification programs for these patients.

14 Targeting heat shock protein 90 to alter evolution of aggressive cancer phenotypes

Nickolas Bacon

Marshall University Joan C. Edwards School of Medicine, Huntington, USA

The evolution of aggressive cancer phenotypes remains a significant challenge in cancer medicine, as they oftentimes become the source of chemotherapeutic resistance, relapse, and metastasis in a patient. Therefore, significant clinical benefit may arise by refocusing cancer treatment on limiting the emergence of these phenotypes. Heat shock protein 90 (HSP90) is a chaperone protein whose function is evolutionarily well conserved and plays

a unique role in modulating phenotypic traits. In cancers, HSP90 gene expression is frequently up regulated and has been linked to a poor overall prognosis. Additionally, HSP90's role in supporting protein function and stability in almost every hallmark of cancer makes it a lucrative therapeutic target to effectively shut down multiple oncogenic signaling networks simultaneously. We focus our investigation on the effect of clinically relevant HSP90 inhibitors on the emergence of aggressive cancer phenotypes as they undergo epithelial-to-mesenchymal transition (EMT) in vitro. We subject A549 lung cancer cells to multiple rounds of HSP90 inhibition, provide a rest and recovery period, and induce EMT via transforming growth factor-beta (TGF- β) treatment. We use flow cytometry to compare changes in distribution of classic EMT markers, cancer stem cell markers, and multidrug resistant transporters between our treated and untreated samples. Significant changes are seen at treatment levels far below clinically recommended doses. This work may shed light on mechanisms associated with the development of aggressive cancer traits as well as generate a discussion on strategic use of HSP90 inhibitors to target cancer evolution.

15 The Kcnq1ot1 Long Non-Coding RNA Regulates Genetic Imprinting Within a Defined 3-Dimensional Chromatin Structure

Abhik Banerjee

University of Southern California and California Institute of Technology, South Pasadena, USA

Genomic imprinting provides an excellent model to understand mechanisms responsible for cis gene regulation, including chromatin insulation, enhancer looping interactions, and long non-coding RNA (lncRNA) function. The Kcnq1ot1 lncRNA is expressed in antisense orientation to Kcnq1 protein coding gene and is responsible for paternal imprinting of a conserved one megabase domain in mouse and human. Disruption of imprinting in this cluster results in an overgrowth disorder called Beckwith-Wiedemann Syndrome. Despite previous studies investigating the regulation and function of the lncRNA itself, little is known regarding its mechanism of silencing or how the lncRNA is able to distinguish between target and non-target genes in cis. In order to answer these questions, we have developed a Kcnq1ot1 doxycycline-inducible mouse embryonic stem cell line. Using this system, we demonstrate that induction of Kcnq1ot1 lncRNA is sufficient to silence endogenous target genes and that the lncRNA primarily localizes to its imprinting targets within a defined topological-associated domain. Based on these results, we hypothesize that Kcnq1ot1 lncRNA scaffolds regulatory factors within a defined 3-dimensional chromatin structure to coordinately silence target genes in cis.

16 Controlled Manipulation of Protein Phosphorylation and Cell Regeneration with Light-Responsive DNA Aptamer Reactions

Ameer S. Basta

University of Florida, Gainesville, USA

Most cells in the human body respond to growth hormone, which binds to cell surface receptors and induces growth and replication for those cells. Our study is focusing on receptor tyrosine kinase (RTK), a cell receptor of growth hormone that phosphorylates downstream proteins inside the cells, leading changes in certain protein expression level that allows for cell growth and replication. Utilizing this pathway has become one of the most popular fields in regenerative therapy, however, uncontrollable cell growth would be oncogenic. In our project, we design the DNA reactions to realize light-responsive switch between the activation/deactivation of the RTK-participated signal pathway.

The activation of RTK pathway requires the close proximity of the two receptor subunits when bound with the growth factor, which would be achieved by using the DNA aptamers of the RTK protein and the formation of the double-stranded structure. The introduction of the PC-linker would allow the feasible cleavage in the DNA structure, causing the disassembly of the receptor pair. The reaction was monitored with FRET and gel-electrophoresis in solution, and flow cytometry on the cell membrane. The phosphorylation of the proteins would be analyzed with western-blotting and other cellular experiments. This design would offer a feasible, fast, and simple platform for controllable cell regeneration.

17 Interplay between the EWS-portion of EWS/FLI and length of GGAA-microsatellite binding elements defines transcriptional activation function in Ewing sarcoma

Ariunaa Bayanjargal

The Ohio State University, Columbus, USA

Ewing sarcoma is an aggressive bone-associated tumor first described by James Ewing in 1921. Most cases contain a translocation between chromosomes 11 and 22 that fuses two genes, EWSR1 and FLI1, creating a potent oncogenic transcription factor: EWS/FLI. EWS/FLI regulates thousands through the coordinated functions of transcriptional activation, via its EWS portion, and DNA binding, via its FLI portion. Many of its target genes are regulated through binding of EWS/FLI to GGAA-microsatellite sequences containing multiple consecutive GGAA repeats. Prior data suggested a relationship between the length of the GGAA-microsatellite and EWS/FLI-mediated transcriptional activity, and other data suggested that the length of EWS-sequence present in the fusion is also important. We therefore hypothesized that the transcriptional activation from GGAA microsatellites is defined by an interplay between the length of the microsatellite and amount of EWS sequence present.

To test this hypothesis, we analyzed engineered mutants of EWS/FLI, containing point mutations and/or deletions in the EWS portion, to activate a luciferase reporter gene linked to GGAA-microsatellites of various lengths cloned upstream of a minimal SV40 promoter. We found that full length EWS/FLI was the most potent activator and demonstrated maximal activity from GGAA-microsatellites of 20-30 GGAA repeats. EWS/FLI mutants with EWS-deletions required a greater number of GGAA repeats in the microsatellites to achieve their peak activities. The full length EWS/FLI construct containing point mutations in key residues showed a 4-fold decrease in activity compared to wild-type EWS/FLI.

These results suggest that the microsatellite mediated activation of genes by EWS/FLI may result from the interplay of the number of GGAA repeats and the sequence length and composition of the EWS portion of EWS/FLI. Studies are being conducted to quantify the binding affinities of these constructs to different lengths of GGAA microsatellites to further elucidate the role of the EWS portion in microsatellite mediated transcriptional activation by EWS/FLI. The current study is a crucial in understanding the role(s) of EWS in the binding characteristic of EWS/FLI to the GGAA microsatellites, and help unearth important biochemical properties of EWS/FLI that contribute to its oncogenic characteristics.

18 Medical Student and Physician Knowledge and Attitudes Towards the Patient Protection and Affordable Care Act

Evan Berger

New York Institute of Technology College of Osteopathic Medicine, New York, USA

Phenomenon: It is important to examine the US healthcare workforce's attitudes and knowledge about the Patient Protection and Affordable Care Act (PPACA), as they communicate details about this act with patients. Understanding the views of medical students is particularly crucial as they are the future of the healthcare workforce. Additionally, it is important to assess whether these views change as individuals go into clinical practice. This study sought to investigate the attitudes and knowledge that medical students and faculty possess about the United States healthcare system and the PPACA, and whether there are differences between the two groups.

Approach: A 42 item survey was developed after review of health policy literature and administered to medical students and faculty of the New York Institute of Technology College of Osteopathic Medicine.

Findings: Very few students (n=2, 5.41%) and practicing physicians (n=4, 9.30%) supported the current healthcare system. 24.32% (n=9) of students supported repeal of the PPACA and 37.21% (n=16) of practicing physicians shared this view. These differences were not statistically significant. 40.54% (n=15) of students and 32.56% (n=14) of practicing physicians believed the PPACA will improve health care quality. 72.97% (n=27) of students and 51.16% (n=22) of practicing physicians believed the PPACA will expand access. These differences were statistically significant.

Insights: Students and physicians differ in their support of the PPACA and in their knowledge about the act. This study highlights the need to educate students about health policy issues in the medical school curriculum and physicians at the CME level.

19 ITIM-Dependent Functions of a Major Histocompatibility Complex Class I-Specific Ly49 Receptor on Natural Killer Cells

Michael D. Bern

Washington University in St. Louis, St. Louis, USA

Natural killer (NK) cells are cytotoxic innate immune cells that express MHC class I (MHC-I)-specific inhibitory receptors, such as murine Ly49A, that prevent killing of healthy cells that express self-MHC-I. Interactions between inhibitory Ly49s and their self-MHC-I ligands also "license" NK cells to become functionally competent and regulate the expression of inhibitory NK cell receptors. Due to the lack of mice with targeted mutations in inhibitory Ly49s, however, the in vivo functions and mechanisms of action of self-MHC-I-specific NK cell receptors have been challenging to investigate. In this study, we developed a mouse with an inactivating mutation in the immunoreceptor tyrosine-based inhibitory motif (ITIM) of Ly49A. This mutation impaired NK cell effector inhibition by Ly49A and rendered Ly49A-expressing NK cells hyporesponsive to stimulation in the presence of its self-MHC-I ligand. NK cells from this mutant mouse also expressed an altered repertoire of inhibitory receptors. These results show that inhibitory receptor signaling controls NK cell self-tolerance through multiple mechanisms.

20 The DYRK1A pathway illustrates a paradoxical program in normal versus malignant lymphopoiesis

Rahul S. Bhansali

Northwestern University, USA

Dual specificity tyrosine-phosphorylation-regulated kinase 1A (DYRK1A) is a serine/threonine (S/T) kinase that regulates diverse pathways such as splicing, cell cycle, differentiation, apoptosis, and transcription. DYRK1A is encoded within the Down syndrome (DS) critical region of chromosome 21, underlying its importance in DS-related pathologies, such as Alzheimer's disease. Children with DS have an increased risk of developing hematologic malignancies, namely acute megakaryoblastic leukemia (AMKL) and acute lymphoblastic leukemia (ALL). We previously reported that DYRK1A is necessary for normal lymphopoiesis through phosphorylation and destabilization of cyclin D3. Dyrk1a-deficient lymphocytes are unable to exit the cell cycle; however, these cells also lose proliferative capacity due to a block at the G2-M transition.

Given the critical role of DYRK1A in lymphopoiesis, we aimed to seek whether DYRK1A is a suitable target in ALL. We first generated murine models of ALL in pan-hematopoietic Dyrk1a conditional knockout mice. Excision of Dyrk1a in leukemic mice increased survival after transplant nearly three-fold. Next, in order to determine viability of targeting DYRK1A, we treated ALL cell lines with EHT1610, a potent and selective DYRK1-specific inhibitor. EHT1610 sensitivity was observed in ALL cell lines harboring various oncogenic mutations, including those associated with both non-DS and DS-ALL. We also found that 50% (9 of 18) of primary ALL samples were sensitive to EHT1610 treatment *in vitro*, with 75% (6 of 8) of the DS-ALL samples displaying sensitivity. Of note, the observed induction of cycling also conferred increased sensitivity to traditional cytotoxic drugs, such as cytarabine. Furthermore, we saw a marked decrease in leukemic burden in ALL-PDX models after treatment with EHT1610, indicating that DYRK1A is a target in ALL.

Last, we performed global and directed phosphoproteomic studies to determine DYRK1A substrates in pre-B cells. Loss of DYRK1A activity in pre-B cells leads to changes in phosphorylation of substrates that regulate cell cycle, splicing, and RNA metabolism. One of the identified targets is serine 329 of FOXO1, a proapoptotic transcription factor that is critical in B lymphopoiesis and negatively regulated by PI3K/Akt signaling. Using a green fluorescent protein-tagged FOXO1, we found that treatment of large pre-B cells with EHT1610 shifted FOXO1 localization from the cytoplasm to the nucleus, where it is active despite intact PI3K/Akt signaling. Moreover, treatment of pre-B cells with EHT1610 and AS1842856, an inhibitor of activated FOXO1, rescued the G2-M blockade. Paradoxically, despite its tumor suppressor role in normal lymphocytes, ALL cell lines are very sensitive to FOXO1 inhibition, suggesting a unique requirement for its role in the survival of ALL cells. In all, these studies indicate that DYRK1A is an effective target in ALL through a loss of proliferative capacity, sensitization to commonly used cytotoxic drugs by induction of cycling, and dysregulation of substrates that are key to lymphocyte survival.

21 Characterization of novel photosensitizers based upon the Janelia Fluor rhodamine scaffold

Thomas C. Binns

Howard Hughes Medical Institute, Janelia Research Campus, USA

Photosensitizing agents are excited by electromagnetic radiation, typically in the form of visible or ultraviolet light, and subsequently generate free radicals via the transfer of energy to adjacent

molecules. Photosensitizers see broad use in the basic sciences through techniques such as targeted cell ablation and chromophore-assisted light inactivation of specific proteins; as well as in the clinic through applications including photodynamic therapy for the treatment of cancers and inactivation of pathogenic microbes. This study describes the characterization of photosensitizing agents based upon HaloTag ligand variants of the Janelia Fluor scaffold using two approaches — halogenation and substitution of the central xanthene oxygen with a sulfur. The resulting candidate molecules are compared for singlet oxygen generation potency, HaloTag binding kinetics, and photosensitization availability due to the lactone-zwitterion equilibrium typical of rhodamine dyes. Experiments in their use for the manipulation of biological systems are currently underway. This study provides the characterization of several new photosensitizing agents for use in the biomedical sciences and compares two canonical approaches to photosensitizer development, highlighting potential pitfalls of each in the context of compatibility with self-labeling enzyme tagging systems such as HaloTag.

22 A model for the analysis of schizophrenia as a disease of brain connectivity

Daniel Biro

Albert Einstein College of Medicine, Bronx, USA

Schizophrenia is a remarkably complex neuropsychiatric disease with complex etiology that is one of the leading causes of disease related disability in the United States and worldwide. The mechanistic causes and effects across multiple levels of biological hierarchy are poorly understood, although progress has been made in recent years. One level of examination which holds significant promise is that of the brain network connectivity. Broadly speaking, brain connectivity approaches utilize tools such as functional magnetic resonance imaging and electroencephalography to measure the interactions between large and meso-scale brain regions. These approaches have been combined with computational models and graph theoretic concepts such as network structure in order to examine how changes in both physical and functional connections can be correlated to the clinical changes seen in schizophrenic patients. We put forward a simple model of brain connectivity and function where a neural network is trained to solve input-output tasks, and then the network is "broken" in a manner consistent seen with the connectivity changes in schizophrenia. We then analyze the patterns in which the neural network fails, and show parallels to the failure of information processing seen in schizophrenic patients. Analogies can be drawn to the inability of schizophrenic individuals to process pertinent information in the same way as healthy individuals.

23 p53 And Your Heart: Role in the Mitochondrial Permeability Transition

Alan Blayney

SUNY Upstate, Syracuse, USA

Recent evidence from animal- and cell-based studies has demonstrated that the p53 tumor suppressor plays a fundamental role in triggering the mitochondrial permeability transition (mPT), leading to necrotic and apoptotic cell death in response to several noxious stimuli. In particular, mPT is thought to result from the surge of reactive oxygen species (ROS) that are generated during the ischaemia-reperfusion injury of myocardial infarction (MI) and cerebrovascular accidents (CVA). The mPT pore complex (mPTP) is famously mysterious in its composition, but it is known to be regulated by cyclophilin D (CypD), a mitochondrial matrix cis-trans proline isomerase, and this has been proposed to be p53's

intramitochondrial target. We have begun preliminary studies to characterize the proposed interaction between p53 and CypD. We have measured direct binding between p53 and CypD with micromolar affinity using fluorescence polarization anisotropy (FP), and investigated the impact of known cyclophilin inhibitor cyclosporine A. We have begun further structural and functional studies using NMR, FP, and analytical ultracentrifugation to identify the binding sites on both proteins, which we propose to be a new target for pharmaceutical therapy to reduce injury post-MI and -CVA.

24 Characteristics of Patients Diagnosed with Catastrophic Cutaneous Carcinomatosis

Nicole Bolick

The Brody School of Medicine at East Carolina University, Greenville, USA

Catastrophic Cutaneous Carcinomatosis (CCC) is a dermatologic condition in which a non-organ transplant patient is diagnosed with 10 or more non-melanoma skin cancers in a one-year period. We identified patients from a large skin cancer data base who had been diagnosed with at least 10 non-melanoma skin cancers in one year. We looked at characteristics of these patients and if they could be diagnosed with CCC.

We performed a retrospective chart review at the Brody School of Medicine of dermatology patients with 10 or more cases of non-melanoma skin cancer in a one-year period to identify characteristics of these patients.

Brody School of Medicine's EHR and paper charts were used to review patients diagnosed with 10 or more cases of basal cell carcinomas and/or squamous cell carcinomas in a one-year period. The characteristics of the 37 patients eligible for the study were compiled and analyzed to determine correlations. One patient's chart was unable to be located.

Of the 37 patients eligible for the study all were Caucasian with 78% of our patients being males. Approximately half (41%) of our patients were immunosuppressed. Hypertension was common with 70% of our patients having high blood pressure. Eight patients diagnosed with diabetes had a comorbidity of hypertension as well. Twenty-one of 37 patients (57%) were deceased. Of the patients who were deceased five (24%) died due to skin cancer. Patients who were immunosuppressed were younger at the onset of their first skin cancer by 15 years. This was a statistically significant difference. There was also a statistically significant difference in the number of basal cell carcinomas; immunocompetent patients had more basal cell carcinomas than immunocompromised patients. Patients who were immunosuppressed showed a greater number of squamous cell carcinomas, however this data was not statistically significant.

The data shows that the majority of patients diagnosed with Catastrophic Cutaneous Carcinomatosis will be Caucasian and male. Many CCC patients will have a comorbidity of hypertension. Differences in the rates of squamous cell carcinomas and basal cell carcinomas exist between patients who are immunosuppressed and immunocompetent. Patients with multiple skin cancers suffer significant morbidity and many die from their disease. Management requires a coordinated multispecialty approach.

25 Associations between Lymphocyte Activation, Senescence, and Pulmonary Function in HIV-infected and HIV-uninfected individuals

Mariam Bramah-Lawani

University of Pittsburgh School of Medicine, Pittsburgh, USA

Rationale: HIV is an independent risk factor for pulmonary dysfunction. Both HIV and COPD are independently associated with chronic inflammation, senescence, and immune activation. Limited reports in HIV-COPD have described associations of activated-senescent T-cell phenotypes and pulmonary function testing (PFT) abnormalities, but comparisons to uninfected persons have not been made. Additionally, abnormal lymphocyte memory subset redistribution is associated with chronic inflammation; memory subsets have not been evaluated in the context of HIV-associated pulmonary dysfunction. We compared surface markers of lymphocyte activation and senescence and proportions of lymphocyte memory subsets to PFTs in HIV-infected and uninfected persons. Methods: HIV-infected and uninfected persons were recruited from an outpatient cohort. Clinical factors including demographics, smoking exposure, and measures of HIV viral control were collected. Participants performed ATS standard PFTs. Peripheral blood mononuclear cell lymphocytes were analyzed by flow cytometry for expression of activation (CD38+, HLA-DR+, CD69+), senescence (CD28nullCD57+), and memory subsets (naïve [Tnaive, CD45RA+CCR7+], central memory [TCM CD45RA-CCR7+], effector memory [TEM CD45RA-CCR7-] and terminally differentiated [TTEMRA CD45RA+CCR7-]). Relationships between T-cell markers and PFTs were tested by Spearman's correlation, t-test, or rank-sum. Regression was used to adjust for clinically relevant variables. Results: 79 participants were enrolled, of whom 60 (77%) were HIV-infected. Mean age of participants was 49.5 years. HIV-infected individuals had a greater smoking history than HIV-uninfected (median pack-years 16.87 vs. 0.15, $p=0.01$). 95% of HIV-infected persons used ART (median CD4 567.5 cells/mm³, range [3-1619]; median viral load 43, range [UD-78771]). PFTs were normal on average, but 16.9% had post-bronchodilator FEV1/FVC < 0.7 and 55.7% had DLCO < 0.8. There were no significant differences in PFTs by HIV status in this cohort. Certain activated and senescent phenotypes (CD38+/CD8+, CD38+/CD28nullCD57+/CD8+, CD28nullCD57+/CD8+; CD69+/CD4+, CD38+/CD28nullCD57+/CD4+, CD69+/CD28nullCD57+/CD4+) were more frequent among HIV-infected (not shown). Higher proportions of naïve CD8 T-cells independently correlated with better DLCO ($\beta = 0.37$, $p = 0.007$), and higher proportions of CD4 TTEMRA were independently associated with greater odds of post bronchodilator FEV1 < 0.8 (OR 3.5 [95%CI:1.4-9.2, $p=0.01$]) in HIV-infected persons only. Higher CD69+/CD8+ expression independently associated with post-bronchodilator FEV1/FVC < 0.7 (OR 6.3 [95% CI: 1.2-33.3, $p=0.03$]), and higher CD28nullCD57+/CD4+ expression associated with lower post-bronchodilator FEV1 percent-predicted ($\beta = -0.03$, $p=0.03$) in HIV-infected persons. Conclusions: Results are consistent with prior findings that upregulation of senescent and immune activation markers are associated with lung dysfunction in HIV. Lymphocyte memory compartments may be novel important markers of T-cell immunopathogenesis in HIV-associated lung dysfunction.

26 Exosomes secreted by mutant SOD1^{G93A} motor cortex reveal an insight into how cortical neurons communicate disease in ALS

Jonathan Brent
Northwestern University Feinberg School of Medicine,
Chicago, USA

Exosomes are extracellular vesicles that carry proteins and RNAs which are secreted by cells into their surrounding milieu. In the nervous system exosomes are thought to function as a means of communication between neurons, glia, and their targets. ALS is a devastating disease characterized by the dysfunction of both upper and lower motor neurons, and upper motor neuron degeneration is an early event in the disease. Corticospinal motor neurons (CSMN) display cortical hyperexcitation prior to any clinical evidence of disease and they degenerate as early as P14, prior to any evidence of spinal motor neuron abnormality in ALS mouse models. The molecular mechanisms that underlie CSMN degeneration are poorly understood and the signals that CSMN and their neighbors use to communicate within the microenvironment of the diseased cortex have yet to be revealed.

We hypothesized that cortical neurons which become vulnerable would utilize exosomes to communicate their cellular pathology with the surrounding cells/neurons in the cerebral cortex and more broadly in the central nervous system. Elucidating which signals act to improve versus propagate disease is critical to our understanding of ALS pathogenesis.

We collected conditioned medium from both healthy and diseased mixed cortical neuron cultures and isolated exosomes secreted to the medium. Then, we performed proteomic assays to determine the content of exosomes secreted with respect to disease. Our findings reveal that diseased cortical neurons secrete 276 proteins within exosomes. These proteins have diverse cellular functions, including transcription factors and kinases, suggesting that active signaling takes place prior to disease symptom onset in the cortex. Our ultimate goal is to define the functional relevance of these proteins and to reveal whether they promote disease progression or are sent as a warning signal to the brain.

27 The preclinical development of a recombinant subunit vaccine against whipworm: immunological characterization of protective efficacy

Neima Briggs
University of Texas - Houston / M.D. Anderson, Houston, USA

Trichuris trichiura, the common whipworm, is a leading cause of chronic colitis in the developing world with an estimated 465 million people living with whipworms in their colon. The disease disproportionately affects children, resulting in growth stunting, anemia, and cognitive deficits. Current approach to the control soil-transmitted helminths, including trichuriasis, in endemic nations is through annual mass drug administration. However, success has been limited due to the combination of poor drug efficacy, high rates of post-treatment reinfection, and failure to co-implement aggressive sanitation programs. Our long-term goal is to develop a vaccine against *T. trichiura*. Because there is no established laboratory animal model for this human pathogen, we adapted the closely related *Trichuris muris* parasite that infects rats and mice causing similar pathophysiology. Both pathogens release macromolecules from a unique anterior organ known as the stichosome, which facilitates intracellular invasion into the colon. The majority of *Trichuris* genes between the two species are orthologs. Vaccination with *T. muris* excretory/secretory (*Tm-ES*) proteins, known to be predominantly

stichosome in origin, elicits protective immunity in AKR mice. Using the protective anti-*Tm-ES* sera, we identified 14 antigens by both immunoscreening the *T. muris* cDNA library and by two-dimensional electrophoretic separation followed by western blotting. The leading three candidate antigens were ranked by their vaccine potential and were tested for efficacy against *T. muris* in the AKR mouse model. The most promising candidate recombinant *Trichuris muris* whey acidic protein 49 (r*Tm-WAP49*) lead to a significant reduction in larval worm burden. Endpoint ELISA titers revealed a high serum IgG1 to IgG2a ratio, reflective of a type 2 humoral immune response in protected groups. Similarly, a profound type 2 cellular immune response (interleukin-4 [IL-4], IL-5, IL-9, and IL-13) was measured in the spleens, mesenteric lymph nodes, and vaccine-draining lymph nodes of protected mice by 23-plex Luminex analysis. Immunofluorescent staining with anti-r*Tm-WAP49* confirmed high production of the native protein in the stichosome of *T. muris*. We also evaluated the translatability of r*Tm-WAP49* as a potential vaccine candidate by testing its serological and cellular reactivity of biological samples collected from 236 individuals in Honduras, a region endemic for *T. trichiura* after confirming active transmission of *T. trichiura* transmission by real-time polymerase chain reaction.

28 Role of Oncometabolite L-2 Hydroxyglutarate in Reprogramming Renal Cell Carcinoma Metabolism

Garrett Brinkley
University of Alabama at Birmingham, Birmingham, USA

INTRODUCTION: Renal cell carcinoma (RCC) is among the ten most common neoplasias in the United States and is well known to undergo extensive metabolic reprogramming. Previous work by our lab has identified high levels of the oncometabolite L-2 Hydroxyglutarate (L2HG) in RCC. It is currently unknown if we can utilize metabolic liabilities created by oncometabolites for personalized RCC therapy.

OBJECTIVES: The primary objective of this study is to understand the mechanism and impact of loss of *de novo* serine and glycine biosynthesis in RCC. In turn, we will assess how this liability can be targeted therapeutically.

METHODS: This project analyzed normal renal cell line HK2 and renal cancer cell lines (RXF-393, OS-RC-2, A498, 786O, 769P, Caki1, Sn12Pm6, and A704) using lentiviral transgene or knockdown expression. Proliferation assays were counted over 4 day periods and inhibitor experiments were done at 10mM. Data was analyzed via real-time PCR and western blot. Patient samples were obtained through proper procedures at UAB. Additionally, The Cancer Genome Atlas was also analyzed.

RESULTS: Phosphoglycerate dehydrogenase (PHGDH), the first and rate-limiting step in the serine synthesis pathway, is commonly reduced in both RCC patient samples and several RCC cell lines. Lentiviral transgene L2HGDH knockdown or re-expression was able to either decrease or increase PHGDH expression respectively. Serine and glycine starvation significantly decreased proliferation in RCC cell lines with reduced PHGDH (OS-RC-2, 769P and 786O) but not in RCC cell lines with higher basal PHGDH (RXF393, Sn12p6). Pharmacologic inhibition of serine and glycine transporters SLC38A1 and SLC38A2 (SNAT1 and SNAT2) with MeIAB decreased proliferation in 769P cells (low PHGDH) but not RXF-393 (high PHGDH), whereas inhibition of SLC1A4 and SLC1A5 (ASCT1 and ASCT2) did not alter growth of either cell line.

CONCLUSION: L2HG controls *de novo* serine and glycine synthesis in RCC cell lines. SNAT pathway inhibition via MeIAB reduces proliferation in low PHGDH RCC cell lines. Targeting serine and glycine transports looks to be a promising direction for novel, personalized RCC treatments.

29 Dynamics of dexmedetomidine-induced loss and return of consciousness across primate neocortex

Jessica B. Briscoe

Geisinger Commonwealth School of Medicine, USA

Consciousness is the experience of perceiving the outside, as well as our internal worlds, by synthesizing multiple sensory inputs, developing emotions, or forming and reflecting on opinions. However, we have yet to understand how the components of the brain interact to mediate consciousness and arousal. Physicians and scientists have manipulated arousal and consciousness for decades, using anesthesia for purposes of surgery and procedures without the knowledge of how it affects the interchange of brain networks. The body's natural neural oscillations that create varying arousal and unconsciousness states during sleep have been shown to be physiologically distinct from the neural oscillation patterns seen during anesthesia-induced arousal and unconsciousness. This distinction may reveal more information about anesthesia's effects, as well as the phenomenon of changes in arousal states. More importantly, electrophysiological studies conducted in rodents, non-human primates, and humans are largely conducted under anesthesia without a basic understanding of how anesthetic agents interfere with baseline brain functional synchrony and neural oscillations. We hypothesize that anesthetic-induced altered states of arousal are generated by highly structured and distinctive oscillations, causing characteristic spatial and temporal neural patterns along the neocortex, thalamus, and brainstem.

We have investigated how the anesthetic dexmedetomidine effects neural oscillations during loss of consciousness (LOC) and return of consciousness (ROC) in the primate neocortex. We conducted microelectrode array intracortical recordings in the somatosensory (S1) and frontal ventral premotor (PMv) networks in primates. Following a behavioral task, to determine alertness and performance measures, dexmedetomidine infusion was administered through a vascular port. Alertness and trial-by-trial performance was then used to analyze the primates' behavior during LOC, ROC, and return of pre-anesthetic performance (ROPAP) using the state-space model.

We first analyzed the change in spectrograms in S1 and PMv. During wakefulness, beta oscillations dominated in S1 and PMv, while the onset of LOC was identified by a brief increase of alpha power oscillations more obvious in S1 than PMv. Throughout anesthesia, slow-delta oscillations appeared, while ROC was associated with a return of alpha oscillation dominance and decrease in slow-delta waves. As the animal recovered, alpha waves appeared to increase its frequency toward the beta range; however, ROPAP did not achieve pre-anesthetic beta oscillation frequency and power. Single neuron spike responses were clearly different in S1 and PMv. The PMv spike firing rate increased upon LOC, while S1 neurons decreased — a response that continued through recovery.

These findings suggest that dexmedetomidine-induced LOC and ROC are both associated with an increase in alpha oscillations in S1 and PM. The slow-delta oscillations are dominant while the animals are unconscious. Spike firing response appears to be region specific, but clearly associated with consciousness changes. Further investigation is underway to identify mechanisms of cortical, thalamic, and brainstem responses under dexmedetomidine anesthesia.

30 Surrounding the enemy: investigating the influence of cervical microbiome and tumor microenvironment on the prognosis of cervical cancer patients.

Dewey Brooke

University of Alabama at Birmingham, Birmingham, USA

While nearly all cervical tumors are infected with HPV, infection alone is not sufficient for tumor development. Although most cervical HPV infections are cleared by cell-mediated immunity, progression to malignancy is linked to an immunosuppressive microenvironment comprising of a subset of protumorigenic lymphocytes and immunosuppressive stromal fibroblasts. While the tumor microenvironment directs the biology of many cancers, recent evidence has linked dysbiosis of the vaginal microbiome with the extensive reprogramming and remodeling of the cervical stroma.

Using expression-based cell deconvolution methods on RNAseq from 372 cervical carcinomas, we performed hierarchical clustering on principle components to identify three patient clusters, which were identified as either immune-rich, stromal-rich, or an intermediate immune/stromal type. Patients with immune enriched tumors exhibited a favorable prognosis. However, both the intermediate and stromal enriched tumors had significantly worse overall and disease-free survival (DFS), with the stromal type carrying the worst prognosis ($p = 0.038$ and 0.0021). Gene Set Enrichment Analysis found that genes implicated with the epithelial-mesenchymal transition were more strongly associated with the stromal subtype, while the immune type was strongly associated with genes involved in p53 pathways and networks. Furthermore, we used microbial transcriptomics to identify microbes that were both elevated in patients with DFS < 3 years and patients relapse free greater than 5 years.

These results are significant in that they confirm previous studies that tumors with higher stromal invasion and marked immunosuppression exhibit the worst prognosis, while identifying for the first time to our knowledge microbes associated with prognosis. Furthermore, we identified possible genetic markers that would aid both in differentiating tumor types and likelihood of recurrence.

31 Enteroendocrine cell activity modulates vagal response in vivo

Kelly L. Buchanan

Duke University, USA

Overeating is linked to an altered perception of the reward value of nutrients. But how this signal is transduced from the gut to the brain remains unknown. Like taste receptor cells in the tongue, the gastrointestinal tract also has cells that sense nutrients. These are called enteroendocrine cells (EECs). EECs are known to respond to luminal stimuli and release hormones that act on vagal nerve fibers. Recently, we discovered that EECs can also form synaptic links with vagal nodose neurons. Here, we sought to establish whether EECs directly transduce stimuli onto vagal nerve fibers. We combined whole nerve electrophysiology of the cervical vagus nerve and EEC optogenetics to dissect the functional connectivity of this gut-brain neuroepithelial circuit. Our results show the following:

First, sugars delivered intra-luminally stimulate vagal firing rate. Sucrose, D-glucose, the non-nutritive sweetener sucralose, and the non-metabolized sugar methyl α -D-glucopyranoside, but not fructose, cause a rapid and significant increase in vagal firing rate when delivered intra-luminally in mice. The response is not observed when the stimulus is applied intraperitoneally or directly onto the

cervical vagus. The effects on cervical vagal firing rate are abolished after a subdiaphragmatic vagotomy, indicating that an intact vagus is necessary for the response.

Second, EECs transduce the stimuli of both nutritive and non-nutritive sugars onto the vagus nerve. Using a mouse in which EECs express the excitatory channelrhodopsin 2, we found that intraluminal stimulation with a 473-nm laser rapidly and significantly increases vagal firing rate. This increase is comparable to the sucrose response. Then, using a mouse in which EECs express the inhibitory halorhodopsin, we found that both sucrose and sucralose vagal responses are attenuated when EECs are stimulated with a 532-nm laser light.

Third, EEC transduction of a sucrose stimulus is dependent upon the sodium glucose transporter SGLT1. We found that the sucrose but not sucralose stimulus is abolished when the solution contains the SGLT1 receptor blocker phloridzin.

These data suggest that EECs modulate vagal activity within seconds in response to D-glucose and that the response is dependent upon the sodium glucose transporter SGLT1. This neuroepithelial circuit represents a therapeutic target to alter the transduction of caloric reward from gut to brain and to modulate appetite.

32 Photoacoustic tomography of intact human prostates and vascular texture analysis identify prostate cancer biopsy targets

Brittani Bungart

Purdue University, Boston, USA

The current methods of the prostate biopsy either do not target potential tumors or require separate imaging for target identification of the biopsy procedure. Our objective is to determine the ability for the multimodal imaging technique of blood and lipid photoacoustic tomography (PAT) imaging and ultrasonography (US) followed by texture-based image processing to identify targets for the purpose of guiding prostate biopsy in real-time.

Nine ex vivo human prostates were imaged with 1064 and 1197 nm PAT and 5-9 MHz US directly following radical prostatectomy. The PAT and US image frames corresponding to whole mount histology slides were used for either texture-based, k-means clustering feature learning or learned-feature testing. Six prostates were assigned to the learning group and three to the testing group. Following cluster center assignment of the testing group's pixels, a regional density filter of the tumor-clustered pixels was applied. The center of mass for each group of tumor-assigned pixels was considered the biopsy targets and compared to histopathology.

Upon assessment of each PAT channel, 1197 nm PAT did not provide a unique contribution to the clustering results, and thus only the 1064 nm PAT and US channels were utilized for further analysis. Biopsy targets identified 100% (3/3) of the primary tumors and 67% (2/3) of the secondary tumors in the testing group. The total number of targets per case are 10, 8, and 10. In conclusion, 1064 nm PAT and US texture-based feature analysis provided successful prostate biopsy targets with lower number of suggested cores compared to current biopsy protocols.

33 Ribavirin as a potential therapeutic for atypical teratoid/rhabdoid tumors

Joshua Casaos

Johns Hopkins University, USA

Atypical teratoid/rhabdoid tumors (AT/RT) are highly aggressive pediatric brain tumors with no current standard of care. A recent

genetic analysis reported AT/RT to have high expression of enhancer of zeste homolog 2 (EZH2), a methyltransferase known to have oncogenic properties in many cancers. Our laboratory previously demonstrated that the antiviral drug ribavirin, approved by the FDA for treatment of hepatitis C, inhibited glioma cell growth in vitro and in vivo, potentially through modulation of EZH2. Based on these findings and the lack of a preclinical model of ribavirin in AT/RT, we investigated the effect of ribavirin on AT/RT in vitro and in vivo. Three different human AT/RT cell lines (BT12, BT16, and BT37) were selected for investigation. Cell proliferation was assessed via cell counting. Cell cycle and cell death processes were quantified using flow cytometry. Tumor migration, invasion, and adhesion capacities were assessed via scratch wound, Boyden chamber, and adhesion assays, respectively. Ribavirin's mechanism of action in AT/RT was studied using Western blots for several known ribavirin targets. Finally, we tested ribavirin efficacy in vivo using an orthotopic xenograft AT/RT model in athymic mice.

We provide evidence that ribavirin significantly impairs AT/RT cell growth, increases cell cycle arrest, and induces cell death, potentially through modulation of the EZH2 and/or eIF4E pathways. We also demonstrate that ribavirin significantly impairs AT/RT cell migration, invasion, and adhesion. Most importantly, we show that ribavirin significantly improves the survival of mice orthotopically implanted with BT12 cells. Ribavirin-treated animals exhibited a significantly increased median survival (56 days) compared with controls (37 days) ($P < 0.0001$).

Our work establishes that ribavirin is effective against AT/RT in vitro and in vivo. Given the lack of standard therapy for AT/RT, these findings fill an area of unmet need and could represent a new therapeutic option for children with this deadly disease.

34 Glucose transporter GLUT3: a novel molecular target in bevacizumab-resistant glioblastoma

Ankush Chandra

University of California, San Francisco, USA

In spite of optimal treatments and recent advances in our understanding of its biology, glioblastoma (GBM) remains the most lethal primary adult brain tumor, with a poor median survival of less than 15 months from diagnosis. While phase II clinical trials showed encouraging results, randomized phase III clinical trials failed to show efficacy of the VEGF neutralizing antibody bevacizumab, which devascularizes the tumor, as most tumors progress during treatment and develop a much more aggressive and invasive molecular phenotype associated with resistance. Our laboratory has identified and found overexpression of the glucose transporter GLUT3 to be a hallmark of resistance to antiangiogenic therapy in GBM causing a metabolic re-circuitry within the tumor. In our studies, we have also shown GLUT3 overexpression to be associated with increased survival and proliferation of bevacizumab-resistant GBM cells, both in vitro and in vivo. We have also found that GLUT3 inhibition using an indirect inhibitor decreased survival of bevacizumab-resistant GBM cells in culture, suggesting GLUT3 as a potential targetable biomarker of resistance. We believe that direct molecular inhibition of GLUT3 will reverse the aggressive biology of bevacizumab-resistant GBM and overcome resistance to antiangiogenic therapies. Using six novel direct GLUT3 inhibitors synthesized and provided by our collaborators, we found that all six inhibitors inhibited bevacizumab-resistant GBM proliferation, with three of the six inhibitors inhibiting proliferation by 45%. We are analyzing the effects of these inhibitors on bevacizumab-resistant GBM cell biochemistry, morphology, invasiveness, and growth in culture and in vivo to fully define the

effect of direct GLUT3 inhibition on bevacizumab-resistant GBM. We believe that elucidating the biological actions of direct GLUT3 inhibitors will define targeting GLUT3 in bevacizumab-resistant GBM as an effective strategy to overcome GBM resistance to bevacizumab and unravel the full therapeutic potential of antiangiogenic agents.

35 The tandem zinc finger mRNA binding protein, Tristetraprolin, is a novel regulator of cardiac fatty acid metabolism through its effect on PPAR α

Hsiang-Chun Chang

Northwestern University, Chicago, USA

Introduction: Altered substrate utilization has been described in type II diabetes and heart failure (HF), but current therapies do not target the metabolic derangements in these disorders. Identification of novel pathways regulating cellular metabolism could facilitate the development of new therapies. Tristetraprolin (TTP) is a tandem zinc finger protein that binds to AU-rich elements (AREs) in the 3' untranslated region (UTR) of mRNA molecules and causes their degradation. Its expression is reduced in patients with diabetes, and its cellular level is regulated by mTOR, a key protein involved in cellular metabolism. Furthermore, the yeast homolog of TTP has been suggested to play a role in metabolism. Thus, we hypothesized that TTP regulates cardiac metabolism and its deletion prevents the development of HF through its effects on substrate utilization in the heart. Results: We first assessed the effects of TTP modulation on cellular substrate utilization, and found that TTP downregulation in cultured cardiomyocytes resulted in higher palmitate uptake and oxidation, while its overexpression had the opposite effect. Since TTP regulates its targets at the mRNA level, we studied the mRNA levels of ARE-containing genes involved in lipid metabolism, and found that only PPAR mRNA to be significantly increased with TTP downregulation. Furthermore, we demonstrated that TTP physically interacts with PPAR mRNA, and the activity of a luciferase reporter harboring full-length PPAR 3'UTR is increased with TTP downregulation. Additionally, PPAR mRNA is stabilized with TTP knockdown. We then studied the role of TTP in cardiac metabolism using mice with cardiac-specific TTP knockout. Although cardiac-specific TTP knockout mice had normal cardiac function at baseline, they displayed higher fatty acid utilization compared to wild type littermate control. We also demonstrated a significantly higher TTP levels in failing human and mouse cardiac samples, suggesting that TTP levels are altered in HF. Conclusion: Our results demonstrate that TTP is a novel regulator of cardiac fatty acid metabolism through its effect on PPAR, and that its levels are increased in HF. Thus, modulation of TTP may be a viable therapeutic approach for HF.

36 NGF signaling in stress fracture healing

Leslie L. Chang

Johns Hopkins University, USA

In contrast to the large body of literature on the role of peripheral nerves in other tissues, few studies have investigated the function of peripheral nerves in the skeleton. Developing peripheral tissues dictate innervation by secretion of specific neurotrophins, which promote neuronal survival by activation of tyrosine kinase receptors. The prototypic target tissue-derived neurotrophin is nerve growth factor (NGF). Importantly, the vast majority of nerves in mature bone are thinly myelinated or unmyelinated sensory neurons, which express the NGF high-affinity receptor TrkA. As sensory nerves have also been shown to be important mediators of early response to mechanical loading, we sought to develop a better understanding of the expression of the neurotrophin NGF and subsequent innervation of bone in a clinically relevant stress fracture model.

In the present study, 18-week-old male Thy1-YFP and NGF-eGFP reporter mice underwent stress fracture injury, using a previously validated cyclic axial compression of the right forelimb. Bone repair was assessed using routine histology as well as immunohistological analysis to assess for inflammatory response (CD45) and vascular proliferation (CD31). In Thy1-YFP reporter samples, immunohistochemistry was performed for the sympathetic marker TH (tyrosine hydroxylase) and sensory nerve marker CGRP (calcitonin gene-related peptide).

Stress fracture induces early and robust NGF reporter activity within the injured bone. At 1 and 3 days after injury, increased NGF reporter activity was observed among the resident periosteal stromal cells as well as inflammatory cells adjacent to the fracture site. CD45 immunohistochemical staining highlighted a dual source of NGF within the early fracture period among both stromal cells and inflammatory cells. Next, neuronal sprouting and ingrowth were examined within the same model using Thy1-YFP reporter animals (a pan-neuronal reporter). In the uninjured periosteum, YFP+ nerve fibers are of thin caliber and indiscrete. Early time points after fracture demonstrated an increased density of YFP+ nerve fibers was observed adjacent to the fracture site. The bulk of YFP+ nerves surrounding the fracture site were found to be CGRP+ sensory nerves, while a small minority were found to be TH+ sympathetic fibers. Additionally, as neural density increased, a trend toward increased vascularity of the fracture site was also observed.

Our data documents a timeline of NGF expression in an appendicular stress fracture model within the early stromal/inflammatory milieu of the soft callus. This robust expansion of an NGF+ domain within early bone healing corresponds to later neural sprouting and ingrowth of predominantly CGRP+ sensory fibers into and around the bone repair site. Moreover, sensory nerve ingrowth seems to be coordinated with vascular ingrowth. These new findings suggest a previously undescribed role for sensory nerves in the trophic support for fracture repair.

37 Using artificial intelligence to identify noninvasive imaging biomarkers in lung cancer — a deep learning radiomic approach

Tafadzwa Chaunzwa

Yale School of Medicine, USA

Lung cancer is the leading cause of cancer death and morbidity. The high degree of intra- and intertumor heterogeneity presents a challenge in treatment. However, early-stage disease, specifically stage I non-small cell lung cancer (NSCLC), is amenable to curative resection. Poor surgical candidates may benefit from stereotactic body radiation therapy (SBRT). Many prognostic molecular and genomic biomarkers have been identified in lung cancer, and there is a growing body of evidence suggesting radiomic phenotypes (drawn from medical images) can augment prognostic power when used in combination with both clinical features and tumor genomic profiles. Recent advances in computation and convolutional neural networks (CNNs) have also opened new avenues to tumor patch analysis and feature extraction from different imaging modalities.

In this study we set out to develop a deep learning model that can act as a noninvasive prognostic biomarker in patients with stage I NSCLC treated with surgery. In contrast to "conventional" radiomics, which relies on engineered quantitative imaging features (e.g., shape compactness, wavelet gray level nonuniformity HLH), deep learning-based image analysis algorithms are able to automatically find optimal rules and parameters from data. Our model would be able to assign patients to short-term or long-term survival groups

based on computed tomography (CT) characteristics.

Initial data mining yielded a discovery cohort of 500 patients who underwent surgery for stage I NSCLC at Massachusetts General Hospital (MGH) between 2004 and 2010. Presurgical CT studies with or without contrast were retrieved for ~300 patients. Image pre-processing included manual tumor identification and segmentation, with seed-point placement to predefine a 50-voxel cubical region of interest (ROI) that contains tumor, and creation of isotropic voxel dimensions in CT data with spatial interpolation. Further data curation yielded 233 volumetric and 2-dimensional imaging samples to feed into our neural networks. A 2-dimensional VGG-16 CNN modeled after the mammalian visual cortex was used to perform visual recognition and data analysis. The model was trained on 186 labeled CT scans, matched to one of two groups based on 2-year survival. Data containing variations of scanners and imaging protocols were used in training to create a model that is robust for the variations.

Our model learned to classify patients with long-term versus short-term survival in a test set of 47 patients, with 83% accuracy. These preliminary findings suggest that artificial intelligence-enhanced radiomic feature extraction and predictive modeling can improve the clinician's ability to assess the benefits of treatment in patients with early-stage NSCLC. An even larger dataset of ~1,300 patients with stage II and stage III lung cancer, treated at MGH, is also being curated and added to separate analyses. In addition, pretrained 3-dimensional models will also be employed.

38 Targeting the vitamin B6 pathway as a novel therapeutic strategy for cutaneous T cell lymphoma

Cynthia Chen

Columbia University College of Physicians & Surgeons, USA

Cutaneous T cell lymphoma (CTCL) is a malignancy of predominantly skin-homing CD4+ lymphocytes. Patients with advanced stages of CTCL have a high mortality rate, and even those with more indolent disease experience severely diminished quality of life due to recurrent skin infections, pain, and pruritus. Currently, there are few specific therapeutic targets known in CTCL, highlighting the need to identify not only key mediators in disease pathogenesis, but also druggable ones. One aspect of CTCL cells that has not been well studied thus far is their dependence on unique metabolic pathways to support dysregulated growth. Here, we identify the vitamin B6 pathway as a novel potential target for the treatment of CTCL. Using an sgRNA-mediated knockout platform, we found that loss of pyridoxal kinase (PDXK), an enzyme that converts vitamin B6 to its active form, pyridoxal phosphate (PLP), resulted in reduced proliferation of the CTCL cell lines MyLa and PB2B. Consistently, administration of the FDA-approved drug isoniazid, commonly used to treat tuberculosis and known to block the vitamin B6 pathway, recapitulated this proliferation defect in vitro. Furthermore, cells cultured with isoniazid demonstrated higher levels of apoptosis and delayed cell cycle progression. Future studies will assess the feasibility of repurposing isoniazid as a new treatment for CTCL by testing the drug's effects on primary samples from patients with CTCL.

39 Pan-cancer Akt pathway synthetic essential long intergenic non-coding RNA LINC00499

Jasper R. Chen

The University of Texas MD Anderson Cancer Center, USA

The Akt pathway is one of the most commonly activated in oncogenesis. To identify gene targets that could lead to the development of therapies across multiple cancer types, we applied the principle of synthetic essentiality, a recently described framework

for identifying potential synthetic lethal interactions by screening for genes that are consistently retained in the context of a tumor suppressor deletion or an oncogene amplification, on a pan-cancer scale to analyze 11,025 cases encompassing 32 cancer types from the Cancer Genome Atlas for genes that possess loss-of-function mutations that are mutually exclusive of loss-of-function in PTEN, gain-of-function in EGFR, PIK3CA, AKT1, AKT2, AKT3, or high phospho-Akt (Ser473) by RPPA. Based on these criteria, 1,010 cases were classified as Akt pathway gain-of-function and 10,015 cases were classified as wild-type. Our screening yielded a lincRNA, LINC00499, that had zero loss-of-function mutations in the Akt gain-of-function cohort and 40 loss-of-function mutations in the wild-type cohort. LINC00499 was overexpressed in PTEN-deficient SF763 glioblastoma and DU145 prostate cancer cell lines, suggesting increased dependency on this lincRNA during the PTEN-deficient state. Thus, we hypothesized that PTEN deletion disinhibits the Akt pathway, thereby inhibiting FoxO, which disinhibits LINC00499 expression. Three conserved FoxO binding sites were found using FIMO to search for the consensus binding motif between -8 kb from the transcription start site to +5 kb from the transcription end site of LINC00499 in aligned sequences of human, mouse, and at least one of cow, rabbit, sheep, pig, dog, cat, or horse with p-value < 0.0001. BLAST against Human RefSeqGene sequences determined putative binding elements in two splice variants of LINC00499. Depletion of LINC00499 by CRISPR-mediated deletion of the binding element for each splice variant yielded a reduction in cell proliferation and survival in PTEN-deficient SF763 GBM cells. The splice variant of LINC00499 with the greater difference in phenotype between PTEN-KO and WT was further analyzed by chromatin isolation by RNA purification in order to validate the 166 potential gene targets identified by BLAST. The binding sites varied from as short as 18 bp in length with 100% sequence identity to the lincRNA binding element to as long as 120 bp with 72% identity. The ErbB signaling pathway was found to be highly represented in this list by KEGG pathway enrichment analysis. Together, these data demonstrate the utility of synthetic essentiality as a powerful tool for identifying pan-cancer vulnerabilities. Furthermore, we explore a novel link between the Akt and ErbB pathways, LINC00499, which highlights the importance of lincRNAs in mediating the crosstalk between key oncogenic signaling to affect cancer viability.

40 Connecting the dots between pain modulation and pain transmission in acute and chronic pain

QiLiang Chen

Oregon Health & Science University, Portland, USA

Chronic pain is a prevalent condition with profound physical, psychological, social and economic impacts. An important factor in both normal and clinically significant pain is the intrinsic pain-modulating system, which regulates nociceptive processing via projections from the brainstem to the dorsal horn. The output of this modulating system, the rostral ventromedial medulla (RVM), can facilitate or suppress nociceptive transmission at the dorsal horn by the respective action of two distinct classes of neurons, "ON-cells" and "OFF-cells". Both classes respond to noxious inputs, however, the pathway through which noxious inputs drive changes in RVM activity is only now being defined. Anatomically, the RVM receives direct spinoreticular and trigeminal reticular inputs, as well as afferents from the parabrachial complex (PB), which is the major target of supraspinal projections from the superficial dorsal horn. The aim of this study was to test the hypothesis that noxious information is relayed to the pain-modulating neurons of the RVM via the PB, under basal conditions and in persistent inflammation. ON-cells and OFF-

cells were recorded in the RVM in lightly anesthetized rats. The ON- and OFF-cell activity were attenuated or blocked by pharmacological inactivation of the lateral PB *contralateral*, but not *ipsilateral*, to the noxious stimulus. By contrast, in animals subjected to chronic inflammation (CFA in one hindpaw), block of PB *ipsilateral* to the inflamed paw interfered with the ON- and OFF-cell activity elicited by normally innocuous stimulation of that paw. This implies recruitment of a normally inactive pathway during inflammation. A direct PB input to RVM was demonstrated using optogenetic methods. Activation of channelrhodopsin2-expressing PB terminals in RVM was able to drive RVM neurons *in vivo*, and in an RVM adult slice preparation, evoked synaptic currents. These data show that a substantial component of the relevant nociceptive drive to RVM pain-modulating neurons is relayed through the parabrachial complex, and that RVM neurons receive direct input from PB. While the *contralateral* PB relays noxious input under basal conditions, the *ipsilateral* PB is recruited in persistent inflammation. Thus, the parabrachial complex, well known as an important relay for ascending nociceptive information, also accesses descending control systems through a connection with the RVM.

41 Mature adipocytes impair the antimicrobial function of reactive dermal adipogenesis: an explanation for impaired cutaneous defense in obesity

Stella X. Chen

University of California, San Diego, USA

To defend against cutaneous infections, the skin must maintain both a physical and immunological barrier. Recently, our laboratory has shown that a layer of adipocytes in the dermis is necessary for antimicrobial defense by producing the cathelicidin antimicrobial peptide (Camp) during a phenomenon known as reactive adipogenesis. However, the increase in mature adipocytes in obesity is paradoxically associated with greater rates of cutaneous infection. In this study, we investigated whether the antimicrobial-adipogenic response of reactive adipogenesis is impaired in obesity, and how this may occur. Using mouse models of diet-induced obesity, we found that obese mice fed a high-fat diet lost dermal adipogenic-antimicrobial activity and had increased susceptibility to *Staphylococcus aureus* infection. *In vitro* studies using mouse primary dermal adipogenic fibroblasts showed that Camp expression peaked 6-fold ($P < 0.05$) during early adipogenesis. This was confirmed using functional antimicrobial assays, which showed that methicillin-resistant *S. aureus* growth decreased by more than three logs when grown in culture supernatant from newly differentiating immature adipocytes. However, as adipocytes continued to mature, *S. aureus* inhibition was lost and Camp mRNA expression decreased nine-fold ($P < 0.05$). Remarkably, we also found that coculturing dermal adipogenic fibroblasts with mature adipocytes or mature adipocyte conditioned media led to a diminished ability of adipogenic fibroblasts to express Camp mRNA, produce cathelicidin protein, and inhibit *S. aureus* growth. These findings suggest that undifferentiated adipogenic fibroblasts in the dermis are an important antimicrobial reserve for cutaneous defense. However, mature adipocytes lose antimicrobial activity and may impair adjacent adipogenic fibroblasts from fighting infection. These results provide a possible explanation for impaired cutaneous defense associated with obesity.

42 Chromosome bridge resolution requires mechanical forces from actin-based contractility

Anna M. Cheng

University of South Florida Morsani College of Medicine, USA

Chromosome bridges result from errors in cell division and form chromatin threads that connect daughter nuclei after division. These bridges eventually break ("resolve"), and the daughter cells inherit broken chromosome fragments. This is thought to initiate a major pathway for oncogene amplification and tumor genome evolution called the breakage-fusion-bridge (BFB) cycle. However, we still lack a complete understanding of the mechanism(s) causing chromosome bridges to break in the first place. Here we present new evidence that bridge breakage requires actin-dependent contractile forces. As daughter cells connected by a bridge move away from each other, the bridge is typically stretched over long distances before breakage. Using fibronectin micropatterns to limit daughter cell separation, we were able to block bridge resolution, with over 90% of bridges still intact as the daughter cells entered the next mitosis. In cells not constrained by micropatterns, bridge resolution was similarly blocked by timed addition of inhibitors of actin contractility. We propose that mechanical forces from actin-based contractility play a central role in bridge resolution.

We are also studying the genomic consequences of bridge breakage. BFB cycles have been observed in association with another form of localized mutagenesis called chromothripsis. It has also been shown that individual cells experiencing telomere dysfunction can grow into clonal populations with chromothripsis. These findings suggest a mechanistic link between bridge breakage and chromothripsis, but the details of this relationship are unclear. To address this question, we are using our "Look-seq" approach, which combines long-term imaging with single-cell sequencing. We will discuss whether bridge breakage occurs directly via chromothripsis, or if the relationship is indirect, with chromothripsis occurring as a downstream consequence, perhaps through formation of micronuclei in subsequent cell cycles.

43 Loss of function of the hepatic fatty acid translocase receptor CD36 is insufficient to protect from liver steatosis in a murine model of parenteral nutrition-induced liver injury

Bennet S. Cho

Boston Children's Hospital, USA

Children with intestinal failure (IF) due to insufficient bowel length or loss of function require intravenous parenteral nutrition (PN). However, long-term PN administration can lead to IF-associated liver disease (IFALD), characterized by cholestasis and hepatic inflammation. IFALD can progress to end-stage liver disease, requiring liver transplantation. Although there is no current Food and Drug Administration (FDA)-approved treatment, replacing the standard soybean oil-based lipid emulsion in PN with a fish oil-based lipid emulsion (FOLE) has been found to reverse IFALD. Our laboratory has demonstrated that FOLE protects from hepatosteatosis in a murine model of PN-induced liver injury, a process that is dependent on G protein-coupled receptor 120 (GPR120). Peroxisome proliferator-activated receptor γ (PPAR γ) expression, a transcription factor associated with hepatic lipogenesis and lipid droplet deposition, is normalized by FOLE treatment. Among transcriptional targets of PPAR γ , CD36 expression is increased in this model of liver injury and is normalized by FOLE treatment in a GPR120-dependent fashion. Fatty acid translocase receptor CD36 is a free fatty acid and lipoprotein transporter receptor associated with increased hepatic fatty acid uptake and triglyceride storage. The

goal of this study was to determine whether loss of function of CD36 is sufficient to protect from PN-induced liver injury.

Cd36-knockout (KO) C57BL/6 male mice and wild-type (WT) littermates were fed ad libitum chow or PN diet for 19 days. Livers, spleens, and kidneys were weighed and stained for hematoxylin and eosin (H&E) histologic analysis. Total RNA was extracted from liver and subjected to quantitative real-time polymerase chain reaction (qPCR) for measurement of hepatic regulators of lipid metabolism, including acetyl-CoA carboxylase 2 (ACC2) and PPAR α .

H&E staining revealed marked steatosis in livers from both WT and KO mice fed PN, whereas WT and KO mice fed regular chow revealed histologically normal livers. qPCR data demonstrated increased expression of ACC2 and PPAR α in PN-fed CD36-KO mice compared with chow-fed WT and KO mice.

The results of this study demonstrate that loss of function of CD36 by itself is not sufficient to prevent development of hepatosteatosis in a murine model of PN-induced liver injury. Increased ACC2 and PPAR α expression in CD36-KO mice suggests compensatory lipid accumulation via parallel pathways in the absence of CD36 function. Further studies investigating these alternate pathways may elucidate the pathologic mechanisms involved in the development of IFALD.

44 Oncogenic potential of noncanonical PIK3CA mutations and implications for molecular targeting strategies in head and neck cancer

Janice Cho

University of California San Francisco, USA

Despite the recent FDA approval of PD1 inhibitors for head and neck squamous cell carcinoma (HNSCC), about 50% of patients succumb to their disease, and predictive biomarkers to guide therapy are lacking. PIK3CA, the most commonly mutated oncogene in HNSCC, encodes the p110 α catalytic subunit of phosphoinositide-3-kinase (PI3K), which triggers downstream pathways involved in cell growth and survival. According to The Cancer Genome Atlas Network (TCGA), approximately 63% of PIK3CA mutations in HNSCC cluster at three canonical, "hotspot" mutation sites (E542K, E545K, H1047R), while 37% of HNSCC-associated PIK3CA mutations occur at noncanonical sites. Although there is considerable evidence illustrating the oncogenic properties of canonical, "hotspot" PIK3CA mutations, the role of noncanonical mutations in HNSCC tumorigenesis is unclear. Preliminary data from our lab demonstrate that PIK3CA mutations may lead to tumorigenesis via hyperactivation of the PI3K/COX2/PGE2 signaling pathway, and that combined therapeutic targeting of PI3K and COX2 may be a viable therapeutic strategy for PIK3CA-altered tumors. Through a genomics-based approach to treatment selection, this project aims to uncover the role of PIK3CA noncanonical mutations in conferring oncogenic driver function, with the goal of identifying viable therapeutic strategies for patient subsets based on PIK3CA mutational status. To accomplish this aim, we are engineering an HNSCC cell line that is sensitive to serum deprivation to express a panel of noncanonical PIK3CA mutations. The oncogenic properties of the noncanonical mutants will then be assessed by examining the engineered cell lines for proliferation in the absence of serum. In addition, activation of PI3K/COX2/PGE2 signaling will be examined via immunoblot analysis. Subsequently, we will determine whether PIK3CA noncanonical mutations exhibiting "driver" tumor growth confer sensitivity to conventional or molecular targeting strategies used in the treatment of HNSCC. If successful, this project will guide therapy for patients possessing PIK3CA-mutated tumors.

45 Using RNA sequencing to understand how steroids induce remission in Eosinophilic Esophagitis

Yash Choksi

Vanderbilt University, Nashville, USA

Background: Current treatments of eosinophilic esophagitis (EoE) include proton pump inhibitors, topical steroids, and elimination diets. While these therapies can be successful, none are specific. A previous study by Katzka et al *CGH* 2014 showed that topical steroid treatment in patients with EoE modified expression of tight junction proteins. In this study, our aim is define transcriptional networks modified by steroids in EoE, specifically with regards to cell adhesion and epithelial to mesenchymal transition (EMT).

Methods: Mid (5-10 cm from GE junction) and distal (2 cm from GE junction) esophageal mucosal biopsies from patients without EoE (defined as undergoing endoscopy for GERD non-responsive to therapy or dysphagia, (n=3; 2 female, 1 male), patients with active EoE (n=5; 3 female, 2 male), and patients with steroid-induced histologic remission (n=3; 1 female, 2 male), were submitted for whole transcriptome analysis using RNA sequencing. Esophageal tissue was obtained from both Vanderbilt and the Mayo Clinic.

Results: Control patients had an average age of 32.3 (range 31-35), patients with active EoE had an average age of 36.2 (range 27-49), and patients in steroid-induced remission had an average age of 63.3 (range 46-75). 542 genes were significantly decreased after steroid treatment, and 965 genes were significantly increased after steroid treatment. The list of 542 genes which were decreased after steroid treatment were compared with both gene ontology (GO) and Kyoto encyclopedia of genes and genomes (KEGG) gene sets. In the GO set, 58 genes associated with cell adhesion were found to be significantly decreased (FDR = 0.0072). In the KEGG set, 67 genes were associated with cell adhesion were found to be significantly decreased (FDR = 3.04e-4). When comparing the list of 542 genes to hallmark gene sets, 96 genes related to EMT were significantly downregulated (FDR = 0.0). 56 genes related to the apical junction were also significantly downregulated (FDR = 0.0158). qPCR was performed to confirm changes in expression of remodeling genes with steroid treatment (ACTG2, COL8A2, POSTN, CAPN14). As expected, there were also 88 genes that were decreased related to inflammatory response (FDR = 0.0090). PHEWAS studies were performed on candidate gene CAPN14, as it is not known to be associated with diseases other than EoE. When comparing known CAPN14 variants to phenotypes associated with infectious diseases, an association with *H.pylori* was identified.

Conclusion: Steroids cause changes in expression of genes associated with cell adhesion and EMT.

46 Myocardial Infarct Zone Imaging with Acoustically Activated Nanodroplets

Songita Choudhury

University of Nebraska Medical Center, Omaha, USA

Introduction: Commercially available Definity (Lantheus Medical) microbubbles (MB) can be compressed to nanodroplets (ND) at the bedside. These ND are sub-micron in size and exhibit significantly different acoustic behavior than the MB. ND may cross defective endothelial barriers and accumulate in non-viable tissue. We hypothesized that ND in combination with diagnostic ultrasound could be utilized to highlight areas of infarcted myocardial tissue. Methods: Rats (n=14) underwent acute myocardial infarction via left coronary artery ligation. At 48-72 hours post procedure, transthoracic ultrasound imaging with contrast specific sequences (Siemens 15L8,

0.5 and 1.5 MI) was performed. Myocardial contrast enhancement in the infarct and normal zones were analyzed and compared after 200 μ L bolus injections of 10% Definity or Definity ND. Triggered imaging was performed at 1 frame/3 cardiac cycles immediately following the bolus injections and again 4 minutes post injection. At the 4 minute time point, the MI was transiently increased to 1.5 to activate, and, subsequently, destroy droplets within the infarct zone. The transient enhanced zone (TEZ) was planimeted and compared to post mortem measurements of infarct size with TTC staining and confocal microscopy. Fluorescently labelled ND were administered to determine accumulation of particles in the normal and infarct zones 10 minutes post injection. Results: Infarct size ranged from 0-25% of the short axis plane (11 transmural, 3 non-transmural). Definity MB injections provided excellent contrast delineation of the infarct zone with clearance of the contrast by 2 min. Transient enhancement of the infarct zone using the ND was observed at 4 min post injection. The area of TEZ correlated closely with infarct size ($r=0.84$, $p<0.001$). ND accumulation within the infarct zone was confirmed by confocal microscopy. Recent studies looking at myocardial infarct detection in a porcine model of acute myocardial infarction appear to confirm that Definity ND can be used to define the infarct zone with delayed enhancement imaging. Conclusions: ND formulated from commercially available MB appear to accumulate in infarct zones following injection. Their detection with delayed echo activation presents a potential method of infarct detection and quantification, as well as targeted drug delivery.

47 A Web-Based Respiratory Pathogen Laboratory Report for Summarizing Key Metrics to Stakeholders

Paul Christensen

Texas A&M Health Science Center / Houston Methodist Hospital, Houston, USA

The Center for Disease Control and Prevention (CDC) provides data regarding Influenza activity. However, daily and weekly statistics summarizing regional hospital system observations are possibly most relevant for local decision making. Our microbiology laboratory implemented a daily web-based report to distribute respiratory pathogen data for our eight-hospital system to clinicians, hospital epidemiologists, infection control committees, system leadership, and the general public.

Molecular and antigen laboratory result data from respiratory pathogen tests are extracted from our lab information system and subsequently inserted into a MySQL database. Using 'PHP: Hypertext Preprocessor', we analyzed the laboratory result data to produce a web-based report using the Chart.js framework. The four charts summarize the number of positive tests over time, the number of positive tests by patient location in our hospital system, the percent positive tests, and the number of each pathogen identified by our molecular test during a set time interval.

We advertised the report at three separate committee meetings, where we requested informal feedback. A link to the report was included in an email from the executive vice president of the hospital system. We monitored the visitor statistics, including Internet Protocol (IP) addresses.

We deployed the report to the cloud (bit.ly/HMFlu). Over 1 week, the report was accessed 932 times. 70% of the originating IP addresses were from our hospital system, 10% were from other locations within the United States, 1% were from locations outside the United States, and 19% were from addresses that could not be mapped. 18% of the views were on mobile devices. The most common browser for desktop computers was Microsoft Internet Explorer (43% of all

views). Visit count peaked at 241 views per hour right after the link was distributed by email. 36% of all hour intervals saw no page views; excluding these, there were on average 8 views per hour.

In summary, we developed a web-based report that presents relevant statistics regarding respiratory pathogen testing in our laboratory. The report is updated daily to provide critical data to all stakeholders, including the general public. We developed the site with mobile devices in mind, which allows the charts and fonts to be readable on any platform. The charts are interactive, allowing the user to switch between daily and weekly reports using radio buttons. Data can be filtered by clicking the data labels in the chart legend. These features are possible because of our decision to develop a web-based report, as opposed to a Portable Document Format (PDF), spreadsheet, or word processing document. Anecdotal feedback collected at the time of rollout was universally positive. The report continues to be viewed daily.

48 Immune profiling of rejection biomarkers in HIV-positive transplant recipients

Simon N. Chu

University of California, San Francisco, USA

HIV+ solid-organ transplant recipients are predisposed to a three times higher rate of rejection episodes when compared to HIV- recipients, but immunological correlates of rejection in this population have not previously been identified. Here we describe our investigation of immunologic phenotype and gene expression profiling to identify functional differences between Rejectors (Rej) and Non-Rejectors (NR).

Donor and recipient peripheral blood mononuclear cells (PBMCs) were collected prior to transplant. Rej were selected based on biopsy-proven acute cellular rejection. Kidney transplant recipients were stratified by Rej ($n=28$) versus NR ($n=56$), as compared to matched HIV- kidney transplant recipients, HIV+ non-transplant controls and HIV-, ESRD- healthy control subjects ($n=25$ per group). These patients were profiled using flow cytometric panels to characterize cellular subsets, activation status, and Treg phenotype. Groups were compared for variance using the Kruskal-Wallis test, with pairwise comparison performed between groups by Dunn's post-test. For gene expression analysis, pre-transplant HIV+ liver recipient PBMCs from Rej ($n=2$) and NR ($n=2$) were co-cultured in mixed lymphocyte reaction (MLR) in vitro with either CD40L-stimulated donor or 3rd party B cells. Donor B cells were removed by immunodepletion and recipient cells were analyzed using a custom NanoString panel. Raw counts were normalized and p-values were adjusted using the Benjamini-Hochberg procedure.

HIV+ Rej were found to have markers of increased pre-transplant immune activation as compared to NR, with a bias toward activation of the innate immune system. They exhibited a significantly altered monocyte phenotype, including decreased HLA-DR expression on CD14+CD16+ intermediate monocytes ($p=0.0042$). Moreover, Rej have increased B cell activation by HLA-DR expression ($p=0.016$) and less activated Tregs by decreased percentage of CD39+ Tregs ($p=0.0271$). The frequency of Tregs did not differ between the two groups. After alloantigen stimulation, Rej showed increased gene expression of T-cell activation markers, CD28 and ICOS ($p=0.0242$, 0.0334). Interestingly, NR displayed upregulation of regulatory ligands in the leukocyte immunoglobulin-like receptor family (LILR), including LILRB4, LILRB1, and LILRA1 ($p=0.0384$, 0.017 , 0.0317). Differential gene expression between Rej and NR was preserved irrespective of stimulus by either donor or 3rd party.

Overall, our results suggest that increased rates of rejection in HIV+ kidney and liver transplants correlate with pre-transplant, recipient-specific immune dysfunction. Concordance in gene expression profile following stimulation with donor or 3rd party suggests that differential gene expression is an intrinsic, recipient-driven propensity to immune activation in Rej and immune regulation in NR.

49 Oral microbiome of braces patients

Jennifer Chung

University of Connecticut School of Medicine, New Britain, USA

There has been a significant increase in the number of patients being treated for orthodontic care over the past decade. Orthodontic treatments, particularly braces, are known for increasing the risk of periodontal disease, but not all patients with orthodontic interventions result in periodontitis. Certain bacteria, predominately gram-negative anaerobic bacteria, have been found to be responsible for periodontal diseases. The human mouth harbors many different microorganisms, collectively they are known as the oral microbiota.

We hypothesize that a distinct oral microbiome increases the likelihood for periodontal disease among braces patients. We have profiled the subgingival bacteria at four sites (first molar, central incisor, buccal first bicuspid, and lingual first bicuspid) in patients receiving brackets(n=9), clear aligners(n=2), and healthy controls(n=5) at three time points (0, 6, 12 weeks) using 16s rRNA gene sequencing and assessed bleeding on probing, plaque, and periodontal status.

We obtained a mean of 23,755 sequences per sample and aggregated to a total of 402 operational taxonomic units (OTUs). In our bracket cohort, we observed that there was a significant increase in microbial richness between samples obtained before braces intervention and six weeks after intervention among three of the four sites. Richness stayed at a similarly high microbial richness by 12 weeks. This increase in richness was accompanied by the decrease in *Streptococcus*, the most abundant genera found across all samples. Similar trends were seen when looking at diversity among samples by Bray Curtis. Samples taken before bracket treatment clustered more tightly and differently compared to the two time points after, which clustered similarly among each other.

In addition, over 30% of our bracket cohort developed periodontitis compared to 15% of our controls by six weeks of intervention. Overall samples that were associated with periodontitis had a lower relative abundance of *Streptococcus*.

We also observed that there were fewer OTUs shared among the four sites in time point one than in time point two and three, suggesting that the whole oral microbiome becomes more uniformed with bracket treatment. Interestingly, the unique OTUs to each site over time did not remain the same, suggesting that the uniqueness of each tooth's bacterial profile maybe very transient.

In conclusion, we observed significant microbial changes in the oral microbiome of patients with bracket intervention and the composition of these communities may contribute to periodontitis.

50 Evaluating ZNF274 as a therapeutic target for Prader-Willi Syndrome

Michael S. Chung

UConn Health, Farmington, USA

Prader-Willi Syndrome (PWS) is a neurodevelopmental disorder affecting ~1/15,000 live births and has no known cure. Individuals with PWS present with hypotonia, hypogonadism and initial failure

to thrive. After about 18 months of normal development, the PWS patients develop obesity and hyperphagia along with short stature and behavioral problems. PWS is caused by the loss of the paternal contribution of the chromosome 15q11-q13 locus. This locus is governed by genomic imprinting and thus the genes are expressed from one parental allele. Although PWS patients lack the paternal contribution of this region, they possess an intact but transcriptionally silent set of genes on the maternal chromosome. Thus the activation of the silent maternal genes may be an attractive potential therapy for PWS. The work previously done in our lab indicated the importance of Zinc Finger Protein 274 (ZNF274) in the repression of the maternal genes on the chromosome 15q11-q13 locus. ZNF274 recruits epigenetic silencing factors that mediate the deposition of repressive H3K9me3 histone marks. Chromatin immunoprecipitation (ChIP) confirmed that both ZNF274 and H3K9me3 marks are specifically enriched in the maternal allele but not the paternal allele. In the subsequent studies, a knockout of ZNF274 was generated in PWS induced pluripotent stem cells (iPSCs). Although the activation of the maternal 15q11-q13 genes was modest in these cells, a full activation of the maternal genes was observed in neural precursors (NPCs) and neurons that were derived from them. In addition, the repressive H3K9me3 marks were also shown to be reduced in ChIP experiments. Thus we hypothesize that ZNF274 is an attractive and viable therapeutic target for PWS. In order to test this hypothesis, we have generated several tools to deplete ZNF274 in PWS cell models. With these reagents, we aim to answer whether the depletion of ZNF274 in neurons will recapitulate the results found in our earlier studies. Furthermore, we will determine whether a sustained depletion of ZNF274 is required to activate the normally silent maternal genes. Lastly, we will determine the genome-wide consequences of ZNF274 depletion. The results of these studies may serve as a proof-of-principle for novel ZNF274 based therapies for the treatment of PWS.

51 Quantitative analysis of RPE morphology after gene therapy rescue in a mouse model of retinitis pigmentosa

Michelle J. Chung

Harvard Medical School, USA

Retinitis pigmentosa (RP) is a disease in which a mutation in >70 different loci leads to a conserved pattern of clinical symptoms and cell death in the eye. Photoreceptors, the cell types that capture and process light, are the cells primarily affected by the genetic lesion. Rod photoreceptors, which we use for dim light vision, die first, followed by cones, the type that we use for our daylight and color vision. Retinal pigmented epithelial cells (RPE) provide support for rods and cones, and they are also affected in RP. We recently showed that an adeno-associated viral (AAV) vector overexpressing Nrf2, a transcription factor that fights oxidation and inflammation, rescues cones and vision in an RP mouse model (rd1). We have more recently found that it also rescues the RPE. My project concerns quantifying the degree of RPE rescue so that we can better score this phenotype and test Nrf2 relative to other RP treatments that we are developing.

Eyes from rd1 mice received a subretinal injection of an AAV encoding for Nrf2 driven by an RPE-specific promoter (BEST1) or an AAV encoding GFP driven by the same promoter. The eyes were then flat-mounted and the RPE cytoskeletons imaged with phalloidin. The uniform hexagonal monolayer of the RPE became increasingly dysmorphic in untreated or control mice but remained regular in Nrf2 treated mice. Manual segmentation of RPE cells and quantification with Fiji found that the RPE of untreated rd1 mice had mean areas

12% larger than in treated mice. Control (AAV-GFP) rd1 RPE also had a mean aspect ratio 16% lower than that found in rd1 RPE from eyes treated with Nrf2. Because of the time-consuming nature of this analysis, we developed a customized eight-step CellProfiler pipeline to automate segmentation. CellProfiler was less effective than manual segmentation for both mean cell area (ROC AUC 0.68 for manual vs 0.56 for CellProfiler) and aspect ratio mean (ROC AUC 0.96 for manual vs 0.77 for CellProfiler).

We were able to demonstrate a quantitative difference between rescued and non-rescued RPE utilizing parameters of cell area and cell aspect ratio. Aspect ratio mean was a better parameter for discriminating between treated and untreated RPE than mean cell area. Although manual segmentation of RPE offers more sensitivity, CellProfiler is able to detect differences in rescued vs non-rescued eyes. Further improvements to the CellProfiler pipeline may bring its performance closer to that of human segmentation.

52 The role of renalase and its potential serum binding partner in pancreatitis

Shang-Lin Chung

Yale School of Medicine, USA

Renalase (RNLS) is a plasma protein secreted by the kidney and other tissues that has been found to be protective in acute injury including models of ischemic injury to the kidney and heart. In addition, it has been shown that renalase appears to disappear from serum during acute kidney injury. Given its apparent cytoprotective properties and connection to other organ systems and disease, we investigate the relationship of renalase with pancreatitis. Using isolated murine pancreatic lobules, pretreatment with recombinant human renalase (rRNLS) blocked zymogen activity caused by both cerulein and carbachol, two agents that can cause pancreatitis *in vivo*. Cerulein-induced histological changes commonly seen in pancreatitis was also prevented with rRNLS pretreatment, and cerulein administration to mice with a genetic deletion of renalase resulted in more severe pancreatitis. Furthermore, serum endogenous renalase was found to be undetectable within an hour after the onset of experimental cerulein-induced murine pancreatitis; RNLS returned to levels higher than basal values once cerulein administration ceased. Similarly, in preliminary studies in human plasma from individuals with acute pancreatitis we observed significant decreases in plasma levels when compared to healthy controls. We found that renalase is transported in serum in a high molecular weight complex, and this complex may have a role in its apparent disappearance from serum during the onset of disease. Through mass spectrometry, we determined that putative murine RNLS binding protein candidates in murine models include murinoglobulin, pregnancy zone protein, C3, and C5, which are members of the alpha-2-macroglobulin domain containing gene family. Together, these results suggest that renalase and its serum binding protein may play an important role in the regulation of injury and recovery in pancreatitis. To better understand how, I am using immunoprecipitation assays to confirm the identity of the binding protein and investigate its interactions with renalase during periods of pancreatic injury and recovery. I am also working with human samples to confirm that the same RNLS binding protein(s) found in murine plasma is the same in humans.

53 Monitoring real-time HIV-1 virion fusion and downstream metabolic consequences with fluorescence lifetime imaging.

Charles Coomer

University of Kentucky and University of Oxford (NIH Oxford-Cambridge Scholars Program), Louisville, USA

Quantitatively monitoring HIV-1 fusion enables mechanistic investigations of viral entry, its downstream consequences, and its pharmacological inhibition. Several assays have been used previously to evaluate viral fusion. However, these approaches (i.e. β -galactosidase-, electron microscopy-, p24-, and virus particle colocalization-based methods) not only lack the capability to track viral fusion in real-time, but also fail to distinguish which viral fusion events resulted in productive or non-productive infection. Furthermore, no attempt has been made to multiplex a viral fusion assay with methods aimed to monitor separate viral-induced cellular events in real-time. We developed a viral fusion assay taking advantage of Forster Resonance Energy Transfer (FRET) multiplexed with FRET biosensors of host cell metabolism and various second messengers. We utilized bimolecular fluorescent complementation (BiFC) to detect fusion positive cells, where Gag-mCherry-labelled JR-FL virions containing nuclear-localized, VPR-tagged C-terminal half-mVenus were used to infect cells expressing activation-induced cytidine deaminase (AID) tagged with N-terminal half-mVenus. Cells that were productively infected were detected with Gag-mCherry while fusion positive cells were detected by BiFC located in the nucleus. This fusion assay was multiplexed with FRET-based sensors of the [ATP]/[ADP] ratio, cAMP, NADH, lactate, pH, Ca^{2+} , and H_2O_2 concentration, which were characterized, optimized, and expressed in TZM-bl cells. Consequently, we detected and monitored HIV-induced changes of cellular metabolism during fusion and infection compared to baseline at the single-cellular level. Fluorescence lifetimes and average intensities per cell were calculated to elucidate the changes in concentration of metabolites and second messengers during fusion and infection. We therefore tracked, viral-induced changes in global host cell metabolism and signal transduction during fusion and productive infection in real-time, at the single-cell level. Our results will add to existing knowledge of several key metabolic changes and signal transduction processes required for HIV to successfully enter and productively infect its host. This data is key for the development of alternative therapeutic strategies to control HIV replication in infected patients.

54 Astrocytes mediate brain reward signaling in the nucleus accumbens

Michelle Corkrum

University of Minnesota, minneapolis, USA

Objective: The present study aims to determine the role of astrocytes in drug addiction, to reveal potential novel cellular targets for the treatment of this brain disorder. Background: Over 200 million people worldwide suffer from the debilitating consequences of drug use and abuse; and, unfortunately, even with treatment, the relapse rate for drug abuse is between 40-60%. The current project specifically examines amphetamine, a psychostimulant that adversely affects multiple organ systems including the brain. Amphetamine works in the brain by blocking and reversing dopamine transporters and increasing the amount of synaptic dopamine. In addition to the disruption of dopaminergic signaling, a major neural circuit disrupted by amphetamine is excitatory transmission in the nucleus accumbens (NAc: a primary brain region implicated in reward and addiction behavior). Most studies on reward and addiction have focused on neurons. Little is known about astrocytes, which are emerging

as important cellular elements of synaptic function regulation. Traditionally, astrocytes have been viewed as passive players in nervous system function. However, although astrocytes are not electrically excitable, astrocytes respond to chemical transmitters with cytoplasmic calcium elevations, which, in turn, can trigger the release of additional chemical transmitters leading to the modulation of synaptic transmission and animal behavior. The present study investigates the effects of dopamine and amphetamine on astrocyte-neuron signaling in the NAc and tests the hypothesis that astrocytes are activated by dopaminergic signaling and mediate excitatory synaptic transmission in the NAc and behavioral sensitivity to amphetamine. **Methods:** We combined confocal calcium imaging with selective optogenetic stimulation of dopaminergic axons to investigate astrocytic responsiveness to dopamine. To investigate the consequences of astrocyte activation on synaptic transmission we performed electrophysiological recordings of excitatory transmission and activated astrocytes with selective optogenetic stimulation of dopaminergic axons and by activating Designer Receptors Exclusively Activated by Designer Drugs (DREADDs) specifically expressed in astrocytes. Behaviorally, we investigated locomotor activity in response to amphetamine in wild-type and transgenic mice with decrease astrocyte activity. **Results:** We found that astrocytes responded to dopamine and amphetamine with intracellular calcium elevations. These dopamine-induced calcium elevations in astrocytes were associated with a depression of excitatory synaptic transmission through activation of adenosine A₁ receptors. Furthermore, specific activation of astrocytes with DREADDs resulted in a depression of synaptic transmission that mimicked the dopamine-mediated synaptic depression. Transgenic mice with decreased astrocyte calcium signaling exhibited attenuated locomotor responses to amphetamine. Present results indicate that astrocytes in the NAc core are involved in reward signaling by responding to dopamine and amphetamine and mediating dopamine-induced synaptic depression and behavioral responses to amphetamine. **Conclusions:** The present results aid in elucidating the cellular mechanisms involved in the neural plasticity associated with drugs of abuse and provides insight into novel therapeutic cellular targets.

55 Broad-spectrum antiviral banana lectin is highly efficacious against lethal influenza virus infection in vivo and inhibits influenza virus fusion

Evelyn Covés-Datson

University of Michigan, Ann Arbor, USA

Influenza viruses cause both seasonal epidemics, resulting in the death of up to 500,000 people each year, and pandemics, which are unpredictable and have the potential to kill millions. Vaccination as a preventive measure and neuraminidase inhibitors as treatment for severe influenza infections are only moderately effective, and resistance to extant therapies is increasing among circulating strains. Thus, there is a strong unmet need for a new antiviral therapeutic for the prevention and treatment of influenza infection, particularly one that is broad-spectrum. We have developed a novel, genetically optimized lectin (sugar-binding protein), originally isolated from bananas, called H84T banana lectin (H84T BanLec, H84T) that has broad-spectrum antiviral activity against multiple, including pandemic and avian, strains of influenza as well as viruses from other families, such as human immunodeficiency virus (HIV) and hepatitis C virus (HCV). We previously demonstrated in vitro that the single amino acid mutation at position 84 from a histidine to a threonine minimizes the mitogenicity of the wild-type lectin while maintaining antiviral activity against influenza, HIV, and HCV. We now report that H84T synergistically inhibits the replication of several strains of influenza in

vitro in combination with the standard of care neuraminidase inhibitor oseltamivir and is active against at least one oseltamivir-resistant strain. In a mouse model of lethal influenza virus infection, H84T is non-mitogenic, and both early and delayed therapeutic administration of H84T intraperitoneally are highly protective. Furthermore, H84T administered via aerosol with the Toll-like 2/6 and 9 receptor agonists Pam2CSK4 and ODN 2395, respectively, is also highly efficacious. In efforts to understand the mechanism of action of H84T against influenza virus, we have found by immunofluorescence that influenza virus replication is inhibited at or before the step of protein translation. Attachment is not inhibited by H84T in quantitative polymerase chain reaction-based and hemagglutination assays. Instead, H84T appears to inhibit influenza virus fusion at submicromolar concentrations using quantitative fluorescence dequenching- and immunofluorescence-based approaches with several different strains. Taken together, these studies reveal that H84T is efficacious against influenza virus both in vitro and in vivo by two different routes of administration and that it inhibits influenza virus fusion, underscoring its potential utility as a new broad-spectrum anti-influenza therapeutic.

56 Frataxin deficiency induces endothelial metabolic dysregulation to promote pulmonary hypertension

Miranda Culley

University of Pittsburgh, Pittsburgh, USA

Pulmonary hypertension (PH) is a progressive vascular disease that causes increased pulmonary arterial pressure, right heart failure, and death. We have previously shown iron-sulfur (Fe-S) cluster deficiency due to repression of iron sulfur cluster assembly protein 1 and 2 (ISCU1/2) promotes mitochondrial dysfunction and PH. Frataxin (FXN), a binding partner of ISCU1/2, is crucial to Fe-S cluster assembly. Genetic FXN deficiency causes Friedreich's ataxia, a disease of neurologic and cardiovascular dysfunction. The latter is often accompanied by PH, but the molecular etiology is unclear. Thus, there may be a direct role for FXN in PH. We hypothesized that FXN deficiency, due to genetic or acquired triggers, disrupts endothelial metabolic function to promote PH.

FXN expression was modulated in human pulmonary arterial endothelial cells (PAECs) by gene transfection and exposure to bromodomain inhibitor I-BET151, hypoxia, and IL-1 β . Simultaneously, analyses were performed in induced pluripotent stem (iPS) cell-derived endothelial cells from patients with Friedreich's ataxia. Fe-S clusters were quantified by fluorescent sensor; glycolytic flux was measured by Seahorse assay. Phenotypic changes, such as apoptosis, migration, vasomotor gene expression, and angiogenesis, were measured. In vivo, cell-specific conditional FXN knockout mice and mice with FXN siRNA delivered to the vascular endothelium were studied.

In PAECs, chronic hypoxia (0.48-fold change \pm 0.05, $P < 0.01$) and IL-1 β (0.47-fold change \pm 0.01, $P < 0.05$) down-regulated FXN expression. I-BET151 inhibition of bromodomain-containing protein 4 (BRD4) as well as siRNA knockdown of BRD4 restored FXN levels following hypoxia (1.98-fold change \pm 0.11, $P < 0.01$) and IL-1 β (2.5-fold change \pm 0.15, $P < 0.01$). FXN deficiency decreased Fe-S cluster assembly (0.57-fold change \pm 0.05, $P < 0.01$) and increased glycolysis (2-fold change \pm 0.05, $P < 0.01$) and ROS production, leading to increased apoptosis, decreased migration, altered effectors of vasomotor tone, and decreased angiogenesis in vitro. Similar phenotypic changes were also observed in endothelial cells derived from iPS cells from patients with Friedreich's ataxia. Endothelial-specific FXN knockdown in chronically hypoxic mice promoted hemodynamic (RVSP 34.31 mmHg \pm 0.18 v. 29.77 \pm 0.93, $P < 0.05$) and histologic indices of PH in vivo.

FXN deficiency induced by hypoxia and IL-1 β promotes endothelial-specific metabolic changes, leading to PH development in vivo. Our results may provide a target for diagnostic and therapeutic intervention for PH and may guide genetic identification of a novel cohort of patients at risk for PH.

57 Mice lacking type-1 interferon receptor generate ADCK antibodies in response to Δ gD-2 vaccination but have defects in ADCK mobilization

Joseph M. Dardick

Albert Einstein College of Medicine, USA

Δ gD-2 is a live-attenuated Herpes Simplex Virus type-2 (HSV-2) strain genetically deleted for glycoprotein D (gD), one of the immunodominant antigens. gD is required for cell entry, limiting Δ gD-2 to a single round of replication in non-complementing cells. Δ gD-2 is a novel immunogen in that it elicits completely protective immunity against HSV-1 and HSV-2 through antibody-dependent cell-mediated cytotoxicity and phagocytosis, collectively referred to here as antibody-dependent cell-mediated killing (ADCK). The mechanisms by which immunogens elicit ADCK activating antibodies are not well understood, but type-1 interferons (IFN α/β) have been shown to play a role activating humoral immunity and Fc γ R-mediated immune modulation.

To investigate the role of IFN α/β in generating an effective ADCK antibody response, we prime-boost vaccinated IFN α/β receptor knockout mice (IFNAR $^{-/-}$) with a fluorescent Δ gD-2 variant and compared the resulting immunity to that of WT mice. Both strains of mice vaccinated with Δ gD-2 generated similar proportions of total activated and gB-specific CD8 $^{+}$ T cells. Additionally, Δ gD-2 vaccinated IFNAR $^{-/-}$ mice developed similar overall and isotype specific anti-HSV IgG titers as compared to WT mice. ADCK assays using bone-marrow derived macrophages (BMDMs) from WT mice showed that serum from vaccinated IFNAR $^{-/-}$ mice induces significantly more ADCK killing than serum from vaccinated WT mice ($p < 0.05$). To determine whether the humoral immunity in IFNAR $^{-/-}$ mice initiated ADCK in vivo, serum from vaccinated IFNAR $^{-/-}$ mice was passively transferred into naive WT and Fc γ RIV $^{-/-}$ knockout mice. WT mice that received the vaccinated serum were partially protected from 10x LD90 challenge with HSV-2 but Fc γ RIV $^{-/-}$ mice were not ($p < 0.05$). However, in a simultaneous experiment, serum from vaccinated WT mice did not confer any protection to naive IFNAR $^{-/-}$ mice, indicating difficulty in mobilizing an ADCK response ($p < 0.01$). Surprisingly IFNAR $^{-/-}$ mice that were prime-boost vaccinated with Δ gD-2 were still completely protected from morbidity and mortality following a 10x LD90 challenge with HSV-2 ($p < 0.0001$). Subsequent quantification of viral copies in the dorsal root ganglia of the challenged mice found no difference in sterilization of infection between vaccinated WT and IFNAR $^{-/-}$ mice. To determine whether the disruption in ADCK during the passive transfer experiments was due to defects in macrophage response, assays were performed using WT BMDMs in the presence of IFNAR blocking Abs. However, the addition of anti-IFNAR antibodies did not affect ADCK activity, indicating that IFNAR signaling is not required for macrophages to carry out ADCK. Together, our data shows that the production of ADCK antibodies in response to Δ gD-2 is independent of IFN α/β , but IFNAR signaling is required for protection by passive transfer. These findings illustrate a novel drawback of the IFNAR $^{-/-}$ model while highlighting the utility of Δ gD-2 as a vaccine vector for pathogens which are commonly studied in IFNAR $^{-/-}$ mice.

58 Reciprocal transplantation and ATAC-seq profiling of fibroblasts reveal scar-forming behavior is cell intrinsic

Heather E. desJardins-Park

Stanford University School of Medicine, USA

Scars can be physically and psychologically devastating, and represent a major financial burden on the US healthcare system. Interestingly, mammalian fetuses heal scarlessly by regenerating native tissue. In mice, the transition from regenerative healing to scarring occurs between embryonic day (e)16.5 and e18.5. A lineage of fibroblasts, the cells known to produce scars, defined by embryonic expression of Engrailed 1 deposits all scar tissue in adult mice. However, these Engrailed 1-positive fibroblasts (EPFs) contribute to scarless healing before e16.5, then transition into a scarring phenotype as development progresses. Therefore, we hypothesized that EPFs accumulate epigenetic changes over time that result in the shift from scarless to scarring phenotype, and that EPF healing phenotype is thus cell intrinsic rather than dependent on cell microenvironment.

Fibroblasts were isolated from En1Cre;R26mTmG mice using fluorescence-activated cell sorting (FACS) at gestational ages e10.5, e16.5, e18.5 and postnatal day (p)1 and p30. Reciprocal transplantation experiments were performed to analyze EPF behavior in vivo, by injecting EPFs from e16.5 or p1 En1Cre;R26mTmG mice into the dorsum of C57BL/6J mice at p1 or e16.5, respectively. Epigenetic analysis was performed using the Assay for Transposase Accessible Chromatin with high-throughput sequencing (ATAC-seq).

EPFs at e16.5 transplanted into a scarring microenvironment (p1) exhibit non-scarring morphology and colocalize with type I collagen in only 2.13% of cells, whereas EPFs at p1 transplanted into a scarless microenvironment (e16.5) exhibit scarring morphology and colocalize with type I collagen in 24.18% of cells. ATAC-seq profiling reveals e10.5 fibroblasts are of a single lineage; they were thus excluded from analysis. Time course analysis of e16.5-p30 EPFs and Engrailed 1-negative fibroblasts (ENFs) demonstrates reliable biological reproducibility. Principal component analysis indicates that while EPFs and ENFs are similar at e16.5, they eventually diverge as distinct populations, with the greatest differences observed at p30. Examining the EPF lineage specifically, the most epigenetic changes occur between e16.5 and e18.5, with fewer epigenetic changes occurring postnatally between p1 and p30 (significant peaks = 124 vs. 20). Upon analyzing the genes for α -smooth muscle actin and vimentin, two genes implicated in fibrosis whose expression is thought to be characteristic of all fibroblasts, we found that their genetic accessibility significantly differs between EPFs and ENFs.

Our data strongly suggest that fibroblast phenotype is linked to transcriptomic regulation. Additionally, fibroblasts, while they may be capable of activation, behave in a stereotyped manner not dependent on cell microenvironment. Directed interventions on EPFs may thus enable scarless healing in adult animals. In future experiments, we hope to identify targets for genetic perturbation using CRISPR-Cas9. By corroborating our ATAC-seq data with functional assays such as Western blots and RNA analysis, we will pinpoint genes regulating fibroblast behavior to ultimately identify novel therapeutic options for human patients.

59 Interactions of calcium, 25-OH vitamin D, and kidney function with parathyroid hormone levels

Sangeet Dhillon-Jhattu

University of Chicago, IL, Chicago, USA

Parathyroid hormone (PTH) is a crucial factor in regulating calcium homeostasis and bone mineral deposition. 25-OH Vitamin D and estimated glomerular filtration rate (eGFR) also interact with PTH, and we aimed to better characterize the interplay between these factors.

Laboratory results performed at Laboratory Corporation of America Holdings (LabCorp) between April 2011 and February 2014 were assessed, if simultaneous PTH, calcium, vitamin D and eGFR were available. Calcium and vitamin D were categorized, and analyses were stratified for National Kidney Foundation stage of chronic kidney disease (CKD). Percentages of tests in which a PTH>65 was observed were calculated and plotted for each combination of calcium, vitamin D, and eGFR.

Among 126,615 patients, 38% were male and mean age was 65.6 years. Compared to those with eGFR>90, PTH levels were more likely to be abnormal in CKD stages 2 and 3A. Higher vitamin D levels were associated with lower PTH in all patients, and this effect became more prominent with decreasing eGFR. The normal U-shaped relationships between calcium and PTH were distorted in CKD stages 4 and 5.

PTH levels become detectably abnormal even in very early CKD. Repletion of vitamin D to levels of 40 ng/mL or greater was associated with significantly lower PTH levels in patients with eGFR \geq 15. Further work is needed to determine if interventions to replete vitamin D >40ng/ml might reduce hyperparathyroidism and its vascular complications in early CKD.

60 Risk Assessment in High-Achieving Adolescents

Anshul Dhingra

Case Western Reserve University, Menomonee Falls, USA

Background: Adolescence is a period of social, physical, and psychological development. While it has its stages of exploration and experimentation, it is accompanied by a fair share of risky behaviors. Most health problems among adolescents are due to risky behaviors as opposed to biological dysfunction (genetic diseases, physiological ailments etc.) Almost 75% of the causes of death in the adolescent population are preventable, and therefore addressing these risky behaviors in health care visits is essential to reducing morbidity and mortality. The Rapid Assessment for Adolescent Preventive Services (RAAPS) is a 21-item questionnaire designed to identify risk factors in adolescents based on generally accepted risk categories. Objectives: Our goal was to evaluate and analyze the most prevalent risk factors in a general adolescent population at Michigan Medicine Health Clinics and compare this to risk-factors of high-achieving adolescents in the MHSPEA program. The goal was to determine whether or not high-achieving students are more or less prone to risky behavior. Methods: RAAPS questionnaire was administered to adolescents, ages 13-19, coming to outpatient clinics at Michigan Medicine Health Clinics for annual health maintenance exams. Demographic characteristics were obtained from a retrospective chart review. The RAAPS questionnaire was constructed in the form of a Qualtrics survey and emailed to the current and previous cohorts in the MHSPEA program. The rates of high-risk behavior in both populations were determined and then compared using the Chi-squared test for categorical variables. Results: The average risky behavior score per adolescent was 1.95 in

the general population and 3.53 in the PEA students. The prevalence in the top 7 risk factors between both groups was also greater in the PEA adolescents compared to the general population. PEA had six statistically significantly larger risky behavior categories, depression (p-value=0.0015), victim of bullying (p-value=0.0005), anxiety (p-value=0.0063), distracted driving (p-value=0.0001), no adult support (p-value=0.0002), and eating disorder (p-value=0.0481). **Conclusions:** PEA students are more prone to risky behavior than a general population of adolescents. High academic performance is not an indicator of reduced risky behavior, and we did not find any correlation at all between the two.

61 The role of spinal meningeal lymphatic vessels in recovery from spinal cord injury

Michael Dong

University of Virginia, USA

Spinal cord injury is a debilitating disease involving damage from initial injury and secondary degeneration with recruitment of immune cells to facilitate repair. However, the trafficking of immune cells between the peripheral immune system and the spinal cord is poorly understood. In addition, the controversy over the beneficial or harmful aspects of the inflammatory response in spinal cord injury has led to greater discussion over immunotherapy strategies.

The spinal meningeal lymphatic network has recently been characterized and provides an unexplored avenue for communication between the nervous system and immune system. The role of spinal meningeal lymphatics has never been studied in the context of spinal cord injury. We demonstrate marked alterations in lymphatic vessels in the spinal cord dural meningeal compartment as a result of spinal cord injury. We have assessed their morphological and functional changes and the role of major lymphangiogenesis-promoting factors in meningeal lymphatic vessel changes associated with spinal cord injury. We hypothesize that spinal meningeal lymphatic vessels respond to injury and communicate with the peripheral immune system to activate the adaptive immune response. Further work is required to establish the causal link between meningeal lymphatic trafficking of immune cells and recovery in spinal cord injury. We aim to set the foundation for spinal meningeal lymphatic modification as a therapeutic option in spinal cord injury.

62 Activation of DAF-16/FOXO by reactive oxygen species promotes longevity in long-lived mitochondrial mutants.

Dylan Dues

Michigan State University College of Human Medicine / Van Andel Research Institute, Grand Rapids, USA

Mild deficits in mitochondrial function have been shown to increase lifespan in multiple species including worms, flies and mice. Here, we study three *C. elegans* mitochondrial mutants (*clk-1*, *isp-1* and *nuo-6*) to identify overlapping genetic pathways that contribute to their longevity. We find that genes regulated by the FOXO transcription factor DAF-16 are upregulated in all three strains, and that the transcriptional changes present in these worms overlap significantly with the long-lived insulin-IGF1 signaling pathway mutant *daf-2*. We show that DAF-16 and multiple DAF-16 interacting proteins (*MATH-33*, *IMB-2*, *CST-1/2*, *BAR-1*) are required for the longevity of all three mitochondrial mutants. Our results suggest that the activation of DAF-16 in these mutants results from elevated levels of reactive oxygen species. Overall, this work reveals an overlapping genetic pathway required for longevity in three mitochondrial mutants, and, combined with previous work, demonstrates that DAF-16 is a downstream mediator of lifespan extension in multiple pathways of longevity.

63 The Scaffolding Protein IQ motif-containing GTPase Activating Protein 1 (IQGAP1) Promotes Hepatic Proliferation and Protects the Liver from Injury

Hanna L. Erickson

University of Illinois at Urbana-Champaign, Champaign, USA

Liver cancer is the second leading cause of cancer-related death worldwide, with 810,000 deaths annually, and the mortality rate is increasing rapidly in the United States. Liver disease, a major risk factor for liver cancer is becoming increasingly prevalent due to its association with the growing obesity epidemic. Bile acids (BA) are known liver tumor promoters but the mechanisms by which BAs promote tumorigenesis are unknown. The scaffolding protein IQ motif-containing GTPase Activating Protein 1 (IQGAP1) is overexpressed in numerous cancers, which is associated with a more aggressive phenotype. We show that elevated BAs induced expression of IQGAP1, and this induction correlated well with BA levels in a dose-dependent manner both *in vitro* and *in vivo*. Treating WT and IQGAP1-null (*Iqgap1*^{-/-}) mice with a 1% cholic acid (CA) diet to increase BA levels revealed that loss of IQGAP1 does not alter BA homeostasis. *Iqgap1*^{-/-} mice fed CA diet showed reduced hepatic proliferation, whereas ectopic adenoviral expression of IQGAP1 in *Iqgap1*^{-/-} livers restored BA-induced proliferation indicating that IQGAP1 is required for hepatocyte proliferation in response to elevated BAs. To determine whether the proliferative defect in *Iqgap1*^{-/-} mice could affect the response to more severe liver injury, WT and *Iqgap1*^{-/-} mice were fed a 0.1% 3,5-diethoxybaronyl-1,4-dihydrocollidine (DDC) diet for 2 weeks. The DDC diet resulted in elevated serum BAs and total bilirubin, which are both higher in *Iqgap1*^{-/-} mice. Consistently, histological analysis revealed more severe liver damage including increased inflammatory cells and fibrosis along with increased BA accumulation in the livers of *Iqgap1*^{-/-} mice. Gene expression analysis further revealed reduced expression of proliferation markers and increased expression of inflammatory markers in the absence of IQGAP1. These results indicate that IQGAP1 could be protective against liver injury by promoting proliferation of hepatocytes and reducing inflammation. To determine whether this could impact liver tumorigenesis, we administered 5 mg/kg diethylnitrosamine (DEN) to 14-day-old mice and assessed tumor burden at 50 weeks post-injection. Preliminary analysis revealed no overt effect of IQGAP1 on the chemically-induced liver tumor development. However, we expect that histological and biochemical analysis of the tumors will reveal more aggressive tumors in WT mice compared to *Iqgap1*^{-/-} mice. Taken together, these data indicate that the short-term role for IQGAP1 downstream of BA signaling includes controlling hepatic proliferation, maintaining biliary homeostasis, and protecting against injury.

64 Data-Driven Computational Drug Discovery for Novel understudied kinase, PNCK

Derek Essegian

University of Miami Miller School of Medicine, Miami, USA

The druggable genome consists of about 3,000 protein-encoding genes that may be amenable to small molecule therapy. Currently, less than 10% of druggable proteins are being targeted by approved drugs. Thus, it is important that this space be explored to identify novel, clinically relevant targets for the treatment of cancer and other diseases. Through integrative analyses of the Cancer Genome Atlas (TCGA) transcriptomic and clinical data, we have identified PNCK as one such understudied target that may be clinically relevant for the treatment of various cancers. Pnck is the most significantly differentially overexpressed kinase in renal cell carcinoma (RCC)

patients. Pnck is also significantly up-regulated in breast carcinoma, lung squamous carcinoma and renal papillary carcinoma patients. In RCC patients, Pnck is overexpressed by 179-fold in tumor tissue compared to adjacent normal tissue. Pnck overexpression correlates with various pathological and clinical outcomes such as Fuhrman grade, T-staging and overall survival (OS). In A498 kidney cancer cell lines, we have determined overexpression of PNCK to be a driver of cancer progression. Genomic editing with CRISPR/Cas9 significantly reduced cellular proliferation and cell viability. Collectively, this evidence validates PNCK as a kinase drug target of interest. As an understudied protein, PNCK has no known crystal structure and no known exogenous ligands. Using related protein crystal structures as templates, we have developed a structural homology model of PNCK to use in structure-based docking screens to identify potential hit compounds against PNCK kinase activity. We have developed ligand-based Laplacian-modified Naïve Bayesian classifiers for the use of machine learning kinase predictive models that leverages data from across the kinome and computed the probability of activity against PNCK of over 7 million commercially available compounds obtained from eMolecules. In a large scale virtual screen, we have identified a series of in-silico hit compounds with diverse chemical scaffolds that we have tested in vitro in RCC cell lines which we have confirmed significant PNCK overexpression. This represents the early stages in a drug discovery pipeline. We will determine binding affinity of top compounds in biochemical assays and will use computational structure-activity-relationship methodologies to improve our hits with medicinal chemistry.

65 TIR: A conserved innate immunity-signaling domain that defines a new family of NADase enzyme

Kow Essuman

Washington University School of Medicine, Saint Louis, USA

The Toll/Interleukin-1 Receptor (TIR) domain is an evolutionary conserved protein domain, present in numerous receptors and adaptor proteins, and is the signature-signaling domain of Toll-Like Receptors (TLRs). In eukaryotes, these TIR domains generally serve as scaffolds that promote the assembly of signaling complexes to trigger activation of pro-inflammatory cytokines and other defense-related products. In plants, TIR domain proteins are known to mediate disease resistance, and in bacteria, they have been associated with virulence. In pursuing our work on axon degeneration, we made the surprising discovery that the TIR domain of SARM1, a TLR adaptor protein, has enzymatic activity. Upon axon injury, the SARM1 TIR domain cleaves Nicotinamide Adenine Dinucleotide (NAD⁺), destroying this essential metabolic co-factor to trigger axon destruction. This finding identified a druggable target for axonopathies such as peripheral neuropathy and other neurodegenerative diseases, and also identified the first enzymatic activity intrinsic to a TIR domain, thereby redefining TIR function. Furthermore, NAD⁺ biology profoundly influences myriad aspects of biology, from metabolism, to aging, to cancer biology, to neurodegeneration, and until our discovery, it was thought that the pathways regulating NAD⁺ biosynthesis and degradation were mostly known. However, our studies showing that the SARM1 TIR domain is a potent NADase necessitates a re-evaluation of the function of this well-studied scaffolding domain and its impact on NAD⁺ metabolism and disease. Here, we dramatically extend our understanding of this protein domain, by demonstrating that the ancestral prokaryotic TIR domains constitute a new family of NADase enzymes. Using purified proteins from a cell-free translation system, we show that TIR domain proteins from both bacteria and archaea cleave NAD⁺ into Nicotinamide and ADP-Ribose (ADPR), with catalytic cleavage

executed by a conserved glutamic acid residue. We find that a subset of bacterial and archaeal TIR domains generates a non-canonical variant cyclic ADPR molecule, and that the full-length TIR domain protein from pathogenic *Staphylococcus aureus* induces NAD⁺ loss in mammalian cells. These findings suggest that the primordial function of the TIR domain is the enzymatic cleavage of NAD⁺, and establishes TIR domain proteins as a new class of metabolic regulatory enzymes.

Washington University, J.M., A.D., K.E., D.W.S., Y.S., X.M., have patent(s) related to this work, and income may be derived from licensing of technology to Disarm Therapeutics and Chromadex. J.M., and A.D., are co-founders of Disarm Therapeutics and members of its scientific advisory board.

66 Myristoylated alanine-rich C-kinase substrate peptide mimetic triggers apoptosis in glioblastoma cells

Nicholas Eustace

University of Alabama at Birmingham, Birmingham, USA

INTRODUCTION: Glioblastoma's (GBM) median survival is just 14 months despite the best standard of care of maximally safe resection, chemotherapy and radiation treatment. Novel therapeutics are needed to target drug and radiation resistant glioblastoma cells (GBM) that remain. Receptor tyrosine kinase (RTK) amplifications, Phosphatase and tensin homolog (PTEN) loss and Phosphatidylinositol-4,5-bisphosphate 3-kinase mutations are all common mutation in GBM which leads to dysregulation of phosphatidylinositol 4,5-bisphosphate (PIP2) enhancing cell proliferation, invasion, chemotherapy and radiation resistance. Myristoylated alanine-rich C-Kinase substrate (MARCKS) effector domain binds and sequesters PIP2 regulating its availability and potentially countering the effects of mutations in GBM.

OBJECTIVES: This study tests the efficacy of a MARCKS effector domain peptide mimetic in suppressing the growth of glioblastoma (GBM) patient derived xenografts (PDX) models, and to better understand its of action.

METHODS: MARCKS peptide sequence containing the PIP2 binding domain and a control peptide sequence of similar length and MW was screened against a panel of molecularly characterized PDX lines for cytotoxicity using the luminescent cell viability assay CellTiter-Glo. Timing of cellular uptake and visualization of MARCKS peptide within GBM was determined using a Cyanine 7 fluorescent peptide and confocal microscopy. An Xcyto10 quantitative fluorescent microscope was used to quantify apoptosis, the impact on cell cycle as well determine concentrations of the peptide in the cytoplasm and nucleus. Kinase signaling was assessed through western blot and gene expression was analyzed using the pan cancer gene set on nanostring.

RESULTS: The proneural line D456 was highly sensitive to MARCKS peptide (>90% kill) at 5uM compared to a control peptide, with classical lines 1046, X14 and 1016 being moderately sensitive (p<0.001) and normal human astrocytes being least sensitive. There was a significant increase in apoptosis following dosing of MARCKS peptide compared to control. Peptide accumulated throughout the cytoplasm and nucleus of D456 in a punctate pattern by 6hrs, kinase signaling and gene expression was significantly altered at 12 and 24 hours after peptide respectively.

CONCLUSION: MARCKS peptide accumulates inside GBM cells and has significant cytotoxicity to subtypes of GBM.

67 Constitutively active STAT5 in antigen-specific CD8 T cells enhances the antitumor effect of adoptive cell transfer with peptide vaccination

Aaron Fan

Augusta University, Augusta, USA

Adoptive cell therapy (ACT) of retrovirally transduced (RV) CD8 T cells is a powerful technique that has shown promise in tumor eradication in cancer patients. However, some major barriers to current methods are that ACT is expensive, time consuming, and requires harmful and toxic adjunct procedures. Our laboratory has demonstrated the use of TriVax, a potent peptide vaccination strategy that dramatically expands ACT cell populations and bypasses the necessity for adjunct procedures. Our purpose was to enhance current methods of ACT+TriVax by testing an antigen-specific antitumor response of RV CD8 T cells and if it could be enhanced with constitutively active STAT5 (CA-STAT5) expression, a protein activated downstream several cytokine pathways that have been shown to play a role in increased CD8 T cell persistence and resistance to apoptosis. Here, we aimed to test the hypothesis that CA-STAT5 in CD8 T cells enhances an antitumor effect by increasing T cell persistence and efficacy.

Our results show that TriVax administration selectively expanded the ACT cell population expressing gp100-TCR in both blood and spleen. When co-transduced with CA-STAT5, an even higher fold expansion of antigen-specific cells was observed. CA-STAT5+ cells were able to expand more robustly than CA-STAT5- cells upon repeated antigen stimulation (vaccine boost), demonstrating 5000-fold increases in tetramer+ CD8 T cells. CA-STAT5+ cells also seemed to persist longer *in vivo* over time, and they expressed lower levels of PD-1. Using B16F10 melanoma, ACT+TriVax of these cell populations into tumor-bearing mice demonstrated a powerful antitumor effect, leading to tumor regression in treated groups. CA-STAT5 seemed to recapitulate similar antitumor effects we observed previously with combinatorial aPD-L1 treatment or IL2/aIL2 mAb complexes (IL2Cx), suggesting a potential role for STAT5 in resisting the PD-1/PD-L1 inhibitory pathway. Altogether, these results demonstrate that RV T cells expressing gp100 TCR and CA-STAT5 are capable of antigen-dependent expansion in response to TriVax. CA-STAT5 plays a role in increasing T cell proliferation and persistence, as well as increasing efficacy through resistance to PD-1/PD-L1 inhibition.

68 Skeletal muscle Krüppel-like factor 15 is a major regulator of systemic lipid metabolism

Liyan Fan

Cardiovascular Research Institute, Case Western Reserve University, Cleveland Heights, USA

Skeletal muscle serves as a major site for insulin-mediated glucose uptake and use, glycogen storage, lipid metabolism, and fatty acid oxidation. Disturbances in skeletal muscle metabolism lead to whole body metabolic dysregulation, resulting in disease such as obesity and insulin resistance. Previous work from our group and others have identified Krüppel-like factor 15 (KLF15) as a major regulator of nutrient homeostasis: for example, *systemic* KLF15 deficiency is associated with reduced exercise capacity, severe hypoglycemia during fasting, and impaired amino acid metabolism. Here we show that *skeletal muscle specific* KLF15 is a critical regulator of systemic lipid metabolism. Additionally, we show that KLF15 expression is downregulated in response to insulin, the major hormonal coordinator of whole body nutrient homeostasis. We utilized mice with skeletal muscle specific *Klf15* knock out (K15-SKO) or skeletal muscle specific *Klf15* overexpression (K15-Skm-Tg) placed on either

a high-fat diet (HFD) or normal chow (NC) for 12 weeks. K15-SKO mice fed NC displayed increased body weight, increased circulating free-fatty acids and triglyceride levels, glucose intolerance, and increased white-adipose cell size compared to controls. With HFD challenge, K15-SKO animals gained significantly more body weight and are severely glucose intolerant. K15-Skm-Tg mice were resistant to HFD-induced weight gain and are more glucose sensitive than controls. Importantly, compared to control animals, expression of lipid flux genes (e.g. *Fatp1*, *Cpt1 β* , *Slc25a20*) were decreased in K15-SKO and increased in K15-Skm-Tg mice. To elucidate insulin's effect on KLF15 expression, C2C12 cells were cultured and differentiated for 7 days and then treated with insulin and pharmacological inhibitors of the insulin signaling pathway. RT-qPCR and chromatin immunoprecipitation assays revealed that KLF15 is negatively regulated by insulin through an Akt-FoxO signaling pathway. These data indicate skeletal muscle KLF15's critical role in regulating whole body lipid homeostasis. Given the central role that skeletal muscle dysfunction plays in the pathogenesis of diseases such as metabolic syndrome and obesity, our findings importantly shed light on the mechanisms that govern metabolic plasticity in skeletal muscle.

69 APOE, Metabolism and Cognitive Function: An Assessment via Indirect Calorimetry

Brandon Farmer

University of Kentucky, Lexington, USA

Both genetic factors and metabolic disturbances are associated with declines in cognitive performance and increased risk of dementia. The gene Apolipoprotein E (APOE) encodes for three isoforms in the human population (E2, E3, and E4), and the E4 isoform – carried by approximately 1/5 of the population – is the strongest genetic risk factor for late onset Alzheimer's Disease (AD). Both AD and E4 have been associated with inefficient brain glucose uptake and impaired metabolism. Interestingly, our preliminary data show that aged mice expressing human E4 demonstrate a metabolic "shift" compared to those expressing human E3. This is reflected as a preference of E4 mice for lipids vs carbohydrates as a fuel source. As the brain relies primarily on glucose as an energy source, these data suggest that E4 may negatively influence metabolic pathways which are critical for cognitive function. We hypothesize that similar apoE differences are present in cognitively normal individuals, and therefore aim to translate these exciting findings to human subjects. We believe an E4-directed shift away from glucose utilization may represent a critical step in the progression of cognitive decline, and thus a potential novel biomarker for AD risk. To test our hypotheses, we aim to measure metabolic rate and respiratory quotient (RQ) – a reflection of substrate preference – using indirect calorimetry (IC). Metabolic analyses employing IC are commonly used in clinical settings and exercise studies. However, while technically feasible, to our knowledge, IC has never been applied to investigate biomarkers of cognitive impairment. Thus, repurposing IC to study the metabolic effects of an AD risk factor such as E4 represents a simple and cost-effective new approach. In the current study, real-time metabolic measures will be assessed in individuals with various APOE genotypes – both at rest and during a cognitive and dietary challenge. Accuracy and interpretation of RQ will be aided by measuring adiposity, blood glucose, and urinary urea nitrogen (for estimation of protein oxidation). Our initial feasibility studies show measurable increases in RQ during a cognitive challenge, as well as a trend toward increased resting energy expenditure (REE). Additionally, an acute dietary challenge (sugar water drink) resulted in a steady increase in RQ following ingestion. Recruitment of ~75 young, cognitively normal subjects is scheduled to begin in January

2018. We hope to expand our methods in future studies to measure elderly subjects (cognitively normal, mild cognitive impairment and AD), as well as potential collaborative efforts in other areas of neuroscience.

70 Protein tyrosine kinase 2 beta is required for cultured beige adipocyte differentiation

Jared S. Farrar

Virginia Commonwealth University School of Medicine, Richmond, USA

Brown adipose tissue (BAT) is a unique adipose tissue which can increase energy expenditure through the thermogenic action of uncoupling protein 1 (UCP1) in mitochondria. Thermogenic adipocytes are therefore an appealing target to promote a significant shift in energy expenditure and increase glucose utilization. White adipose tissue (WAT), in contrast to BAT, has an energy storing, rather than consuming function. However, WAT can be "browned" leading to the generation of functional thermogenic brown-in-white (brite) or beige adipocytes. Previously, several receptor and non-receptor kinases have been identified as important molecular targets in thermogenic adipocyte differentiation and function. However, knowledge of specific protein kinase actions in thermogenic adipocyte differentiation and function remains limited. In this study, we demonstrate that the non-receptor protein tyrosine kinase 2 beta (PTK2B, also known as PYK2 or FAK2) plays a critical role in beige adipocyte differentiation. In order to study the role of PTK2B in UCP1 mediated thermogenesis, an immortalized murine inguinal WAT preadipocyte cell line was generated which could be differentiated to either beige or white adipocytes. We observed that PTK2B protein expression was elevated during beige adipocyte differentiation in this cellular model. Using the generated cell line, *Ptk2b* was knocked-out using CRISPR/Cas9 genome editing. When *Ptk2b* KO (PKO) preadipocytes were differentiated to beige adipocytes, they had altered expression of thermogenic adipocyte signature genes and proteins. Furthermore, beige adipocyte differentiation was delayed in PKO preadipocytes and mature PKO beige adipocytes had increased lipid droplet accumulation. We also deleted *PTK2B* in human subcutaneous fat preadipocytes to extend the findings of our mouse model. Together, our data establish a unique role for PTK2B in the differentiation of functional beige adipocytes and suggest PTK2B may be a potential therapeutic target to increase thermogenic adipocyte capacity and improve treatment of obesity and type-2 diabetes.

71 A Retrospective Analysis: Sleep Disordered Breathing In Patients With Cystic Fibrosis

Noor Fatima

Xavier University of Louisiana, Metairie, USA

Objective: Cystic Fibrosis (CF) is an autosomal recessive disease that causes exocrine gland dysfunction; this leads to thick mucus that results in obstruction of airways in the lungs and also affects the GI tract and other organs. Previous research in CF and sleep has shown daytime sleepiness and impaired neurocognitive function as an effect of poor sleep quality.^{1,2} The goal of this study is to assess sleep disordered breathing (SDB) and differences in sleep architecture in patients with CF as compared to age-matched non-CF controls.

Methods: This is a retrospective study on 43 CF patients with age matched controls (0-66 years of age) with no sleep pathology, who had a sleep study at University of Michigan sleep laboratory between the years 2009 and 2017. Patient data such as demographics and

polysomnogram values were taken from Epic and analyzed via SPSS software.

Results: TST, CAI, OI, oxygen desaturation, and OSA are all statistically significant for the total populations as well as for some age groups. The difference between sleep efficiency mean percentage for the two populations is trending towards significance; it is significant for the ≥ 19 age group. There is no statistically significant difference in sleep stages between the two total populations, but some trends and significant differences exist in the age groups ≤ 12 and ≥ 19 for N1, N2, and R. Interestingly, the CF ≥ 19 population spent more time in N1 sleep than the age-matched controls, with a prolonged transition period between being awake and going to sleep. There is no statistically significant difference in any variables in the 13-18 age range, only a trend in oxygen desaturation. Hypothesis 1 is correct as sleep of CF population is disturbed with apnea, oxygen desaturation, inefficient sleep, and reduced sleep time. Hypothesis 2 is rejected as the younger age group did not show increased rates of OI, nor did the older population show a statistical difference in CAI. Small sample size could lead to skewed results.

Conclusions: There are statistically significant differences in the sleep patterns of the CF compared to non-CF patient populations. This warrants regular sleep studies (polysomnographies) for CF patients to evaluate for SDB and provide intervention as needed.

72 A mammalian steroidal Na-pump ligand marinobufagenin is synthesized from the intermediates in the acidic and classical bile acid pathways

Olga V. Fedorova

National Institute on Aging, NIH, Baltimore, USA

Objectives: The bioactive steroidal Na/K-ATPase inhibitor marinobufagenin (MBG), a pro-hypertensive and a pro-fibrotic factor, is involved in the pathogenesis of preeclampsia, salt-sensitive hypertension, and chronic renal failure. MBG synthesis in mammals is controlled by the Cyp27a1 enzyme (cytochrome P450, family 27, subfamily a, polypeptide 1), which initiates the acidic bile acid (BA) pathway in extra-hepatic tissues, i.e., in rat adrenal cortex and human placenta. Nevertheless, the knockout of Cyp27a1 in a mouse model did not reduce MBG production. Moreover, down-regulation of Cyp27a1 was accompanied by an upregulation of Akr1d1 enzyme (aldo-keto reductase family 1, member D1), which participates in the final steps of both acidic and classical BA pathways. We hypothesized (i) that MBG is synthesized from the intermediates in the acidic and classical BA pathway under Cyp27a1 and Akr1d1 control, and (ii) that inhibition of Akr1d1 will decrease MBG production in Cyp27a1 knockout (Cyp27a1^{-/-}) homozygous mice.

Methods: All-trans retinoic acid (atRA) suppresses Akr1d1. Four-month old homozygous Cyp27a1^{-/-} (HO) male mice and wild type male mice (WT) were fed atRA diet (150 mg/kg of diet) or control diet (CTRL) for 10 days (n=8/group). Hepatic Cyp27a1 and Akr1d1 mRNA and protein abundance, and MBG excretion were assessed before (baseline) and after atRA diet. Data were analyzed using 2-way ANOVA, and are presented as mean \pm standard error.

Results: Hepatic Cyp27a1 mRNA level was down-regulated by 70% in HO vs. WT (p<0.01), hepatic Akr1d1 mRNA level was twofold overexpressed in HO vs. WT (p<0.01). AtRA decreased expression of hepatic Akr1d1 mRNA in both strains (HO: by 180% vs. CTRL, p<0.01; WT by 170% vs. CTRL, p<0.01). Hepatic Akr1d1 protein level was decreased in both genotypes by atRA (HO: fourfold vs. CTRL, p<0.05; WT: threefold vs. CTRL, p<0.01). Baseline urine MBG level was twofold higher in HO vs. WT (p<0.05). Inhibition of

Akr1d1 by atRA was associated with a decrease in urine MBG in HO (5.3 \pm 0.5 vs. 2.9 \pm 0.2 pmol/24hr; baseline vs. atRA; p<0.05), but not in WT (2.1 \pm 0.4 vs. 2.6 \pm 0.9 pmol/24hr; baseline vs. atRA; p>0.05).

Conclusions: The up-regulation of hepatic Akr1d1 enzyme in Cyp27a1^{-/-} mice may compensate for a lack of Cyp27a1 and promote production of MBG. Inhibition of Akr1d1 resulted in a decrease of MBG production in Cyp27a1^{-/-} mice only, indicating that Cyp27a1 is a predominant enzyme in MBG biosynthesis. Thus, mammalian steroid MBG is synthesized from the products and intermediates in the acidic and classical BA pathways. Further investigation of MBG biosynthesis will help to counteract MBG level elevation observed in devastating human diseases.

Acknowledgement: This work was supported by NIH/NIA Intramural Research Program

73 Translocation of a pathobiont induces lymphocyte migration to internal organs and systemic autoimmunity

Rebecca L. Fine

Yale School of Medicine, USA

The mechanisms and sites of host-microbiota interactions in autoimmunity are largely unknown. We hypothesized that certain commensals traverse the gut barrier in autoimmune-prone hosts and interact with immune cells in non-gut organs to promote systemic autoimmunity. During this process, gut-imprinted lymphocytes are expected to migrate to sites of pathobiont colonization. To test these hypotheses, we used the lupus-prone (NZWxBXSB)F1 mouse model which carries a duplication of toll-like receptor 7 (TLR7) on the Y chromosome.

We first determined the importance of the microbiota by modulating the commensal community with single antibiotics. Treatment with oral vancomycin reduced activated CD44⁺ T cells, Th17 cells, T follicular helper cells, anti- β 2GPI, -RNA IgG, -dsDNA autoantibodies, and protected mice from autoimmune deaths. Culture of small intestinal segments, mesenteric lymph nodes (MLN), livers, and spleens revealed progressive translocation of the gram-positive commensal *Enterococcus gallinarum* that was suppressed by vancomycin. Intramuscular vaccination of (NZWxBXSB)F1 males with *E. gallinarum*, but not other commensals, prevented translocation, autoantibody production, and autoimmune-related deaths.

To elucidate the contribution of host genetics to *E. gallinarum*-driven lupus, we tested whether internal organs of female (NZWxBXSB)F1 mice, which do not carry the TLR7 duplication and develop milder disease than males, are colonized by translocated *E. gallinarum*. *E. gallinarum* translocated to MLN in females only after first depleting the niche with broad spectrum antibiotics. To determine the role of *E. gallinarum* in the development of lupus in the absence of genetic predisposition, we next studied whether dense monocolonization of non-autoimmune prone C57BL/6 germ-free mice with *E. gallinarum* could induce signs of systemic autoimmunity. In this gnotobiotic setting, *E. gallinarum* was able to translocate, and induce Th17 cells and serum autoantibodies. Aged monocolonized C57BL/6 mice had also greater levels of Peyer's patch and splenic CD4⁺ T cells than germ-free controls. Gut-homing α 4 β 7⁺ CD4⁺ T cells were significantly increased in spleens, suggesting that lymphocytes previously imprinted in the gut follow *E. gallinarum* to internal organs. Furthermore, in (NZWxBXSB)F1 males, circulating CD3⁺CD4⁺ cells expressing α 4 β 7⁺ or CCR9 increased with age and were reduced with oral antibiotics. Lastly, *E. gallinarum* was detected in human livers of patients with autoimmune hepatitis and systemic lupus erythematosus but not non-autoimmune cirrhotic livers.

Together, these data support that a gut commensal translocates spontaneously to initiate autoimmunity in genetically prone hosts by inducing Th17 responses, autoantibodies, and homing of gut-imprinted lymphocytes to internal organs colonized by the pathobiont. Vaccination against this pathobiont prevented translocation and autoimmune deaths. Because the same species was detected in human livers from autoimmune patients, similar processes may occur in humans. Overall, these discoveries represent a new paradigm of host-microbiota interactions in autoimmunity and reveal a novel treatment target aimed at the microbiota.

75 *Bdnf* rs6265 variant confers a differential response to pharmacotherapies in early-stage Parkinson's disease

D. Luke. Fischer

Michigan State University, Grand Rapids, USA

Background: Patient response to antiparkinsonian therapies is heterogeneous, so the use of patient genotype to inform optimal treatment strategies would be a powerful tool. Brain-derived neurotrophic factor (BDNF) is a critical modulator of neurotransmission and synaptic plasticity within the basal ganglia. Preclinical work has implicated BDNF signaling in the antiparkinsonian efficacy of both levodopa and deep brain stimulation (DBS). Several single nucleotide variants exist in the gene *Bdnf* with one in particular (rs6265) resulting in reduced activity-dependent BDNF release. We have previously shown in a pilot study that early-stage Parkinson disease (PD) subjects carrying the rs6265 minor allele exhibit a less robust response to levodopa therapy.

Objective: We validated the impact of the rs6265 variant and explored the effect of additional *Bdnf* variants in two additional, larger subject cohorts: 1) early-stage PD subjects from the NIH NINDS Exploratory Trials in Parkinson's Disease Long-term Study-1 (NET-PD LS-1) treated over two years with either levodopa alone (n=56) or any combination of dopaminergic medications (n=540), and 2) early-stage PD subjects from the Parkinson Progression Markers Initiative (PPMI) treated with dopaminergic pharmacotherapy (n=361).

Methods: All subjects were genotyped for *Bdnf* variant rs6265, and NET-PD LS-1 subjects were also genotyped for rs908867, rs10501087, rs11030094, rs1157659 and rs1491850. Response to therapy was assessed by Unified Parkinson Disease Rating Scale (UPDRS) scores at various visits over 36 months. Mean UPDRS scores were stratified by variant allele status and adjusted for site, age, race, PD duration, therapy dose, and treatment group.

Findings: In NET-PD LS-1 subjects only treated with levodopa, rs6265 minor allele carriers (38%) and rs11030094 major allele carriers (86%) exhibited higher mean UPDRS scores than those without the risk allele at 24 months (37.6 vs. 30.7, p=0.04 for rs6265; 35.0 vs 23.8, p=0.01 for rs11030094). Neither allele was associated with an altered response to other dopaminergic medications. Analysis of PPMI subjects is ongoing.

Interpretation: Presence of risk alleles for *Bdnf* variants was associated with a worsened therapeutic response to levodopa. Genotyping for specific *Bdnf* variants may be a useful, 'precision medicine' approach to counsel PD patients regarding the efficacy of levodopa or other dopaminergic medications.

This research was supported by grants from the National Institute of Neurological Disorders and Stroke (NINDS, #NS095656) and the Saint Mary's Foundation.

76 Pro-efferocytic nanotherapy in atherosclerosis

Alyssa M. Flores

Stanford University School of Medicine, USA

Atherosclerotic cardiovascular disease continues to be the leading cause of death worldwide. It is now known that defective clearance of apoptotic tissue (efferocytosis) is a key driver of atherosclerotic plaque progression. We previously demonstrated that blocking the "don't eat me" signal CD47 can reverse this defect and prevent plaque expansion, however this antibody-based therapy also caused off-target clearance of red blood cells. To avoid this toxicity, we are evaluating single-walled carbon nanotubes (SWNTs) as a novel platform that may be able to deliver CD47 inhibitors specifically to the atherosclerotic plaque, without any off target toxicity.

Small-molecule inhibitors of CD47 signaling were evaluated in vitro in RAW264.7 macrophages to verify disruption of tyrosine phosphatase SHP1, the common downstream signaling pathway of CD47. SWNTs were prepared by loading carbon nanotubes with polyethylene glycol (PEG) for solubilization, Cy5.5 fluorophore for detection by fluorescence-activated cell sorting (FACS), and pro-efferocytic therapies (small-molecule inhibitors of CD47-SHP1 signaling). SWNTs were then evaluated for their ability to be taken up by monocytes/macrophages and promote efferocytosis in vitro by FACS. To study SWNT accumulation in the arterial plaque and other systemic tissues, samples of atherosclerotic aortae, blood, spleen, liver, lung, and heart were dissociated and analyzed 24h, 48h, and seven days after tail vein injection of SWNTs into atheroprone mice (apolipoprotein-E deficient, apoE^{-/-} mice).

Immunofluorescence staining confirmed that small-molecule SHP1 inhibitors suppress phosphorylation of SHP1 in macrophages. Dye-conjugated (naked) SWNTs rapidly and preferentially accumulated in mouse RAW264.7 and human THP1 macrophages in vitro (>80%), compared to other immune cells and vascular smooth muscle cells. In vivo pharmacokinetic studies showed enhanced uptake of SWNTs into intraplaque macrophages of apoE^{-/-} mice over time. Following seven days in circulation, total SWNT detection decreased in mouse blood, liver, lung, spleen, and heart, indicating minimal systemic accumulation. Standard in vitro efferocytosis assays demonstrated that SHP1-loaded SWNTs effectively promote clearance of apoptotic cells (4.3-fold), compared to naked SWNTs and SHP1 inhibitors alone. This effect was similar to efferocytosis rates induced by anti-CD47 antibodies in vitro.

Future studies will evaluate pro-efferocytic SWNTs for their ability to stably deliver to macrophages and enhance lesional phagocytosis in mouse models of atherosclerosis, without causing anemia. If effective, SWNTs may form the basis of a new "Trojan horse" platform for delivery of pro-efferocytic therapies to prevent atherosclerosis.

77 EWS-FLI1 driven transcription suppressed by a combination therapy of mithramycin and cyclin-dependent kinase 9 inhibition

Guillermo Flores

Michigan State College of Human Medicine/Van Andel Institute Graduate School, Grand Rapids, USA

Background: Ewing sarcoma (ES) is a pediatric soft tissue tumor with a poor prognosis. ES is dependent on the presence and activity of the oncogenic transcription factor, EWS-FLI1, that dysregulates gene expression at hundreds of targets. We have previously identified mithramycin (MMA) as a potent inhibitor of EWS-FLI1 driven transcription. However, only sub-therapeutic concentrations have been achieved in pediatric patients. To maximize inhibition, we

conducted an siRNA screen to identify gene targets that potentiated the effects of MMA in ES. Knock-down of several transcriptionally related genes significantly sensitized ES cells to the effects of MMA. We next developed a drug matrix screening platform to identify commercially available transcriptional inhibitors that also potentiated the effects of MMA on EWS-FLI1 driven transcription and ES cell viability. PHA-767491, a cyclin-dependent kinase 9 inhibitor (CDK9i), reverses the effect on EWS-FLI1 on several targets at both the mRNA and protein level across multiple ES cell lines when combined with MMA.

Methods: We utilize matrix drug screening to identify that PHA-767491 synergizes with MMA in terms of a reduction in cell viability as measured by MTS and cell growth as measured by time-lapse microscopy. We use RT-qPCR to measure changes in gene expression across multiple well characterized targets of EWS-FLI1 driven transcription. We use western blot analysis to measure changes at the protein level for these targets as well. We then use an orthotopic xenograft mouse model to measure changes in tumor size after administration of our MMA-CDK9i combination therapy.

Results: Our combination of MMA and PHA-767491 displays strong synergy as measured by Bliss-Independence. Multiple ES cell lines become unviable, with minimal effect on non-ES cells, and this effect is stable after removal of the compounds. This synergy is recapitulated as a reversal of EWS-FLI1 driven transcription across multiple targets at both the mRNA and protein levels. We see a similar effect in our animal model with a significant decrease in tumor volume with our combination therapy when compared to control or either agent alone. Importantly, our MMA-CDK9i combination uses drug concentrations that are clinically achievable.

Conclusions: We describe an MMA-CDK9i combination that displays excellent activity against EWS-FLI1 driven transcription. We confirmed this using multiple independent assays in both *in vitro* and *in vivo* models. We complete this work with the hope that it can eventually be translated to patients.

78 DXM: a novel algorithm to deconvolve genomic DNA methylation data to understand epigenetic clonality.

Jerry Fong

MD-PhD Program, Washington University in St. Louis, St. Louis, USA

DNA methylation refers to the presence of 5-methylcytosine in a CG dinucleotide context. Cancer exhibits globally altered patterns of DNA methylation, and in some instances, promoter methylation can silence expression of tumor suppressor genes. One study in diffuse large B-cell lymphoma (DLBCL) demonstrated that patients with increased heterogeneity in DNA methylation at presentation had worse prognosis. However, this study did not analyze the subclonal architecture that underlies epigenetic heterogeneity, and individual tumor subclones have been implicated in cancer progression, treatment resistance, and metastasis. Given that experimental techniques to identify epigenetic subclones have some limitations and that there is a plethora of bisulfite sequencing data being generated from heterogeneous tumor samples, there is a need to develop computational methods to analyze this methylation data at the subclonal level.

We have developed a novel algorithm, DXM, to deconvolve methylation sequencing data of a heterogeneous clinical sample into the number of major subpopulations, their prevalence, and their respective methylation profiles. Briefly, for each gene, DXM solves for the number of subpopulations (alleles) iteratively. The percent

composition and methylation profiles are solved with an alternating optimization scheme including a modified Hidden Markov Model. Afterwards, the allelic methylation profiles for all genes are assigned to their corresponding subpopulations by solving a mixed-integer quadratic program.

Training for DXM was conducted with bisulfite sequencing data of somatic tissues available from the Roadmap Epigenomics Project. To test DXM and benchmark its performance, reads from bisulfite sequencing experiments of various lymphocytes (Blueprint Epigenome Project) and cell lines (ENCODE) were subsampled and combined to form synthetic "mixtures," where the read counts from each underlying cell type reflected its expected percent composition in the mixture. DXM accurately deconvolved these mixtures into the number of major subpopulations, their prevalence, and their respective methylation profiles. On these mixtures, DXM also outperformed existing methylation-deconvolution algorithms such as methylPurify and methylFlow. To validate DXM, methyl-Seq (Agilent promoter capture) was conducted on primary DLBCL samples. DXM accurately deconvolved these samples, as compared to reference methylation profiles and to clinical flow data for these samples. We are currently planning analyses to identify epigenetic subclones of DLBCL and acute myeloid leukemia (AML), where genetic subclonal architecture is well-characterized. In the future, we hope that DXM can be broadly applied to understand epigenetic clonality of multiple cancer types and improve patient prognostics and therapy.

79 Grand Valley State University Pre-MD/PhD Club

Alexia Frantzeskakis

Grand Valley State University, Canton, USA

The Pre-MD/PhD Club at Grand Valley State University focuses on promoting awareness of MD/PhD programs and developing individuals to bridge the gap between scientific research and clinical medicine. The club advocates professional and personal development, emphasis on research, and networking skills. Career exploration on physician-scientists and clinical-physicians is provided by guest speakers, university Career Services, videos such as TED Talks, and conferences. Students are provided with the resources to dissect medical journals and understand the scientific literacy of articles. The Pre-MD/PhD club aids its members in discovering research interests, how to build strong applications for medical/graduate school, and balance school life.

80 The Influence of Phosphomimetic Nato3 on Dopamine Neuron Gene Expression

Melina Frantzeskakis

Grand Valley State University, Canton, USA

Midbrain Dopamine neurons (mDA) can arise from the floor plate of the midbrain and are responsible for the symptoms of Parkinson's disease when they cease to function. mDA neurogenesis and maturation are regulated by multiple genes such as Shh, Foxa2, and Lmx1a/b among others. Genes that promote formation of mDA have potential to be used for clinical therapy development in Parkinson's disease. One gene involved in dopamine neurogenesis is the basic helix-loop-helix transcription factor Nato3. However, its mechanism of action is not well known. Nato3 is expressed throughout the entire floorplate, however it only produces dopamine neurons in the caudal region of the midbrain. To better understand the mechanism of Nato3, specific amino acids were altered to mimic the charge at putative phosphorylation sites, creating multiple variants of phosphomimetic Nato3 (PM Nato3). We hypothesized that PM Nato3 had the ability to upregulate the dopamine neuron marker expression *in vivo* and

in vitro more effectively than wildtype Nato3. These current data show greater upregulation of genes important for the formation of dopamine neurons by some variants of PM Nato3 than wild type Nato3 in vivo and the immortalized mouse midbrain cell line. PM Nato3 upregulation of these genes suggest that the phosphorylation status of Nato3 can influence the expression of genes known to drive dopamine neurogenesis, raising it as a potential target for therapeutic development.

81 Exploring the Role of Arid1a and Chromatin Remodeling in the Pancreas and Kras-mediated Transformation

Scott Friedland

University of Rochester School of Medicine and Dentistry, Rochester, USA

Introduction: Pancreatic Adenocarcinoma (PDAC) is an almost universally fatal disease, lacking effective treatments. PDAC develops mainly from two precursor lesions, pancreatic intraepithelial neoplasia (PanIN) and intraductal papillary mucinous neoplasm (IPMN). Similar mutations are found in PanINs and IPMNs, which arise from acinar cells and ducts, respectively. Frequently mutated genes in PDAC including KRAS, TP53, SMAD4, and CDKN2A have been extensively studied. However, the SWI/SNF complex (an ATP-dependent chromatin remodeling complex) has mutations in more than 1/3RD of cases, and has not been well explored in this disease. A DNA-binding subunit, ARID1A, is deleteriously mutated in about 8-15% of cases. Our objective is to understand the effects of ARID1A loss on pancreatic function and PDAC development, and its opposition to Kras-mediated transformation. **Methods:** Compound-mutant mice containing pancreas-specific expression of Cre recombinase (C), one or two conditional null alleles of Arid1a (Af/+ or Af/f), with or without activation of oncogenic KrasG12D (K) were studied longitudinally. In vitro studies used mouse embryonic fibroblasts (MEFs) with the same alleles, treated with Cre-EGFP or EGFP control adenoviruses. **Results:** Arid1a-null (CAf/f) mouse pancreases show progressive attrition of the acinar population with acinar to ductal metaplasia, and ductal expansion. The pancreas of CAf/f mice have significantly higher rates of proliferation and apoptosis than controls, and this proliferative phenotype is driven by the ductal compartment. When combined with KrasG12D, loss of Arid1a produce cystic pancreases that resemble human IPMNs, as opposed to PanIN that predominate in the KC and KCAf/+ cohorts, which decreases survival in the KCAf/f cohort. In both the KCAf/f and KCAf/+ cohorts there were rare malignancies with metastases. MEFs with the KAf/f alleles show replicative immortality, and other phenotypes associated with transformation, much faster than controls. RNA-seq and ATAC-seq were used to identify important gene sets in the transformed state, and assess the chromatin landscape in nearby gene-regulatory regions, respectively. **Conclusions:** Here we demonstrate the importance of ARID1A in pancreatic tissue homeostasis, and cancer development. ARID1A restrains proliferation in ducts and Kras-mediated expansion of cystic IPMNs. Our in vitro work is beginning to uncover the gene regulatory alterations that allow Kras-mediated transformation after Arid1a deletion.

82 Elucidating endocrine functions of peripheral neuromedin U in regulating metabolism

Mollie S.H. Friedlander

Stanford University School of Medicine, USA

Metabolic diseases are polyhormonal disorders, and a subset of the hormones that regulate these diseases remain uncharacterized. Previous research has focused on understanding hormones that regulate insulin secretion in the fed state, but it is apparent that

sustained fasting also alters the dynamics of insulin regulation, resulting in diminished insulin output, glucose intolerance, and "starvation diabetes." While the role of incretins in promoting insulin secretion during feeding is well-documented, a counter-regulatory hormone that decreases insulin output (a "decretin") during fasting has not yet been identified in mammals. Recently, our group characterized an index decretin hormone in *Drosophila* and identified its mammalian orthologue, Neuromedin U (NMU).

NMU encodes a secreted peptide that is expressed in the hypothalamic "feeding center" and gastrointestinal cells. Both NMU deficiency and excess have been linked to altered glucose metabolism in mammals. Mice expressing a truncated form of NMU demonstrate increased adiposity and hyperinsulinemia, and a familial variant of NMU encoding a missense substitution (R165W) cosegregates with early-onset obesity and hypertriglyceridemia in humans. Conversely, ubiquitous overexpression of NMU in mouse results in hypoinsulinemia and reduced body weight, and our group previously reported ectopic NMU expression in pancreatic tissue from patients with pancreatic ductal adenocarcinoma, a disease associated with pancreatogenic diabetes.

While prior research has investigated the role of NMU in central regulation of satiety, our studies aimed to characterize the function of peripheral NMU in regulating insulin secretion and metabolic homeostasis. Specifically, we (1) profiled NMU-expressing enteroendocrine cell gene expression by RNA-Seq, (2) evaluated the effects of NMU and peripheral NMU receptor (NMUR1) signaling on insulin secretion from pancreatic islets, and (3) generated transgenic models to explore the role of NMU misexpression in pathological states associated with insulin dysregulation. Consistent with a decretin profile, circulating NMU levels increased during fasting in both mice and humans. Following FACS purification, RNA-Seq data revealed that NMU-expressing cells demonstrate a unique enteroendocrine signature. NMUR1 expression was detected in insulin+ cells of human and murine pancreatic islets and, while NMU suppressed glucose-stimulated insulin secretion from wildtype islets, this effect was lost in mice lacking NMUR1. To investigate the role of peripheral NMU in vivo, we developed a conditional knockout allele and an inducible NMU misexpression allele in mice.

Collectively, our results support a model in which NMU secreted from enteroendocrine cells of the gastrointestinal tract during fasting interacts with pancreatic islets to suppress insulin secretion in an NMUR1-dependent manner. Furthermore, we present mouse models to investigate the link between NMU misexpression and altered metabolism in human disease. These studies address essential questions about links connecting peripheral NMU function and insulin biology, and a better understanding of the role of decretins in insulin regulation may transform current therapeutic approaches to treating metabolic diseases.

83 Exome sequencing uncovers the molecular pathogenesis of vein of Galen cerebral arterio-venous malformations

Jonathan R. Gaillard

Yale School of Medicine, USA

Vein of Galen malformations (VOGMs) are particularly severe arterio-venous malformations of the developing brain. If untreated, VOGMs cause high-output cardiac failure, hydrocephalus, brain hemorrhage, and death. Our limited knowledge of the molecular genetics of VOGMs has hindered the development of novel therapies. We hypothesized that the apparent sporadic occurrence of VOGM may frequently be attributable to damaging de novo mutation events or incomplete penetrance of rare transmitted variants. Unbiased whole-

exome sequencing (WES) can overcome these barriers for gene discovery.

Using a dynamic and innovative HIC/IRB-approved social media campaign and teaming with multiple domestic and international collaborators, we recruited the largest VOGM cohort to date in less than 1.5 years. Germline DNA was isolated from 50 unrelated probands harboring radiographically-confirmed VOGMs. Both parents were available for 48/50 probands. WES was performed on all participating individuals (n=148). Variants in both cohorts were called using the Genome Analysis Toolkit (GATK) Haplotype Caller and annotated for allele frequencies in Exome Aggregation Consortium (ExAC), 1000 Genomes, Kaviar, and Exome Variant Server (EVS). De novo mutations were identified using TrioDeNovo and the impact of missense mutations was inferred using MetaSVM and a custom bioinformatics pipeline. Transfections of constructs harboring VOGM mutations in HEK293 cells, followed by immunoprecipitation and immunoblotting, were performed to determine impact on biochemical function. Further functional validation *in vivo* was performed in *Xenopus tropicalis* using CRISPR/Cas9 gene editing.

Gene burden analysis revealed exome-wide significant enrichment of rare transmitted damaging mutations in ephrin type-B receptor 4 (EPHB4; n=4; p=2.34 x 10⁻⁷, 80.52-fold enrichment), a key regulator of arterio-venous differentiation. Additional damaging rare inherited mutations were identified in the upstream EPHB4 ligand ephrinB2 (EFNB2); the downstream EPHB4 effector Ras GTPase-activating protein 1 (RASA1), mutated in CM-AVM type 1; and the associated EphrinB2-EphB4 regulator activin A receptor like type 1 (ACVRL1), mutated in Hereditary Haemorrhagic Telangiectasia. Two novel damaging mutations were identified in the ACVRL1 paralog activin A receptor type 1 (ACVR1), not previously implicated in human disease. Together, mutations in EPHB4 signaling components accounted for 9/50 (18%) of cases. VOGM-associated EPHB4 mutants, relative to wild type, are associated with significant impairment of RAS/MAPK/ERK1/2 and PI3K/AKT/mTOR signaling in mammalian cells. X. tropicalis embryos injected with CRISPR/Cas9 targeted against RASA1 or EPHB4 harbored severe neural tube defects compared to controls, and decreased and irregular expression of *msr* and *prox1*, demonstrating widespread impairment of vascular and lymphatic development.

This work demonstrates the power of social media to recruit actionable genetic cohorts for rare diseases in unprecedented time, and has uncovered the critical genetic determinants and molecular mechanisms of VOGM. These results have potential diagnostic screening implications for family members, and identify specific genes and pathways for the development of targeted therapeutics.

84 Regulation of IgA protease expression in nontypeable *Haemophilus influenzae* during persistence in chronic obstructive pulmonary disease

Mary Gallo

University at Buffalo Jacobs School of Medicine and Biomedical Sciences, Buffalo, USA

Nontypeable *Haemophilus influenzae* (NTHi) is the most common cause of acute exacerbations of chronic obstructive pulmonary disease (COPD). NTHi also persistently infects the lower airways of adults with COPD, causing worsening of inflammation and symptoms. One virulence factor of NTHi is IgA proteases that cleave human mucosal IgA1 antibody at the hinge region and mediate intracellular survival in respiratory epithelial cells. There are two distinct IgA protease genes at different loci, *igaA* and *igaB*, each with two variants. Each of the 4 IgA protease variants has a

characteristic cleavage specificity for the hinge region of human IgA1. We hypothesize that expression of IgA protease changes during persistent infection of lower airways in COPD.

IgA protease expression was determined by immunoblot assay after incubation of broth culture supernatants with purified human IgA1 antibody. We analyzed IgA protease gene sequences from genome sequences in strains that demonstrated changes in enzymatic activity during persistence.

As part of a 20-year longitudinal study of adults with COPD at the Buffalo VA Medical Center, 101 strains of NTHi that persisted in adults with COPD from 2 to 56 months were assessed for IgA protease activity. Two of the 50 strains that expressed IgA protease A1 upon acquisition by the patient showed absent expression after persistence in COPD airways. Two of the initial 11 strains expressing IgA protease A2 upon acquisition stopped expressing and two of the initial 23 strains expressing IgA protease B1 stopped expressing after persistence. Sequence analysis revealed that insertions or deletions ranging in size from 1 to 49 basepairs causing the genes to be out of frame conferred these phenotypic changes in each of the strains that shut off expression of IgA protease A1, A2 and B1 during persistence.

The change in IgA protease B2 expression was not explained by examining the open reading frames, but instead we discovered an upstream "TCAAAAT" simple sequence repeat that varied in number among strains with the IgA protease B2 gene. Analysis of 10 strains revealed that when the number of this 7-nucleotide repeat caused the gene to be out of frame, it was not expressed, whereas when the number of repeats caused the gene to be in frame, it was expressed. Thus, IgA protease B2 expression varies during persistence, and its expression is regulated by slipped strand mispairing.

In summary, IgA proteases A1, A2, and B1 undergo genetic changes that result in altered expression during persistence. Expression of IgA protease B2 is regulated by slipped-strand mispairing of an upstream 7-nucleotide repeat during persistence in adults with COPD. We conclude that NTHi regulates expression of IgA proteases during persistence in the human respiratory tract.

85 Fibrotic scar formation in the retina following laser injury

Ryan A. Gallo

University of Miami Miller School of Medicine, Miami, USA

Injury to the central nervous system (CNS) leads to scar formation that has both glial and fibrotic components. Scar formation is important for repairing the lesion, but also results in inhibition of nerve regeneration. Unlike the glial scar, much less is known about the fibrotic scar. We characterize fibrotic scar formation in the CNS using *in vivo* retinal laser trauma and imaging. Transgenic mice in which GFP is expressed under the control of the collagen promoter (Col1α1-GFP mice) were subjected to retinal injury by a photodisruptive Nd:YAG laser. In each animal, the retina of one eye was lasered while the contralateral eye was used as a non-lasered control. Spectral domain optical coherence tomography (SD-OCT), confocal scanning laser ophthalmoscopy (cSLO), and fluorescein angiography (FA) were performed at baseline and at various time points following injury. Antigenic profiling was carried out two weeks after injury to define the cellular identity of recruited Col1α1-GFP cells that contribute to fibrotic scar formation. Baseline cSLO and FA imaging revealed Col1α1 fibroblast cells promptly localized within the major retinal blood vessels. A weaker GFP signal was observed within the choroidal vascular bed. Col1α1 cells were observed around the site of injury as early as three days after laser injury, and recruitment peaked at approximately two weeks

later. SD-OCT and cSLO imaging demonstrated that disruption of Bruch's membrane was necessary for Col1 α 1 recruitment. Col1 α 1-GFP signal was confined only to the choroid, and not retina, in both control eyes and areas of damage that lacked Bruch's membrane disruption. In areas of injury with Bruch's membrane damage, Col1 α 1-GFP signal was observed between the choroid and the retina. Cellular profiling of the fibrotic scar two weeks after injury revealed positive antigenicity for PDGFR- β , CD45, and vimentin. Damage to the retina in mammals results in scarring and irreversible loss of retinal neuronal phenotypes. Using transgenic mice, we show that Col1 α 1 cells contribute to the fibrotic scar in the retina following injury. In vivo imaging strongly suggests that perivascular Col1 α 1 cells migrate to the injury site from the arteries or choroidal vascular bed of the eye after disruption to Bruch's membrane. At two weeks after injury, Col1 α 1 cells in the fibrotic scar express characteristics of perivascular cells with their PDGFR- β ⁺ immunoreactivity. Other cell types contribute to scar formation that are Col1 α 1⁺ and express CD45 or vimentin, which are fibrocyte/leukocyte and mesenchymal cell markers, respectively. A better understanding of the underlying mechanisms of fibrotic scar formation in the retina offers promise for promoting retinal regeneration.

86 Investigating key residues of PCSK9 processing and modulators of PCSK9-mediated degradation

Adri M. Galvan

Pennsylvania State University College of Medicine, USA

Proprotein convertase subtilisin/kexin type 9 (PCSK9) binds the LDL receptor (LDL-R) and induces lysosomal-mediated degradation, increasing LDL cholesterol (LDL-C), and, consequently, cardiovascular risk. Thus, PCSK9 has emerged as a prime therapeutic target against heart disease. Self-proteolysis of PCSK9 produces a mature, yet catalytically inactive protein which is shuttled extracellularly to bind and chaperone LDL-R for degradation. We previously identified PCSK9 processing as occurring via two independent mechanisms: proteolysis and proteolysis-independent secretion. We then developed parallel high-throughput luminescence assays capable of assessing each step. These assays allowed us to analyze key residues for both events using saturation mutagenesis libraries determining residues P6 and P4 through P1* of the cleavage sequence to be highly specific for maintenance of function. We also evaluated single nucleotide polymorphism (SNP) effects on each mechanism of PCSK9 processing and found a high percentage of the SNPs analyzed to alter proteolysis. Based on our results, we examined potential structural implications of the SNPs, defined proteolysis to be the rate limiting step of PCSK9 processing, and identified a region of the protein involved in allosteric regulation of PCSK9 proteolysis.

While PCSK9 processing involves these two steps for production, little is known about mediators of PCSK9 and LDL-R binding. Cell-based studies have shown LDL-C inhibits PCSK9-mediated degradation, though the mechanism of its effect is unclear. Recently, heparan sulfate proteoglycans (HSPG) were suggested to act as co-receptors on the hepatocyte facilitating the LDL-R:PCSK9 interaction. By adapting our high-throughput assay, we investigated the relationship of these two effectors on PCSK9 uptake to elucidate the mechanism of LDL-C's inhibitor effect on PCSK9. We also compared the inhibitory effects of LDL-C variants, such as oxidized LDL-C and lipoprotein(a), on PCSK9-mediated degradation. We found the inhibition of PCSK9 uptake to be additive with the introduction of exogenous heparin, competing for HSPG chaperone binding, and LDL-C. However, maximal inhibition of PCSK9 uptake

could be achieved with heparin alone indicating related pathways which supports previous data demonstrating a similar N-terminal PCSK9 binding region for both mediators. Our studies provide further insight into PCSK9 biochemical processing and modulators of PCSK9 metabolism, with implications for finding new targets to lower LDL cholesterol and prevent atherosclerosis.

87 A tale of two viruses: cognitive recovery in the post-infectious CNS

Charise Garber

Washington University in St Louis, School of Medicine, Saint Louis, USA

Cognitive dysfunction following viral encephalitis is associated with persistent reactive changes in microglia and astrocytes. T-cell infiltration into the CNS is necessary for viral clearance, however subsequent persistence of memory T-cells after the acute insult may lead to altered neuroimmune communication and contribute to delayed recovery of cognitive function. Using an established model of West Nile Virus (WNV) neuroinvasive disease, we show that persistent CD8 T-cells in the CNS express cytokines that influence normal cognitive function, including interferon (IFN)- γ . Lack of IFN- γ signaling leads to delayed clearance of infectious virus, and increased persistence of viral genome in the hippocampus, but protection from WNV-mediated deficits in spatial learning. Microglial specific deletion of IFN γ R or administration of IFN- γ neutralizing antibody to WT mice is sufficient for cognitive protection. Finally, lack of IFN- γ signaling leads to cognitive protection from a related flavivirus, Zika virus (ZIKV), despite differences in neural tropism. Our results reveal that postinfectious interactions between infiltrating T-cells and resident microglial cells may prevent complete cognitive recovery, and provide a novel target for therapeutic intervention following viral encephalitis.

88 Induced pluripotent stem cell modeling of sarcomere disruption in human hypertrophic cardiomyopathy

Amanda Garfinkel

Harvard Medical School Department of Genetics, Boston, USA

Hypertrophic cardiomyopathy (HCM) is a dominant myocardial disease caused by missense mutations in sarcomere proteins. The pathophysiology of HCM has been long described as one of cellular hypercontractility with poor relaxation (a hallmark of diastolic insufficiency) and energetically expensive cardiac sarcomeres, but the link between pathogenic genotypes and this characteristic phenotype remains incompletely elucidated. Uncertainty persists regarding how sarcomere mutations increase sarcomere power, as mutated amino acids more commonly reduce the function of proteins, and how amino acid substitutions perturb sarcomere relaxation.

Cryo-electron microscopy of tarantula striated muscle predicts an interacting-heads motif (IHM) that plays an important role in healthy sarcomere function. In this dynamic interaction, one or both heads of a myosin head pair bind the thick filament backbone, inhibiting myosin ATPase and limiting its ability to bind actin. IHM stability is important to maintain appropriate sarcomere relaxation, and IHM destabilization may promote sarcomeric hypercontractility and energy expenditure by enabling extra myosin heads to hydrolyze ATP. We believe IHM disruption represents an important part of disease pathogenesis in certain HCM variants.

Using human induced-pluripotent stem cell-derived cardiomyocytes (hiPSC-CMs) together with CRISPR/Cas9, we introduce HCM-linked sarcomere mutations into isogenic hiPSC lines, generating heterozygous and homozygous variants in genes that may impact

the IHM, including *MYBPC3* truncations and missense mutations in *MYH7*, *TNNT2*, and *TNNI3*. To analyze hiPSC-CM contractility to model disease, we introduce our patient-specific mutations into a line with a GFP-fusion reporter tagged to the N-terminus of titin; this fluorescent tag illuminates the Z-disc boundaries of sarcomeres without disrupting sarcomere assembly or function.

Isogenic edited and wild type hiPSC-CMs are characterized to assess contractile parameters including resting sarcomere length, relaxation time, and shortening fraction, using pacing (1 Hz) to approximate the adult human heart rate. Imaging is acquired with a Keyence BZX microscope using a GFP filter cube and a Nikon 100x objective and analyzed using a custom-built MATLAB program that enables tracking of fluorescent sarcomeres. To investigate if mutations alter IHM properties, permeabilized cells are studied using Mant-ATP, which is a fluorescent, non-hydrolysable analogue of ATP. From biochemical analyses, the relative proportions of myosin heads in the bound versus unbound states of the IHM are deduced, yielding insight into sarcomere pathophysiology in human HCM cardiomyocytes. Each of these assays are repeated after treatment with a small molecular myosin ATPase inhibitor to determine if this therapy corrects functional aberrations.

89 Recording from large ensembles of neurons in primate primary visual cortex

Anupam Garg

Salk Institute for Biological Studies, San Diego, USA

Decades of previous work have revealed the functional and anatomical organization of primate primary visual cortex (V1) at the level of cortical layers and columns. However, recent technological advances in extracellular electrophysiology and two-photon calcium imaging have allowed for investigation of more detailed cortical organization at the cellular level. We aim to develop and further refine approaches to link large ensembles of neurons in V1 to their laminar identity, cell types, functions, and connectivity. In this study, we demonstrate the ability of high-density Neuropixels electrode arrays and two-photon calcium imaging using GCaMP6f to increase our understanding of the principles and mechanisms by which large populations of neurons transform sensory input to give rise to patterns of neuronal activity in macaque V1. Integrating multiple imaging and recording technologies enables us to perform detailed studies revealing computational and organizational principles of functional cortical connectivity.

Using next-generation Neuropixels electrode arrays, we demonstrate the ability to simultaneously record from 50-100 V1 neurons across all cortical layers. In these experiments, we present a series of chromatic and achromatic visual stimuli consisting of stationary and moving gratings, which allows us to characterize cellular receptive fields of a wide array of cell types. Simultaneously recording from large ensembles of neurons enables us to use reverse correlation and cross-correlation analyses to reveal circuit mechanisms between functionally connected pairs or groups of neurons. Combining these results with current source density (CSD) analysis, in which we assign a laminar identity to each recorded neuron, enables us to reveal the laminar organization of color-responsive neurons in macaque V1.

In combination with our work using extracellular electrophysiology, we robustly express GCaMP6f in V1 using the TET-Off inducible gene expression system, allowing simultaneous imaging of calcium responses from hundreds of neurons. Using these results, we can align the calcium imaging responses with postmortem cytochrome oxidase staining to identify the locations of blobs and inter-blobs, and compare the differences between neuronal activity in each of these locations in response to a variety of visual stimuli.

90 Molecular evolution of adeno-associated virus for targeting of microglia in Parkinson's disease

Aysegul Gezer

Michigan State University, Grand Rapids, USA

Parkinson's Disease (PD) is a neurodegenerative disorder with multisystem failure. The pathological hallmark of PD is protein aggregates, termed Lewy bodies, found inside neurons and implicated in the disease process. Ongoing research demonstrates that neuroinflammation plays an important role in the pathophysiology of PD. Accumulating evidence from studies, including post-mortem investigations of human PD brains, attests the contribution of chronic inflammation to the death of dopaminergic neurons of the substantia nigra in PD. Microglia, the dominant antigen presenting cells of central nervous system (CNS), play a crucial role in neuroinflammation; yet, the exact role of these cells in PD disease etiology isn't well defined. One of the challenges to study microglial biology is the lack of an experimental tool to specifically manipulate microglia. The aim of this project is 1) to generate a novel tool to study microglial biology and 2) investigate role(s) of microglia in neurodegeneration in PD.

Adeno-associated virus (AAV) is the most commonly used tool for gene therapy because of sustained gene expression and safety profile. In the central nervous system, AAV transduces neurons, however microglia remain remarkably refractory to transduction. Viral capsid, encoded by the CAP gene, determines AAV tropism. A plethora of natural and recombinant AAV serotypes are discovered so far differing in capsid structure. This study utilizes two techniques to engineer AAV capsids to selectively and specifically target microglia. First is random DNA family shuffling of natural and recombinant capsids. This involves digestion of various cap genes from different AAV serotypes and randomly reassembling them into full length chimeric capsids. The second method is using a peptide display library where short peptides, 7-20aa long pieces of known microglial surface receptor ligands, are introduced into the AAV capsids. Capsid libraries are then selected for microglia in vivo.

We aim to utilize the microglial-specific AAVs to study the role of alpha-synuclein (α -syn) in PD. α -syn is the chief component of Lewy bodies and α -syn-mediated neurotoxicity is thought to involve neuroinflammation. Here we hypothesize that overexpression of α -syn in microglia will exacerbate neurodegeneration.

Finally, it is crucial to note that microglia-specific AAV vectors are promising tools to study not only PD, but also other neuroinflammatory diseases of which the role of microglia is being increasingly recognized.

91 Investigation of changes in extracellular vesicles from glioblastoma cells treated with gene-mediated cytotoxic immunotherapy

Alexandra M. Giantini Larsen

Brigham and Women's Hospital

Glioblastoma (GBM) is a devastating malignant brain cancer whose progression is driven by a subset of GBM stem-like cells (GSCs). In order to improve survival, novel therapeutics using gene-mediated cytotoxic immunotherapy (GMCI) are being studied. GMCI inserts the gene for a therapeutic enzyme or protein into cells using an engineered virus. One use of GMCI to target GBM involves intratumoral injection of a non-replicating adenovirus (AdV) that expresses the herpes simplex virus thymidine kinase (HSV-tk) gene. An anti-herpetic prodrug that requires activation by HSV-tk is administered and the activated toxic nucleotide causes cell death that promotes an immune response. GMCI is now in clinical trials

for patients with GBM. However, the identification of biomarkers that measure tumor responsiveness to the treatment is still needed. Extracellular vesicles (EVs) are important mediators of intercellular communication, and can transmit biological information. Tumor-derived EVs are found in several biological fluids, including CSF and blood, and represent an excellent source of biomarkers. The goal of this study was to identify changes in EVs secreted by GBM cells treated with GMCI compared to control cells.

To determine the time of maximum expression of the HSV-tk gene and optimal time for exosome collection, the expression of green fluorescent protein (GFP) was monitored after cells were infected with an AdV-expressing the GFP gene. Maximal expression occurred at 24 hours. Viral infection of cells with an AdV-expressing the HSV-tk gene (AdV-tk) was confirmed by treatment of cells with increasing concentrations of the anti-herpetic prodrug ganciclovir (GCV). GCV showed strong cytotoxicity against the GSCs with an IC50 of 0.1 μ M at 96 hours. Differences in EV size were detected between control cells and virally infected cells using the Nanosight at 24 and 48 hours after infection. The concentration of EVs in virally infected cells was 100-fold less than control cells at 24 and 48 hours. However, control EVs showed a main population of EVs around 100 nm, while virally infected cells secreted two different populations of EVs around of 85 and 140 nm. At 48h after infection, the size of the main population of EVs remained consistent while the virally infected cells secreted EVs shifted more to the larger population.

Our results suggest that AdV-tk treatment of glioblastoma cells may alter EV quantity and size. Ongoing studies are being performed to further characterize these EVs.

92 Identifying functionally informative multiple sequence alignments

Nelson H. Gil

Albert Einstein College of Medicine, Bronx, USA

Although high-throughput genome sequencing technologies have made on the order of 100,000,000 unique protein sequences available in current public databases, there are only approximately 1,000 detailed annotations of protein function. In other words, roughly only a single protein function is known for every 100,000 available sequences. A central goal of bioinformatics is to close this monumental gap through functional annotation of genomes. The principal motivation for this is that detailed functional annotations are necessary for progress in biomedicine, particularly in the area of rational drug design. A common approach to functional annotation is the analysis of conservation patterns in multiple sequence alignments (MSAs) - the idea being that evolutionarily conserved amino acid positions in proteins (MSA columns) are functionally important. However, the optimal selection of sequences to obtain biologically informative MSAs is poorly-explored, and has traditionally been performed manually, which is tedious and subjective.

We present Selection of Alignment by Maximal Mutual Information (SAMMI), an automated, sequence-based approach to objectively select an optimal MSA from a large set of alternatives sampled from a general sequence database search. The hypothesis driving this approach is that the mutual information (a mathematical quantity indicating strength of correlation) among MSA columns will be maximal for those MSAs that contain the most diverse set possible of the most structurally and functionally homogeneous protein sequences. This is based on the idea that correlation patterns among amino acid positions in protein sequences encode a structural and functional fingerprint that uniquely defines a set of evolutionarily-related proteins.

SAMMI was tested to select MSAs for functional residue prediction by analysis of conservation patterns on a diverse cross-section of the proteome consisting of a set of 435 proteins obtained from protein-ligand (peptides, nucleic acids and small-molecule substrates) and protein-protein interaction databases. Our results demonstrate that in the majority of proteins, the conservation pattern of an appropriately selected MSA can capture on average 70% of functionally important residues compared to 25% in controls ($p < 0.01$); these results double the current state-of-the-art. Furthermore, a detailed analysis of the minority of proteins whose functionally important residues were "missed" indicates that the conservation patterns of MSAs selected by SAMMI are likely to represent unannotated functional residues. This suggests that "failed" cases are simply "unannotated" and represent no specific failing of our algorithm.

Addressing the genome functional annotation problem will only increase in importance as the number of available protein sequences exponentially grows. Finding ways to extract useful knowledge from this mass of information is critical to biomedical progress. SAMMI represents an important contribution to solving this problem by providing an objective, data-driven way of selecting optimal MSAs, which are a central tool for genome analysis in bioinformatics.

93 AIRE in pregnancy: autoimmune regulator gene may support maternal-fetal tolerance via deletion of reactive maternal T cells

Eva M. Gillis-Buck

University of California San Francisco, USA

Complications of pregnancy, such as recurrent miscarriage, may represent a failure of maternal-fetal immune tolerance. The autoimmune regulator gene (AIRE) is a crucial component of tolerance to self-antigens, but its relevance for maternal-fetal tolerance has not yet been explored. AIRE contributes to both central and peripheral tolerance via the presentation of tissue specific antigens (TSAs), leading to the clonal deletion of self-reactive T cells. These TSAs include placental antigens, which we call "distant self" antigens, since they are encoded in the maternal genome, but have not been expressed since the mother was herself an embryo with a placenta. We hypothesize that AIRE-driven maternal tolerance of "distant self" placental TSAs are critical for successful embryo implantation and development. To test this, we first investigated AIRE expression in pregnant and nonpregnant female mouse tissues. Using qPCR, RNAscope, and immunohistochemistry, we found AIRE-expressing cells in the uterine draining lymph nodes. To test the functional role of AIRE during pregnancy, we next used an AIRE-diphtheria toxin receptor (DTR) transgenic mouse model to ablate AIRE-expressing cells during the first nine days of an allogeneic pregnancy. We found significantly smaller litter sizes ($p < 0.0001$) and smaller embryos ($p = 0.005$) in a subset of AIRE-DTR pregnancies (30% of $N = 10$), compared to wildtype (WT) pregnancies given DT ($N = 11$). Flow cytometry of maternal tissues showed AIRE-DTR pregnancies had more CD4+ T cells ($p = 0.003$) and fewer FoxP3+ Tregs ($p = 0.003$) in the uterus, and more CD25+CD4+ T cells ($p = 0.019$) in peripheral lymph nodes. AIRE-DTR mice were less likely to be pregnant after a confirmed plug (rate of pregnancy on embryonic day 9.5: 67% AIRE-DTR vs 92% WT), suggesting decreased fertility or early pregnancy loss. Thus, although AIRE expression may decrease during pregnancy, AIRE-expressing cells may still play an important role in maternal-fetal tolerance by deleting reactive maternal T cells and promoting maternal Treg differentiation. Future work will use RNA-sequencing to compare transcription profiles of thymic and peripheral AIRE-expressing cells in pregnant versus nonpregnant

female mice, with the goal of identifying candidate placental TSAs that may be responsible for maternal T cell reactivity towards the placenta and developing embryo.

95 Establishment of a Murine Behavioral Model to Investigate the Role of the Microbiome in Major Depressive Disorder and Crohn's Disease

Adrian S. Gomez-Nguyen

Case Western Reserve University, Cleveland, USA

The microbiome plays an intimate and multifaceted role in Crohn's Disease (CD). Increasing evidence has demonstrated that CD patients exhibit an inappropriate immune response to the microbiome. In addition, recent evidence has cemented the connection between the microbiome, the gut, and the brain. This is significant because patients with CD have disproportionately high rates of depression and anxiety. Alterations in the microbiome leads to major changes in behavior which reinforces the microbiome as a previously unrecognized, but significant, therapeutic target which will revolutionize the therapeutic landscape of treating patients with CD and depression. The aim of this study is to establish a mechanistic link between the microbiome and depression in CD. Our ultimate goal is to improve patient's behavioral diagnoses through manipulation of the microbiome.

To establish a behavioral baseline for our model, we performed behavioral studies using male SAMP mice (n=10) at various ages with AKR/J (AKR), C57BL/6, SAMP6, and SAMR1 mice as controls. Behavioral studies included tail suspension (TS), open field (OF), elevated plus maze (EPM), rota-rod, grip strength, Barnes maze, and Y-maze. Flow cytometry sorted microglial, immunohistochemistry, and 9.4T brain MRI were used to analyze brains. Ileal myeloperoxidase activity, histological severity, and cytokine transcription and secretion were used to measure disease severity. Fecal microbiome was analyzed using 16s rRNA gene sequencing.

As expected, our SAMP mice exhibited marked ileal inflammation when compared to AKR mice. Gross cobblestoning, increased MPO activity, and worse histology score all indicated severe ileitis. Surprisingly, the SAMP mice did not develop depressive or anxiety-like behavior with increasing inflammation (depressive behavior measured with TS and anxiety-like behavior measured with EPM and OF). Conversely, despite a benign inflammatory phenotype, the AKR mice demonstrated marked depressive behavior when compared to SAMP ($p < 0.0001$). These changes were not due to changes in motor function as demonstrated by non-significant differences in the rota-rod, grip strength, and open field activity ($p > 0.066$, $p > 0.49$, and $p > 0.085$ respectively). Microbiome results are pending but will be available at the time of the conference.

The ability of the SAMP mice to maintain a constant behavioral phenotype despite worsening disease is a welcomed surprise. With these results, we now have a model of spontaneous CD that does not naturally develop depressive behavior. In addition, we also have a model that does not develop intestinal inflammation but does develop spontaneous depressive behavior. These powerful models will allow us to manipulate behavior and microbiome to further elucidate the connection between CD and depression.

96 Optimizing Success of Physician-Scientists

Ruth Gotian

Weill Cornell Medicine, New York, USA

This qualitative case study was designed to explore with a group of exemplar physician-scientists what factors contributed to their success. The study was based on the following assumptions: (1) Exemplar physician-scientists can be easily identified; (2) Qualities

of success of physician-scientists are tangible; (3) Qualities of success of physician-scientists can be measured; and (4) Exemplar physician-scientists know how to reflect on their success, understand and clearly articulate what has led to their success.

This was a national study with the most exemplar physician-scientists of our generation. Two earlier phases of the study provided a national definition of success, which was used to identify exemplar physician-scientists. The primary sources of data were: in-depth interviews of nineteen exemplar physician-scientists, a focus group with physician-scientists, and document analysis.

Key findings of the study revealed: (1) Exemplar physician-scientists are overwhelmingly intrinsically motivated by both the need to understand the science and the desire to help their patients; (2) Exemplar physician-scientists are actively engaged in overseeing the design and execution of experiments, bringing in the unique perspective of both the physician and scientist; (3) Perseverance was identified as the most critical factor of success; and (4) Informal means played an integral role in the learning of physician-scientists, most notably through dialogue and formal mentoring programs.

Informal learning was described by Coombs (1985) as self-directed, incidental, and socialization or tacit learning was used to understand the manner in which physician-scientists learn and underscored the synthesis and analysis of the study.

Numerous recommendations were provided for current and future physician-scientists, as well as to the numerous stakeholders—those who hire, train, and fund them. These recommendations include suggestions for admissions practices that more accurately showcase the qualities of exemplar physician-scientists, rethinking the architecture of our spaces to allow for more collaborative dialogue, suggestions for how to make the most of informal learning opportunities, and an emphasis on mentoring, specifically, mentoring the mentors.

97 Analysis of the role of Glutamatergic and GABAergic periaqueductal gray neuronal subpopulations in a mouse model of persistent inflammatory pain

Jose G. Grajales-Reyes

Washington University School of Medicine, Saint Louis, USA

It has been estimated that 100 million adults suffer from chronic pain in the United States, with an annual societal cost of approximately 600 billion dollars. Endogenous analgesic pathways represent an alternative route for the development of new therapies. Pharmacological and electrical stimulation studies of the ventrolateral periaqueductal gray (vlPAG) have implicated its role in descending pain modulation. The GABA disinhibition hypothesis put forward by Basbaum and Fields proposes that tonic GABAergic neurotransmission at the level of the vlPAG serves to inhibit output excitatory projections that mediate descending analgesia, and disinhibition of vlPAG excitatory neurons that project to the rostral ventromedial medulla (RVM) is thought to allow subsequent activation of RVM cells that project to the dorsal horn of the spinal cord and inhibit nociceptive transmission. Numerous lines of evidence are consistent with this hypothesis, but experimental manipulations used in prior studies lack cell-type specificity, preventing unambiguous determination of the role of specific subsets of vlPAG neurons in analgesia. Techniques such as chemo- and opto-genetics now afford us the opportunity to selectively manipulate identified subclasses of vlPAG neurons. With the GABA disinhibition hypothesis as our model, we hypothesized that stimulation of excitatory vlPAG neurons or a reduction of in vlPAG GABAergic

tone would result in analgesia. We find chemogenetic stimulation of glutamatergic neurons or inhibition of GABAergic vPAG neurons results in an elevation of withdrawal thresholds to noxious stimuli in naïve animals. In the context of persistent inflammatory pain, we find that optogenetic stimulation of Vglut2 or chemogenetic inhibition of Vgat vPAG neurons results in attenuation of inflammation-induced hyperalgesia. Using an intersectional genetic approach, we provide direct experimental evidence for the proposed analgesic role for glutamatergic projections from the PAG to the RVM. In brief, our findings support the GABA disinhibition hypothesis, highlighting the role of local tonic GABAergic neurotransmission as an analgesic gatekeeper at the level of the vPAG.

98 Vesicular Ca²⁺ sensor Synaptotagmin 1 mediates neurotransmission from mammalian rod photoreceptors

Justin Grassmeyer

University of Nebraska Medical Center, Omaha, USA

Rod photoreceptors initiate vision by converting light into neuronal signals that are passed to downstream neurons in the retina and beyond. Dysfunction of molecules that mediate photoreceptor neurotransmission can lead to visual dystrophies and blindness. Rods are depolarized in darkness, allowing Ca²⁺ ions to enter the cell and stimulate the release of glutamate-laden vesicles. Exocytotic Ca²⁺ sensor proteins bind intracellular Ca²⁺ and trigger the vesicular release process; most neurons utilize one or more Synaptotagmin isoforms as a Ca²⁺ sensor. The identity of the Ca²⁺ sensor that operates in mammalian rods, which appear to exhibit an atypical relationship between Ca²⁺ influx and neurotransmitter release, remains unknown. We hypothesized that Synaptotagmin 1 (Syt1) serves as the exocytotic Ca²⁺ sensor at mammalian rod synapses. To investigate the role of Syt1 in vision, we generated novel mouse lines in which Syt1 expression was specifically abolished in rods and compared these conditional knockouts to littermate controls. Rod and cone function was evaluated using ex vivo electroretinogram (ERG) recordings of responses to light stimuli. Immunohistochemistry was used to evaluate the efficacy of conditional Syt1 removal and examine retinal anatomy. Our results confirm the presence of Syt1 in mouse rod terminals and demonstrate that Syt1 serves as the principal Ca²⁺ sensor regulating neurotransmitter release from rods. Syt1 is therefore an essential protein for rod-mediated vision in mammals. Although deletion of Syt1 from rods disrupted neurotransmission, its absence did not appear to alter outer retinal anatomy, suggesting that normal synaptic release from rods is not required for development of proper connections between rods and second-order retinal neurons. In contrast to release from other Syt1-mediated neurons, release from mammalian rods appears to exhibit a nearly linear relationship between Ca²⁺ and exocytosis, suggesting that accessory proteins also shape Ca²⁺ sensitivity at this synapse.

99 Identifying Novel Therapeutics to Inhibit the Wnt Self-Renewal Pathway in Leukemia Stem Cells

Meghan Green Haney

University of Kentucky, Lexington, USA

The relapse rate of pediatric Acute Lymphoblastic Leukemia (ALL) is 15-20%, and these patients have limited treatment options and a poor prognosis. Relapse rate is likely due to a small population of cells known as leukemia stem cells (LSCs), which have the ability to self-renew and can reform a leukemia from a single cell. Additionally, a major clinical concern is whether these LSCs are effectively killed by conventional cytotoxic chemotherapies. Current efforts to study LSCs have faced serious limitations, which have impeded our understanding of this important population of cells.

Prior work in our lab has established a zebrafish Myc-induced T-cell acute lymphoblastic leukemia (T-ALL) model that mimics the most aggressive and treatment resistant form of human T-ALL. Using this system, we isolated single LSCs through a novel transplantation strategy. Limiting dilution analysis showed significant differences in the rate of self-renewal between different LSCs, suggesting heterogeneity in LSC relapse potential. We generated a library of zebrafish T-ALL with high self-renewal rates (about 1 in 10 leukemia cells is a LSC) for use in bulk RNAseq, as well as single cell qPCR and single cell RNAseq to identify a self-renewal signature unique to LSCs. Single cell analyses showed a population of cells that expressed known self-renewal genes and clustered separately from the rest of the leukemia cells in the population. Ongoing work in our laboratory is focused on functionally testing whether this gene expression profile is linked with self-renewal. Additionally from this analysis, the Wnt pathway, more specifically β -catenin, was enriched in the putative LSC population. These data support previous finding in mammalian models of ALL.

We hypothesize that inhibitors of the Wnt pathway will inhibit self-renewal of LSCs and force them to terminally differentiate. However, there are no WNT inhibitors clinically available due to undesirable side-effects. We are currently using a 6xTCF/LEF:GFP zebrafish Wnt reporter model for high throughput screens to identify new, less toxic Wnt pathway inhibitors. Thus far, several compounds have showed significantly decreased TCF/LEF activity after drug treatment, with no effects on animal health. Future studies will test these inhibitors in our zebrafish high LSC leukemia samples and patient derived xenograft models. Ultimately, these inhibitors may represent a potential therapeutic strategy for targeting treatment-resistant LSCs and preventing ALL relapse.

100 Dietary sodium restriction following high salt intake reduces arterial stiffness, vascular wall transforming growth factor-beta (TGF- β)-dependent fibrosis and marinobufagenin level in young normotensive rats

Yulia N. Grigorova

National Institute on Aging / NIH, Baltimore, USA

High salt intake (HS) is accompanied by blood pressure (BP) increases in salt-sensitive hypertension. HS stimulates marinobufagenin (MBG), an endogenous Na/K-ATPase ligand, which activates profibrotic signaling in the cardiovascular system. In normotensive animals, HS did not cause BP elevation. Nevertheless, it was associated with MBG increase and aortic fibrosis. Here we investigated whether HS activates an aortic TGF- β profibrotic signaling and MBG production in normotensive young Sprague-Dawley rats (SD), and whether these changes are reversible by normal salt diet (NS).

SD (3-month old males) received NS for 4 and 8 weeks (0.5% NaCl; NS4 and NS8), or HS for 4 and 8 weeks (4% NaCl; HS4 and HS8), or HS for 4 weeks following by NS for 4 weeks (HS4/NS4), n=8 per group. Systolic BP (SBP), pulse wave velocity (PWV), MBG excretion, aortic collagen1 α 2 and TGF- β mRNA, and total collagen abundance were measured at baseline (BL), and on weeks 4 and 8. Statistical analysis was performed using a one-way ANOVA.

HS increased MBG (164 \pm 19 vs. 103 \pm 19 pmol/24hr/kg, HS4 vs. BL, p < 0.05) and PWV (3.7 \pm 0.2 vs. 2.7 \pm 0.2 m/s, HS4 vs. NS4, P < 0.05), while SBP was not affected (126 \pm 6 vs. 128 \pm 7 mmHg, HS4 vs. BL, p > 0.05). HS8 was associated with further increase in MBG and PWV, with an increase in aortic Col1 α 2 (twofold), *Tgfb1* (30%) and *Smad3* (70%) mRNAs, and aortic wall collagen (180%) vs. NS8 (all p < 0.05). NS following HS downregulated HS-induced factors: in HS4/NS4 MBG level was 91 \pm 12 pmol/24hr/kg (twofold

lower vs. HS8, $p < 0.01$), PWV was 3.7 ± 0.3 vs. 4.7 ± 0.2 m/s (HS4/NS4 vs. HS8, $p < 0.05$), aortic wall *Tgfb1*, *Col1a2*, *Smad3* mRNAs, and collagen abundance were reversed by salt reduction to the BL levels ($p < 0.05$).

HS in young normotensive rats was associated with an activation of TGF- β signaling, aortic fibrosis, and aortic stiffness accompanied by MBG increase in a pressure-independent manner. Reduction of dietary salt following HS decreased MBG, PWV, aortic wall collagen and TGF- β . Thus, HS-induced aortic stiffness in normotensive animals occurred in the context of elevated MBG, which may activate pressure-independent TGF- β -dependent profibrotic signaling. This data suggests that decreases in salt consumption could help to restore aortic elasticity and to reduce the risk of cardiovascular disease.

Supported by the NIH/NIA Intramural Research Program.

IO1 Diagnostic utility of whole-exome sequencing for kidney disease

Emily E. Groopman
Columbia University, New York, USA

Hereditary etiologies account for ~10% of adult and >70% of pediatric kidney disease, and often differ markedly from acquired forms in their prognosis, course, and clinical management. However, due to high genetic and phenotypic heterogeneity, diagnosis can remain elusive using traditional modalities alone, and in more than 1 in 10 patients with end-stage renal disease, the primary cause is “unknown.” Whole-exome sequencing (WES) has illuminated the genetic basis of a variety of disorders, and is becoming increasingly deployed as a first-line diagnostic across clinical medicine. However, its broad clinical value for patients with nephropathy, particularly among adults, has yet to be examined. To this aim, we performed WES in a large cohort of patients with all-cause chronic kidney disease (CKD), and assessed the diagnostic yield and prevalence of other medically relevant (secondary) findings.

2,187 CKD patients underwent WES at the Columbia Institute for Genomic Medicine (Roche or IDT capture kits). 87% were adults and 49% were non-Caucasian. Sequence data was processed using GATK v3.6 best practices, and annotated using ATAV and ANNOVAR. Genetic variants were interpreted using the American College of Medical Genetics (ACMG) guidelines. Diagnostic yield was calculated using counts of ACMG-pathogenic and likely pathogenic variants.

Diagnostic variants were detected in 204 (9%) of patients, encompassing 74 different genetic diseases. In 74% of cases, the genetic diagnosis gave novel clinical insight, informing subsequent clinical workup and management, disease prognosis, and/or family counseling. 57% of positive cases had autosomal dominant disorders, 21% autosomal recessive, and 22% X-linked. 3% of positive cases had dual molecular diagnoses. 43% of diagnostic variants had been previously reported, and 57% were novel. The most recurrent phenotypes were *COL4A3-5*-associated nephropathies, *UMOD*-associated tubulointerstitial disease, and *TRPC6*-associated focal segmental glomerulosclerosis. However, 60% of molecular diagnoses were detected in a single case. Diagnostic yield was highest among patients with a clinical diagnosis of a Mendelian form of CKD, with positive findings in 66%; however, 57% of positive cases did not have a clinical diagnosis of a hereditary nephropathy. Strikingly, the second-highest diagnostic yield was found in patients with CKD of “unknown etiology,” with diagnostic genetic findings identified in 19%. 41 (2%) of patients had a secondary finding in one of the ACMG 59 medically actionable genes, and the *APOL1*

risk genotypes were noted in 30% of African American and 8.5% of Hispanic patients.

Our findings highlight the genetic and phenotypic heterogeneity of hereditary nephropathies, supporting the value of WES for the detection of genetic forms of CKD. The high diagnostic yield observed among patients with CKD “of unknown etiology” suggests that WES may have substantial diagnostic utility for patients with undiagnosed CKD as well as for those clinically suspected to have a hereditary form of disease.

IO2 MYC family members drive chemoresistance in small cell lung cancer

Eli Grunblatt
University of Washington-Fred Hutchinson Cancer Research Center, Seattle, USA

Small cell lung cancer (SCLC) is a highly aggressive, frequently metastatic cancer that accounts for approximately 35,000 new cases annually in the United States alone. While many patients initially respond well to cisplatin-based chemotherapy, relapse within months is nearly universal. Relapsed disease is frequently resistant to chemotherapy, contributing substantially to the poor overall prognosis of SCLC patients. Decades of study have yet to produce an FDA-approved targeted therapy or a detailed understanding of chemoresistance, severely limiting treatment options for patients with relapsed disease. However, recent studies indirectly suggest that overexpression of MYC family members, such as *MYCL* and *MYCN*, may play a role in SCLC chemoresistance. Therefore, detailed investigation of MYC family member overexpression in SCLC could lead to meaningful clinical advances. We used genetically engineered mouse (GEM) models of SCLC to study the effects of *MYCN* and *MYCL* overexpression on SCLC chemoresistance. Upon treating cohorts of GEMs with cisplatin/etoposide, we found that while SCLC tumors in control mice exhibited a cytostatic response to chemotherapy, tumors in mice that overexpressed either *MYCL* or *MYCN* did not respond to treatment and continued to grow. In parallel, we used lentiviral vectors to overexpress *MYCN* in patient derived xenograft (PDX) models of SCLC that had previously been shown to be chemosensitive. We then injected these PDX models, alongside empty controls, into the flanks of immunocompromised mice and treated with either saline or cisplatin/etoposide once tumors developed. We found that while control tumors regressed when treated with cisplatin/etoposide, tumors that overexpressed *MYCN* did not respond to treatment and continued to grow through multiple cycles of chemotherapy. Taken together, our findings show that MYC family members can drive the development of chemoresistance in SCLC. To elucidate a potential mechanism for MYC family member driven chemoresistance, we performed RNAseq analysis of SCLC tumors derived from control, *MYCL* overexpressing, and *MYCN* overexpressing mice. Our preliminary results show that multiple ABC transporters, anti-apoptotic factors, and cyclin dependent kinase inhibitors are upregulated in MYC family member overexpressing samples. These pathways have previously been implicated in the development of chemoresistance in other cancers, and we hypothesize that *MYCN* and *MYCL* driven SCLC chemoresistance occurs through one or more of these avenues. Further work in this ongoing study will follow up on these hits to determine potentially druggable targets in pathways downstream of MYC members. These results can ultimately inform development of novel therapies to successfully target chemoresistance in SCLC and alleviate suffering for patients with this disease.

IO3 Examining the postmitotic roles of STAG2 mutations in solid tumors

Mary L. Guan

University of Michigan Medical School, USA

Mutations in the cohesin complex are associated with cancer, namely Ewing's Sarcoma (EWS) and bladder cancer (BC). The STAG2 subunit of cohesin is essential for its loading onto chromatin and proper function of the complex. EWS and BC patients who carry a STAG2 mutation show decreased survival. How STAG2 functions as a tumor suppressor is not fully understood. Some studies show that STAG2 mutations causes aneuploidy in cancers; while other data suggest that STAG2 mutations result in altered gene expression. We hypothesize that in EWS, where the EWSR1-FLI1 fusion is pathognomonic, the genetic epistasis of EWSR1-FLI1 and STAG2 is due to the suppressive role of STAG2 on EWSR1-FLI1.

In this study, we used co-immunoprecipitation (co-IP) to examine a ternary interaction between EWSR1-FLI1 and STAG2. We explored the phenotypic effect of STAG2 knockdown in vitro in HT1376 BC cells and A673 EWS cells via siRNA knockdown and proliferation curves. Finally, we determined the effect of STAG2 knockdown on expression of EWSR1-FLI1 and its downstream targets using RT-PCR.

We did not detect any physical interaction between STAG2 and EWSR1-FLI1 in A673 EWS cells via co-IP with STAG2 or EWS-FLI1. Phenotypically, in vitro proliferation was not affected upon STAG2 knockdown in HT1376 BC cells. We also counted HT1376 cell at 7 days post siSTAG2 transfection. Consistently, no significant difference was observed from cell count between siSTAG2 and negative control (siNC). Utilizing CellTiter-Glo Luminescent Cell Viability Assay, we further confirmed that the growth curve of siSTAG2 HT1376 cells was not significantly different from that of siNC HT1376 cells. RT-PCR of siSTAG2 EWS A673 cells showed increased expression of the fusion protein EWSR1-FLI1. Expression levels of EWSR1-FLI1 targeted genes were also increased after STAG2 knockdown in A673 cells.

In summary, our results suggest STAG2 mediates expression of EWSR1-FLI1 and its targeted genes, however not through physical interaction. Instead, STAG2 could act on chromatin to regulate oncogenic transcriptional programs associated with EWSR1-FLI1. Currently there exists no medical therapy for EWS, as the only treatments are chemotherapy, radiation therapy, and surgery. If STAG2 regulates oncogenesis of EWS, this will shed new light on the treatment of EWS, by targeting STAG2 in a specific, non-invasive way.

IO5 Specific TGF- β isoform targeting in combination with local tumor destruction with radiation therapy is associated with anti-tumor efficacy in mouse models of cancer

Aditi Gupta

Memorial Sloan-Kettering Cancer Center, USA

TGF- β is a pleotropic cytokine, which has emerged as a potential target in cancer treatment due to its dual role in tumorigenesis and homeostasis. There are three isoforms of TGF- β (TGF- β 1, TGF- β 2 and TGF- β 3), which are secreted by immune and non-immune cells as a latent complex. Depending on the local context, TGF- β adopts opposing roles in carcinogenesis and in modulating the immune system. These dueling roles of TGF- β are dependent on its secretion and activation. Local radiation therapy (RT) can activate TGF- β via reactive oxygen species. Such TGF- β expression is linked to radioresistance and dose-limiting toxicities, reducing the effectiveness of RT. In these studies, we aim to characterize the

effect of RT on the temporal and cell-specific expression patterns of TGF- β isoforms in mouse tumor models. This will inform treatment regimens combining isoform specific anti-TGF- β therapy with RT.

Fluorescence-activated cell sorting (FACS): C57BL/6 mice were implanted on the hind limb with B16-F10 melanoma cells. On day 10, tumors were irradiated locally with 15 Gy. Expression of TGF- β isoforms was measured at 1, 3 and 5 days post-RT by FACS.

In-vivo: C57BL/6 mice were implanted with tumors and irradiated as described. Mice were treated (10/group) with anti-TGF- β 1, anti-TGF- β 3 or a pan-TGF- β antibody beginning 1 day after RT given intraperitoneally (200 ug/mouse) every other day for 8 doses. Tumor growth and overall survival were monitored. A similar experiment was conducted in the 4T1 breast cancer model, in which mice were treated 1 day prior to radiation.

FACS data indicated that TGF- β 1 and TGF- β 3 expression increases on most immune cells in the tumor 1 day after RT, decreases 3 days after RT and reaches a peak 5 days after RT. Preliminary in-vivo studies demonstrate that both α TGF- β 1 and α TGF- β 3 as monotherapies have activity against B16 melanoma. In combination with RT, α TGF- β 3 shows greater anti-tumor activity compared to α TGF- β 1 in melanoma. Similar observations were obtained in a 4T1 breast model; however, α TGF- β 3 alone and in combination with RT as well as α TGF- β 1 + RT showed a significant delay against tumor growth. No significant differences in survival were seen in either tumor model. Analysis of tumor, lymph node and spleen from animals treated with isoform-specific anti-TGF- β therapy with and without RT is underway to understand the contribution of α TGF- β 1 versus α TGF- β 3 to anti-tumor efficacy.

TGF- β 1 and TGF- β 3 are expressed on numerous lymphoid and myeloid cells in B16 tumors and spleens. TGF- β isoform expression peaks 5 days post-RT. Anti-TGF- β therapy is effective in delaying tumor growth and may synergize with RT in certain cancers. This demonstrates rationale for the use of anti-TGF- β therapy to enhance the effectiveness of RT in cancer.

IO6 To analyze the aliphatic amyloid forming oligo peptides, their catalytic activities and nano-structure evolution of the resulting self-assembly.

Pardeep Guru

Hunter College, USA

The self-assembly is nature's intrinsic phenomenon to stimulate the functionality in a molecule so it can execute several functions such as producing adhesive properties in cell matrix, binding into DNA or assisting in replication itself. Studying self-assembly and catalysis of short peptides is a strategy to understand the catalytic effectiveness as well as understanding peptidic precursors of natural enzymes. In order to analyze the enzyme mimic catalysis, the ester hydrolysis of synthetic tetra-peptides with p-nitrophenyl acetate (p-NPA) was performed. Hydrolase is the most abundant studied reaction to understand the peptide that mimics the natural enzyme properties. These tetra-peptide sequences contain Lys and His as nucleophilic units, Leu as hydrophobic enforcer for aggregation and Met, Thr as polar residues that could assist potentially in hydrolytic activity. The enzyme-substrate affinity and the saturation kinetics for each peptide was analyzed by the UV-Spectroscopy which helped in analyzing the enzyme-substrate complex formation into enzyme and product. Moreover, the protein aggregation study was performed by using Thioflavin-T dye as an indicator which can help identifying the high molecular weight catalytic aggregates. Also, the structural components of these peptides were visualized at a nanoscale by

using the atomic force microscopy which helped in determining the morphology of peptides. Combination of self-assembly with peptide catalysis is a rational move towards artificial enzymes to produce biologically inspired catalysts.

107 Noninvasive Imaging of Fluorescent Probe Delivery in Intracranial Tumor Xenografts Using Fluorescence Molecular Tomography

LeMoyné Habimana-Griffin

Washington University in Saint Louis, Saint Louis, USA

The blood-brain barrier (BBB) is a significant obstacle to detecting and treating brain tumors. Development of methods to monitor delivery of diagnostic and therapeutic agents to the brain is imperative to overcome this challenge. In this work, we developed optical imaging methods to provide a highly sensitive, noninvasive, low cost platform to monitor delivery of diagnostic and therapeutic agents utilizing nonionizing radiation for preclinical brain tumor models. Utilizing fluorescence molecular tomography (FMT), we quantified the uptake of near-infrared fluorescent probes in an intracranial tumor xenograft model. We used FMT to longitudinally monitor BBB breakdown in this model. Furthermore, we demonstrated earlier detection of tumors using focused ultrasound (FUS) to permeabilize the BBB. These methods provide a framework for future studies in brain tumors as well as other neurological diseases.

108 Age-dependent hypertension development is associated with cognitive function decline and behavioral activity changes in Dahl Salt-Sensitive rats

Madeleine Hagood

National Institute on Aging / NIH, Baltimore, USA

Background: Blood pressure (BP) increases may be accompanied by a cognitive decline, however, it remains unclear what cognitive impairments emerge due to the development of hypertension with an advancing age. Hippocampal memory changes were described in Dahl Salt-Sensitive rats (DSS), which develop age-associated hypertension and cardiovascular changes even in the absence of high salt intake. Here we study what cognitive functions will decline and what behavioral abnormalities will be associated with age-dependent hypertension in DSS.

Methods: Fifty-three males DSS and Sprague-Dawley rats (SD) were kept on a normal 0.5% NaCl diet for the duration of the cross-sectional study. BP (plethysmography tail cuff method) and a battery of behavioral tests were performed at 3-mo and 12-mo old animals (n=11-14/group). Behavioral tests were aimed to assess the differences in memory, exploratory behavior, and anxiety, and include: open field test (OFT) to assess vertical activity and distance traveled; Rotarod test to examine balance and motor coordination learning; novel object recognition test to examine memory and object exploration; a version of Morris Water Maze (MWM) test to examine hippocampal-dependent memory. Statistical analyses were performed using T-tests and ANOVA.

Results: 3-mo SD and DSS did not differ in BP, cognitive function, and motor learning tasks. 12-mo DSS showed higher BP vs. 3-mo DSS (170 ± 5 vs. 128 ± 2 mmHg, $p < 0.01$), unlike SD. 12-mo SD and DSS differed from 3-mo counterparts on OFT in total distance traveled ($p < 0.0001$) and vertical activity ($p < 0.0001$), on the latency during rotarod test with a main effect of strain ($p < 0.0001$), on time exploring objects in the test phase of the novel object recognition task with a main effect of age ($p < 0.0001$) and an interaction of age and strain ($p = 0.0088$). 12-mo DSS demonstrated impairment in identifying the location of the invisible platform in a MWM (distance

traveled: 6.06 ± 1.26 vs. 4.00 ± 0.99 m, DSS vs. SD, $p < 0.01$).

Conclusion: Development of hypertension in aged DSS is associated with impairments in several components of cognition. Variations in cardiovascular function and observable behavior may reflect differences in sympathetic activation, anxiety, hyperactivity, or memory impairments. While age-induced decline in cognition, such as memory, may be accelerated in DSS compared to SD, the change in motor function is delayed. Investigation of the brain and cerebral vascular structural changes associated with memory decline and corresponding behavioral changes in a rat model of hypertension may merit future studies.

Acknowledgement: Supported by the NIH/NIA Intramural Research Program.

111 Proper centromere mechanical maturation is required to maintain the fidelity of chromosome segregation during mitosis

Lauren A. Harasymiw

University of Minnesota, Minneapolis, USA

During mitosis, tension develops across the chromosome's centromere as a result of spindle-based forces. In metaphase, tension at the centromere may play a critical role in preventing chromosome segregation errors. In human cells, disrupting the centromere's normal structure and function has been shown to increase the rate of chromosome missegregation, a cellular phenotype which is strongly implicated in cancer progression. However, the role of centromere mechanics in influencing the magnitude and cell-cycle specificity of tension at the centromere, and their effect on chromosome segregation outcomes, remains unknown. We combined quantitative, biophysical microscopy with computational analysis in order to elucidate the mechanics of the centromere in unperturbed, mitotic mammalian cells. Our approach revealed that the mechanics of the mammalian centromere mature with a signature pattern during mitotic progression. This maturation leads to amplified centromere tension, specifically at metaphase. Further, we found that a disruption in centromere mechanical maturation led to diminished tension at metaphase in human cancer cells, and that this disruption increased in severity with increasing chromosome number. Strikingly, the rate of lagging chromosomes at anaphase, which result from tension-based kinetochore-microtubule attachment errors, was elevated in cells with disrupted centromere mechanical maturation. Further, these errors persisted into chromosome segregation defects at telophase. Thus, we reveal a novel role for the centromere in regulating tension during mitosis, and demonstrate a direct link between aneuploidy, centromere mechanics, and chromosome missegregation.

112 PAX8 increases migration and metastasis of ovarian cancer through upregulation of PKCa and Rho GTPases

Laura Hardy

University of Illinois - Chicago, Chicago, USA

High grade serous ovarian cancer, the most lethal subtype of ovarian cancer, can originate in either the fallopian tube epithelium (FTE) or ovarian surface epithelium (OSE). PAX8 is a lineage specific transcription factor that is ubiquitously expressed in HGSO. We have shown that knockdown of PAX8 using shRNA in multiple ovarian tumor cells lines leads to apoptosis, suggesting that PAX8 plays an essential role in cancer survival. In this study, we used CRISPR genomic editing to delete PAX8 from the OVCAR8 cell line. PAX8 deletion led to a decrease in migration and invasion in vitro and an increase in survival and a reduction in tumor volume in vivo. Previous work using RNA sequencing and ChIP-sequencing identified cell adhesion as a top differentially expressed gene between malignant

ovarian cancer and benign fallopian tube cell lines. We performed quantitative proteomic analysis of the OVCAR8-PAX8^{-/-} cell line to define PAX8 altered proteins. We also performed quantitative proteomics and transcriptomic analyses on a previously generated murine OSE cell line with forced PAX8 expression (MOSE-PAX8). These analyses identified several genes that contribute to an increase in migration and EMT. Specifically, our data indicates PAX8 upregulates key drivers involved in altering cell morphology including PKC α and the GTPases: RhoA, Cdc42, and Ras. Upregulation of PKC α increased the migratory ability of OVCAR8 while inhibiting PKC α decreased this ability. Inhibition of RhoA led to a greater decrease in migration for both OVCAR8-PAX8^{-/-} and MOSE-PAX8 when compared to control. Inhibition of Ras had a greater effect in OVCAR8-PAX8^{-/-} while inhibition of Cdc42 had a greater effect in MOSE-PAX8. These data provide a mechanistic explanation for the role of PAX8 on increasing migration and metastasis in ovarian cancer.

113 HIV-infected macrophages induce endothelial cell dysfunction and metabolic reprogramming to promote HIV-associated pulmonary arterial hypertension

Lloyd Harvey

University of Pittsburgh School of Medicine, Pittsburgh, USA

Background & Hypothesis: Pulmonary arterial hypertension (PAH) is an enigmatic vascular disease characterized by complex pulmonary vascular remodeling, an increase in pulmonary vascular resistance, subsequent right ventricular hypertrophy, and right heart failure. There is an increased predisposition to PAH in HIV-infected populations, and as a historically neglected vascular disease, the pathogenesis of HIV-induced PAH (HIV-PAH) remains largely unknown. Recently, our laboratory has demonstrated a novel paradigm of metabolic reprogramming secondary to vessel stiffening as a pathogenic driver of PAH. More specifically, extracellular matrix stiffening induces the mechanosensitive transcriptional co-activators YAP and TAZ, resulting in the upregulation of the microRNA (miR) cluster miR-130/301 and glutaminase (GLS1) in human pulmonary arterial endothelial cells (HPAECs). The implications of this discovery are two-fold: (1) increased miR-130/301 further promotes matrix remodeling, (2) while upregulated GLS1 increases glutaminolysis—an anaplerotic reaction that sustains energetic demands in proliferating, neoplastic-like HPAECs. In addition, our laboratory has demonstrated that miR-21 is upregulated in the plasma of HIV-PAH patients, and that miR-21 is linked to the miR-130/301 cluster to exert broad influence over PAH. Taken together, we hypothesize that HIV-infected macrophages actively secrete miR-21 to promote vessel stiffening, glutaminolysis, and the pathogenesis of HIV-PAH.

Methods: Peripheral blood mononuclear cells are isolated from human blood by pull-down of CD14⁺ monocytes. CD14⁺ monocytes are then stimulated with granulocyte-macrophage colony stimulating factor (50 ng/mL) for five to seven days to produce monocyte-derived macrophages (MDMs). MDMs are infected with the HIV-1_{BAL} strain for two days using a multiplicity of infection of one or left uninfected. MDMs are subsequently co-cultured with HPAECs for two days before experiment termination.

Results: Our data are consistent with a previously defined model of the YAP/TAZ-miR-130/301-GLS1 axis as a novel paradigm in PAH. Using a co-culture system, miR-21 expression is upregulated in HPAECs, MDMs, and the conditioned media in which the cells were raised—suggestive of possible cell-to-cell transmission. Additionally, inducers of vessel stiffening and glutaminolysis—YAP/TAZ and the miR-130/301 cluster—are increased in HPAECs. Downstream targets

of YAP/TAZ and the miR-130/301 cluster are also upregulated, such as the collagen isoform 3 and its cross-linking enzyme lysyl oxidase and the anaplerotic enzymes GLS1 and pyruvate carboxylase.

Conclusions: Taken together, the upregulation of the matrix remodeling components and anaplerotic enzymes implies that HIV infection may be acting, in part, through our previously established YAP/TAZ-miR-130/301 GLS1 axis in the development of PAH, and that upregulation of this axis may be under regulatory control of miR-21. The implications of our data suggest that GLS1 may have a critical role in HIV-PAH pathogenesis, and that the GLS1 inhibitor CB-839—currently in clinical trial for cancer—may be rapidly repurposed for this devastating vascular disorder.

114 Amino acid metabolism as a drug target to treat persistent Mycobacterium tuberculosis

Erik Hasenoehrl

Albert Einstein College of Medicine, New York, USA

Most chemotherapeutics currently used in the treatment of Mycobacterium tuberculosis (Mtb) target hallmark systems of antimicrobial therapy, like cell wall and DNA biosynthesis. While targeting pathways essential for proliferation is sufficient to cure most bacterial infections, these approaches require at least six months to treat tuberculosis (TB) in order to clear persistent cell populations that are phenotypically tolerant to antibiotics. The severity of the TB epidemic mandates the development of drugs that target pathways essential during persistence. The “aspartate pathway” is responsible for the biosynthesis of essential amino acids (lysine, threonine, isoleucine, methionine), the peptidoglycan precursor diaminopimelate and the co-factor s-adenosyl methionine. We have previously demonstrated that a methionine auxotroph induced rapid killing and was avirulent in immunocompromised mice. Here, we investigate the requirement of three branch-point enzymes in the aspartate pathway during persistence and characterize the cellular response to pathway inhibition. Using a genetic inducible knockdown system we found that that all three enzymes were required for both acute and chronic infection in a mouse model. Transcriptomic and metabolomic characterization of inactivation of the aspartate pathway revealed a novel killing mechanism by which threonine auxotrophy causes a toxic accumulation of cytosolic lysine. We demonstrate that this occurs through a loss of threonine-mediated feedback regulation of the pathway, and that the cell tries to compensate for this toxicity by upregulating novel pathways for lysine degradation and export. In summary, our results strongly indicate that the aspartate pathway is a valuable and target rich space for development of drugs that can clear persistent TB infection.

115 Nox4 Modulates Lung Macrophage Polarization in Pulmonary Fibrosis Via Regulation Of Mitochondrial Biogenesis

Chao He

University of Alabama at Birmingham, Birmingham, USA

The phenotype of macrophages can contribute to fibrotic development. We have previously shown that lung macrophages from subjects with pulmonary fibrosis have elevated pro-fibrotic gene expression and increased mitochondrial dynamics compared with lung macrophages from normal subjects. Here, we found that lung macrophages isolated from subjects with pulmonary fibrosis have a significant increase in nox4 gene expression, suggesting a pivotal role of NOX4 in regulating macrophage phenotype and promoting fibrosis development. We hypothesize that NOX4 is required pro-fibrotic polarization of lung macrophages. We found that NOX4 overexpression increases TGF- β 1 promoter activity as

well as pro-fibrotic markers expression (TGF- β 1, FIZZ1 and Ym-1) in vitro suggesting the importance of NOX4 in pro-fibrotic gene regulation. Conversely, macrophages transfected with NOX4 siRNA have decreased TGF- β 1 production compared with cells transfected with a scrambled siRNA. These data were recapitulated in vivo with bleomycin-induced injury. Lung macrophages from NOX4^{-/-} mice had a significant decrease in pro-fibrotic gene expression (TGF- β 1, FIZZ1 and Ym-1) compared to WT mice. Furthermore, NOX4^{-/-} mice were protected from developing pulmonary fibrosis. Mitochondrial dynamics is crucial for macrophage polarization, and lung macrophages from pulmonary fibrosis subjects have increased mitochondrial biogenesis. NOX4 overexpression increased tfam gene expression, whereas inhibition of mitochondrial biogenesis reduced pro-fibrotic polarization of macrophages. These observations suggest a critical role for NOX4-mediated regulation of pro-fibrotic polarization of macrophages via modulation of mitochondrial biogenesis in pulmonary fibrosis.

I16 Measurement in health: Advancing assessment of delirium

Benjamin K.I. Helfand

University of Massachusetts Medical School, Newton, USA

Delirium, an acute clinical syndrome characterized by inattention and cognitive disturbances, is a common, preventable, and costly problem for older persons. Over 12 million Americans develop delirium annually, accounting for over \$160 billion in annual Medicare expenditures. While prevention of delirium can happen in 30-40% of cases, under-recognition of the syndrome occurs in about two-thirds of cases. A problem plaguing delirium research is difficulty in identification. Different clinicians in different clinical settings have developed many tools to aid in delirium identification. The lack of consensus on key features and approaches has posed a major barrier to progress in the field of delirium. Thus, the overarching goal of this project is to use advanced methods in measurement to improve the identification of delirium.

The specific aims of this project are to: (1) determine the 4-5 most commonly used and well-validated instruments for delirium identification; (2) harmonize the 4-5 most commonly used and well-validated assessment instruments to evaluate their level of agreement, generate an item bank, and create a harmonized measure; (3) identify the threshold (cut point), which will best identify delirium (vs. absence of delirium) rates for the harmonized measure. Accomplishing the first aim will occur through a rigorous systematic review of the published medical literature with quality rating of the articles. Performing the second aim will happen by implementing modern psychometric methods and harmonization methods on a secondary analysis of the Better Assessment of Illness (BASIL) study and other studies which have simultaneously administered multiple delirium measures of interest. The third aim will apply Monte Carlo approaches utilizing psychometric and harmonization methods to conduct over 10,000 simulations. This will allow for identification of the optimal cut-point to determine whether a patient has delirium or not.

The significance of the proposed research is the creation of the harmonized measure to provide a unified approach to identification of delirium allowing for the comparison of studies regardless of their method of delirium identification. Ultimately, the measure will facilitate combining studies, paving the way for meta-analyses of existing studies to advance clinical decision-making and guideline development. Additionally, the harmonized measure will provide the means to create big datasets for future research studies (e.g., -omics studies, population-based investigations).

The authors report no conflicts of interest.

I17 The Effects of Acarbose on Healthspan: A Functional and Tissue Level Assessment

Jonathan Herrera

University of Michigan, Ann Arbor, USA

With advances in modern health care, the global population is living longer. The US population aged 65 and over will double by 2050, and comprise 20% of the total population. Although individuals are living longer, aging is a prominent risk factor for chronic disease and comorbidities, which can compromise healthspan (i.e. healthy and longevity). The oral diabetic drug Acarbose (ACA) extends lifespan in genetically heterogeneous male and female mice (UMHET3) by 22% and 5%, respectively. To determine whether ACA improves healthspan or affects aging physiological systems, we focused on the musculoskeletal and cardiovascular systems. UMHET3 male (M) and female (F) mice were treated with ACA (1000 ppm) or a control diet from 8 months to 22 months of age. At 22 months, both old treated (OACA) and control (OC) groups, along w/a 4 month young control diet (YC) group, underwent motor function and echocardiography testing. Grip strength was reduced w/age (YC-M: 0.511 kg x 10⁻²/g BW vs. OC-M: 0.292 kg x 10⁻²/g BW, YC-F: 0.534 kg x 10⁻²/g BW vs. OC-F: 0.302 kg x 10⁻²/g BW; p<0.01) and improved w/ ACA (OACA-M: 0.358 kg x 10⁻²/g BW, OACA-F: 0.371 kg x 10⁻²/g BW; p<0.01). Acceleration fall latency (YC-M: 86.4s vs. OC-M: 39.8s, YC-F: 103s vs. OC-F: 50.6s; p<0.01), measured using a rotarod, declined w/aging. Acceleration fall latency improved w/ ACA (OACA-M: 62.9s, OACA-F: 66.9s; p<0.01), while endurance fall latency showed a trend toward improvement w/ACA (OC-M: 9.59min vs. OACA-M: 11.5min, OC-F: 10.1min vs. OACA-F: 15.5min; p=0.06). Echocardiography revealed a male-specific left ventricular mass increase w/age (OC-M: 120mg to 176mg; p=0.001), which was diminished by ACA (OACA-M: 145mg, p=0.04). Other measures of cardiac structure and function were unchanged w/age or treatment. Following functional testing, hearts from male mice were processed for TMT labeled mass spectrometry. Preliminary evaluation using Gene Set Enrichment Analysis (GSEA), gene ontology w/ IPATHWAYGUIDE, and pathway analysis w/Reactome, detected consistent changes in proteins involved in cardiac structure and metabolism. Specifically, collagen pathways involving proteins Col6a1 and Col6a1 decreased in OC-M compared to YC-M, and increased w/ACA treatment. GSEA demonstrated decreases in glucose metabolism pathways in OACA-M vs. OC&YC-M, while Reactome detected upregulation of pathways involved in Insulin-like growth factor (IGF) regulation in OACA-M vs OC&YC-M. Overall, ACA not only extends lifespan but also improves healthspan, as observed by improvement in motor function using clinically relevant assays. Furthermore, cardiac age-related left ventricular hypertrophy in male mice was attenuated by ACA treatment. Initial examination of a comprehensive proteomics analysis suggests that the treatment effects of ACA at the level of cardiac tissue involve restoration of age-related decreases in collagen and metabolic proteins and pathways.

I18 Missing the Diagnosis of Hyperparathyroidism in Patients With Kidney Stones: A Possible Explanation

Brendon Herring

University of Alabama Birmingham School of Medicine, Birmingham, USA

OBJECTIVE(S): Although hyperparathyroidism is a significant cause of kidney stones, there are frequently substantial delays in diagnosis that lead to recurrent kidney stones and a significant reduction in quality of life. We hypothesized that patients with hyperparathyroidism and kidney stones experience delays in diagnosis because they

present with more mild elevations in calcium and/or parathyroid hormone (PTH). **METHODS:** We reviewed a prospective database of 1836 patients with primary hyperparathyroidism who underwent parathyroidectomy by one endocrine surgeon. Of these patients, 18% had kidney stones. We compared patients with and without kidney stones using either the Pearson Chi-Square, Fisher's Exact Test, or Student's T-Test where appropriate. **RESULTS:** The mean age of our cohort was 60 ± 14 years, with 77% females. Patients with kidney stones were younger (57 vs. 60 years, $p=.004$) and more males had kidney stones than females (23 vs. 16%, $p=.002$). Normocalcemic hyperparathyroidism was more common in those with kidney stones (84 vs 78%, $p=0.016$). Patients with kidney stones also had a lower mean preoperative PTH (117 vs.134 pg/ml, $p=.004$). **CONCLUSIONS:** Patients with kidney stones due to hyperparathyroidism are more likely to present with mild parathyroid disease characterized by normal calcium and lower PTH levels. Primary care providers, endocrinologists, and urologists must be aware of this to avoid missing or delaying the diagnosis of hyperparathyroidism. Therefore, we recommend that patients with kidney stones be evaluated with a serum calcium and PTH level.

119 Discrete dopamine systems for learning and motivation converge to maximize reward behavior

gabriel Heymann

University of Washington, Seattle, USA

The capacities to assign value, associate environmental cues with positive or negative outcomes, and motivate goal-directed actions are fundamental aspects of adaptive behavior. These coordinated elements of **reward processing** are regulated by **Ventral Tegmental Area (VTA) dopamine neurons** and their diverse projections to forebrain structures. While it is appreciated that distinct VTA dopamine populations and pathways mediate discrete aspects of goal-directed behavior, attributing specific functions to select cell populations and circuits has proven difficult. Here, we utilize novel Cre-driver lines to isolate genetically distinct VTA dopamine subpopulations with dissociable roles in reward association and motivation, as well as complementary innervation profiles within the Nucleus Accumbens (NAc): *Crhr1* – NAc_{CORE}; *Cck* – NAc_{SHELL}; Channel rhodopsin (ChR2) mediated activation of *Crhr1* VTA dopamine neurons, with restricted innervation of the NAc_{CORE} subdivision, is sufficient to facilitate the acquisition of instrumental responding for optical intracranial self-stimulation (oICSS). In contrast, activating the *Cck* VTA population with a NAc_{SHELL}-specific projection cannot promote initial learning, but will sustain and augment an already learned operant reward behavior. Interestingly, concerted activity of both subpopulations and dual activation of NAc_{CORE} and NAc_{SHELL} VTA dopamine pathways is required for maximal oICSS. While these results suggest discrete associative and motivational processes that work in a coordinated fashion to drive behavior, future experiments will combine optical inhibition and excitation during Pavlovian and extinction learning to further probe the dissociable functions of *Crhr1* and *Cck* subpopulations. Furthermore, we employ combinatorial genetic strategies to selectively abolish dopamine signaling and confirm the dopamine dependence of independent reward behaviors. Our findings begin to consolidate the operational roles of discrete dopamine populations and signals, a crucial step in identifying more precise therapeutic targets for drug addiction and depression, disorders associated with aberrations in mesolimbic dopamine signaling.

120 Influence of neurogenesis timing on cerebellar circuitry

Kelly K. Hill

Washington University in St. Louis, St. Louis, USA

Neurons are connected in elaborate circuits underlying specific functions, yet little is known about how these circuits are established during development or how they go awry in the context of neurodevelopmental disorders. This study tests the hypothesis that the timing of neurogenesis is a key regulator of cerebellar cortical development. Specifically, we evaluate whether the birthdate of a cerebellar granule neuron influences its function in the mature circuit. Several lines of evidence support this hypothesis including anatomical and in vitro differences between early- and late-born granule neurons. To test our hypothesis, we first demonstrate a methodology to fluorescently tag in vivo cohorts of granule neurons in a birthdate-dependent manner. We next evaluate the functional responses of hundreds of mature granule neurons by performing in vivo calcium imaging of transgenic mice that express the GCaMP6f calcium indicator in cerebellar granule neurons. Finally, by intersecting our birthdating technique with our transgenic approach, we compare the functions of early- and late-born granule neuron cohorts in the mature cerebellar circuit.

121 The role of miR-29 in B cell development and function

Marcus Hines

NYU School of Medicine, New York, USA

We previously published a paper showing that miRNAs are important in regulating PTEN and PI3Kinase signaling pathway downstream of the B cell receptor. We hypothesize miR-29, specifically, regulates the PTEN-PI3Kinase axis in B cells and can control B cell survival and signaling. The miR-29 family of miRNAs is transcribed from two different loci: the miR-29ab1 locus generates miR-29a and miR-29b while the miR-29b2c locus generates miR-29b and miR-29c. Mature sequences of miR-29b from both the miR-29ab1 and miR-29b2c loci are identical. The seed region used to recognize the 3'UTR of mRNA targets are identical for miR-29a, miR-29b, and miR-29c. Previously the members of the miR29 family have been implicated in immune-related diseases such as acute myeloid leukemia (AML) and T-cell acute lymphoblastic leukemia (T-ALL), but the role that miR-29 plays in B lymphocyte physiology has not been fully examined. Using mice deficient for the miR-29ab1 locus, the miR-29b2c locus, or both miR-29 loci (double KO), we have begun to investigate how miR-29 affects B lymphocyte development and function. Our observations suggest that ablation of both miR-29 loci did not have appreciable impact on early B cell hematopoiesis but had a profound impact on the survival of splenic B lymphocytes. Using intracellular FACS we examined the contribution of each of the two miRNA clusters on the regulation of PI3K signaling and also assessed the direct impact on B cell survival. We have also performed a series of in vitro differentiation assays to examine the role of miR-29 family miRNAs on proliferation, survival, class switch recombination and plasma cell differentiation. Our data suggests a critical role for the miR-29-PI3Kinase regulatory axis in mature B cell survival and terminal differentiation.

122 Functional characterization of lncRNAs in melanoma maintenance

Kate Hockemeyer

New York University School of Medicine at NYU Langone Health, New York, USA

Accumulating data suggest that mutations in coding genes are not sufficient to explain melanoma maintenance and progression to metastasis. Nearly 20,000 non-coding RNAs are expressed at various

stages of development and disease, of which lncRNAs comprise a major and heterogeneous class. lncRNAs have diverse roles within the cell, and recent findings implicate numerous lncRNAs in the onset, progression, and/or metastasis of cancer. While lncRNAs have been shown to play roles in apoptosis, proliferation, and invasion in melanoma, a comprehensive, unbiased study of lncRNA expression and involvement in melanoma progression has not been performed, and the role of lncRNAs in melanoma formation and metastasis remains poorly understood. Application of our in-house lncRNA pipeline identified novel and annotated lncRNAs differentially expressed in melanoma relative to melanocytes and in metastatic relative to primary sites. To identify critical dependencies on lncRNAs in melanoma, we carried out a focused CRISPRi loss of function screen in a melanoma cell line expressing inducible dCas9-KRAB *in vitro* and *in vivo*. We designed a library targeting the transcription start site (TSS) of lncRNAs significantly upregulated in melanoma patient samples relative to melanocytes. Using stringent criteria, this screen identified expected lncRNAs such as MALAT1 and SAMMSON as well as lnc-RGS5, GMDS-AS1, and novel XLOC-030781. GMDS-AS1 was highly expressed across all stages of melanoma, and knockdown resulted in modest proliferation defects. Intriguingly, the expression correlates strongly with nearby genes. We will elucidate the mechanism by which GMDS-AS1 supports melanoma survival. This work will elucidate the complex epigenetic and transcriptional programs underlying melanoma pathogenesis and provide basis for novel therapeutic strategies leveraging this information to improve patient outcomes.

123 Multi-parametric liquid biopsy analysis of circulating tumor cells (CTCs), cell-free DNA (cfDNA), and cell-free RNA (cfRNA) in metastatic castrate resistant prostate cancer (mCRPC)

Emmanuelle Hodara

Keck School of Medicine of USC, Beverly Hills, USA

Background: Molecular profiling of prostate cancer using liquid biopsies such as CTC capture and cell-free nucleic acid analysis yield informative yet distinct datasets. Additional insights may be gained by simultaneously interrogating multiple liquid biopsy components to construct a more comprehensive molecular disease profile. We have conducted an initial proof of principle study aimed at piloting this multi-parametric approach.

Methods: Blood was drawn under an IRB-approved protocol from 20 mCRPC patients. Samples were analyzed simultaneously for the following: CTC enumeration and single CTC and matched white blood cell capture for whole genome amplification and low-pass copy number variation; CTC DNA and matched cfDNA for somatic single nucleotide variant analysis; plasma cfRNA extraction and qRT-PCR for AR, AR-V7, and PCA3. When available, liquid biopsies were compared with matched tumor profiles.

Results: Fifteen of 20 patients (75%) had detectable CTCs by CellSearch (range: 1-692/7.5mL, median: 16.5/7.5mL). Thirteen of 20 patients (65%) had detectable SSNVs in CTC DNA and/or matched cfDNA, including mutations in *TP53*, *PIK3CA*, *HRAS*, and *EGFR*. Matched CTC DNA and cfDNA demonstrated both shared and distinct SSNVs. Copy number analysis of single CTCs was performed in 2 patients, and both had CNVs in multiple cancer relevant genes. A majority of CNVs were present in matched solid tumor profiles, but some were exclusive to the liquid biopsies. Plasma PCA3 and AR transcripts were detected in 18/20 (90%) and AR-V7 in 4/20 (20%) cfRNA samples. Unique SSNVs were detected at second time points at disease progression (more are being collected).

Conclusions: In this pilot cohort, simultaneous multi-parametric

profiling was feasible for CTC DNA mutations and CNVs, and matched plasma cfDNA mutations and cfRNA gene expression. These disease-specific molecular profiles were often concordant with tumor tissues but also contained new, potentially actionable alterations unique to CTC DNA or cfDNA. Expanded studies will build upon this approach to optimally leverage liquid biopsies for molecularly directed patient management.

COI Declarations: EH, DZ, GM, AC, YX, JC, PD, TD, DQ, and AG: None. PD, JU, KD, FB, AK, PC, MM, SG are employees of companies (see affiliations) that developed platforms utilized in this work.

Funding: 5P30CA014089-42. Partial support provided by Cynvenio, Liquid Genomics, Menarini Silicon Biosystems, and ResearchDX for assays conducted using their respective platforms.

124 Novel Crystal Forms of the Antibiotic Cefixime

Win Hon

Grand Valley State University, Allendale, USA

In the pharmaceutical field, solid form selection is often plagued by low bioavailability, a property determined by intestinal permeability and water solubility of a drug. The poor performance of these pharmaceuticals, however, can be improved through the use of novel crystal forms. Methods used to approach and adjust the solubility include the use of various crystallization techniques as well as crystal engineering of multicomponent forms, such as solvates or cocrystals. Crystals are analyzed using different techniques including optical microscopy, Raman spectroscopy, and powder X-ray diffraction. Herein, we describe the novel crystalline forms discovered for the antibiotic cefixime. Crystallization conditions used in our research include evaporation at room temperature, heated evaporation, cooling, addition of an antisolvent, vapor diffusion, grinding, and slurring. Our results show that molecules containing carboxylic acids interact best to form crystals with cefixime. Scale up is needed in order to perform further characterization on these novel crystal forms.

125 Mast cells promote Japanese encephalitis virus penetration of the blood-brain barrier

Justin Hsieh

Duke-NUS Medical School, Singapore, Singapore

Japanese encephalitis virus (JEV) is the leading cause of viral encephalitis in Asia. However, the mechanisms of JEV penetration of the blood-brain-barrier (BBB) remain poorly understood. Here, we identify that mast cells (MCs), which are key immune sentinel cells located throughout peripheral connective tissues and in the central nervous system (CNS), contribute to BBB leakage during JEV infection. JEV infection induces activation and degranulation of MCs both *in vitro* and *in vivo*. Consistent to the role of MCs during infection by related flaviviruses, we observed that they play a role in peripheral clearance of JEV. However, MCs also induced significant BBB leakage in JEV-infected animals. In MC-deficient mice, both BBB leakage and JEV infection of the CNS were reduced. While wild-type mice developed neurological deficits during JEV infection, these effects were absent in the MC-deficient mice. Our results support a role for MCs in peripheral immunosurveillance against JEV, but indicate that MCs also facilitate BBB penetration by JEV. Thus, MCs play a previously unrecognized role in worsening viral encephalitis.

126 A complement protein mediates neuroprotection in a model of Parkinson's disease via a gut-neuron axis

Paishiun Hsieh

Case Western Reserve University, Cleveland, USA

Aging is accompanied by an increased risk of chronic disease, notably neurodegenerative diseases such as Parkinson's disease. Therefore, a central challenge of aging research is the extension of time spent free of age-related debility, or healthspan. Over the last several decades, studies in model organisms like the roundworm *Caenorhabditis elegans* have identified transcriptional regulators (e.g. FOXO) which modify the fundamental biology of aging, modulating lifespan as well as delaying the onset of aging-associated pathology. Recently, we demonstrated that the Krüppel like factors, a conserved subfamily of zinc-finger transcription factors, are bona fide regulators of aging in worms and also influence cardiovascular aging in mice. Here we show that a long-lived worm overexpressing *klf-3* is resistant to age-related neurodegeneration in a model of Parkinson's disease overexpressing mutant α -synuclein. Interestingly, we find that the neuroprotective effect of *klf-3* is localized to the intestine, as intestine specific overexpression of *klf-3* is sufficient to phenocopy systemic overexpression. Further, using RNA-seq analysis, we identify a secreted C-type lectin, *clec-186*, which is required for and mediates the neuroprotective effect of intestinal *klf-3*. Systemic deletion or intestine specific knockdown of *clec-186* completely abolishes *klf-3* mediated neuroprotection while dopamine specific knockdown of *clec-186* has no effect. Sequence analysis of *C. elegans klf-3* points to the complement protein COLEC11 as a mammalian ortholog. COLEC11 is detectable in rat brains and CSF and studies currently ongoing will assess a conserved neuroprotective role for COLEC11 in mammals. Collectively, these observations identify a mechanism mediating neuroprotection via a gut-neuron axis whereby intestinal *klf-3* regulation of the secreted complement protein *clec-186* modulates distant neuronal responses to proteotoxic stress due to misfolded α -synuclein. Our findings additionally shed light on the mechanisms coupling longevity with extension of healthspan and have implications for targeting the underlying aging biology in age-dependent diseases, which currently pose an enormous burden on healthcare systems worldwide.

127 Plasma kidney injury molecule-1 and monocyte chemoattractant protein-1 correlations with kidney histopathology

Isabel J. Hsu

Princeton, Dearborn Heights, USA

More than one in seven adults in the United States—30 million people—have chronic kidney disease (CKD). CKD cannot be reversed, so early detection and prevention is crucial. Currently serum creatinine (SCr) and proteinuria are used to indicate kidney function. However, SCr lags in response to kidney injury or disease, and proteinuria lacks diagnostic specificity. Better biomarkers are needed for earlier, more accurate diagnoses and for monitoring the course of kidney disease progression.

Kidney injury molecule-1 (KIM-1) and monocyte chemoattractant protein-1 (MCP-1, also CCL2) have shown promise as nephrology biomarkers in animal and cohort studies. KIM-1 is a protein highly upregulated in proximal tubular cells after acute ischemic kidney injury. Increases in MCP-1, a chemokine that recruits specific leukocyte populations, have been detected in response to inflammation as in active lupus nephritis. We hypothesized that plasma KIM-1 and MCP-1, independent of estimated glomerular filtration rate (eGFR) and proteinuria, would identify acute tubular

injury (ATI) and inflammation on biopsies. Biomarker studies published to date have used endpoints such as renal function decline and mortality rather than histopathology. We reasoned that kidney biopsy histopathology would serve as a novel approach to biomarker identification and validation.

We enrolled patients undergoing native kidney biopsy at three Boston-area hospitals into the Boston Kidney Biopsy Cohort (BKBC). Urine, plasma, and DNA were collected at the time of biopsy from patients who provided written informed consent. Kidney histopathological lesions were independently adjudicated by two study pathologists, who scored each biopsy on a semiquantitative scale. We used Spearman correlations and multivariable linear regression to test associations between biomarker concentrations and clinical and histologic findings.

We measured KIM-1 and MCP-1 in 522 patients with available plasma samples. The mean age was 53 ± 17 years, 51% were female, and 35% were nonwhite. The most common reasons for biopsy were proteinuria, abnormal eGFR, and hematuria. The most common clinicopathological diagnoses were proliferative glomerulonephritis (29%), non-proliferative glomerulonephritis, and diabetic nephropathy. KIM-1 levels were inversely correlated with eGFR ($r = -0.60$, $P < 0.001$) and directly correlated with proteinuria ($r = 0.26$, $P < 0.001$) and highest in patients with diabetic nephropathy and tubulointerstitial disease. After adjusting for estimated glomerular filtration rate and proteinuria, KIM-1 levels were higher in those with more ATI, mesangial matrix expansion, and interstitial fibrosis/tubular atrophy (IFTA). MCP-1 levels were not associated with eGFR or proteinuria but were elevated in patients with more tubulointerstitial inflammation.

Histopathological findings from kidney biopsies can be noninvasively determined from plasma biomarkers. Plasma KIM-1 and MCP-1 could be used to provide diagnostic information and to track response to therapies in patients with a variety of kidney diseases.

128 Mouse endothelial cell transcriptomes in healthy and diseased states

Jennifer C. W. Hu

Cleveland Clinic Lerner College of Medicine of Case Western Reserve University School of Medicine, USA

Endothelial cells line the interiors of blood and lymphatic vessels. Depending on the vessel type (e.g., capillary, vein, artery, sinusoid), they have diverse morphologies and functions. Somatic mutations have been identified in endothelial cells isolated from sporadically occurring vascular malformations; these include: PIK3CA mutations in lymphatic and venous malformations and GNAQ mutations in congenital hemangiomas. How a mutation in an endothelial cell gives rise to a specific type of vascular malformation is unknown.

We hypothesize that a somatic mutation's effect depends upon the transcriptome of the endothelial cell in which the mutation arose. For instance, baseline transcriptional differences between sinusoidal and arterial endothelial cells account for the ability of a somatic GNAQ mutation to produce a hepatic hemangioma in the former and no malformation in the latter. To begin testing this hypothesis, we are performing RNA sequencing on mouse endothelial cells freshly recovered from different vascular compartments.

Thus far, we have immuno-affinity purified endothelial cells from collagenase digested lung, liver, aorta, inferior vena cava/jugular veins, and uterus samples from adult C57BL/6J mice using anti-CD31 antibodies. Our highest yield came from the liver (~1 million cells) and our lowest yield came from the aorta (~13,000 cells). Extracted RNA

was used to create RNA-seq libraries which were characterized using an Illumina MiSeq. As expected, known endothelial cell transcripts (e.g., Vwf) were present in every sample. However, our ability to detect differences in the transcriptomes of the different endothelial cell populations was confounded by contaminating neighboring cells. For example, albumin transcripts (Alb) were enriched in endothelial cells isolated from liver and surfactant associated protein transcripts (Sftpb) were enriched in endothelial cells isolated from lung.

We are currently developing more stringent enrichment methods to recover endothelial cells, applying computational methods to eliminate contaminating transcripts from endothelial cell datasets, and performing single cell RNA sequencing to precisely define different endothelial cell transcriptomes. Once this work is complete, we will begin determining endothelial cell transcriptomes in mice with a conditional *Pik3ca* p.H1047R allele that has been associated with venous and lymphatic malformations or a *GNAQ* p.Q209L allele that has hepatic malformations. Finally, endothelial cells from different vascular compartments of wild-type and conditional mutant mice will be co-cultured with wild-type cells to determine how mutant endothelial cells affect the behavior of non-mutant neighbors.

Completion of these experiments will elucidate the transcriptional profiles of endothelial cells from different vascular sites in the absence or presence of a malformation-causing somatic mutation. It will also identify cell autonomous changes in gene expression that can recruit non-mutant cells into the malformation process. This knowledge could lead to therapies that halt the development or progression of a vascular malformation, or promote the malformation's regression.

129 MRI functions as a DNA damage response adaptor during non-homologous end joining

Putzer J. Hung

Washington University School of Medicine, New York, USA

Non-homologous end joining (NHEJ) is the primary DNA double-strand break (DSB) repair pathway in G1-phase cells and involves the direct ligation of two DNA ends. In developing lymphocytes, NHEJ is required for the repair of DSBs generated by the RAG endonuclease during the antigen receptor gene assembly process, and dysregulation of this pathway can lead not only to impaired lymphogenesis, but also to chromosomal deletions or translocations that predispose towards lymphoid malignancies. NHEJ is carried out by a set of essential core factors, including Ku70/80, DNA ligase IV, and XRCC4, which recognize broken DNA ends and catalyze their rejoining. Additionally, several other accessory factors, such as XLF, ATM, and H2AX, also function redundantly during NHEJ to tether broken DNA ends and protect them from nucleolytic degradation. Yet, how the NHEJ machinery is assembled and retained at DSBs remains unclear. Using a genome-wide genetic screen, we identified the modulator of retrovirus infection (MRI), a small peptide of unknown function, as a new component of the NHEJ pathway. Here, we show that MRI interacts with numerous DNA damage response (DDR) factors at its termini to form large multimeric complexes and that it rapidly localizes to DSBs, where it promotes the association of these proteins with chromatin. Loss of MRI results in increased cellular sensitivity to ionizing radiation, a hallmark of defective NHEJ. Remarkably, the requirement for MRI in NHEJ is even more pronounced in the absence of XLF. Mice deficient in MRI and XLF exhibit embryonic lethality caused by widespread neuronal apoptosis in a manner similar to that of mice deficient in the core NHEJ factors DNA ligase IV or XRCC4. Furthermore, knocking out MRI in XLF-deficient pre-B cells almost completely abolishes the NHEJ-mediated repair of RAG DSBs and leads to aberrant joining of unrepaired DNA

ends. We thus propose that MRI is an adaptor which, through its multivalent interactions, increases the avidity of DDR factors for damaged chromatin to promote NHEJ.

130 Age-dependent effects of apoE reduction using antisense oligonucleotides in a model of β -amyloidosis

Tien-Phat V. Huynh

Washington University School of Medicine, Saint Louis, USA

The apolipoprotein E (*APOE*) gene is the strongest genetic risk factor for late-onset Alzheimer disease. Previous studies suggest reduction of apoE levels through genetic manipulation can reduce A β pathology. However, it is not clear how reduction of apoE levels after birth would affect amyloid deposition. We utilize an antisense oligonucleotide (ASO) to reduce apoE expression in the brains of APP/PS1-21 mice homozygous for human APOE- ϵ 4 or APOE- ϵ 3 allele. ASO treatment starting after birth led to a significant decrease in A β pathology when assessed at 4 months of age. Interestingly, ASO treatment starting at the onset of amyloid deposition led to an increase in A β plaque size and a reduction in plaque-associated neuritic dystrophy, despite no change in overall plaque load. These results suggest that manipulation of apoE levels can strongly affect the initiation of A β pathology *in vivo*, while modulating plaque size and toxicity during the later stages of amyloid deposition.

131 Neutrophil extracellular traps propagate post-traumatic heterotopic ossification

Charles Hwang

University of Michigan, USA

Neutrophil extracellular traps (NETs), a component of the host defense mechanism, have been implicated in pro-inflammatory conditions such as arthritis and autoimmune disorders. Heterotopic ossification (HO) is a pathology of impaired musculoskeletal wound healing characterized by ectopic osseous lesions that cause joint immobility, disfigurement, and pain. This acute-on-chronic inflammatory process has both clinically and experimentally exhibited an association between mechanical strain and increased local inflammation. We show that mechanically disrupted NETs independently induce NETosis, thereby augmenting inflammation in response to injury, and causing wound pathology. Furthermore, interrupting signaling downstream to nascent NETs attenuated ectopic formations.

Wild-type mice underwent hindlimb Achilles tenotomy to generate trauma-induced HO. Mice were allowed to ambulate with the injured hindlimb either mobile or cast-immobilized. Mice were treated with vehicle control, i.v. DNase-I to chemically disrupt NETs, or ODN-2088 (TLR 7/8/9 inhibitor) to inhibit DNA receptor activity. Inflammation was assessed by flow cytometry to quantify infiltrate at 48 hours and cartilage was assessed histologically (Safranin O) at three weeks. For *in vitro* studies, neutrophils were isolated from wild-type mice and treated with phorbol-12-myristate 13-acetate (PMA) to induce NETosis. NETs were mechanically disrupted using proven protocols or left intact. Neutrophils treated with ODN-2088 were exposed to either disrupted or intact NETs followed by quantification of "secondary" NETosis using anti-citH3/DAPI staining. For mCT analysis, mice received 150ng/g i.p. injections daily with ectopic lesions quantified at nine weeks. All significant results were calculated at $p < 0.05$.

Immobile hindlimbs reduced normalized neutrophil (1.0 v. 0.27) and macrophage (1.0 v. 0.26) counts compared with mobile hindlimbs 48 hours after injury corroborated by histology showing increased citH3 immunostaining in the mobile hindlimb. Chemical disruption of NETs

through DNase-I also significantly increased normalized neutrophil (1.0 v. 6.39) and macrophage (1.0 v. 3.0) counts in the immobile hindlimb at 48 hours; however, no differences were observed in the mobile hindlimb (n=5/group). Treatment with DNase-I to chemically disrupt NETs also led to the presence of ectopic cartilage. TLR interruption via ODN-2088 significantly reduced inflammation in the mobile hindlimbs. In vitro studies confirmed that mechanically disrupted NETs induce robust secondary NETosis compared with intact NETs (46.6/hpf v. 20.2/hpf). Treatment of secondary neutrophils with ODN-2088 reduced secondary NETosis (92.7/hpf v. 0.90/hpf) validating the role TLRs serve as major receptors for NET-induced NETosis. Post-traumatic treatment with ODN-2088 successfully reduced the CT volume of ectopic bone (5.36 v. 9.52mm³), confirming the signaling and recruiting role of NETosis in HO.

These results strongly suggest mechanical or chemical disruption of NETs augments joint inflammation and endochondral ectopic bone formation by inducing further NETosis among neutrophils. TLR 7/8/9 inhibition via ODN-2088 prevents this secondary NETosis and downstream development of ectopic lesions, suggestive of a valuable target in preventing NETotic pathologies and dysregulated inflammation.

132 Prevalence of Advanced, Precancerous Colorectal Neoplasia in Black and White Populations: a Systematic Review and Meta-analysis

Thomas F. Imperiale

Indiana University School of Medicine, Indianapolis, USA

Background: Colorectal cancer (CRC) incidence and mortality is higher in Blacks than in Whites. While the reason(s) for these disparities is unclear, some guidelines recommend CRC screening in Blacks starting at age 40-45.

Objective: To compare the prevalence of advanced adenoma (AA) or advanced, precancerous colorectal neoplasia (ACN) between asymptomatic Black and White screen-eligible adults.

Methods: We performed a systematic review and meta-analysis by first searching OvidMEDLINE, PubMed, EMBASE, and the Cochrane Library to identify published literature from database inception to June 2017. We included studies measuring the prevalence of AA or ACN in average-risk Black and White persons undergoing screening colonoscopy. Two authors independently assessed study quality and risk for bias using a modified NIH quality assessment instrument for cross-sectional studies, and independently abstracted descriptive and quantitative data from each study. A random effects model for meta-analysis was used, providing the I² measure for heterogeneity, risk differences (RD) and odds ratios (OR).

Results: From 1653 titles, we identified 9 studies that included 302,128 subjects. The largest single study included 292,494 (97%) of all subjects. Six of 9 studies were of high methodological quality and low risk for bias. Overall prevalence of AA/ACN was no different between Blacks and Whites: OR=1.03; 95% CI, 0.81-1.30 and RD=0.00; 95% CI, -0.01 to 0.02; I²=52% showing moderate heterogeneity. Proximal AA/ACN prevalence was greater in Blacks than in Whites: OR=1.20; CI, 1.12-1.30 and RD=0.01; CI, 0.00 to 0.01; I²=0 showing low heterogeneity. Excluding the largest study resulted in no difference in the prevalence of overall AA/ACN (OR=0.99; CI, 0.73-1.34) or proximal AA/ACN (OR=1.48; CI, 0.87-2.52). Including only the highest quality studies for which pathology was available (study N = 5, subject N = 8,503) showed no difference in AA/ACN prevalence (OR=1.06; CI, 0.75-1.50) or proximal AA/ACN prevalence (study N = 3, subject N = 7,187): OR=1.44; CI, 0.84-2.49.

Conclusion: Prevalence of AA/ACN is similar in average-risk Black and White screen-eligible persons, findings that support CRC screening beginning at age 50, irrespective of race.

133 Uptake, Efficacy and Sustainability of a Fitbit Based Lifestyle Program for Patients with Non-Alcoholic Fatty Liver Disease (NAFLD)

Donovan Inniss

Saint John's University/The College of St. Benedict, Collegeville, USA

Abstract: Non-Alcoholic Fatty Liver Disease (NAFLD) is a highly prevalent disease affecting approximately 30% of the US population. It is associated with metabolic diseases including diabetes, obesity, and high cholesterol. Currently there are no FDA approved pharmacologic therapies to halt or reverse liver injury. Prior studies have found that improvement of liver histology and metabolic parameters has been achieved with increases in physical activity and nutritional lifestyle interventions. However, it has been difficult for many patients to initiate and maintain these lifestyle changes. Hypothesis & Aims: We hypothesize that a less vigorous and minimally time-consuming approach to implement these lifestyle changes will serve as an effective and sustainable option for patients. Therefore, the goal of this study is to assess the efficacy, feasibility, and sustainability of a technology (Fitbit) based lifestyle intervention program for patients with NAFLD.

Methods: To assess this, a pilot trial of 40 patients was designed. To date, 23 patients have been enrolled. Baseline metabolic, physical activity, nutritional and Health Related Quality of Life (HRQOL) parameters were collected for each patient, and will be compared to the same measures taken at the end of the 6-month study. Over the course of the study, patients are given weekly individualized feedback on their step counts. Results: The current approached/enrolled ratio of 52%, is comparative to other lifestyle based programs and is indicative of the general appeal of the program to this patient population. The median age of the cohort is 52.5 years, with 52% males and 96% whites. The median baseline BMI is 33.4 and 39% have diabetes. Median baseline AST is 40 and HgA1c is 6. On the Fibrosan the median F score is F0-2 and CAP percentage of steatosis is 348. Among the enrolled patients, 74% are wearing the Fitbit ≥80% of the time. The baseline weekly step count was 5,733 steps and 50% of patients had stable or increasing step counts thus far over the course of the study. Conclusion: As enrollment is ongoing, knowledge gained from the study will improve understanding of the optimal methods to help implement lifestyle changes for patients with NAFLD. This study can then be used to help design larger trials comparing structured lifestyle intervention programs to other NAFLD therapies.

134 The Circulatory Sialyltransferase ST6Gal-1 is a Systemic Regulator of Bone Marrow B Lymphopoiesis at the Transitional B cell Stage

Eric Irons

University at Buffalo, Buffalo, USA

Hematopoiesis generates the cellular components of blood essential to health during homeostasis and stress. Dysregulated hematopoiesis, a feature of many inflammatory and autoimmune diseases, is an attractive but underutilized therapeutic target. As the interface between immune cells and their interactants, glycans are increasingly appreciated as critical mediators of immune cell production, turnover, and function. Although canonical glycosylation is restricted to the ER/Golgi, glycosyltransferases such as ST6Gal-1 are also

secreted into blood during inflammation as part of the acute phase response. We have recently described a novel, extrinsic pathway of glycosylation by which these extracellular glycosyltransferases modify cell surface glycans in a non cell-autonomous manner. This paradigm predicts that circulating glycosyltransferases are global regulators of glycan-dependent processes. Indeed, we have shown that the serum sialyltransferase ST6Gal-1 influences IgG sialylation and inhibits bone marrow granulocyte production. In this study, we present evidence that extrinsic ST6Gal-1 is also a systemic positive regulator of B lymphocyte development. ST6Gal-1 deficiency impeded the development of transitional and marginal zone B cells *in vivo*. However, the discordance between ST6Gal-1 expression and cell surface α 2,6-sialylation during B cell development suggested that intrinsic expression could not completely account for B cell sialylation. Given the association of serum ST6Gal-1 with stress and inflammatory states, we hypothesized that serum ST6Gal-1 could upregulate production of B cells during inflammation in anticipation of imminent antigen presentation. Bone marrow transplantations between WT and ST6Gal-1 deficient mice showed that intrinsic ST6Gal-1 expression was necessary for marginal zone B cell development, but extrinsic ST6Gal-1 was necessary for transitional B cell development. The cellular targets of extrinsic sialylation were identified as the bone marrow immature and transitional B cell populations, which exhibited decreased α 2,6-sialylation in chimeras lacking host ST6Gal-1. *Ex vivo*, treatment of immature B cells with extrinsic ST6Gal-1 supported differentiation into transitional B cells and increased CD23 expression. Our findings show an unexpected role for extrinsic sialylation by ST6Gal-1 in B lymphopoiesis. This novel axis sheds light on the long elusive function of circulating sialyltransferases and adds complexity to the glycan-dependent control of immune cell production - an emerging theme in hematology. As primary targets of negative selection, transitional B cells are a labile population that can harbor self-reactive clones towards the development of autoimmunity. Thus, our observations are consistent with the well-documented role of sialylation in immune tolerance, but potentially represent a target more amenable to clinical manipulation by intravenous administration of recombinant enzyme or inhibitors. Future studies will determine the mechanism by which extrinsic ST6Gal-1 influence B lymphopoiesis, and its consequences for autoimmunity.

135 Type-2 cGMP dependent protein kinase has a tumor-suppressive role in the colon epithelium

Bianca N. Islam

Augusta University, Augusta, USA

The cGMP level plays a central role in regulating homeostasis in the colon epithelium and is emerging as a potential target for colon cancer prevention. The signaling components downstream of cGMP, and the tumor suppressive mechanism remain poorly understood. The present study has examined the expression of cGMP-dependent protein kinase isoforms (PKG1, PKG2) in normal intestinal mucosa and in colon cancer from human specimens. Immunohistochemical analysis detected PKG1 in supportive cells in the lamina propria and in smooth-muscle tissue, but not in the epithelium of normal intestine and colon. In contrast, PKG2 was detected exclusively in the epithelium. In colon cancer, PKG1 was restricted to the stroma where it colocalized with vimentin, whereas PKG2 was only detected in the tumor epithelium where it colocalized with cytokeratin. This pattern of PKG isoform expression was similar in the mouse intestine and colon, where only PKG2 was detected in purified colonic crypts. PKG2 knockout (KO) mice were used to interrogate possible anti-carcinogenic roles in the colon epithelium. When subjected to the

AOM/DSS model of colon carcinogenesis, the PKG2 KO animals produced significantly more polyps than wild type controls (1.75-fold, $p=0.0037$). While the polyps from PKG2 KO animals were slightly smaller than those from wild type, the trend was not significant ($p=0.13$). Wild type and PKG2 KO mice responded equally to DSS treatment, but the PKG2-deficient animals exhibited crypt hyperplasia and increased apoptosis in luminal epithelium relative to wild type animals. Taken together these findings suggest that PKG2 has a tumor suppressive role in the colon epithelium, and that reducing the proliferative compartment may be part of the mechanism.

136 Sonoreperfusion of microvascular obstruction: a step toward clinical translation

Filip Istvanic

University of Pittsburgh School of Medicine, USA

Microembolization during percutaneous coronary intervention for acute myocardial infarction causes microvascular obstruction (MVO). We have shown that sonoreperfusion therapy using ultrasound (US) and lipid microbubbles restores microvascular perfusion in an *in vitro* model of MVO, and that reperfusion efficacy increases with US pulse length. To enable clinical translation of this technique, we compared the reperfusion efficacy of an experimental long-pulse US system (modified Philips EPIQ) to that of a clinical short-pulse US system (Philips Sonos 7500), which has been shown to enhance perfusion in a rodent hindlimb arterial ligation model of ischemia. We hypothesized that the experimental long-pulse US delivery system would relieve MVO to a greater extent in a rat hindlimb model of MVO than would the clinical short-pulse US delivery system.

Our rat hindlimb model of MVO was created by injecting microthrombi into the hindlimb muscle microvasculature via the contralateral femoral artery. Lipid encapsulated microbubbles were infused through the femoral artery while therapeutic US was delivered to the obstructed microvasculature for two 10-minute treatment sessions using either a long pulse (1600 cycles, 1.6 MHz, 1.1 MPa, 0.33 Hz framerate) or a "short" pulse (5 cycles repeated 7 times, 1.3 MHz, 1.3 MPa, 0.33 Hz framerate). Control rats were injected with microthrombi but did not receive US therapy. Contrast enhanced US perfusion imaging (Sequoia, CPS, 7 MHz) of the microvasculature was conducted at (1) baseline (BL), (2) post-MVO, (3) post-treatment 1 (Tx1), and (4) post-treatment 2 (Tx2). DEFINITY® microbubble contrast agent was infused through the jugular vein during perfusion imaging. Microvascular blood volumes (MBV) were calculated from videointensity-time data measured in hindlimb muscle regions of interest. Data are expressed as mean \pm standard deviation.

MBV were similar at baseline and markedly reduced after MVO for all groups. In the long-pulse rats ($n=4$), MBV increased to 91% of BL after Tx2 (15.7 ± 1.9 dB, n.s vs BL, adj p value <0.0001 vs MVO, adj p value <0.0001 vs Short-pulse Tx2, adj p value <0.0001 vs No Treatment Tx2). In the short-pulse group ($n=4$), MBV remained reduced at 22% of BL after Tx2 (4.0 ± 5.0 dB, n.s. vs MVO). In the "No Treatment" group ($n=4$), MBV remained reduced at 7.2% of BL after Tx2 (0.98 ± 1.0 dB, n.s. vs MVO).

These data demonstrate the superior reperfusion efficacy of a long-pulse (1600 cycles) vs. short-pulse (35 cycles) US delivery system for the treatment of MVO. This *in vivo* observation aligns with our previous *in vitro* findings showing that longer pulse length is associated with greater reperfusion efficacy. Results obtained from this study should inform clinical translation and optimization of sonoreperfusion of MVO.

137 Deciphering the functional heterogeneity of the human macrophage response to *Mycobacterium tuberculosis* infection

Christopher Y. Itoh

Harvard T.H. Chan School of Public Health, USA

Mycobacterium tuberculosis (Mtb), the causative agent of tuberculosis, is the leading cause of infectious death in the world. Macrophages are critical to both the progression and control of Mtb infection, providing a protected niche for the bacterium in some cases but clearing the bacterium in others. We understand little about how differences in macrophage antimicrobial capacity are established and maintained. Canonically, M1 macrophages are thought to be antimicrobial and M2 macrophages are immunoregulatory. However, several lines of evidence now indicate that there is extensive transcriptional and functional heterogeneity within macrophage populations that is not captured by these classifiers. To define the dynamics of macrophage memory and plasticity, we developed HERMES (High-dimensional Evaluation of Response to Macrophage Environmental Stimuli), an in vitro platform to characterize macrophage responses and assess their phenotypic stability. This assay captures both static and dynamic features of macrophage state, including surface marker expression, cytokine production, and antimicrobial capacity. HERMES involves a tiered checkerboard assay in which we polarized macrophages with a primary differentiation stimuli, M-CSF or GM-CSF, modulated their state with LPS, IFN- γ , IL-4, IL-6 or IL-10, and measured their response to different TLR stimuli. Macrophages were indistinguishable by canonical surface markers; however, by using a strategy that is both combinatorial and state specific, we uncovered routes of macrophage state modulation that are both terminal and plastic as indicated through their cytokine release profiles. Furthermore, we observed that polarized macrophages had differential capacity to control Mtb growth indicating that macrophage antimicrobial programs were also differentially engaged. In conclusion, macrophage exposure and stimulation history give rise to combinatorial plasticity, as well as differential response in Mtb control. HERMES allows us to investigate the complexity of macrophage plasticity and help define strategies capable of activating a pathway for the most effective macrophage state to control disease.

138 Elucidation of an exquisite synthetic lethal interaction between ATR inhibitors and alkylating agents in MGMT-methylated glioma cells

Christopher B. Jackson

Yale University, USA

Glioblastoma is the most common primary brain tumor in adults. The current standard of care for this condition consists of surgery with maximal resection followed by concurrent temozolomide (TMZ) and radiation therapy. TMZ belongs to a class of alkylating agents which are thought to exert their main cytotoxic effects on cells via methylation of DNA bases, including guanine bases at the O6 position (O6meG). O6-methylguanine-DNA methyltransferase (MGMT) is a suicide enzyme that repairs TMZ-induced DNA damage by removing these alkyl adducts.

The promoter region of MGMT contains CpG island regions that are methylated in approximately 45% of glioblastoma cases. Patients with methylation of the MGMT promoter respond more readily to TMZ and survive approximately 9 months longer than patients with an unmethylated MGMT promoter. Despite this prognostic benefit, these patients still have a median survival of only 21.7 months. Ample opportunity still exists to better understand the relationship between MGMT and TMZ and to introduce treatments that further extend survival in these patients.

Here, we report exquisite synergistic interactions between TMZ and inhibitors of a key DNA damage response protein, ataxia telangiectasia and rad3-related protein (ATR). Preliminary data suggest a mechanism of action which involves acute replication stress leading to fork collapse, and consequent induction of DNA double-strand breaks. TMZ induces activation of ATR specifically in MGMT-methylated glioma cells, and inhibition of ATR signaling sensitizes the glioma cells to TMZ. The magnitude of TMZ sensitization by ATR inhibition is marked—over 100-fold—and entirely dependent on MGMT status. These data lay the foundation for future clinical trials testing this combination specifically in MGMT-methylated glioma, and they challenge previously described mechanisms of action proposed for the differential sensitivity of TMZ in MGMT-methylated tumors.

139 The role of Teneurins in neurodevelopmental disorders

Hudin N. Jackson

University of Connecticut School of Medicine, USA

Neurodevelopmental disorders (NDD) encompass conditions in which development of the central nervous system is perturbed and manifest as neuropsychiatric problems or impaired motor function, learning, language, or non-verbal communication. The underlying etiologies for these disorders are highly complex, but increasing evidence has shown that different rare and common genetic alterations can contribute to similar disease mechanisms underlying shared clinical phenotypes. This suggests that determining the genetic basis and pathogenic mechanisms of rare monogenic disorders has the potential to provide critical insights for many highly prevalent NDD. Therefore, we developed a large-scale collaborative effort to identify individuals with either rare conditions or rare genetic etiologies and to determine the functional consequences of the human gene alterations in a high-throughput *Drosophila* system.

Through multi-institutional collaborations, several individuals with neurodevelopmental disorders were identified with candidate pathogenic variants in vertebrate teneurin genes. These individuals exhibit a range of neurological deficits that were not previously shown to be associated with this gene family. The evolutionarily conserved teneurins encode transmembrane proteins involved in a number of processes integral to the proper development of the nervous system, including neuronal outgrowth, synaptic organization, and synaptic transmission. Previous studies of the fly teneurins, *ten-a* and *ten-m*, demonstrated that knockdown of *ten-m* and *ten-a* causes synaptic loss, impaired apposition of pre- and post-synaptic partners and defective synaptic transmission. Teneurin knockdown in flies results in locomotor deficits, marked by poor crawling. Studies in vertebrates demonstrated that *TENM1* knockout mice display impaired odor discrimination and *TENM4* knockout mice exhibit tremors. *TENM4* knockdown also causes hypomyelination of small axons and inhibition of oligodendrocyte differentiation within the spinal cord of *TENM4* mutant mice.

In order to determine the pathogenic nature of the rare human variants, we employed a genetic system where the endogenous locus for the fly homolog is disrupted resulting in a loss of function allele that simultaneously expresses the yeast transactivator gene (*GAL4*) under the same spatiotemporal regulation of the endogenous locus. To study the human teneurins, we generated a novel *ten-a-T2A-GAL4* allele and obtained the *ten-m Gal4* allele (*w1118; PBac(IT.GAL4)Ten-m0257-G4/TM6B, Tb1*). The *ten-a-T2A-Gal4* and *ten-m-Gal4* alleles are used in conjunction with transgenic fly alleles expressing wildtype and variant fly and human teneurin cDNAs (hcDNA) under the regulation of Upstream Activating Sequences (UAS). The UAS-GAL4 system allows us to perform

a high-throughput in vivo analysis of the consequences of human gene variants on nervous system development and function. These findings have the potential to elucidate the role of teneurins in human NDD and identify shared pathogenic mechanisms that may provide insight into novel therapeutic avenues.

140 Basal interferon stimulated gene expression influences the productive infection of oncolytic HSV in malignant peripheral nerve sheath tumor cells

Joshua Jackson

Univeristy of Alabama at Birmingham, Birmingham, USA

Introduction: Malignant peripheral nerve sheath tumors (MPNSTs) are aggressive cancers of the nerve sheath. Nearly half arise sporadically while the other half are associated with neurofibromatosis type 1 (NF1). Among all patients, median survival is a dismal 24 months following diagnosis. MPNSTs are typically refractory to traditional chemotherapy and radiotherapy, with surgical resection as the only demonstrable benefit to survival, therefore oncolytic HSV virotherapy has been suggested as a therapeutic alternative.

Objective: Determine the extent to which MPNST cells resist the productive infection of oncolytic herpes simplex virus (oHSV) through activation of the JAK/STAT1 pathway and resultant upregulation of interferon stimulated genes (ISGs). ISGs encode diverse proteins that mediate intrinsic antiviral resistance in infected cells.

Methods: Twenty-one human and mouse MPNST cells were used to explore the relationship between STAT1 activation and the productive infection of $\Delta\gamma$ 134.5 oHSVs.

Results: STAT1 activation in response to oHSV infection was found to associate with diminished $\Delta\gamma$ 134.5 oHSVs replication and spread. Multi-day pre-treatment, but not co-treatment, with a JAK inhibitor significantly improved viral titer and spread. ISG expression was found to be elevated prior to infection and downregulated when treated with the inhibitor, suggesting that the JAK/STAT1 pathway is active prior to infection. Conversely, upregulation of ISG expression in normally permissive cells significantly decreased oHSV productivity. Finally, a link between NF κ B pathway activation and ISG expression was established through the expression of inhibitor of κ B (IkB) which decreased basal STAT1 transcription and ISG expression.

Conclusion: While cancer-associated ISG expression has been previously reported to impart resistance to chemotherapy and radiotherapy, these data show that basal ISG expression also contributes to oncolytic HSV resistance.

141 Generation of functional lung alveolar epithelial cells from human pluripotent stem cells

Anjali Jacob

Boston University School of Medicine, Boston, USA

Pulmonary alveolar epithelial type II cell (AEC2) dysfunction has been implicated as a primary cause of pathogenesis in many poorly understood lung diseases that lack effective therapies, including interstitial lung disease (ILD) and emphysema. AEC2s are inaccessible to study in the developing human embryo and difficult to study in patients. They proliferate poorly and rapidly transdifferentiate into other cell types when isolated and cultured, severely limiting research in alveolar development and disease. Using iPSC technology and directed differentiation to generate AEC2s de novo would provide novel opportunities to study both normal AEC2 development and the pathogenesis of monogenic alveolar diseases. AEC2s have been challenging to generate in vitro from pluripotent stem cells (PSCs), however, in part because alveoli are a tissue type that arose late in evolutionary time, existing only in air-breathing

organisms, and with limited lower organism model systems available to provide the necessary developmental roadmaps to guide in vitro differentiation.

Here we report the successful directed differentiation in vitro of human PSCs into AEC2s, the facultative progenitors of lung alveoli. Using gene editing to engineer multicore fluorescent reporter PSC lines (NKX2-1^{GFP};SFTPC^{tdTomato}), we track and purify human SFTPC+ alveolar progenitors as they emerge from NKX2-1+ endodermal developmental precursors in response to stimulation of Wnt and FGF signaling. Purified PSC-derived SFTPC+ cells are able to form monolayered epithelial spheres ("alveolospheres") in 3D cultures without the need for mesenchymal co-culture support, exhibit extensive self-renewal capacity, and display additional canonical AEC2 functional capacities, including innate immune responsiveness, the production of lamellar bodies able to package surfactant, and the ability to undergo squamous cell differentiation while upregulating type 1 alveolar cell markers. Importantly, despite weeks to months of *in vitro* culture, these cells exhibit a normal karyotype. Guided by time-series global transcriptomic profiling we find that AEC2 maturation involves downregulation of Wnt signaling activity, and the highest differentially expressed transcripts in the resulting SFTPC+ cells encode genes associated with lamellar body and surfactant biogenesis. Finally, we apply this novel model system to generate patient-specific AEC2s from induced PSCs (iPSCs) carrying homozygous surfactant mutations (SFTPB^{121ins2}), and we employ footprint-free CRISPR-based gene editing to observe that correction of this genetic lesion restores surfactant processing in the cells responsible for their disease. Thus, we provide an approach for disease modeling and future functional regeneration of a cell type unique to air-breathing organisms.

142 FGF2-FGFR1 Signaling Regulates Release of Leukemia-Protective Exosomes from Bone Marrow Stromal Cells

Nathalie Javidi-Sharifi

Oregon Health and Science University, Portland, USA

The bone marrow microenvironment provides support for normal hematopoiesis, but also shields leukemic cells from the effects of chemotherapy through various mechanisms. This protection leads to persistence of malignant cells, development of resistance and disease relapse. We previously identified fibroblast growth factor 2 (FGF2) as a protective signal in both chronic myeloid leukemia (CML) and acute myeloid leukemia (AML) with FLT3 ITD after tyrosine kinase inhibitor (TKI) therapy. FGF2 is expressed in bone marrow stromal cells and FGF2 expression increases during exposure to therapy. Here, we demonstrate that FGF2 is delivered from stromal cells to leukemia cells via exosomes, and stromal exosomes protect leukemia cells during TKI exposure. Expression of FGF2 and its receptor, FGFR1, are both increased in a subset of stromal cell lines and patient-derived AML stroma. FGFR inhibition or gene silencing in stromal cells abrogates FGF2-mediated autocrine growth signaling and significantly decreases secretion of FGF2-containing exosomes. This results in decreased stromal protection of leukemia cells. In a mouse model of BCR-Abl leukemia, FGF2-/- mice survive significantly longer than wt counterparts when treated with TKI. Exosomes from wt mouse stroma supported increased BCR-Abl colony formation under TKI exposure compared to FGF2-/- exosomes. We conclude that exosomes are important purveyors of protective signaling in the leukemia microenvironment and their production is regulated in part by FGF2-FGFR1 autocrine signaling in bone marrow stroma. Inhibition of FGFR can interrupt this protective stroma-leukemia interaction and restore TKI sensitivity to leukemia cell in the bone marrow niche.

143 “TIPSTer” to the rescue: A rapid and sensitive method for detecting tumor cells in pleural fluid from lung cancer patients

Samuel R. Jean-Baptiste

University of Pennsylvania, Philadelphia, USA

Pleural effusions (PE) is a potentially life-threatening condition afflicting up to 1.5 million people in the U.S. each year. The etiology of PE can range from inflammation/infection to cancer; it is especially essential to determine whether an effusion is of malignant origin due to profound implications for staging and treatment. Analysis of PE via standard cytology is however labor-intensive, lacks sensitivity, or requires large samples for accurate identification of cancer cells. Here we describe a novel method to identify cancer cells efficiently and accurately in small samples of pleural fluid.

We have developed a new diagnostic methodology, which we refer to as Tumor cell Identification in Pleural fluid via Size and TelomERase activity (or TIPSTer), for detecting rare cancer cells in limited amounts of pleural and other bodily fluids. TIPSTer employs a microfluidic-based system (CelSee chip) to isolate cancer cells based on size (cells larger than 8 μm) and deformability (cancer cells are relatively more rigid than monocytes) in conjunction with an adenoviral probe that drives GFP expression in the presence of the elevated human telomerase promoter activity that is characteristic of almost all cancer cells but not normal cells. Tumor cells expressing GFP are then identified based on size, shape, and fluorescence intensity.

We first tested and validated TIPSTer in human lung cancer cells in culture and spiked into control blood. To confirm that the GFP-expressing tumor cells isolated via TIPSTer were of tumor origin, we assessed for thyroid transcription factor 1 (TTF-1) and Napsin A (expressed respectively by well and poorly differentiated lung adenocarcinoma). The usefulness of TTF-1 and Napsin A for this purpose was previously confirmed via western blotting and immunofluorescence staining of positive and negative control cell lines. To simulate a patient PE sample, U251 cells tagged with mCherry were spiked into fluids of human origin and then isolated via a CelSee microfluidic chip to validate its applicability in capturing tumor cells. Finally, we show that malignant cells can be successfully identified in 10 ml PE samples from patients with non-small cell lung cancer, via the TIPSTer method.

We present promising preclinical and clinical results with this method. This method should be useful for rapidly assessing if PE (or other bodily fluids) are due to malignant disease. Furthermore, downstream molecular analysis such as for next generation genetic sequencing require cells of substantial quality and quantity, which TIPSTer could provide. We describe future plans for further validation including to identify targetable pre-existing mutation(s) of driver mutations in genes such as KRAS and EGFR in tumor cells isolated from PE and matched blood samples.

144 The Role of STIM1, Orai1 and Orai3 in Regulating ASM Remodeling in Asthma

Martin Johnson

Penn State, Hummelstown, USA

Asthma is a chronic obstructive pulmonary disease that affects 358 million people worldwide. A major pathological hallmark of asthma is airway smooth muscle (ASM) remodeling, which is characterized by ASM proliferation and migration. Calcium (Ca^{2+}) is a major regulator of ASM remodeling. Ca^{2+} entry channels including those activated by depletion of internal Ca^{2+} stores (Stored Operated Calcium Entry; SOCE) and those independent of Ca^{2+} depletion (nonSOCE) have recently been implicated in ASM remodeling. The sarcoplasmic

reticulum calcium sensor, STIM1, and the plasma membrane protein, Orai1, activate SOCE. While Orai1, Orai3, STIM1, and the inflammatory mediator leukotriene C_4 (LTC_4), activates nonSOCE. We have previously shown that SOCE is augmented in asthma. However, the role of nonSOCE including STIM1, Orai3, and Orai1 in ASM remodeling is unclear. It has been shown in vascular smooth muscle (VSM) remodeling that upregulation of Orai3 and nonSOCE causes enhanced migration through activation of mTOR/AKT. ASM remodeling shares many features with VSM remodeling.

Through cultured ASM obtained from postmortem human lung donors (HASM), the Ca^{2+} signaling of Orai1, Orai3, and STIM1 in airway remodeling was investigated. Intracellular Ca^{2+} in HASM was measured using fura2-AM. SOCE and nonSOCE was demonstrated using the Ca^{2+} off/ Ca^{2+} on protocol in the presence of thapsigargin and physiological agonists. Three normal and asthmatic human donors displayed SOCE and were reversed through SOCE inhibitors. HASM remodeling through cellular migration was studied using the wound-healing assay. HASM migration was compared at 0 and 12 hours in siOrai1, siOrai3, siSTIM1, and non-targeting siRNA. To explore a mechanism, phosphorylation of AKT in siSTIM1, siOrai1, and siOrai3 HASM was measured when stimulated with growth factors.

In conclusion, these results elucidate a novel calcium-signaling pathway through nonSOCE and mTOR/AKT that allows HASM remodeling and pathogenesis of asthma. Further studies unraveling this pathway will reveal novel therapeutic targets in asthma.

145 Characterization of Transforming NTRK2 and NTRK3 Mutations in Leukemia

Sunil K. Joshi

Knight Cancer Institute, Oregon Health & Science University, Portland, USA

Introduction: The neurotrophic tyrosine receptor kinases (NTRK) are a family of neuronal transmembrane receptors that comprise of an: extracellular domain for ligand binding, transmembrane domain, and intracellular domain with kinase activity. These receptors signal through several pathways including JAK/STAT, PI3K/AKT, and MEK/ERK to promote proliferation, differentiation, and survival. Although much of the literature has focused on the importance of these receptors in neuronal development, over the past decade, gene fusions containing NTRK family members have been implicated in driving tumor growth in salivary gland, breast, lung, colon, and neuronal cancers.

Moreover, expression of NTRK2 and NTRK3 has been reported in lymphoid and myeloid malignancies (Li, Z *et al.* Blood, 2009). Interestingly, NTRK3 expression has been associated with poorer prognosis (Hillis, J *et al.* Cellular and Molecular Life Sciences, 2016). Despite these initial studies, the role of NTRK receptors largely remains under-investigated in the setting of hematologic malignancies. Herein, we describe somatic mutations in NTRK2 and NTRK3 that were identified using next-generation sequencing of primary leukemia patient samples. We evaluated changes in downstream signaling driven by these mutations in our previously validated Ba/F3 transformation model system. Lastly, we demonstrate that selective inhibition of NTRK2 and NTRK3 with entrectinib, a well-validated NTRK inhibitor currently in clinical trials for NTRK-fusion positive cancers, can inhibit proliferation and induce apoptosis of NTRK transformed cells.

Results: We found two point mutations in NTRK2 that were transforming — one in the extracellular domain (A203T) and one in the juxtamembrane domain (R458G). Similarly, we found two

point mutations that were transforming in NTRK3. One was in the extracellular domain (E176D) and the other within the transmembrane domain (L449F).

Immunoblot results suggest that expression of total and phosphorylated NTRK2 and NTRK3 is increased in mutant-transformed Ba/F3 cells relative to wild-type cells. Furthermore, NTRK2 and NTRK3 mutant-driven cells exhibited enhanced phosphorylation of AKT, SRC, and ERK compared to wild-type cells. While phosphorylation of STAT3 was significantly increased in Ba/F3 cells transfected with both NTRK3 mutants, it was increased only in one of the NTRK2 mutants (A203T).

Upon treating NTRK mutant-transformed Ba/F3 cells with entrectinib (0, 5, 25, 100 nM), we observed a dose-dependent decrease in total and phosphorylated NTRK2 and NTRK3 in all mutants except for NTRK2 mutant R458G. With R458G, total and phosphorylated NTRK2 expression decreased up to 25 nM of entrectinib but that effect was diminished at 100 nM.

Conclusions: Taken together, our data demonstrates mutations in NTRK2 and NTRK3 have transformative potential to promote downstream survival signaling and leukemogenesis. More importantly, these activated pathways can be pharmacologically attenuated using entrectinib. Our findings contribute to ongoing efforts to understand molecular changes that drive hematological malignancies and could potentially alter current treatment modalities.

146 Littoral Cells of the Human Spleen: A Specialized Barrier Cell?

Sandeep Jubbal

University of Massachusetts Medical School, Marlborough, USA

Human spleen was historically viewed as a vestigial organ that was not critical for survival, thus early studies were limited. In the 1970s a vital role in the regulation of RBC turnover and prevention of sepsis was established. More recently, functions in the prevention of ischemic heart damage, several cancers, auto-immune and even metabolic diseases have been revealed based on epidemiologic research.

The spleen is the largest secondary lymphoid organ in humans though it is uniquely accessed by the circulatory system. Unlike lymph nodes, the spleen lacks an afferent lymphatic supply and is not connected to the lymphatic system. Only cells and pathogens that circulate are interrogated, destroyed and/or released from spleen. Human spleen is highly vascularized and has a unique open microcirculation. Splenic arterioles and the capillaries do not drain into venules, but instead release blood directly into an open meshwork of reticular fibers. Blood is then collected into small cavities called the venous sinuses lined by a uniquely human cell population known as littoral cells (LCs). LCs regulate the inter-cellular slit size that facilitates return of passenger cells and particles to the circulation. The precise mechanism(s) through which this is achieved is unknown. RBCs and other cells must deform to squeeze through these narrow inter-cellular slits from outside to inside the venous sinuses or many pass through these cells in a process known as transcytosis.

LCs emerged late in evolution only in higher primates. They exhibit a unique phenotype as they express antigens common not only to endothelial cells (CD 31) but also to macrophages (macrophage mannose receptor, signal regulatory protein- α -SIRP α), smooth muscle cells (formin homology protein-1-FHOD1), and lymphoid cells (CD8 α), though they lack the common lineage-associated markers CD34 (endothelial) and CD45 (hematopoietic). Morphologically,

these cells contain prominent cytoplasmic "stress" fibers, pinocytotic vesicles, lysosomes, phagocytosed cells and debris.

The morphologic appearance as well as presence of a unique spectrum of antigens on LCs, support the hypothesis that LCs serve as a major filter of circulating cells and pathogens - determining which products will return to the general circulation. The mechanisms that they use to achieve to process circulating pathogens, altered cells, aged erythrocytes, and other debris (e.g. directly (phagocytosis, entosis) or by presenting them to the neighboring T cells and the macrophages) are entirely unknown. Our current work is focused on establishment of a platform for characterization of LCs in situ and elucidating the cellular mechanisms they utilize to process different cells, pathogens and particles. Work on visualization of LCs in situ through advanced microscopy, purification and culturing using specialized media to support ex-vivo survival will be reported as a prelude to experiments that address the mechanism(s) by which different cell types are processed by LCs.

147 Structural tools for clinical problems: Ubiquitin-specific protease 7 and p53, a critical regulatory complex in cancer

Timofey Karginov

Department of Molecular Biology and Biophysics, University of Connecticut Health Center, New Britain, USA

Ubiquitin-specific protease 7 (USP7) is a deubiquitinase regulating turnover of proteins involved in tumor suppression, DNA damage, and immune response. USP7 consists of a tumor necrosis factor receptor-associated factor (TRAF)-like domain at its N-terminus, a catalytic domain, and five Ubiquitin-like regions (Ubl1-5). Structures of all individual domains of USP7 have been resolved. However, the tertiary folding of the full-length protein is currently unknown; a full-length structure of USP7 could subsequently help to elucidate this folding pattern as well as binding of USP7 to its substrates. The TRAF-like domain of USP7 is known to bind to the transcription factor p53, a tumor suppressor involved in cell cycle arrest and apoptosis that is often found mutated in cancers. In order to investigate USP7's full-length structure, we successfully purified full-length USP7 and observed complex formation with a recombinant p53 construct. We further conducted both negative stain electron microscopy as well as cryo-electron microscopy experiments to elucidate structure and binding patterns of full-length USP7 and USP7-p53 complex. Here, we demonstrate supporting evidence for production of both USP7 and USP7-p53 complex. These results can further be used to determine the structure of full-length USP7 and investigate binding of p53 to USP7. Given USP7's regulation and binding of p53 as well as its role in cancers, characterization of USP7 structure and substrate binding would help to elucidate interactions that could be targeted for inhibition and subsequent use in cancer therapy.

148 Acta2 R149C mutation causes atherosclerosis via proliferative and inflammatory pathways.

Kaveeta Kaw

University of Texas Health Science Center at Houston, Houston, USA

Heterozygous missense mutations in ACTA2 account for 14% of familial ascending thoracic aortic aneurysms and dissections (TAAD). Patients carrying the ACTA2 R149 variant are pre-disposed to both TAAD and early onset coronary artery disease. To understand why this mutation leads to two distinct disease processes and which molecular mechanisms underlie the pathology, our lab utilized CRISPR/Cas9 technology to generate a transgenic mouse model, Acta2R149C/+. The Acta2R149C/+ mouse does not show aortic

enlargement; however the mouse has increased atherosclerotic plaque burden when crossed into an ApoE^{-/-} background and fed a high fat diet. Interestingly, there is no significant difference in lipid levels between the ApoE^{-/-} mouse and the ApoE^{-/-} Acta2R149C/+ double mutant. Both smooth muscle cell proliferation and inflammation have been shown to be involved in atherosclerotic plaque pathogenesis. Acta2R149C/+ smooth muscle cells (SMCs) are more proliferative than wild-type cells in culture. The Acta2R149C/+ mouse does not have reduced contractile gene expression or altered localization of MRTF-A, suggesting that proliferation is not due to classic phenotypic switching. We previously identified a pathway involving focal adhesion kinase, altered cellular p53 localization, and increased expression of PDGFR as the mechanism driving increased proliferation in Acta2^{-/-} SMCs. Acta2R149C/+ cells also have altered focal adhesions, but it is not yet established whether the same pathway drives proliferation in these cells. Additionally, we have found increased inflammatory markers in Acta2R149C/+ aortas at six months of age. SMCs can transdifferentiate into macrophages in atherosclerotic plaques; to model this in culture we conducted a cholesterol loading experiment, and Acta2R149C/+ cells were found to express macrophage markers at a much lower cholesterol dose than wild-type cells. Taken together, our data suggests that mutant SMCs are prone to both increased proliferation and inflammation, and both mechanisms may explain why Acta2R149C/+ mice are prone to atherosclerosis. Future studies will investigate the specific mechanisms linking the R149 mutation in actin with proliferation and inflammation to determine how this mutation causes atherosclerosis.

149 Human species-specific loss of the CMP-N-acetylneuraminic Acid Hydroxylase fuels atherosclerosis development via intrinsic and extrinsic mechanisms

Kunio Kawanishi

Department of Cellular and Molecular Medicine, University of California, San Diego, La Jolla, USA

Introduction: Cardiovascular disease (CVD) events due to atherosclerosis are very common in humans, but rarely occur spontaneously in other mammals, absent experimental manipulation. CVD events are rare even in closely related chimpanzees in captivity, despite human-like atherogenic blood lipid profiles, hypertension and sedentary lifestyle. All humans exhibit a species-specific deficiency of the common mammalian sialic acid N-glycolylneuraminic acid (Neu5Gc), due to pseudogenization of the CMP-N-acetylneuraminic acid (Neu5Ac) hydroxylase (CMAH) gene, which occurred in hominin ancestors about 2-3 million years ago. Human-like *Cmah*^{-/-} mice that express only the precursor sialic acid Neu5Ac are more prone to insulin resistance and have more reactive macrophages and T cells. Human dietary consumption of Neu5Gc (primarily from red meat), can act as a foreign "xenoantigen" in humans that gets metabolically incorporated into endogenous glycoproteins. Humans with circulating anti-Neu5Gc "xeno-autoantibodies" can thus potentially develop local chronic inflammation or "xenosialitis" at sites of Neu5Gc accumulation such as endothelial cells and in atherosclerotic plaques. Notably, dietary red meat-associated enhancement of CVD is not seen in other carnivorous mammals, and the human risk is typically explained by increased cholesterol and saturated fat in red meat, conversion of choline and carnitine into trimethylamine N-oxide, and/or oxidant damage due to dietary heme iron. However, none of these mechanisms fully explain the human propensity for atherosclerosis, nor the red meat-specific nature of the dietary component of risk.

Hypothesis: Human CMAH deficiency contributes to CVD via multiple intrinsic and extrinsic mechanisms.

Methods: *Cmah*-deficient *Cmah*^{-/-} and WT mice were bred into an *Ldlr*^{-/-} background and fed a Neu5Gc-free high fat diet (HFD) to induce atherogenesis and assess the impact of CMAH loss. Next, *Cmah*^{-/-} *Ldlr*^{-/-} mice were immunized with control antigens or with Neu5Gc-bearing antigens to generate human-like levels of anti-Neu5Gc antibodies and subsequently fed a Neu5Gc-rich diet, to determine the contribution of diet-induced xenosialitis on atherogenesis.

Result: *Cmah*^{-/-} *Ldlr*^{-/-} mice had increased atherogenesis on a HFD, compared to *Cmah*^{+/+} *Ldlr*^{-/-} mice. This was not associated with cytokine levels in plasma, but increased cytokine expression was seen in *Cmah*^{-/-} *Ldlr*^{-/-} macrophages in comparison to *Cmah*^{+/+} *Ldlr*^{-/-}. The baseline relative hyperglycemia of the *Cmah*^{-/-} *Ldlr*^{-/-} mice was also enhanced on a HF diet. When such mice were immunized to develop human-like levels of anti-Neu5Gc antibodies, they had a 2.5-fold increase in atherosclerosis on a Neu5Gc-rich HFD compared to control Neu5Ac-rich or sialic acid-free HFD feeding. Drastically advanced lesions with increased necrotic core areas and infiltration of macrophages and T-cells accompanied increases in atherosclerotic area and lesion volume. None of these differences were explained by changes in lipoprotein profiles or insulin sensing.

Conclusion: Human evolutionary loss of CMAH likely contributes to atherosclerosis propensity, via both intrinsic mechanisms such as amplified chronic inflammatory response and hyperglycemia; and extrinsic mechanisms such as red meat-derived Neu5Gc-induced xenosialitis.

150 High resolution immune function analyses reveal markedly attenuated IL-7 signaling function restricted to the CD8 T cell compartment in an immunocompromised neonate.

Aaruni Khanolkar

Ann and Robert H. Lurie Children's Hospital of Chicago; Northwestern University, Chicago, USA

A female infant was referred to our institution on day nine of life following a T cell receptor excision circle count of zero (normal value $\geq 250/\mu\text{L}$ of blood) observed during the mandatory statewide newborn screen for severe combined immunodeficiency (SCID). Longitudinal analyses of circulating lymphocytes revealed a persistent paucity of T cells (CD8 T cells \ll CD4 T cells) while the B cell and NK cell counts were consistently within the age-associated normal ranges as were the assessments for serum immunoglobulins. Stringent anti-microbial prophylaxis was initiated from the time of initial referral and the patient's caregivers were instructed to avoid live-vaccine administration. Maternal T cell engraftment was ruled out by chimerism analyses as were DiGeorge Syndrome (by multiplex ligation-dependent probe amplification) and Bare Lymphocyte Syndromes-Types I and II by flow cytometry. Mitogen-induced lymphocyte proliferation was normal albeit lower compared to the control sample assessed in parallel. Given the critical role IL-7 plays in T cell development and homeostasis we next investigated aberrations in the IL-7 signaling axis. We detected higher than normal levels of plasma IL-7 levels in the patient and marked downregulation of IL-7 receptor α (IL-7R α ; CD127) expression specifically on the patient's CD8 T cells as well as almost complete abrogation of CD8 T cell-associated signal transducer and activator of transcription (STAT)5 phosphorylation by phospho analysis following treatment of the patient's whole blood sample with recombinant-human IL-7. Similar treatment of the patient sample with IL-2 did not reveal an inhibition of STAT5 phosphorylation thereby ruling out any intrinsic functional deficits in the signaling components shared by the two pathways [STAT5, common γ chain and Janus Kinase 3 (JAK3)]. Flow cytometry also revealed normal cytosolic expression of the JAK3 protein in the

patient's T cells. However, whole exome sequencing revealed that the patient was a compound heterozygote for two *JAK3* variants [the paternally-derived c.349C>T (p.R117C) and the maternally derived c. 1972G>A (p.E658K) variants]. Homozygous R117C-*JAK3* variant has been described to be associated with atypical T-B+NK+ SCID and E658K is predicted to be a variant of uncertain significance. T cell associated IL-7R α expression and IL-7 signaling analyses performed on samples from the patient's parents and siblings failed to demonstrate similar aberrations thereby casting doubt on the role of the *JAK3* variants in inducing the immunopathology observed in our patient. It is likely that unidentified variants in the relevant regulatory regions of the genome could likely be contributing to the observed immunological findings in our patient. The patient recently underwent a hematopoietic stem cell transplant (HSCT) and is being followed up in the stem cell clinic at our institution.

151 Reprogrammed human cells identify distinct pathogenic mechanisms in myotonic dystrophy disease subtypes

Ellis Y. Kim

University of Chicago, Chicago, USA

Myotonic dystrophies type 1 and type 2 (DM1 and DM2, respectively) are nucleotide repeat expansion disorders where DM1 is characterized genetically by CTG trinucleotide repeat expansion in the *DMPK* gene and DM2 by CCTG tetranucleotide repeat expansion in the *CNBP* gene. In DM1, transcription of nucleotide repeat sequences leads to the formation of intranuclear double stranded RNA foci that bind splicing factors including the muscleblind-like (MBNL) family of RNA-binding proteins, resulting in a functional depletion in MBNL and missplicing of downstream genes. Specific missplicing events are thought to contribute to distinct aspects of pathogenesis in DM1, including muscle myotonia and cardiac dysfunction. The degree to which this same pathogenetic mechanism causes DM2 is not known, as the very large repeats that characterize DM2 have not been effectively modeled. To evaluate whether these mechanisms are shared or distinct between DM1 and DM2, we used direct and indirectly reprogrammed urine-derived cells from human patients with myotonic dystrophy, evaluating both skeletal muscle and cardiac muscle models. Cardiomyocytes were differentiated from induced pluripotent stem cells (iPSCs) (control: n=2, DM1: n=2, DM2: n=4) and skeletal myocytes were differentiated from cells using MyoD overexpression (control: n=2, DM1: n=1, DM2: n=1). Both DM1 cardiomyocytes and skeletal muscles demonstrated intranuclear MBNL clusters, whereas no distinct MBNL clusters were observed in DM2 and control cells. When MBNL target genes in cardiomyocytes were probed using RT-PCR, DM1 displayed missplicing in *SCN5A*, *ANK3*, and *RYR2*, while DM2 cells had splicing patterns similar to control cells. Similarly, when skeletal muscles were probed for misspliced genes, DM1, but not DM2, cells showed a shift towards embryonic splicing pattern in genes such as *INSR*, *mTTN*, *zTTN*, *SERCA*, and *ZASP*. These findings suggest distinct pathogenetic models for DM1 and DM2 where MBNL sequestration and missplicing events characterize DM1 but not DM2. We also studied calcium handling properties with Indo-1 dye by pacing the cardiomyocytes at four different frequencies (0.25, 0.5, 0.75, and 1 Hz, average of 10-15 transient measurements per frequency). Compared to control cells, DM2 cells displayed significantly decreased diastolic calcium and increased calcium release and reuptake rates at every frequency. On the other hand, DM1 cells showed similar diastolic calcium to control cells, but increased calcium release and reuptake rates trending towards significance ($p=0.08$) at lower frequencies (0.25, 0.5, 0.75 Hz). The difference in diastolic calcium between DM1 and DM2 suggests that the increases in calcium release and reuptake

rates may arise from distinct mechanisms in each disease subtype. Together, the results from the cardiomyocyte and skeletal muscle models together implicate that DM1 and DM2, while both nucleotide repeat expansion disorders, have distinct pathogenetic mechanisms.

152 Combinations of Health Status, Access, and Demographic Variables that Predict Cancer History

Uriel Kim

Case Western Reserve University, Cleveland, USA

Traditional research in disparities employs parametric regression methods that identify independent risk factors for disparities. Using this reductionist approach, many independent risk factors for cancer disparities have been identified including race/ethnicity, socioeconomic status, health behavior, and health care access. In reality, risk factors occur in constellations, and distinct patterns of risk may emerge because of the intersection, interaction, and interdependence of many factors. Thus, this study aimed to identify combinations of risk factors that predict cancer history. Data from the 2015 Ohio Medicaid Assessment Survey (OMAS), a complex-designed dual-frame random digit dial telephone survey, was analyzed. For a representative sample of all Ohioans (43,000 Adults), the OMAS reported on the respondents' health status, insurance status, and use of preventive and other health services. The analysis used a machine-learning, nonparametric technique called classification and regression tree (CART) analysis, which examined all the main effects and possible interactions of 17 covariates. The covariates were broadly classified into measures of health care access, health status, health behavior, and demographic characteristics. There were ultimately 25 unique combinations of covariates (termed "phenotypes") associated with cancer history ("never diagnosed with cancer" or "diagnosed with cancer"). Generally, the low-risk phenotypes were constituted by "younger" age individuals (under 44 years old) and the high-risk phenotypes were constituted by "older" age individuals (over 45 years old). There was a "negative deviant phenotype" associated with many more cancer cases than expected. This phenotype was constituted by younger, rural Appalachian females reporting fair health without disabling mental conditions. In the highest risk phenotype, approximately 30% of the individuals have been diagnosed with cancer. This phenotype was constituted by "older" age, widowed individuals who self-reported fair or poor health, have not had major medical bills recently, and have had at least one emergency visit in the past year. In conclusion, there is considerable variation in the "phenotypes" that predict cancer history. Modeling the combinatory effects of covariates advances the understanding of the subpopulations at the highest risk of cancer history, and can inform precision public health interventions aimed at reducing cancer disparities.

153 Rev-erba dynamically modulates chromatin looping to control circadian gene transcription

Yong Hoon Kim

Perelman School of Medicine at the University of Pennsylvania, Philadelphia, USA

Mammalian physiology exhibits 24-hour cyclicity due to circadian rhythms of gene expression controlled by transcription factors (TF) that comprise molecular clocks. The clock orchestrates all-encompassing aspects of physiological homeostasis. As such, genetic and environmental perturbation of the clock can result in devastating health consequences, including neuropsychiatric disorders and metabolic derangements. Core clock TFs bind to the genome at enhancer sequences to regulate circadian gene expression, but not all binding sites are equally functional. Here we demonstrate that

circadian gene expression in mouse liver is controlled by rhythmic chromatin interactions between enhancers and promoters. Rev-erba, a core repressive TF of the clock, opposes functional loop formation between Rev-erba-regulated enhancers and circadian target gene promoters by recruitment of the NCoR-HDAC3 corepressor complex, histone deacetylation, and eviction of the elongation factor BRD4 and the looping factor MED1. Thus, a repressive arm of the molecular clock operates by rhythmically modulating chromatin loops to control circadian gene transcription.

154 Oocytes and embryos from mice of advanced maternal age show decreased mitochondrial mass but no changes in imprinted methylation

Audrey J. Kindsfather

University of Pittsburgh School of Medicine, USA

Over the last several decades, the average age of first-time mothers has risen steadily. Advanced maternal age, defined in humans as above 35 years old, is known to increase the risk of spontaneous abortion, stillbirth, preterm birth, aneuploidy, and other chromosomal abnormalities and birth defects. As a woman ages, molecular changes occur in her oocytes that can affect the ability of the oocytes to be fertilized and the viability of the embryo. These changes include oxidative stress, which is known to damage mitochondria. In addition to other cellular processes, mitochondria likely play a role in regulating epigenetic mechanisms, such as genomic imprinting. Genomic imprinting is an epigenetic phenomenon that restricts expression to predominantly one parental allele through various mechanisms including cytosine methylation. Mitochondria provide both the ATP and methyl groups used for imprinted methylation acquisition in germ cells and imprinted methylation maintenance in preimplantation embryos as the rest of the genome is demethylated. The aim of this project is to determine whether maternal age affects mitochondrial activity and methylation of the imprinted genes Snrpn, H19, and Kcnq1ot1 in mouse oocytes and preimplantation embryos.

Female C57BL/6(CAST7) mice from very young (<2 months), young (2-5 months), middle (6-10 months), and advanced (>10 months) age groups were mated with C57BL/6 males. Morula and blastocysts were collected at day E3.5 by flushing the uterus and oviducts with M2 medium. Oocytes were collected by treating the ovaries with collagenase and trypsin/EDTA. All samples were stained with Mitotracker Red to visualize active mitochondria, Mitotracker Green to visualize total mitochondria, and Hoechst to visualize nucleic acids, and imaged with confocal microscopy. Total and active mitochondria levels were quantified by the green and red intensity, respectively. In oocytes, total and active mitochondrial patterning was characterized as perinuclear, peripheral, homogenous, or aggregated. Individual oocytes, morula, and blastocysts were subjected to bisulfite mutagenesis and assessed for Snrpn, H19, and Kcnq1ot1 imprinted methylation levels.

Our data show that there was a significant decrease in active mitochondrial mass in both oocytes and blastocysts with increasing maternal age. While the mitochondria in oocytes from young and middle-aged mothers was usually arranged in perinuclear and homogenous patterns, oocytes from mothers of advanced age show peripheral and aggregated patterns more frequently. However, our data to date have not shown any difference between imprinted methylation levels of Snrpn, H19, and Kcnq1ot1 in oocytes and blastocysts between mice of any of the age groups. Future studies will determine the consequences of the observed mitochondrial dysfunction, as well as examine how assisted reproductive technologies such as superovulation and embryo culture affect

mitochondrial activity and imprinted methylation in oocytes and embryos from mice of advanced maternal age.

155 Understanding Marburg virus protection through therapeutic antibody MR191

Liam King

University of California San Diego, San Diego, USA

The filovirus family contains Ebola virus (EBOV), Marburg virus (MARV) and other pathogens that can cause severe disease in humans. Ebola virus caused a sustained outbreak in West Africa with >11,000 fatalities from >28,000 cases. Marburg virus has a similar outbreak potential. The 2004-2005 Marburg virus outbreak in Angola caused 90% lethality. It re-emerged in 2007, and in 2008, travelers to Uganda were hospitalized in the United States and Europe with severe Marburg virus disease. A large panel of antibodies was isolated from the American patient by the Crowe lab at Vanderbilt University and characterized for binding and neutralization. One of the antibodies in this panel is MR191, which protects 100% of non-human primates against MARV challenge and is a candidate for an emergency post-exposure immunotherapeutic. Here we present the crystal structure of MR191 in complex with the trimeric, pre-fusion, uncleaved Marburg virus surface glycoprotein (GP). This crystal structure and accompanying biochemistry illuminates the precise interactions made by this extremely potent antibody and illustrates how it neutralizes infection by binding to the receptor binding site at the apex of GP. This site is largely conserved across the filovirus genus. The structure explains how a candidate immunotherapeutic functions, and provides a template by which interactions could be modified to improve filovirus cross-reactivity.

156 IRF8 controls T cell survival and the CD44-osteopontin axis to regulate T cell antitumor activity

John Klement

Augusta University, Augusta, USA

The transcription factor interferon regulatory factor 8 (IRF8) plays an essential role in lineage differentiation and function of hematopoietic cells. Loss of IRF8 leads to defective NK cell activity, perturbations in B cell development and, in mouse models, an accumulation of CD11b⁺Gr1⁺ immature myeloid cells. However, the role of IRF8 in T cell development and antitumor activity remains unclear. Here, we aimed to test the hypothesis that IRF8 plays a critical role in host cancer immunosurveillance by regulating T cell homeostasis and activation. *In vitro* T cell responses were assayed by stimulation with anti-CD3/CD28 antibodies. To examine the role of IRF8 in T cells, a peptide-based vaccine was utilized to measure *in vivo* responses. Mixed-chimera mice were generated by lethal irradiation of recipient host followed by reconstitution with CD45.1⁺ WT and CD45.2⁺ IRF8-KO bone marrow. To further elucidate T-cell intrinsic role of IRF8, IRF8 T cell-specific knockout (IRF8-TKO) mice were generated by crossing IRF8^{fl/fl} mice with *lck-cre*⁺ mice.

Loss of hematopoietic IRF8 allowed for engraftment of an allogeneic mouse breast tumor and enhanced the growth of a spontaneous sarcoma model, and, similarly, *in vivo* stimulation of CD8⁺ T cells demonstrated defective T cell proliferation in IRF8-KO mice. However, isolated T cells from IRF8-KO mice displayed no deficiency following *in vitro* polyclonal stimulation or an *in vivo* mixed chimera model. Loss of IRF8 led to the accumulation of a CD44^{hi}CD8⁺ population in IRF8-KO mice that was not present in a mixed-chimera model or IRF8-TKO. This was accompanied by a twelve-fold increase in the IRF8-KO splenocyte expression of the CD44 ligand osteopontin, which we showed to be a potent inhibitor of T cell proliferation *in*

vitro. Surprisingly, reconstituted IRF8-WT mixed chimera mice demonstrated preferential engraftment and survival of T cells derived from WT, rather than IRF8-KO bone marrow, with further analysis showing a progressive loss of IRF8-KO T cells during their maturation and development process. Given that IRF8 regulates a variety of pro- and anti-apoptotic molecules in tumor and myeloid cells, we hypothesized that IRF8 controls the peripheral survival of T cells. To test this hypothesis, resting and *in vitro* stimulated WT and KO T cell viability was measured by Annexin V/PI staining. IRF8-KO cells, but not WT, demonstrated a pro-apoptotic phenotype.

Therefore, IRF8 intrinsically regulates T cell survival to mediate T cell differentiation and homeostasis while extrinsically regulating osteopontin in myeloid cells to mediate T cell activation and expansion. Together, these intrinsic-extrinsic mechanisms of IRF8 control T cell function in the context of the tumor microenvironment.

157 Aspirin use predicts successful outcomes after percutaneous angioplasty of arteriovenous fistulas and grafts used for hemodialysis

Malgorzata A. Kochanek

University of Chicago, Oak Park, USA

Arteriovenous fistulas (AVF) and arteriovenous grafts (AVG) may develop venous stenoses caused by neointimal hyperplasia (NH), which may be treated with percutaneous transluminal angioplasty (PTA). While the standard criteria for treatment of a clinically significant venous stenosis is estimated at 50%, there is a paucity of data that defines factors associated with clinical success after PTA. We prospectively evaluated the associations of clinical characteristics and procedural measurements with one month outcomes of PTA to find potential predictors of patency.

All persons referred for PTA of a patent AVF or AVG from 1/2016-10/2017 who consented were included in the study. Demographic and clinical data were obtained from records; indication for PTA and the type and location of each lesion were collected. Each stenosis was evaluated in two orthogonal planes so percentage of stenosis could be calculated, compared to a reference vessel, before and after PTA. Clinical outcomes were ascertained from dialysis units one month after PTA. Success was defined as dialyzer blood flows of 450 mL/min during dialysis, without: prolonged bleeding, cannulation pain, high venous pressure, low arterial pressure, pulling clots, infiltrations, poor clearance, infections, or swelling of the arm neck or head.

We observed 115 stenoses in 80 participants of whom 52.5% were female, 98.8% were African American, with a mean age of 58.4 years old and mean BMI 28.8. Of these participants, 96.2% had hypertension. Success at one month after intervention was seen in 56 patients who had 80 stenoses. Success was positively associated with use of aspirin ($P = 0.007$) and with referral for high venous pressures as opposed to any other indication ($P = 0.01$). There was no statistically significant association between success and diabetes ($P = 0.2$), tobacco use ($P = 0.9$), statins ($P = 0.6$), renin-angiotensin aldosterone inhibitors ($P = 0.8$), or multiple stenosis ($P = 0.4$).

Success after PTA of a hemodialysis AVF or AVG malfunction was positively associated with use of aspirin and with referral for high venous pressures as opposed to any other indication. We could not demonstrate any significant associations between procedural success and any anatomic features or measurements. Future work is needed to examine longer term outcomes, validate the current findings, and investigate the beneficial biologic mechanism of aspirin use in patients with hemodialysis vascular access.

158 Discovery and Characterization of VU0529331, the First Small Molecule Activator of G Protein-gated Inwardly-rectifying Potassium (GIRK) Subunit-2-Containing Channels

Krystian Kozek

Vanderbilt University, Nashville, USA

The nationwide opioid epidemic claims tens of thousands of lives each year as people addicted to opiates overdose on them. The cravings of addiction are extremely difficult to ignore, a behavior dependent in part on dopamine signaling. Addiction-associated dopaminergic (DA) neurons exist in specific brain areas, such as the substantia nigra and the ventral tegmental area (VTA). In addition to signaling via the neurotransmitter dopamine, these neurons differ from the majority of central nervous system (CNS) neurons in the expression of specific G protein-gated inwardly-rectifying potassium (GIRK) channels. Throughout most of the CNS, GIRK channels are composed of the GIRK1, GIRK2, and/or GIRK3 subunits, which assemble into homotetramers and heterotetramers. More specifically, DA neurons in the VTA express only non-GIRK1-containing GIRK (non-GIRK1/x) channels, namely GIRK2 and GIRK2/3. Experiments where non-GIRK1/x channel expression was modulated have demonstrated that these channels are implicated in the regulation of substance abuse in rodents. To further investigate whether GIRK channel modulation in DA neurons can affect drug abuse in wildtype animals, we sought means of pharmacologically modulating non-GIRK1/x channels. However, small molecules that modulated the activity of non-GIRK1/x channels did not exist. Therefore, we discovered and characterized the first small molecule modulators of GIRK2 channels

From a high-throughput screen of >110,000 compounds, we identified VU0529331 (VU331) to be the most efficacious small molecule activator of GIRK2 channels. Using high-throughput thallium-flux assays, we determined that VU331 activates both GIRK2 and GIRK1/2 channels. VU331 has a potency of ~5 μ M on both channels, and the activity of VU331 has been validated using whole-cell patch-clamp electrophysiology. VU331 application increased GIRK currents in both GIRK2 and GIRK1/2-overexpressing HEK293 cells; these currents are sensitive to barium ion inhibition. Because GIRK channels are gated by the activated $G_{i/o}$ $\beta\gamma$ -subunit, which is an effector of G protein-coupled receptor (GPCR) signaling, we examined whether inhibition of GPCR signal transduction perturbs VU331 activity. We demonstrated that inhibition of GPCR signaling using pertussis toxin does not prohibit the activation of GIRK channels with VU331.

The first of its kind, VU331 will enable us to study how GIRK channel modulation may affect DA neuron activity in *in vitro* and *ex vivo* experiments. Although VU331 did not demonstrate non-GIRK1/x channel selectivity, future studies will explore analogs of VU331 in search of compounds that are more potent, more efficacious, and selective for non-GIRK1/x channels. Selective analogs that are capable of penetrating into the brain will enable the study of non-GIRK1/x channels in rodent behavioral models of addiction. Such probes will help identify whether non-GIRK1/x channel regulation affects DA neuron activity and, therefore, can modulate drug abuse in rodents.

159 Characterizing the consequences of DEPDC5 deficiency in cortical neurons differentiated from patient-derived induced pluripotent stem cells as a model of epileptogenesis

Lindsay K. Kozek

Vanderbilt University, Nashville, USA

Despite numerous available anticonvulsant drugs, over one-third of epilepsies are refractory to treatment. Pathogenic mutations in *DEP domain-containing protein 5 (DEPDC5)* are a significant cause of focal epilepsies, epilepsies which are both drug-resistant and are linked to sudden unexpected death in epilepsy (SUDEP). DEPDC5 negatively regulates mTORC1 activity when amino acid levels are low, decreasing protein translation and disinhibiting autophagy. DEPDC5 mutations are proposed to cause impaired nutrient sensing, resulting in dysregulation of both mTORC1 and autophagy. Hyperactivation of mTORC1 and impairment of autophagy are independently linked to epileptogenesis, thus suggesting possible pathogenic mechanisms for DEPDC5 mutations. We use patient-derived induced pluripotent stem cells (iPSCs) differentiated into cortical neurons to define the extent to which DEPDC5 haploinsufficiency alters neurodevelopment and metabolism and to link these changes to the pathogenesis of epilepsy.

Methods: iPSCs were derived from fibroblasts from a patient with epilepsy and DEPDC5 mutation via integration-free reprogramming using Sendai virus. An isogenic control line was created using CRISPR/Cas9-mediated genomic editing via homology-directed repair to correct the DEPDC5 point mutation. iPSCs were differentiated into excitatory cortical neurons using a three-stage process based on dual-SMAD inhibition that mimics cortical development. Cortical interneurons were differentiated in a process utilizing dual-SMAD inhibition followed by Wnt antagonism and Sonic hedgehog activation. Neurons were fixed and stained at various timepoints during development to characterize expression of neuronal differentiation markers. mTORC1 activation was assayed by quantifying phospho-S6 expression via immunoblot.

Results: DEPDC5-mutant iPSCs are able to differentiate into mature excitatory and inhibitory neurons, as determined by staining for VGluT1 and PSD-95 or GABA and GAD67, respectively. Early in differentiation, cells express neural progenitor cell (NPC) markers Pax6 and Nestin. After 30 days, cells express markers of mature neurons such as Tuj1, MAP2, and NeuN. At baseline, DEPDC5^{+/-} and control cells show equivalent levels of mTORC1 activation, but not during starvation.

Conclusions: We created an iPSC-based model of DEPDC5-haploinsufficient epilepsy using excitatory and inhibitory neurons to investigate the connection between DEPDC5 deficiency, defects in autophagy, and epilepsy. We find that DEPDC5^{+/-} iPSCs are able to go through a neuroprogenitor phase to form mature excitatory and inhibitory neurons with similar levels of mTORC1 activation in a nutrient-rich environment. Further studies will examine signaling activity following nutrient deprivation and also evaluate neuronal morphology and dendritic arborization. Improving our understanding of how DEPDC5 haploinsufficiency contributes to epileptogenesis may suggest new drug targets and provide fundamental knowledge about the pathogenic mechanisms driving the development of epilepsy.

160 Dissecting the genetic regulatory elements of cold sensation in white fat

Daniel J. Kramer

Weill Cornell/Rockefeller/Sloan Kettering Tri-Institutional MD-PhD Program, New York, USA

The brain can stimulate heat-production (thermogenesis) in adipocytes in response to cold temperatures. This occurs via norepinephrine released by neurons to fat cells. The effect of this signaling is increased Ucp1 transcription. Stimulation of this pathway can promote weight loss, but the amount of cold required makes it less feasible on a large scale. Further, therapeutic activation of this pathway by added norepinephrine is limited by the ubiquity of adrenergic signaling and catecholamines across cell types whose alteration is undesired. Recent work suggests white and beige fat can increase thermogenic gene expression by alternative mechanisms of activation. These mechanisms are incompletely understood, and if elucidated could provide a novel therapeutic target for treatment of obesity and the metabolic syndrome.

We are characterizing this phenotype using a genome-wide CRISPR-based phenotypic screen using reporters for thermogenic gene expression. Cells can be sorted by quantified reporter expression and flow cytometry using surface markers associated with thermogenic capacity. Cells will then be sequenced to determine which guide RNAs are disproportionately present among the low-expression cell population. This method will give us a preliminary set of candidate genes, and gain- and loss-of function studies will then be performed to determine the intermediate steps of this mechanism.

This novel phenotype has been validated in cells differentiated from immortalized F442A preadipocyte lines as well as cultured primary subcutaneous white adipocytes. Transgenic and knockout mouse lines have been developed with increased and decreased expression of PR domain containing 16 (Prdm16), a factor complexed with key regulators of Ucp1 transcription in classical thermogenesis. The effect of Prdm16 expression is currently being measured. Establishing the potential roles of known transcriptional regulators in a novel process will help us determine where in the architecture of thermogenic gene expression cold exposure exerts its effects. Clues such as these will be important for developing our list of candidate genes that will come out of the genome-wide screen. Further studies are also underway to determine the physiologic role of this mechanism in vivo by profiling transcriptional changes in fat and fat-adjacent cells.

162 Altered cerebrospinal fluid flow patterns in a mouse model of chronic neuropathic pain

Benjamin T. Kress

University of Rochester Medical Center, USA

Altered neuronal connectivity and hyperexcitability of nociceptive neurons is generally believed to represent the causal substrate of persistent neuropathic pain. It is now accepted that, in addition, a deviation from the normal supportive functions of glial cells, in particular astrocytes and microglia, contributes to both the initial rewiring of spinal pain pathways, as well as the maintenance of the hypersensitivity believed to underlie the persistent component of neuropathic pain. To date, the exact impairment of the supportive functions of glial cells that contributes to the establishment and maintenance of neuropathic pain remains unknown. Here we tested the hypothesis that peripheral nerve injury triggers functional and structural changes in astrocytes that results in pathologically significant alterations in cerebrospinal fluid (CSF) flow patterns. We theorized that impaired clearance of interstitial fluid and solutes may

lead to the accumulation of excitatory or pro-inflammatory mediators (e.g., cytokines, ATP, or glutamate), which could subsequently contribute to maladaptive synaptic plasticity and the sensitization of nociceptive neurons. To test this hypothesis, we used fluorescence imaging to monitor flow patterns of tracers infused into the CSF of awake mice that had (i) received either the spared nerve injury (SNI) model of peripheral neuropathic pain or (ii) sham injury. The accumulation of tracers from the brain and spinal cord parenchyma, as well as the expression of markers of astrogliosis (glial fibrillary acidic protein [GFAP] and aquaporin 4 [AQP4]), or microgliosis (CD68), were then quantified after multi-channel fluorescence imaging of ex vivo brain and spinal cord slices. In the SNI model, neuropathic pain behavior, including thermal hyperalgesia and mechanical allodynia, peaked at 3 days following SNI. Accumulation of tracers within the parenchyma was markedly altered between mice that received SNI vs. sham-injury. Altered CSF flow patterns were detected as early as 3 days following SNI, and positively correlated with both pain behavior and astrogliosis, determined by increased expression of GFAP/AQP4. The early administration of the analgesics pregabalin and clonidine, but not morphine, prevented the suppression of glymphatic clearance. We are currently evaluating CSF flow in awake nerve injured vs. sham-injured mice in vivo, using serial contrast-enhanced computed tomography. Our results suggest altered glial cell function and CSF flow patterns may contribute to the onset and maintenance of chronic neuropathic pain.

163 Progress towards developing zebrafish models to study the link between SoxC transcription factors and CHARGE syndrome

Laura A. Krueger

University of Kentucky, Lexington, USA

CHARGE syndrome (coloboma, heart defects, choanal atresia, growth retardation, genital abnormalities, and ear abnormalities) is a complex congenital genetic disorder resulting in severe defects in multiple organ systems with an occurrence of 1:8,000-10,000 live births. Mutations in chromodomain helicase binding protein 7 (*CHD7*) and defects in neural crest cell development and migration have been implicated in the pathogenesis of CHARGE syndrome, however the mechanisms underlying the ocular birth defects observed in CHARGE patients have not been identified. Our laboratory studies the development of the vertebrate visual system using zebrafish (*Danio rerio*). Previous work from our lab has shown that knockdown of *Sox11*, a member of the SoxC family of transcription factors, in zebrafish results in microphthalmia, coloboma, brain, trunk, and heart defects, all phenotypes observed in CHARGE syndrome. Furthermore, a duplication of *Sox11* has been identified in a patient clinically diagnosed with CHARGE syndrome, and *CHD7* has been shown to directly interact with *Sox11* and *Sox4* in neural stem cells. Taken together, these data strongly suggest that loss of SoxC expression contributes to the ocular and other phenotypes observed in *Chd7*-associated CHARGE syndrome. In this study, we begin to further investigate the role that *Sox11* plays in the phenotypes seen in CHARGE syndrome by generating *Sox11*-mutant zebrafish using the CRISPR-Cas system. Zebrafish have two co-orthologs of *SOX11*, *sox11a* and *sox11b*. CRISPR target sites were chosen to disrupt the high mobility group (HMG) DNA-binding domain and the transactivation domain of *sox11a* and *sox11b*. Corresponding single strand guide RNAs (sgRNAs) were generated and microinjected with Cas9 protein into fertilized zebrafish embryos at the one-cell stage. The resulting *Sox11* mutant lines will be characterized for phenotypes related to CHARGE syndrome and will be compared to an established *CHD7* mutant line. We will also characterize the role

of *Sox11* in neural crest cell development and migration by crossing the *Sox10:RFP* transgenic line (which fluorescently labels neural crest cells) with the *Sox11* mutant lines and performing live imaging of neural crest cell dynamics. These experiments will provide a better understanding of the potential role of *Sox11* in the pathogenesis of CHARGE syndrome.

165 A pharmacological neuroprotective approach to severe traumatic brain injury: targeting mitochondria and lipid peroxidation

Jacqueline Kulbe

University of Kentucky College of Medicine, Lexington, USA

In the United States over five million people live with a TBI-related disability. Currently, acute treatment for severe TBI entails supportive care. To date, there are no FDA-approved pharmacotherapies available to prevent the devastating neurologic consequences of TBI. Due to the complex pathophysiology which occurs following TBI, innovative targeting strategies must be developed.

Following TBI, mitochondria take up increases in intracellular Ca²⁺ in an attempt to maintain homeostasis, however, increases in intra-mitochondrial Ca²⁺ lead to generation of reactive oxygen and nitrogen species (ROS/RNS), induction of lipid peroxidation (LP), and formation of LP-derived neurotoxic aldehydes, which covalently bind mitochondrial proteins, exacerbating mitochondrial dysfunction. Eventually, mitochondrial dysfunction leads to opening of the mitochondrial permeability transition pore (mPTP), cessation of ATP production, extrusion of Ca²⁺ back into the cytosol, cytoskeletal and neuronal degeneration, and neurologic impairment. Therefore, mitochondria make promising therapeutic targets for prevention of cellular death and dysfunction following TBI. Here we evaluate 1) the neuroprotective effects of cyclosporine A (CsA) on synaptic and non-synaptic mitochondria 2) the neuroprotective effects of a continuous infusion of CsA combined with phenelzine (PZ) and 3) the neuroprotective effects of PZ, hydralazine (HZ) and pargyline (PG).

Mitochondria are heterogeneous, consisting of both synaptic and non-synaptic populations, which have distinct properties, including differential responses to pharmacotherapy. Our results indicate that compared to non-synaptic mitochondria synaptic mitochondria sustain greater damage 24h following severe controlled cortical impact injury (CCI) in young male rats, and are protected to a greater degree by (CsA), an FDA-approved immunosuppressant, capable of inhibiting mPTP.

Additionally, because the TBI secondary injury cascade is complex, combinational therapies should offer greater neuroprotection than single agents. The first 72h following TBI are critical, as peak mitochondrial dysfunction and LP occur 72h following TBI. Therefore, continuous delivery of drug over the first 72h following TBI may offer the best chance at neuroprotection. We utilized a 72h subcutaneous continuous dosing paradigm to evaluate the combination of CsA and the aldehyde scavenger PZ, an FDA-approved monoamine oxidase (MAO) inhibitor class anti-depressant. Our results indicate that individually both CsA and PZ are able to attenuate mitochondrial aldehydic modification, PZ is able to maintain mitochondrial respiratory control ratio, a general measure of mitochondrial health, and cytoskeletal integrity, but together, PZ and CsA, are unable to maintain neuroprotective effects.

Finally, although PZ was chosen for these experiments based on its aldehyde scavenging properties, the fact that it is capable of inhibiting the mitochondrial enzyme MAO, must not be overlooked. Therefore, we are currently evaluating the effects of PZ (aldehyde-scavenger & MAO-inhibitor), HZ (aldehyde-scavenger), and PG (MAO-inhibitor) on cognitive deficits following TBI.

166 Rapid approach to deriving a safe and immunogenic live attenuated Zika viral strain

Swee Sen Kwek

Duke-NUS Medical School, Singapore, Singapore

The microcephaly outbreak in Brazil between late 2015 and early 2016 brought Zika virus (ZIKV) to the world's attention. Even though the incidence rates of ZIKV infection have since fallen, epidemiological observations suggest that ZIKV will emerge periodically to cause large epidemics with uncertain intervals of low-level transmission. As such, a replicating live attenuated vaccine (LAV) capable of inducing long-term humoral and cellular immunity is essential to prevent the re-emergence of epidemic Zika and the associated congenital Zika syndrome. The yellow fever 17D (YF17D) vaccine remains one of the best LAVs to date and serves as a benchmark for LAV development: a single dose confers lifelong immunity. However, in addition to displaying the same phenotype as YF17D, any ZIKV LAV candidate must also be attenuated in causing persistent infection in organs associated with severe disease and non-vector (e.g. sexual) transmission. We demonstrate here that ZIKV strains with desired attenuation phenotypes can be isolated and screened from a genetically heterogeneous viral population that arose during *in vitro* culture of ZIKV. This shortens the LAV development process considerably as compared to the time-consuming traditional approach of serial passaging in either cell culture or laboratory-reared animals. We plaque-purified and rescued a small-plaque variant, DN-2, using an infectious clone. Similar to YF17D, DN-2 displayed IRF3-restricted plaque size and also induction of innate immune responses in primary monocyte-derived dendritic cells. Additionally, DN-2 showed decreased infectivity in both mature endothelial cells (ECs) and endothelial progenitor cells, likely due to a concomitant early activation of a type I interferon (IFN) response and increased susceptibility to type III IFN. This attenuated infectivity in ECs translated to decreased organ infection and vertical transmission when DN-2 was tested in a type I IFN receptor-deficient A129 mouse model. Furthermore, all mice survived initial inoculation with DN-2, which elicited a protective response against a lethal challenge with the H/PF/2013 strain. Our findings thus suggest the possibility of rapidly deriving safe and immunogenic LAV candidates for ZIKV and other flaviviruses from a genetically diverse pool of the target virus by screening for defined molecular characteristics of attenuation.

167 Genetic determinants of heart failure in human induced pluripotent stem cell model

Feria Ladha

University of Connecticut, New Britain, USA

Genetic determinants of heart failure in a human induced pluripotent stem cell model

Heart failure is a leading cause of premature death and cardiac transplant, and has been defined as a global pandemic affecting approximately twenty-six million individuals worldwide. Unfortunately, only four new heart failure medications have been approved since 1995, due in part to lack of drug targets. The goal of our research is to better understand the mechanisms of inherited cardiovascular disorders, especially those that lead to heart failure. More specifically, this study is focused on identifying novel genes involved in heart function in order to provide mechanistic insights into heart failure pathogenesis and identify a platform for potential drug targets. We will be utilizing CRISPR/Cas9 genome-wide pooled screening methods to identify genetic modifiers of sarcomere function in human iPSC-derived cardiomyocytes (iPS-CMs) labeled with fluorescent markers for sarcomerogenesis.

An important marker of sarcomere function is B-type natriuretic peptide (BNP), which is secreted by the ventricles in response to excessive stretching of cardiomyocytes. Furthermore, BNP is a clinical biomarker for heart failure prognosis and efficacy of treatment. The understanding of how BNP expression is regulated is still very limited and therefore our CRISPR screen will allow us to identify novel regulators of BNP and sarcomere function. In order to achieve this, we have used CRISPR/Cas9 to develop a BNP reporter line where eGFP levels correlate with BNP expression. Our reporter line can be activated and inhibited by drugs known to regulate BNP expression. Furthermore, the system is responsive to different substrate stiffness when cardiomyocytes are plated on polyacrylamide gels of varying stiffness.

Our next step is to utilize the BNP reporter assay to conduct a CRISPR/Cas9 genome-wide screen by transducing a lentiviral gRNA library into our cells. We will be using the Brunello library, which includes around 76,000 gRNAs that target 19,000 human genes. This screen will help us identify novel genes that regulate cardiac function in hope of finding new therapeutic targets for heart failure.

168 Lysosomal calcium stores mediate ultraviolet light responsiveness in human melanocytes

Brandon M. Law

Massachusetts General Hospital, USA

Mutations in genes encoding lysosome-related organelles are implicated in impaired pigmentation, but the exact mechanism of this relationship remains poorly understood. Pigment production by human epidermal melanocytes occurs in response to ultraviolet (UV) light. In this study, we hypothesize that lysosomes in melanocytes play a critical role in mediating UV response. To query this hypothesis, we use live-cell imaging to probe for UV light-evoked response in cultured primary human melanocytes. We show that UV light evokes rapid lysosomal calcium release. Pharmacologic pathway modulation indicates that this calcium release is GPCR-mediated and requires the presence of a retinaldehyde chromophore, suggesting that a phototransduction cascade mediates this UV-response rather than a nonspecific cell damage pathway. Action spectrum studies show that calcium response robustly corresponds to the wavelength sensitivities of known UV-specific photoreceptors. UV-induced lysosomal calcium release is attenuated by pharmacologic blockade of lysosomal acidification or depletion of lysosomal calcium stores, further implicating the role of lysosomal ion homeostasis in UV response. Additional studies using CRISPR/Cas9 to genetically edit candidate lysosomal ionic transporter genes in primary human melanocytes derived from individuals with light, medium, and dark skin tones are ongoing. Taken together, these findings suggest a general paradigm that lysosomes serve as critical signaling organelles for UV response and provide additional mechanistic evidence for the emerging role of lysosome-related organelles in diseases of pigmentation.

170 Microglial inflammasome activation after penetrating ballistic-like brain injury

Stephanie Lee

University of Miami Miller School of Medicine, Miami, USA

Penetrating traumatic brain injury (PTBI) remains a significant cause of death and disability in the United States without effective therapies. A rodent PTBI model, penetrating ballistic-like brain injury (PBBi) has uncovered several secondary pathophysiological mechanisms such as reduced glucose uptake, neurodegeneration, inflammation, and apoptosis that magnify the primary injury. Targeting components of these mechanisms may help improve PTBI outcomes. Activators of

innate immunity contribute to secondary injury mechanisms following traumatic brain injury (TBI). Inflammasomes are the key regulators of interleukin-1 β (IL-1 β) mediated inflammation after TBI and present as clinically relevant targets for therapy. The role of inflammasomes in PBBI pathophysiology has yet to be determined. Towards this, adult male Sprague-Dawley rats were subjected to unilateral sham or PBBI surgery and sacrificed at various time points. Tissues were assessed for expression of cytokines IL-1 β , interleukin-18 (IL-18) and components of the inflammasome-- caspase-1, apoptosis-associated speck like protein containing a caspase activation and recruitment domain (ASC), X-linked inhibitor of apoptosis protein (XIAP), NOD-like receptor protein 3 (NLRP3), and gasdermin-D (GSDMD)-- by immunoblot analysis and assessed for ASC cell-type expression by immunohistochemistry. Cortical IL-1 β and IL-18 expression increased 4h-48h and 48h-72h, respectively after injury. PBBI also increased caspase-1, ASC, XIAP and NLRP3 expression from 24h-48h. Brain protein lysates from PTBI animals showed pyroptosome formation evidenced by ASC laddering, and also contained increased expression of GSDMD at 48h after injury. ASC-positive immunoreactive neurons within the perilesional cortex were observed at 24h. At 48h, microglial numbers significantly increased in the ipsilateral cortex compared to sham and contralateral cortices and ASC expression was predominantly increased in morphologically activated microglia. This expression of ASC in activated microglia persisted until 12 weeks following PBBI in the cortex and internal capsule. This is the first report of inflammasome activation after PBBI. Our results demonstrate cell-specific patterns of inflammasome activation and pyroptosis predominantly in microglia suggesting a sustained pro-inflammatory state following PBBI that could underlie the long-term sequelae of PBBI. Inhibition of the inflammasome in PBBI will evaluate its therapeutic potential for PTBI.

171 Interacting with the wrong crowd: a CRISPR/Cas9-edited inducible human cell system designed to reveal the chronology of events leading to proteotoxic stress in tauopathies

Mackenzie Lemieux
Cornell University, Ithaca, USA

A key open question in the tauopathy field is how tau proteins aggregate and cause proteotoxic stress in neurons. We recently published a first in-depth tau interactome, which revealed that tau carrying the P301L frontotemporal dementia mutation exhibits reduced interactions with heat shock proteins and the proteasome. Our previous work captured steady-state interactions of a specific mutated and plasmid-encoded tau isoform. However, as disease evolves dynamically, critically needed are next generation models that can be induced to reveal the chronology of events underlying tau's aggregation and proteotoxicity.

We are poised to fill this unmet need with novel CRISPR/Cas9-generated cell models that can be induced to express human tau alleles. Specifically, inducible tau IMR-32 human neuroblastoma cells were created in a two-step gene engineering workflow: first, a pair of foundation lox sites was inserted into the AAVS1 human genome safe harbor locus via a CRISPR/Cas9 nickase strategy. Second, wild-type or P301L tau C-terminally fused to the enhanced green fluorescent protein were inserted into the primed AAVS1 locus via Cre recombinase-mediated heterologous gene exchange using the foundation lox sites. The system can be used for time-course transcriptome and proteome analyses. Accurate transgene insertion was confirmed by genomic PCR and sequencing. Marked induction and tight leakage control of the inducible model were validated by Western blotting after treating the cells with doxycycline for 0-18 hours.

A preliminary mass spectrometry analysis confirmed that tau interacts with a large segment of the cellular ribonucleoproteome and chaperones. Data collected to date establish the successful implementation of an inducible tau-EGFP expression system that will allow us to dissect the time-course of aberrant tau interactions underlying proteotoxic stress.

Targeted insertion minimizes the deleterious effects of random integrations, and the flexible two-step process can potentially accommodate any genes of interest. In the future, we can use this cell model to find suitable time intervals for in depth interrogation and also polish the system to express both the three and four repeat tau domains to even better recapitulate the endogenous pathological brain state.

172 Small molecule activation of Protein Phosphatase 2A functions through regulation of the c-terminal tail of the catalytic subunit

Daniel Leonard
Cleveland Clinic Lerner College of Medicine at Case Western Reserve University, Cleveland Heights, USA

The success of molecularly targeted therapies for the treatment of select cancers has revolutionized our diagnostic and therapeutic approach to cancer overall. Unfortunately, the genetic heterogeneity and activation of multiple molecular drivers in even a single tumor often results in incomplete therapeutic responses and/or the development of treatment resistance. This heterogeneity and therapeutic hurdle present in cancer highlights the need for continued pursuit of novel treatment approaches. Contrary to the well-studied oncogene targeted therapies, re-activation of tumor suppressors has not been fully characterized. Enhancing the activity of tumor suppressors provides an endogenous cellular mechanism to simultaneously inhibit multiple oncogenic targets, enhancing the generalizability and efficacy of this approach. One major class of tumor suppressor enzymes, Protein Phosphatase 2A (PP2A), is functionally inactivated in the majority of human malignancies, highlighting its potential as a therapeutic target. PP2A consists of a core dimer including a requisite scaffold subunit and an enzymatic catalytic subunit, coupled to one of four classes of regulatory subunits; creating the functional heterotrimer and enabling a broad range of tumor suppressive functions. Despite the low overall rate of somatic mutation of PP2A, cancer employs several mechanisms to dysregulate PP2A function including increased expression of endogenous inhibitors, epigenetic silencing, and post-translational modifications of various subunits. Our lab has engineered a novel class of small molecules (SMAPs) which bind to the scaffolding subunit of PP2A to drive PP2A dependent tumor inhibition in mouse models of both solid and hematologic malignancies. Mechanistic insight into SMAP driven regulation of PP2A is critical for identifying SMAP sensitive patient populations for effective clinical translation of this approach. Evidence presented here, including molecular modeling, hydroxyl radical footprinting and cryo-electron microscopy, highlight the ability of these SMAPs to protect the regulatory c-terminal tail of the catalytic subunit. Post translational modification of this c-terminal region has been shown to direct holoenzyme assembly, regulate substrate specificity, and influence protein stability. Cellular and tumor xenograft co-immunoprecipitation studies suggest that this SMAP induced protection of the C-terminal tail of the catalytic subunit regulates the methylation of the unique terminal leucine (L309) thus influencing holoenzyme composition and substrate directed catalysis. Importantly, cancer derived mutations in the scaffolding subunit of PP2A, such as R183W, demonstrate resistance to SMAP therapy

in tumor xenograft models, further highlighting the importance of identifying an appropriate clinical population for the utilization of these small molecules. Future studies aimed at identifying the tumor suppressive PP2A regulatory subunits enhanced by this SMAP dependent protection of the catalytic subunit will better inform the clinical placement of these small molecules and direct future drug development efforts to enhance PP2A activity in cancer.

173 Transcriptional regulation of wound healing over time in human gingiva and skin.

Trevor Leonardo

University of Illinois - Chicago, Chicago, USA

Injury of epidermal barriers initiates a highly complex set of events to contain, cover, and prevent contamination of the wound site. While most wounded tissues eventually form a scar, wounded oral epithelium exhibits reduced scarring, less angiogenesis, a decreased inflammatory response, and decreased wound closure time as compared to skin. Using a bioinformatics-based approach, we sought to define the transcriptional regulatory networks of wound healing in each tissue over time. A microarray dataset was generated from human full-thickness excisional biopsies in gingival mucosa and ventral forearm, with subsequent biopsies done at six, 24, 72, and 168 hours. Analysis of the data showed that oral and skin wounds have specific differences in their transcriptional response to injury that might explain the differential outcomes in wound healing. Our analysis will provide new information about the factors involved that make wound healing in oral tissue unique in its ability to heal rapidly and to produce less scarring compared to other tissue sites.

174 Transdiagnostic Multimodal Neural Correlates of Cognitive Control in Psychosis: Dimensions of Alteration from Healthy to Disease

Dov B. Lerman-Sinkoff

Washington University in St. Louis, SAINT LOUIS, USA

Psychosis, classically the hallmark of schizophrenia, is nonetheless present in numerous other disorders. Mounting evidence suggests that psychosis may consist of multiple dimensional traits that span the spectrum from normative to disordered. Here, we expand our prior work in the normative population by using multimodal image analysis to examine the replicable transdiagnostic patterns of neural variation in psychosis related to cognitive control. Cognitive control refers to the set of neural functions employed to perform coordinated, purposeful decision-making processes in support of task demands. Persons with psychosis frequently exhibit alterations in cognitive control performance and many imaging studies have identified relationships between cognitive control performance and neural alterations in structural, resting-state, and functional imaging. However, many of these studies only examine a single type of imaging and thus provide a limited view of neural function.

In the present work, structural, resting-state, working memory task functional MRI, and cognitive control performance data were collected and analyzed for 31 healthy controls, 27 persons with psychotic bipolar, and 23 persons with schizophrenia spectrum disorders. Data were collected and processed identically to the Human Connectome Project (HCP) enabling assessment of relationships with prior replicable multimodal correlates of cognitive control in the HCP. Two main analyses were performed: First, two replicable independent components (ICs) derived using multitest canonical correlation analysis + joint independent component analysis (mCCA+jICA) that were predictive of cognitive control in the HCP were directly applied to the present dataset. The resultant subject-specific weights on

these ICs were used to predict cognitive control performance in our psychosis sample. Second, mCCA+jICA was applied de-novo to the present dataset, resultant ICs were visually examined, and subject-specific weights were correlated with cognitive control performance. Both analyses corrected for group differences in cognitive control performance and FDR was used to correct for multiple statistical comparisons.

Partial correlations using the two a-priori ICs predicted significant relationships between working memory imaging and cognitive control in psychosis ($r=0.366$ $p=0.001$, $r=0.300$ $p=0.008$; other modalities not significant). De-novo mCCA+jICA identified a single group-discriminative IC. Post-hoc partial correlations identified that the same IC also significantly or trend-level correlated with cognitive control performance (structural: $r=0.263$ $p=0.020$; resting-state: $r=0.221$ $p=0.051$; working-memory task $r=0.293$ $p=0.009$). Highly contributing structural regions included insular, somatomotor, cingulate, and medial visual areas; task regions included precentral, posterior parietal, cingulate, and visual areas.

The present analyses partially replicated a-priori normative results in individuals with psychosis. De-novo analyses identified a single group-discriminative IC that was significantly related to cognitive control performance and points towards joint contributions of identified regions in supporting cognitive control across the healthy-to-psychosis spectrum. These results support transdiagnostic conceptualizations of psychosis and may aid in future efforts to move beyond the DSM in diagnosis and treatment of mental disorders.

175 Kidney resident macrophages decrease MHCII expression after acute kidney injury

Jeremie M. Lever

University of Alabama at Birmingham, Birmingham, USA

Kidney resident macrophages (F4/80^{Hi}CD11b^{Low}) arise from the fetal yolk sac rather than bone marrow-derived precursors, and are thought to promote organ development during embryonic and postnatal life and recovery, secondary to acute kidney injury (AKI), in adults. We previously demonstrated that resident macrophages are not exchanged with the peripheral blood in uninjured kidneys. We hypothesized that kidney resident macrophages are not replaced by extra-renal precursors *after injury* and that they promote recovery by recapitulating a developmental program, with respect to the transcriptome and epigenome, after AKI.

To test the hypotheses that: 1) kidney resident macrophages are not replaced by monocyte-derived macrophages from the peripheral blood after AKI, and 2) kidney resident macrophages recapitulate a developmental phenotype in the adult after AKI.

To address hypothesis 1, parabiosis was established between CD45.1 and CD45.2 C57BL/6 congenic pairs of mice resulting in stable immune cell chimerism in the peripheral blood and kidney. After 28 d, one pair member was subjected to bilateral renal ischemia-reperfusion (IR) injury. The presence of chimerism in a given intrarenal cell subset after AKI, by flow cytometry and confocal IF microscopy, indicated infiltration of cells from the peripheral blood. To address hypothesis 2, we determined the phenotype of kidney resident macrophages as a function of age (E14.5-P28) and compared those to the same subpopulations after AKI in adults.

After IR-AKI in parabiotic mice, chimerism among F4/80^{Hi}CD11b^{Low} resident macrophages remained low (3.3% injured vs 0.9% sham, $p = 0.07$), indicating that even in the setting of injury-induced inflammation, kidney resident macrophages are minimally replaced by renewing precursors from the peripheral blood. Confocal IF

microscopy 3 d post-injury revealed a predominantly medullary and peritubular localization for F4/80⁺ macrophages and F4/80 protein colocalized with the native CD45 allotype at a higher rate than the chimeric CD45 allotype ($p < 0.0001$). In developing C57BL/6 mice, we observed that the proportion of resident macrophages positive for MHCII expression increased from 5.3% at E14.5 to 96.3% at P28 and expression was maintained in healthy adults. Within 2 d after IR-AKI, MHCII⁺F4/80^{hi} kidney macrophages reappeared and increased in proportion up to 6 d post-injury (36.8%, $p < 0.05$). MHCII⁺F4/80^{hi} cells do not appear to have arrived from the peripheral blood, because in injured parabiotic mice, their chimerism remained low, increasing only slightly after injury (0.28% vs 1.36%, $p = 0.047$).

Kidney resident macrophages are not replaced by renewing precursors from the peripheral blood after AKI. They do not express MHCII during embryonic and neonatal life, but gain expression as the mice progress to adulthood. Notably, kidney resident macrophages lose expression of MHCII after AKI, suggesting that they recapitulate a developmental genetic program after injury.

176 Development of a novel chemotherapeutic agent for fibrolamellar hepatocellular carcinoma

Solomon N. Levin

The Rockefeller University, USA

Fibrolamellar Hepatocellular Carcinoma (FL-HCC) is a rare and lethal liver cancer that primarily affects adolescents and young adults. Surgical resection is the mainstay of treatment; however, due to the non-specific nature of the disease symptoms (e.g., weight loss, abdominal pain), FL-HCC is often diagnosed at a fairly late stage, at which point the tumor has often metastasized and surgery is no longer an option. There is a lack of systemic therapies for the disease, and the mortality rate is high with a five-year survival of only 30-40%.

Previously, our lab discovered a recurrent genetic mutation found in all FL-HCC tumor samples sequenced. The mutation is an in-frame deletion of approximately 400 kilobases on one copy of chromosome 19. This deletion results in a fusion gene that contains the first exon from DNAJB1, which encodes for a member of the heat shock protein family, and exons 2-10 from PRKACA, which encodes for the catalytic subunit α of Protein Kinase A (PKAc). This chimeric gene leads to a chimeric mRNA, and ultimately, a chimeric protein that retains the full catalytic activity compared to the native kinase. More recently, we have found that creating the deletion, and the resulting fusion gene, with CRISPR/Cas9 in mouse liver is sufficient to produce the tumor. The tumor is not the result of the deletion, or loss of a tumor suppressor, since when a transposon containing the chimera is hydrodynamically transfected into the liver of mice, the mice also develop the tumor. When the same chimera is expressed with a point mutation to kill the kinase activity, no tumors are formed. Together these data implicate the kinase activity of the DNAJB1-PRKACA as the oncogenic driver for this cancer.

Here we initiate the discovery and development of a novel drug to target the kinase activity of the chimeric protein via a high-throughput drug screen. The chimeric protein was produced in BL21-CodonPlus (DE3)-RIL E. coli cells. The protein was purified in a single affinity step using a 20-residue peptide derived from Protein Kinase Inhibitor, a naturally occurring inhibitor of PKAc. This allowed for the purification of the chimera without the use of an affinity tag. The pure protein was found to have comparable activity to the native kinase, and was inhibited by H89, a known potent inhibitor of PKAc.

The kinase activity screen was optimized and had a Z-factor of

0.85 with H89 as the positive control. The screen included close to 400,000 compounds. The positive threshold was set to 15% normalized percentage inhibition with a z-score ≥ 3.5 . There were 82 compounds that met this cut-off. Secondary screens of these "hits" are in process, and these will ultimately be tested in cells and mouse models of FL-HCC.

177 Examining the role of Dyrk1a in the development and function of inhibitory neurons.

Rachel V. Levy

University of Florida, Plantation, USA

Dual-specificity tyrosine phosphorylation-regulated kinase 1A (Dyrk1a) has a crucial role in brain development, and studies have revealed links to Down Syndrome (DS) and autism spectrum disorders (ASDs). The purpose of this study was to determine whether deletion of Dyrk1a alters the number and distribution of parvalbumin (PV) neurons in the cortex and innervation of neurons by PV neurons. The overall goal was to reveal how this genetic mutation plays a role in the development of ASD.

Cre-lox technology was used to produce the genetically mutated mice carrying heterozygous deletion of Dyrk1a in inhibitory neurons. Perfusion was performed on both mutant and control mice at 8 weeks old. After perfusion, the mice were dissected, and their brains were sectioned and treated with immunofluorescent staining for PV and GAD67. They were then analyzed through fluorescent and confocal microscopy, with a focus on the cerebral cortex.

Data analysis showed that Dyrk1a mutation disrupts the development of PV neurons. These trends were present in the density and size of PV neurons, as well as in the distribution of synaptic terminals. This study could serve as a base for future research into ASD in humans, including potential for treatment and preventative measures.

178 Xylose donor transport is critical for fungal virulence

Lucy X. Li

Washington University School of Medicine, Saint Louis, USA

Cryptococcus neoformans, an opportunistic fungal pathogen, infects more than one million people annually and kills two hundred thousand individuals worldwide each year. Glycoconjugates are crucial mediators of cryptococcal metabolism and determinants of pathogenesis, making these carbohydrate structures attractive therapeutic targets. Glycan modifications of cryptococcal proteins and lipids incorporate significant amounts of xylose. This monosaccharide also constitutes over one-fourth of the mass of the polysaccharide capsule, the definitive cryptococcal virulence factor that surrounds the cell. Incorporation of sugar moieties into cryptococcal carbohydrate structures requires activated donors, usually nucleotide sugars like the UDP-xylose that serves as the xylose donor for synthetic reactions. While nucleotide sugars are generally synthesized in the cytosol, only a small fraction of these precursors is consumed there. Most nucleotide sugars are translocated into the secretory pathway, where the majority of glycan biosynthesis occurs, to modify critical proteins, lipids, or capsule polysaccharides. Nucleotide sugar transporters (NSTs) are thus required to transport the raw materials to the site of glycan synthesis. However, despite their key role in glycan synthesis, the identity and regulation of the complete set of cryptococcal NSTs remains elusive.

We identified two putative UDP-xylose transporters in *C. neoformans*, Uxt1 and Uxt2, which exhibited distinct subcellular localization, expression patterns, and kinetic parameters. We further demonstrated that Uxt1 and Uxt2 are required for xylose incorporation into capsule polysaccharides and glycoproteins; they

were also necessary for *C. neoformans* to cause disease in mice, although surprisingly not for fungal viability in the context of infection. These findings advanced our understanding of glycan biosynthesis, setting the stage for further studies of fundamental glycobiology and cryptococcal pathogenesis.

179 Translational machinery heterogeneity in circulating tumor cells

Selena S. Li

Harvard Medical School, USA

Metastasis is the primary cause of morbidity and mortality in cancer patients and the most important prognostic indicator. During metastatic progression, a cancer cell must detach from the primary site, intravasate into a blood vessel, survive in the circulation, extravasate from the bloodstream, survive and proliferate in a distant location. Circulating tumor cells (CTCs) are neoplastic cells that have accessed the circulation and are a critical intermediate in the metastatic cascade. Survival of CTCs in the bloodstream is a major determinant of metastatic spread as the majority of CTCs are eliminated in the harsh conditions of the bloodstream. Although CTC heterogeneity is thought to underlie the differential survival of the tumor initiating cells, the key differences of CTC heterogeneity and their potential contribution to survival remain unclear.

Single cell RNA-sequencing and clustering of patient-derived CTCs was conducted to determine the most differentially regulated genes, and our results showed distinct populations defined by high and low ribosomal protein (RP) expression. Interestingly, this translational signature correlated with worse prognosis of patients from whom the CTCs were acquired. We hypothesize that the dramatic shift in cell phenotype that occurs as tumor cells undergo metastasis likely requires equally dynamic changes in protein synthesis and translational machinery. To better understand the dynamics of ribosomal protein regulation, we fused three ribosomal protein gene promoters (RPS6, RPL10a, RPL12) to a destabilized green fluorescent protein (GFP) gene, allowing quantification of GFP fluorescence to serve as a dynamic readout of RP expression. We stably infected both a breast cancer CTC line and an immortalized breast epithelial cell line to study temporal changes in ribosomal protein expression at both a single cell and bulk population level. We are currently investigating the regulation of the protein biosynthetic pathway and its potential role in mediating CTC survival. Ultimately, this study aims to characterize the regulation of translational machinery and its contribution to CTC biology, expanding our understanding of metastasis and identifying potential novel targets for inhibition.

180 Restoration of social encoding by individual neurons in an adult mouse model of Autism

Songjun W. Li

Boston University School of Medicine, Boston, USA

Social dysfunction is among the most prominent features of autism spectrum disorder (ASD) as well as many other developmental and neuropsychiatric conditions. The precise neuronal mechanisms that are disrupted in ASD, however, remain unknown. The goal of this study is to provide a basic cellular-level understanding and treatment model for ASD. To this end, we developed an alternating appetitive/aversive paradigm in which socially-paired mice experienced both acute stress and food reward while we simultaneously recorded neuronal activity from the medial prefrontal cortex. We compared wild-type (WT) to SHANK3 -/+ mice as a model of ASD, to explore the neuronal correlates of socially relevant information and its dysfunction. Individual medial

prefrontal neurons in SHANK3 -/+ mice displayed markedly different response profiles compared to that of WT. Specifically, neurons in WT mice demonstrated integration of both the identity of the paired mouse and the valence of the condition, whereas neurons of the SHANK3 -/+ mice dissociated these two features. Our study reveals some of the basic neuronal coding mechanisms that are disrupted in ASD. In particular, they demonstrate that, at the cellular level, autistic mice separately encode social and conditional stimuli. This selective lack of response to other's experience (i.e., 'what' they are experiencing) is associated with an inability to distinguish between other-and-self but does not adversely affect their ability to encode to the other's identity (i.e., 'who' is experiencing it). Cre-flex mediated restoration of *Shank3* expression reverses this cellular imbalance in the mPFC of adult mice and temporally precedes an increase in prosocial behavior. Our study suggests a neuronal encoding substrate for ASD and demonstrates that it may be possible to functionally restore social encoding within mature adult cells. Taken together, this neuronal response provides a putative neural mechanism for disrupted capacity for theory of mind, a hallmark characteristic of ASD and suggests a basic model for testing neurobiologically plausible treatments for individuals with autism.

181 The Role of Twist2 in Regulating Myogenesis

Stephen Li

University of Texas Southwestern Medical Center, Dallas, USA

Ageing-related muscle atrophy (sarcopenia) is a process that affects nearly every person, contributing to debilitations and reductions in quality of life. During aging, fast-twitch muscle fibers are selectively atrophied resulting in motor weakness. Normally, muscle regenerates through a population of stem cells called satellite cells, which differentiate and non-selectively fuse to existing myofibers in order to repair the damaged muscle tissue. Thus, it's possible that loss of an alternative muscle precursor that fuses specifically to fast-twitch fibers may be a mechanism by which aging-related muscle atrophy occurs. Through the technique of lineage-tracing (fate-mapping) of the transcription factor Twist2, we have identified a novel muscle progenitor that fuses specifically to type IIb/x (fast-twitch, glycolytic) muscle fibers during both aging and regenerative conditions. These Twist2+ cells are transcriptionally distinct from satellite cells and are intrinsically myogenic. Additionally, loss of Twist2+ cells in vivo results in specific atrophy of fast-twitch myofibers. We are capable of isolating Twist2+ cells and differentiating them in culture. Through further in vitro assays, we identified Twist2 as a regulator of myogenic differentiation. We confirmed these findings through RNAseq and ChIP-Seq, where found that Twist2 overexpression drives global repression of the myogenic program. Additionally, we identified several interesting Twist2 target genes such as Neuropilin 1, which may mediate the fiber-type specificity through repulsive interactions with Semaphorin 3a. Our data so far suggests Twist2 plays a multifaceted role in regulating the biology of Twist2-dependent progenitors.

183 Tumor-induced immunosuppression promotes brain metastasis in patients with non-small cell lung cancer

Yuping D. Li

Feinberg School of Medicine, Northwestern University, USA

Brain metastases are a significant source of morbidity and mortality for patients with lung cancer. While effective innate immune responses can combat early malignancy, many cancers have the potential to induce local and systemic immunosuppression, promoting tumor growth and metastasis. One mechanism of immunosuppression is the tumor-induced expansion of programmed death-ligand 1 (PD-L1) positive suppressive myeloid cells. We recently demonstrated that in patients with glioblastoma, circulating monocytes have

increased PD-L1 surface expression, which was associated with worse survival in patients receiving a vaccine immunotherapy. Here we evaluate the role of tumor-induced suppressive myeloid cell expansion on the development of brain metastases in patients with non-small cell lung carcinoma.

Peripheral blood was collected from patients undergoing resection of lung metastatic brain tumors (n = 27). Immunosuppressive monocytes (CD45+ CD11b+ CD163+/- PD-L1+/-) and myeloid-derived suppressor cells (MDSCs) (CD11b+ CD33+ HLA-DR^{lo} PD-L1+/-) were quantified through flow cytometry. Tumor tissue was obtained from resection of brain metastases and used to generate cell cultures (n = 6) from which tumor conditioned media (TCM) was collected. TCM was analyzed for immunosuppressive cytokines, including interleukin-6 (IL-6), by enzyme-linked immunosorbent assay (ELISA). Naïve monocytes were stimulated with TCM for 24 hours in the presence of antibodies targeting the IL-6 receptor (tocilizumab), IL-6 (siltuximab), or IgG control.

Patients with brain metastatic lung carcinoma demonstrated increased peripheral monocyte PD-L1 compared to healthy controls (p<0.05), with an average 2.5-fold increase. All patients exhibited an increased abundance of MDSCs (p<0.05), with an average 14.9-fold increase. Elevated plasma IL-6 was associated with increased peripheral myeloid PD-L1 in patients with brain metastatic lung carcinoma (p<0.05). TCM stimulated monocytes expressed increased PD-L1 compared to unstimulated controls (17.7 vs. 7.4% PD-L1 positive, p<0.001). Correlation of TCM IL-6 levels with PD-L1 expression in TCM stimulated monocytes demonstrated a dose-dependent relationship (R² = 0.87, p<0.01). In addition, treatment with anti-IL-6 and anti-IL-6 receptor antibodies inhibited the increase in monocyte PD-L1.

Patients with lung cancer and brain metastases exhibit signs of peripheral immunosuppression, including increased PD-L1+ monocytes and MDSCs. IL-6 was found to stimulate induction of immunosuppressive myeloid cells. Monitoring of these immunosuppressive factors in peripheral blood may be used as a biomarker to predict patients at greater risk for brain metastases and suggest a new target for therapeutic intervention.

184 Evaluating Use Of Telemedicine For Interfacility Transfer Handoffs

Monica Lieng

University of California, Davis, Sacramento, CA 95817, USA

Interfacility transfers – transitions in care between different hospitals — have been associated with serious adverse events, many of which stem from breakdowns or inefficiencies in communication. Nursing reports between outside emergency departments (EDs) and receiving inpatient wards may include inaccuracies regarding the severity of illness of the patient, which may lead to a mismatch in the level of resource preparation and utilization upon admission. One solution to improve care coordination between nurses at referring hospitals with nurses at receiving hospitals is through telemedicine. Utilizing telemedicine instead of telephone for report may allow nurses to interact with patients and their families prior to their transfer while enabling direct visual assessment of the patient and illness severity. While the use of telemedicine has been investigated during physician communication during interfacility transfers, no studies have evaluated the use of telemedicine for nursing communication during these handoffs. We hypothesize that handoffs using telemedicine will improve handoff quality and nursing perception of preparedness at patient admission compared to handoffs using telephone, the current standard of care.

This is a prospective, observational study that uses a telemedicine network that connects a university based, 24-bed tertiary care Pediatric Intensive Care Unit with 26 remote EDs. Pediatric transfers from outside EDs are eligible if the nurse receiving report is also the admitting nurse upon admission. Receiving nurses complete a three-page survey that includes the validated Handoff Clinical Evaluation Exercise (Handoff CEX) instrument for handoff quality, additional items on nursing preparedness and the technology acceptance model. This study was approved by the local institutional review board.

To date, data have been collected on 27 nurse-patient dyads: 11 by telemedicine and 16 by telephone. Before commencing the study, preliminary data were collected on three transfers during the study implementation phase: two telemedicine reports and one telephone report. During both telemedicine reports, receiving nurses visually assessed the patient and communicate with the family whereas in the telephone report, neither of these occurred. In one telemedicine report, the use of telemedicine was particularly helpful in determining the severity of illness of the patient; which was previously not assessable in the preceding physician-physician report over telephone. Data collection and analysis will be finished by March 2018. We expect to enroll 120 transfers with oversampling of telemedicine transfers.

This prospective study assesses the feasibility of implementing telemedicine for nurse-led communication between distant hospitals. In the planned analyses, we will evaluate the impact of telemedicine on perceived preparedness and the quality of interfacility handoffs utilizing mixed-model logistic regression. We plan to use this data to demonstrate a feasible model of care that can be scaled across healthcare systems nationwide to improve care coordination during patient transfers.

185 The Role of Exosomes in Renal Cell Carcinoma Immune Suppression

Aaron R. Lim

Vanderbilt University School of Medicine, Nashville, USA

Renal cell carcinoma (RCC) is one of the leading causes of cancer-related deaths in the United States. Although activating the immune system with anti-programmed death-1 (PD-1) immunotherapy was recently approved to treat metastatic RCC, only 20% of patients respond to this treatment. Previous work in our labs demonstrated that RCC has the highest infiltration of CD8+ T lymphocytes, which have been known to play an anti-tumor role, of all solid tumors in the Cancer Genome Atlas. However, we found that CD8+ tumor-infiltrating lymphocytes isolated from freshly resected RCC patient tumors have elevated expression of PD-1 and are functionally exhausted. Thus, understanding how RCC evades our immune system is critical to improve the efficacy of immunotherapy. One potential mechanism by which tumors can evade the immune system is the release of exosomes, nanosized extracellular vesicles secreted by most tissues. These particles, which carry protein cargo, are gaining considerable attention in the field of cancer biology for their roles as intercellular communicators and biomarkers. Studies of plasma exosomes from cancer patients revealed cargo that are known to suppress the immune system, such as programmed death-ligand 1 (PD-L1) and TNF-related apoptosis-inducing ligand (TRAIL). However, the role of exosomes in RCC has been understudied. We hypothesized that RCC secretes exosomes containing PD-L1 and TRAIL to suppress the function of tumor-infiltrating lymphocytes and thus create an immunosuppressive environment. To test this hypothesis, we used differential ultracentrifugation and an Optiprep

density gradient to isolate and purify exosomes from the culture media of 786-O cells, a human RCC cell line. Using nanoparticle tracking analysis and transmission electron microscopy, we confirmed that 786-O cells secrete vesicles consistent with exosome size (~100nm) and morphology. With western blot, we found that these exosomes contain both immunosuppressive proteins PD-L1 and TRAIL. In addition, flow cytometric measurement of activation markers showed that RCC-derived exosomes decreased the activation of human CD8+ T cells. Taken together, our results indicate that RCC releases exosomes with immunosuppressive cargo, such as PD-L1 and TRAIL, that can suppress the immune system.

186 Egr2-dependent microRNA-138 is dispensable for peripheral nerve myelination

Hsin-Pin Lin

University of Florida, Gainesville, USA

Recent studies have elucidated the crucial role of microRNAs in peripheral nerve myelination by ablating components of the microRNA synthesis machinery. Few studies have focused on the role of individual microRNAs. To fill this gap, we focused this study on miR-138, which was shown to be drastically reduced in Dicer1 and Dgcr8 knockout mice with hypomyelinating phenotypes, and potentially target the negative regulators of Schwann cell differentiation. Here, we showed that of two miR-138 encoding loci, miR-138-1 is the predominant locus transcribed in Schwann cells. miR-138-1 is transcriptionally upregulated during myelination, and downregulated upon nerve injury. EGR2 is required for miR-138-1 transcription during development, and both SOX10 and EGR2 bind to an active enhancer near the miR-138-1 locus. Based on expression analyses, we hypothesized that miR-138 facilitates the transition between undifferentiated Schwann cells and myelinating Schwann cells. However, in conditional knockouts, we could not detect significant changes in Schwann cell proliferation, cell cycle exit, or myelination. Overall, our results demonstrate that miR-138 is an Egr2-dependent microRNA, but is dispensable for Schwann cell myelination.

187 Biomimetic stimuli-responsive glucose-based polymeric nanocarriers for cancer therapeutics

Yen-Nan Lin

Texas A&M University, Bryan, USA

Nanocarriers that improve the efficacy of chemotherapy are essential to the control of cancer progression. This talk will focus on the development of novel biomimetic cellular membrane-camouflaged stimuli-responsive glucose-based nanocarriers that overcome various biological barriers during systemic chemotherapeutics delivery. Upon systemic administration, nanocarriers encounter a series of biological challenges, including protein adsorption, mononuclear phagocyte system uptake, off-target accumulation and drug release, drug efflux and excretion. Nanocarriers should be designed to avoid these obstacles in order to maximize bioavailability of drugs to tumors and reduce off-target toxicity. Organocatalyzed sequential controlled ring-opening polymerization of cyclic glucose monomer and cyclic lactide monomer, followed by post-polymerization modification via thiol-yne click chemistry, led to functional amphiphilic polymers. Optimization of glucose-based polymer assemblies and cell membrane coating led to biomimetic stimuli-responsive sugar-based polymeric nanoparticles. The impact of cell membrane coatings on the pH-responsive behavior of the sugar-based polymeric nanoparticles will be discussed through evaluation of particle size, surface charge, colloidal stability, drug release kinetics, and morphology under physiological and tumor-

mimicking environments. The relationship of systemic delivery challenges and the behaviors of these nanoparticles will be further discussed.

188 An immunogenomics approach to neoantigen identification in preclinical models of glioblastoma

Connor J. Liu

Washington University School of Medicine, USA

Glioblastoma (GBM) remains the most common and lethal malignancy of the central nervous system (CNS) in adults. The past decade of GBM research has seen limited progress in improving patient survival beyond the current standard-of-care surgical resection followed by radiation and temozolomide chemotherapy. However, recent success in the use of immunotherapy to treat other solid and blood malignancies, in addition to experimental evidence challenging the notion of the CNS as an immunologically privileged environment, has generated new interest in using immune-based treatments for GBM patients. In particular, 'cancer immunogenomics' describes an approach to immunotherapy design aimed at leveraging the tumor-specific mutant peptides presented on a patient's individual human leukocyte antigen (HLA) molecules, as therapeutic targets. These tumor specific mutant peptides, called neoantigens, have come under intense focus as the immunodominant targets mediating anti-tumor responses to immunotherapy.

Most recently, using DNA whole exome sequencing, RNA-sequencing, and computational algorithms to prioritize neoantigens predicted to bind major histocompatibility complexes (MHC), our group isolated neoantigen-specific CD8+ T-cells from tumor infiltrating lymphocytes (TIL) in two checkpoint sensitive mouse glioma models, GL261 and SMA560. To assess the anti-glioma immune response following neoantigen vaccination, here we demonstrate that peptide vaccination with a mutant Imp3 neoantigen confers a significant survival advantage in mice bearing intracranial GL261. To our understanding, these findings represent the first documentation of a personalized 'mutation-to-vaccine' pipeline in a preclinical GBM model and provides a framework for studying the cellular basis of neoantigen dependent responses to immunotherapy. Additionally, we show that the CT2A syngeneic mouse glioma model recapitulates the highly aggressive and checkpoint blockade resistant phenotype seen in the human GBM setting. Applying DNA whole exome sequencing we identified 2,392 nonsynonymous mutations in the CT2A tumor genome, of which 802 were also expressed in RNA-sequencing. We used the open-source, in silico neoantigen prediction software pVAC-seq to identify top-ranking H-2Kb and H-2Db restricted CT2A candidate neoantigens for synthesis and immunogenicity screening by IFN γ ELISPOT. Thus, by determining the immunogenicities of high priority neoantigens in CT2A, we extend our neoantigen discovery pipeline to a third and highly immunosuppressive glioma model. In conjunction with our work in GL261 and SMA560, characterization of the CT2A neoantigen landscape will help establish a GBM immunotherapy model that captures clinically relevant biology and that will provide a platform to further study combination immunotherapies in GBM.

189 Activation of Akt by Wnt4 as a Novel Regulator of Uterine Leiomyoma Stem Cell Function

Shimeng Liu

Northwestern University, Chicago, USA

Introduction: Uterine leiomyomas (LM) represent the most common tumor in women. We recently demonstrated the presence of 3 distinct LM cell populations based on the expression of CD34 and CD49b:

CD34⁺/CD49b⁺ (LSC, leiomyoma stem cells), CD34⁺/CD49b⁻ (LIC, intermediate cells), and CD34⁻/CD49b⁻ (LDCs, differentiated cells), but the mechanism underlying LSC activation followed by differentiation to LIC and LDC remain unclear. In this study, we report the activation of Akt by Wnt4 as a novel regulator of LSC function.

Materials and Methods: Cells from LM tissues (n=4) were sorted by FACS into three populations: LSCs, LICs, and LDCs. MethylCap-Seq and microarray were used to profile genome-wide DNA methylation and mRNA expression differences among the three cell populations. Total primary cells and sorted cells were maintained using a 3D spheroid model. The function of Wnt/b-catenin and PI3 kinase/AKT signal pathways in LM cells were evaluated using real-time PCR and western blot analyses.

Results: Integrative analysis of gene expression and DNA methylation data of the three cell populations demonstrated that Wnt/b-catenin and PI3 kinase/AKT pathways are highly enriched in genes differentially methylated and expressed between LSC and LIC populations. Specifically, Wnt4 gene is hypomethylated and overexpressed in LICs, while its receptors FZD6 and LRP5 are primarily expressed in the LSCs, suggestive of potential paracrine interactions between these two populations recently reported by our group (N=8, P<0.001). Wnt4 (200ng/ml) treatment at different time points (15 min, 30min, 1h, 2h, 6h) did not significantly alter the protein levels of active b-catenin. Interestingly, Wnt4, in a time-dependent manner, dramatically increased AKT phosphorylation (pAKT), peaking at 15 min (N=3). Additionally, Wnt4 significantly increased c-Myc and cyclin D1 (downstream targets of Akt pathway) protein levels at 1h, 2h, and 6h after treatment. Real-time PCR assay confirmed that mRNA levels of both c-Myc and cyclin D1 were also upregulated by Wnt4 (N=4, P<0.05). Long-term treatment (2 days) with Wnt4 not only increased protein levels of c-Myc and CyclinD1 but also those of PCNA (a cell proliferation marker), and these stimulatory effects were reversed by co-treatment with MK-2206 (an AKT inhibitor). To investigate whether Wnt4 regulates LSC function, we treated each freshly FACS-sorted population of LM cells with Wnt4. We found that Wnt4 upregulated c-Myc expression specifically in LSCs which was blocked in the presence of MK-2206, suggesting that Wnt4 regulates LSC function indeed through AKT activation (N=4, P<0.001).

Conclusions: Our data suggest that Wnt4 plays a vital role in regulating LSC proliferation via activating AKT signaling pathway. Our studies represent a key step towards the better understanding of stem cell regulation and indicate potential novel therapeutic targets to refine the treatment for LM.

190 Protein o,o'-Dityrosine Cross-Linking Disrupts Cystic Fibrosis Mucus Viscoelastic Dynamics

Morgan Locy

University of Alabama at Birmingham, Birmingham, USA

Rationale: Cystic fibrosis (CF) is a multi-organ disease with lung morbidity being the primary cause of early mortality. Cardinal features of CF airway disease include increased viscosity and decreased clearance of neutrophil-laden mucus. Although oxidative stress has been implicated in CF pathogenesis, its role in mucus viscoelasticity are not well understood. Oxidative tyrosine modifications, including o,o'-dityrosine, have been shown to be increased in sputum of CF patients. o,o'-Dityrosine is a stable, covalent, irreversible modification that is catalyzed by hydrogen peroxide (H₂O₂)-mediated oxidation of a heme peroxidase (hPx), such as myeloperoxidase (MPO) produced by neutrophils and macrophages. In this study, we explored the mechanisms by which protein-associated o,o'-dityrosine contributes to disease pathogenesis.

Methods: Patient-derived primary human bronchial epithelial (HBE) cells were grown in an air-liquid interface. H₂O₂ measurements were performed utilizing the hPx-dependent homovanillic acid assay. Micro-resolution Optical Coherence Tomography was used to evaluate mucociliary transport (MCT). Data were analyzed by student t test (mean ± SEM, statistical significance was defined as p≤0.05).

Results: We observed that CF donor-derived HBE cells (F508del homozygous) produce increased extracellular H₂O₂ when compared to non-CF control cells (n=3-4 donors; 2.56 ± 0.87 vs. 0.64 ± 0.15 pmol/min; p≤0.05). MPO treatment decreased MCT by 2.6-fold in CF HBE cells when compared to vehicle treated cells (n=3 donors; p≤0.05), and co-treatment with L-tyrosine, which competitively inhibits protein o,o'-dityrosine cross-linking, abrogated the effect of MPO on MCT. MPO had no effect on MCT in non-CF donor-derived HBE cells, which lack the H₂O₂ hyperproduction observed in CF HBE cells, a necessary reactant to induce o,o'-dityrosine.

Conclusions: These studies suggest that o,o'-dityrosine cross-linking delays MCT in CF, and may contribute to the elevated viscoelastic properties of CF mucus. Delineating the source of H₂O₂ production, the proteins modified by o,o'-dityrosine cross-linking, and how this modification changes mucus dynamics within the lung could lead to the development of novel therapies targeting o,o'-dityrosine in CF patients.

191 ADAM10 Sheds ICOS Ligand on B Cells and is Necessary for Proper T Cell ICOS Regulation and T Follicular Helper Responses

Joseph C. Lownik

Virginia Commonwealth University, Richmond, USA

Introduction: A Disintegrin and Metalloproteinases (ADAMs) are a family of zinc dependent proteinases which can mediate intramembrane proteolysis and ectodomain shedding of a large range of substrates. We have shown that loss of ADAM10 on B cells results in loss of the marginal zone B cell compartment as well as a dramatic defect in antigen-specific antibody responses. In addition to B cells, T cells are necessary for most antibody responses (T-dependent). The interaction between T cell inducible costimulator (ICOS) and its ligand (ICOSL) on B cells is essential for proper T-dependent antibody responses. Loss of either of these molecules has been shown to dramatically impact antibody responses as well as allergic responses.

Methods: To examine the role of ADAM10 on B cell ICOSL regulation, we utilized a B cell conditional knockout of ADAM10 (ADAM10^{B-/-}). Flow cytometry and ImageStream analysis were used to examine ICOS and ICOSL levels. Follicular helper T cell (T_{FH}) and antibody responses were examined using NP-KLH immunizations. Allergic airway responsiveness was examined using a house dust mite (HDM) model in which HDM extract is intranasally administered for four days followed by intranasal challenge with HDM extract ten days later. Autoimmune responses were examined using the experimental allergic encephalomyelitis (EAE) model.

Results: ADAM10^{B-/-} mice exhibited a 15-fold increase in surface levels of ICOSL on B cells, while T cells exhibited an almost complete loss of surface ICOS. T cells downregulated surface ICOS levels through internalization and lysosomal degradation following interaction with ICOSL. Physiologically, inability to shed ICOSL caused disruption of the ICOS:ICOSL axis and caused severe defects in T_{FH} development. Blockade of elevated ICOSL rescued T cell ICOS surface expression and rescued both T_{FH} numbers and the abnormal antibody production in these mice. Additionally, using

the HDM model of allergic airway inflammation, we demonstrated that ICOS:ICOSL dysregulation through ADAM10 deletion caused defective Th2 polarization. In contrast Th1 and Th17 responses, which are less dependent on ICOS/ICOSL are increased. This change was exemplified in that autoimmune responses in the EAE model were clearly more severe both with respect to symptomatology and percent of mice developing disease.

Conclusions: Overall this study not only confirms the importance of ICOSL shedding in ICOSL/ICOS function, but it also identifies ADAM10 as the most important sheddase for this function. Our work also defines a novel post-translational mechanism for ICOS regulation, namely internalization in response to ICOSL interaction as well as differences in endosomal shuttling pathways when TCR stimulation occurs concomitantly combined with ICOSL. In summary, these findings present a novel pathway to modulate ICOSL and ICOS expression and alter the humoral immune response.

192 Epithelial-specific p85 α KO Affords Survival Advantage After Radiation Injury Through Enhanced Crypt Resilience

Evan B. Lynch

University of Kentucky College of Medicine, Lexington, USA

High-dose radiation targets highly proliferative compartments, making radiation an attractive option for aggressive cancers. However, radiation exerts stress on high cycling cells, including intestinal epithelial cells (IEC), where it causes significant, debilitating side effects (diarrhea, bleeding, etc). Here we examine the role of PI3-Kinase (PI3K) signaling in promoting epithelial repair after radiation injury. Previously, we found that reductions in class IA PI3K (*pik3r1*) (regulatory subunit p85 α) induces the anti-apoptotic protein survivin and promotes IEC expansion in an ileocecal resection repair model. Preliminary data obtained in histopathologic sections from radiation proctitis patients reveal a 29.3% enhancement of survivin+ nuclei compared to normal colonic biopsies. To interrogate the role of IEC PI3K in radiation injury, we utilized *VillinCre-p85^{fl/fl}* (p85KO) and *VillinCre-p85^{+/+}* subjected to high dose (12Gy) radiation. IEC Western blot (WB) data of unperturbed p85KO mice revealed a complete ablation of p85 α , with subsequent increases in p-Akt^{Ser473} along with p-PTEN, p-GSK3 β ^{Ser9}, as well as p-p70S6K and survivin compared to WT controls, suggesting a deregulation of PI3K machinery. RT-PCR studies performed at baseline revealed increases in TA-enriched Wnt target genes, *Axin2* (56%) and *c-myc* (39%) and reserve intestinal stem cell (ISC) markers *HopX* (33%), and *Bmi1* (20%), at the expense of the active cycling Lgr5+ stem cells (-25%). Histopathologic sections highlight a distinct shift in the zone of proliferation with more than a 2-fold increase in BrdU+ cells at the reserve stem cell position 4 compared to controls. **Following lethal radiation** dosage, p85KO mice exhibited a 20% increase in survival as compared to wildtype (WT) littermates along with increased crypt survival (proportion of crypts with >5 BrdU+ cells/crypt, WT vs p85KO: 72% +/- 3 Vs 84% +/- 1, pSer552, p-PTEN). In p85KO mice, radiation induced lower levels of WB PUMA and cleaved caspase 3 compared to WT controls. Concomitantly, crypt lengths increased in p85KO (+9%) compared to WT (-20%). Taken together, our data suggest PI3K signaling enhances recovery from radiation injury through expansion of reserve ISC populations capable of creating proliferative Lgr5+ ISC and accelerating crypt IEC recovery from radiation-induced cell death. We posit this pathway limits apoptosis and enhances survival of proliferating progenitor populations which increases overall crypt survival. Given results suggesting p85 α KO IEC increase PI3K signaling, we propose p85 α as a potential drug-targetable target capable of enhancing recovery from radiation therapy.

193 Defining the role of the immune system in aneuploid cell clearance

Emily C. MacDuffie

Warren Alpert Medical School of Brown University, USA

Aneuploidy, the loss or gain of one or more chromosomes, is a hallmark of oncogenic transformation. Although aneuploidy is rare in normal tissues (0-4% of cells), it is estimated to be present in 90% of solid cancers. Despite its pervasiveness in cancerous tissue, experimentally-derived aneuploid cells have a significant proliferative disadvantage compared to euploid cells both in vitro and in vivo.

To assess the effects of aneuploidy on cellular fitness and tumorigenesis, mouse models were developed that lack a functional spindle assembly checkpoint (SAC). Without a functioning checkpoint, cells initiate anaphase before correct kinetochore attachments are made, resulting in aneuploid daughter cells. Mouse models of chromosomal instability (CIN) due to disruption of the SAC show high levels of aneuploidy in tissues that are formed during embryogenesis such as brain. However, tissues that regenerate during adulthood, such as skin, intestine, and peripheral blood harbor very low levels of aneuploidy. It is unknown how aneuploid cells are selected against in these tissues. We tested the possibility that aneuploid cells are cleared via apoptosis. We quantified cleaved caspase 3, a marker of apoptosis, in the intestine of CIN mouse models but detected no increase in apoptotic cells compared to control mice, suggesting that other mechanisms may be responsible for aneuploid cell elimination. We hypothesized that aneuploid cells exhibit immunogenic stress responses that are recognized by the immune system and result in their ultimate removal.

To test the above hypothesis, we optimized a protocol to generate arrested aneuploid cells with complex karyotypes from RPE1 cells. Broad protein profiling of secreted cytokines in the cellular supernatant revealed increased levels GM-CSF, IL-6, and CCL2, inflammatory cytokines known to attract cells involved in both innate and adaptive immunity. Co-cultures of aneuploid RPE-1 cells and natural killer (NK) cells have previously demonstrated NK-mediated cell killing. Continuing investigations are exploring the interactions between aneuploid cells and phagocytic cell types including macrophages and dendritic cells.

To determine if immune mediated clearance of aneuploid cells occurs in vivo, tissue inflammation was assessed in two mouse models expressing mutated components of the SAC. Intestine, skin, kidney, liver, and brain tissue were stained with immune cell markers and the number of immune cells per area was quantified. Preliminary experiments suggest that macrophages are more abundant in the regenerating tissues of CIN models but that the number of CD4+ helper T cells does not differ between CIN models and controls. Ongoing experiments are evaluating quantity of NK cells, CD8+ cytotoxic T cells, and dendritic cells in CIN tissues.

Understanding immune system recognition of these non-cancerous aneuploid cells is the first step towards the development of therapies that can augment the immune system's response to cancerous aneuploid cells.

194 CT Scan Findings in Microcephaly Cases During 2015-2016 Zika Outbreak: A Cohort Study

Jessika T. da S. Maia

Centro Clinico da Dor, Natal, Brazil

Objective: This study aimed to evaluate CT scan findings in living babies whose mothers had exanthematous diseases (ED) compatible with ZIKV infection during their pregnancy.

Background: Studies have demonstrated radiological findings in microcephaly (MCP) related to Zika virus (ZIKV). The 2015-2016 ZIKV epidemic led to an increase in the prevalence of MCP in the northeast region of Brazil. Rio Grande do Norte State (RN), a Brazilian northeast state, was highly impacted by this outbreak.

Design/Methods: We evaluated the CT brain scan images of 38 subjects up to 17 months whose mothers had ED during pregnancy. All these MCP cases were followed at a reference center for children rehabilitation in RN. Cohort enrollment occurred within babies born between January 2015 and May 2016.

Results: All subjects had brain volume reduction, followed by intracranial calcification (N=27). Lissencephaly and ventricular dilatation were found in 19 cases. Pachygyria was observed in 11 subjects (28.9%) and cerebellar atrophy was observed in 8 subjects (21%). All subjects reported with pachygyria had lissencephaly. In addition, all subjects observed with intracranial calcifications had pachygyria.

Conclusions: It is a large and well detailed case series of CT brain scan performed in living babies with MCP related to ZIKV. These findings observed are supportive evidence to prove the severity of brain damages caused by ZIKV due to its neurotropism. This pattern of CT scan images should be compared with CT brain images observed in others studies in MCP cases related to ZIKV. Furthermore, our results might be compared with CT brain scan images from MCPs related to other infectious diseases (STORCH positive) that can also lead to central nervous system alterations. It will certainly help differentiating the etiology of MCPs.

195 Repurposing triclosan as an aminoglycoside adjuvant for the eradication of *Pseudomonas aeruginosa* biofilms

Michael Maiden

Michigan State University/MSUCOM, Lansing, USA

A major problem in the management of cystic fibrosis (CF) is antibiotic treatment failure due to biofilms produced by *Pseudomonas aeruginosa*. The current *Pseudomonas* eradication protocol is 300 mg of aerosolized tobramycin twice a day for 28 days in on-off cycles, reaching mean sputum concentrations of 737 µg/g (~1,440 µM per dose). However, despite the routine use of this protocol, by early adulthood, nearly 80% of CF patients are chronically colonized with *P. aeruginosa*. The ability of this pathogen to survive eradication by tobramycin and pathoadapt into a hyper-biofilm state leading to chronic infections is key to its success. Retrospective studies have demonstrated that preventing this pathoadaptation by improving eradication is essential to extend the lives of CF patients. To identify adjuvants that enhance tobramycin eradication of *P. aeruginosa*, we performed a high throughput screen (HTS) of 6,080 compounds from four drug repurposing libraries. We identified that the Food and Drug Administration (FDA) approved compound, triclosan, combined with tobramycin resulted in a 2-log reduction of viable cells within biofilms at six hours, but neither compound had significant antimicrobial activity against biofilms on their own. This synergistic treatment significantly accelerated killing of biofilms compared to tobramycin treatment alone, and the combination was effective against 6/7 CF clinical isolates tested including a tobramycin resistant strain. Further, triclosan and tobramycin killed persister cells, causing a 2-log reduction by 8-hrs and eradication by 24-hrs. Additionally, triclosan synergized with other aminoglycosides such as gentamicin or streptomycin. Triclosan is an aminoglycoside adjuvant that could improve current *Pseudomonas* eradication protocols.

196 Evaluation of non-random X-inactivation in blood cells as a marker for cardiovascular disease and adverse health risk

Emily A. Marre

Rosalind Franklin University of Medicine and Science, USA

Age-related clonal hematopoiesis (CH) is a common condition that is associated with an increased risk of hematologic malignancies (HM) and cardiovascular disease (CVD). The majority of candidate driver mutations occur in epigenetic regulatory genes such as ASXL1, DNMT3A, and TET2 genes. However, a significant proportion of older people harbor clonal hematopoiesis without candidate driver mutations. In older women, clonal hematopoiesis can be detected by the human androgen receptor A gene (HUMARA) assay regardless of the presence or absence of candidate driver mutation(s). The HUMARA assay evaluates non-random X inactivation (NRX-I) as a marker for clonal hematopoiesis. The purpose of this study is to evaluate the association between NRX-I and cardiovascular risk factors and other health correlates.

We screened for NRX-I in 744 women ages 65 and older participating in an ongoing, prospective cohort study in Oregon (Women Engaged in Advancing Health Research [WEAR] study). This approach was used to enhance the efficiency of identifying a subpopulation of women harboring impactful, high-risk mutations. We examined the HUMARA results and any association with previous health history using a cross-sectional study design. Analysis of variance and logistic regression analyses were used to examine the relationship between HUMARA assay results and baseline CVD risk, controlling for age and race.

Women displaying highly skewed NRX-I were 2.5 times as likely to report a history of diabetes controlled with insulin injection (p-value 0.078, 95% CI: 0.76, 8.99) compared to women without NRX-I. They were 1.4 times as likely to report hypercholesterolemia (p-value: 0.39, 95% CI: 1.00, 1.97) and 1.5 times as likely to report use of cholesterol lowering medication (p-value 0.01, 95% CI: 1.08, 2.24). Women with NRX-I were 2.54 times as likely to report a history of myocardial infarction (p-value: 0.077, 95% CI: 0.761, 8.98). Women with NRX-I were 1.48 times more likely to report daily aspirin use, (p-value=0.016, 95%CI: 1.05, 2.0) than women without NRX-I. Women with and without NRX-I were not found to differ with respect to race, age, body mass index, smoking history, hypertension, family history of CVD, or previous history of transient ischemic attack and stroke.

Prediction of major adverse cardiac events is based the presence of traditional risk factors including high blood pressure, high cholesterol, uncontrolled diabetes, smoking, and family history. Yet there is significant residual risk; many will still die from CVD without these risk factors. NRX-I, in addition to enriching for mutations known to confer CVD and HM risk, may be a marker for additional and unique health risk. An association between NRX-I and DM as well as hypercholesterolemia, supports the current biological hypothesis that clonal hematopoiesis, perhaps irrespective of the cause or underlying driver mutation, is a driver of CVD.

197 Atypical Xist RNA localization to the inactive X in a female-biased murine model of systemic lupus erythematosus

Anna R. Martin

Perelman School of Medicine, University of Pennsylvania, USA

Systemic lupus erythematosus (SLE) is a severe autoimmune disease that affects women at a rate nine times higher than men. The genetic basis for this bias is the X-chromosome, where the greatest concentration of immunity related genes on any chromosome can

be found. Females have two X chromosomes (XX), and through a process, known as X-chromosome inactivation (XCI), silence one of their X-chromosomes randomly to have a similar level of X-linked gene expression as males (XY). In XCI, XIST RNA, a long non-coding RNA, is expressed from the future inactive X (Xi) and is bound to it in cis by the transcription factor YY1. As XIST RNA coats the Xi, it recruits heterochromatin modifiers to condense and silence it. Previous research has shown that human SLE patient B cells exhibit altered localization of XIST RNA, which indicates that they have partial reactivation of the Xi. To explore this relationship, we worked with NZB/W F1 mice, which are a well-characterized murine model of SLE-like disease that also displays a female bias. The hypothesis of our study is that the Xi in splenic B cells of NZB/W F1 mice during disease progression will exhibit compromised silencing due to reduced epigenetic modifications, resulting in increased expression of X-linked genes. Preliminary results indicate that the protein and mRNA levels of YY1, which is required for Xist RNA localization to the Xi, is reduced across all stages of disease in female NZB/W F1 when compared to age-matched wild type (WT) mice. Using Xist RNA FISH, we have observed that the activated B cells of late stage disease NZB/W F1 mice have decreased localization of Xist RNA to the Xi when compared to WT, suggestive of compromised silencing of the Xi. In addition, we observed that the expression of Tlr7 and Cxcr3, two important immunity-related X-linked genes, is increased in diseased NZB/W F1 when compared to age-matched WT. We conclude that there is evidence of perturbations with XCI in the female-biased lupus mouse model that could explain how X-linked genes become abnormally overexpressed in B cells during SLE.

198 Toward the Discovery of a Novel, Functionally Selective Dopamine 1 Receptor Agonist for the Treatment of Parkinson's Disease

Michael Martini

Icahn School of Medicine at Mount Sinai, New York, USA

Parkinson's Disease (PD) is the second most common neurodegenerative disease in the world with a prevalence estimated to be approximately 1% in people over the age of 60, making it an increasingly important medical problem in our aging population. L-DOPA is the current standard of care for PD and functions by increasing levels of dopamine centrally in the dopamine-depleted nigrostriatal pathway. Despite its success in managing PD, L-DOPA is known to induce motor fluctuations, termed L-DOPA-induced dyskinesias (LIDs), in patients chronically receiving it. LIDs are estimated to occur in over 50% of patients after 5 to 10 years of treatment and present a considerable limitation to the viability of using L-DOPA long term as patient function and quality of life are compromised while individual and societal costs rise.

Recent research has elucidated that, in addition to G protein signaling, dopamine receptors are also capable of signaling through a distinct β -arrestin2 (β -arr2)-dependent pathway. This pathway is important in regulating downstream responses at the Dopamine 1 Receptor (D1R) and plays a significant role in converting dopamine signaling into motor function. Importantly, previous studies have also shown that genetic modulation of β -arr2-mediated D1R signaling results in improved motor functioning, while preventing LIDs.

These promising results inspired this project, which is the first to develop new D1R ligands with functional selectivity biased towards stimulating the β -arr2 signaling pathway over the G protein pathway in order to reduce the incidence of LIDs, while maintaining anti-parkinsonian properties. Based on a lead compound identified via high-throughput screen, we synthesized several analogue

compounds and tested them in cellular assays to assess their relative potencies towards activating the G protein and β -arr2 signaling pathways. Based on this data, we developed a preliminary structure-activity relationship (SAR) between our agonist scaffold and functional selectivity at D1R.

Future directions will focus on optimizing our chemical scaffold, improving our SAR by incorporating sophisticated computational modeling of ligand-receptor bias, and testing our compounds in acute and chronic animal models of PD to assess the ability of these ligands to reverse motor deficits without inducing dyskinesia-like behaviors.

199 Mast cells promote thrombocytopenia during dengue virus infection.

Mohamad Fadhli Masri

Duke-NUS Medical School, Singapore, Singapore

Dengue fever, an infection caused by dengue virus (DENV), has become an increasing health concern worldwide. Thrombocytopenia, a reduction in platelet counts, is a classical trait of dengue fever. Our previous studies have highlighted that DENV can activate mast cells, resulting in the release of mast cell mediators which can influence the severity of dengue. We hypothesize that mast cell-derived products contribute to thrombocytopenia during DENV infection. Using an *in vitro* model, we have shown that activated mast cells release mediators that result in platelet activation. DENV infection of wild type (WT) mice induced thrombocytopenia, which was characterized by increased platelet activation and phagocytosis. Using mast cell-deficient (Sash) mice, as well as pharmacological inhibition of mast cell activation with ketotifen, we have been able to demonstrate a reduction in DENV-induced thrombocytopenia. Reduction in thrombocytopenia was characterized by a reduction in platelet activation and phagocytosis. Reconstitution of the Sash mice with mast cells restored the phenotype of thrombocytopenia seen in wild type mice. Furthermore, platelets of both WT and Sash mice could be activated *ex vivo*, suggesting no intrinsic activation deficit in the platelets of mast cell-deficient mice. Our findings point to mast cells promoting thrombocytopenia during DENV infection through the release of mediators, increasing platelet activation and phagocytosis. One mediator released by mast cells that is known to be able to affect platelets is serotonin. Pharmacological inhibition of serotonin with the 5HT_{2A} receptor antagonist, ketanserin, in DENV-infected WT mice reduced thrombocytopenia compared to vehicle treated mice. Conversely, treatment of DENV-infected Sash mice with exogenous serotonin restored the thrombocytopenic phenotype that is absent in Sash mice. Thus, we have implicated mast cells as a previously unidentified component of thrombocytopenia during DENV fever, revealing a potential therapeutic target of disease.

200 Electrophysiological Effects of NAD⁺ Supplementation and Depletion on the Cardiac Sodium Channel

Daniel Matasic

The University of Iowa, Iowa City, USA

Background: Nicotinamide Adenine Dinucleotide (NAD⁺) is a central mediator of metabolism within the heart. Previous studies demonstrated that the metabolic state of the heart influences cardiac electrophysiology and the propagation of arrhythmias. The sodium channel Na_v1.5 is responsible for the initiation of the cardiac action potential and has been implicated in metabolic regulation. To further study the role of metabolism in the regulation of the electrical activity of the heart, we examined the effect of modulating NAD⁺ on Na_v1.5 by: (1) NAD⁺ precursor supplementation, utilizing Nicotinamide

Riboside (NR) and Nicotinamide (NAM), and (2) NAD⁺ depletion by FK866, an inhibitor of the NAD⁺ biosynthetic enzyme NAMPT.

Objective: To evaluate the effects of NAD⁺ supplementation and depletion on Na_v1.5 activity and channel properties.

Methods: To test the effect of NAD⁺ supplementation on Na_v1.5, HEK293 cells expressing Na_v1.5 (Na_v1.5-HEK293 cells) were treated with the NAD⁺ precursor NR (500 μM, 48 hours) and subjected to whole cell patch clamp to measure sodium current (I_{Na}). I_{Na} from native Na_v1.5 channels was then evaluated neonatal rat cardiomyocytes (NRCMs) subjected to treatment with either NR or NAM (500 μM or 5 mM, 24 hours). Similarly, to test the effect of NAD⁺ depletion on Na_v1.5, Na_v1.5-HEK293 cells and NRCMs were treated with FK866 (100 nM, 24 hours). The NAD⁺ metabolome in response to these treatments were measured by Liquid Chromatography-Mass Spectrometry (LCMS).

Results: Both 500 μM and 5 mM NR significantly increased I_{Na} in Na_v1.5-HEK293 cells and NRCMs compared to control. Interestingly, the NAD⁺ precursor NAM stimulated I_{Na} at 500 μM but inhibited I_{Na} at 5 mM in NRCMs. Both NR and NAM significantly elevated NAD⁺ levels with NR being more effective at equimolar concentrations. Furthermore, depletion of NAD⁺ by FK866 increased I_{Na} in Na_v1.5-HEK293 cells but had no effect in NRCMs. By LCMS quantification, FK866 treatment reduced NAD⁺ content by approximately 86% in NRCMs. In addition, FK866 decreased levels of NAD⁺-related metabolites including NADP⁺, NAM, and ADP-ribose.

Conclusions: Interestingly, both NAD⁺ supplementation by NR and NAD⁺ depletion by FK866 increased Na_v1.5 activity in Na_v1.5-HEK293 cells. In addition, NAD⁺ supplementation by NAM yielded differential dose-dependent effects on Na_v1.5. Changes alone in NAD⁺ are insufficient to explain these observed effects on Na_v1.5 activity and suggestive of a complex regulatory mechanism.

Conflicts of Interest: DSM: None, CB: a stockholder and Chief Scientific Adviser of ChromaDex, which manufactures and sells nicotinamide riboside as a nutritional supplement in addition to developing NAD⁺-boosting therapeutics, BL: None.

201 Decreased editing of endogenous RNA by ADAR1 protects from RNA virus infection

Megan Maurano

University of Washington, Seattle, USA

Detection of nucleic acids leading to production of type I interferons (IFN) and the induction of antiviral states in both infected and nearby cells is essential to antiviral defense, but can cause autoimmune disease if dysregulated. Adenosine Deaminase Acting on RNA 1 (ADAR1) catalyzes the deamination of adenosine to inosine in double stranded RNA. Without this ADAR1 "editing" of endogenous RNA, unedited RNA activates the cytosolic RNA sensor MDA5. Complete absence and abrupt deletion of ADAR1 in mice are both rapidly lethal secondary to an MDA5-dependent IFN response, demonstrating the requirement for ADAR1 to specifically regulate MDA5 throughout life. MDA5 is critical to recognizing Picornaviruses and Flaviviruses, but hyperactive forms are found in the Mendelian autoimmune disease Aicardi-Goutieres Syndrome (AGS), as well as the more common Type 1 Diabetes and Systemic Lupus Erythematosus. ADAR mutations are found in AGS as well as other IFN-driven inflammatory conditions. Recent studies have shown mice with hyperactive MDA5 are predisposed to autoimmunity, but protected during RNA virus infection. Unlike MDA5, ADAR1 mutations must be biallelic to cause AGS, and disease associated with ADAR haploinsufficiency is characterized by mildly elevated IFN. We hypothesize that mutations

in ADAR1 confer a pathway-specific heterozygous advantage that protects from RNA virus infection but predisposes to autoimmunity by allowing accumulation of RNA such that MDA5 is closer to a threshold of activation upon exogenous stimulation. Though it is known that ADAR1 editing is predominantly in noncoding regions, ADAR1 is a prolific editor and which targets are essential to MDA5 regulation is unknown, so we have developed a new system to isolate and identify the RNA that mediates ADAR1-MDA5 interactions.

We infected ADAR^{-/-} and ADAR^{+/+} Mouse Embryonic Fibroblasts (MEF), with and without MDA5, with encephalomyocarditis virus (EMCV), a picornavirus specifically sensed by MDA5, or transfected RNA or DNA pathway ligands. Unstimulated ADAR1^{-/-} MEF have unchanged IFN and interferon stimulated genes (ISG) transcription, but ADAR^{-/-} MEF exhibit increased survival and IFN/ISG transcription in EMCV infection. Similarly, live ADAR1^{+/+} mice have increased survival in oral EMCV infection. Elevated IFN/ISG in ADAR^{-/-} MEF were only observed in response to triggers of the MDA5 pathway, suggesting protection is pathway-specific. To address our threshold hypothesis, we developed a system to abruptly delete ADAR1 in response to tamoxifen administration both in vitro and in vivo, recapitulating the robust and lethal MDA5-dependent IFN response. We will use this system to identify the MDA5 ligand[s] edited by ADAR1. Future studies will extend these findings to a novel mouse model of the most common ADAR mutation in the human population to examine the interaction between viral infection, polymorphisms of ADAR and autoimmune disease.

202 Defining a Novel Role for Isocitrate Dehydrogenase 3 in Glioblastoma

Jasmine May

Northwestern Feinberg School of Medicine, Chicago, USA

Glioblastoma (GBM) is a highly malignant brain tumor and is the most commonly diagnosed primary brain tumor in adults. It has a poor prognosis of only 15 months. The gold standard treatment consists of radiotherapy and the chemotherapeutic temozolomide. While these therapies lengthen prognosis from 3 to 15 months more research must be done to discover druggable targets that have fewer side effects and improve prognosis. Of late there have been investigations on a group of enzymes called isocitrate dehydrogenases (IDH). They are key enzymes that convert isocitrate (ICT) to α-ketoglutarate (αKG). IDH1 carries out this conversion in the cytosol while IDH2 and IDH3 function as part of the tricarboxylic acid (TCA) cycle. αKG is important for fatty acid synthesis and acts as a co-factor for enzymes that regulate histone methylation and protein degradation. IDH1 and IDH2 are frequently mutated in the setting of GBM, especially in secondary GBM, GBM that develops from low grade gliomas, while wild type IDH1 is more commonly found in primary GBM, GBM that arises de novo. Our lab determined that wild type IDH1 promotes primary GBM growth and receptor tyrosine kinase inhibitor resistance. While IDH1 and IDH2 have been the focus in GBM research, very little has been discovered with regards to IDH3. IDH3 is rarely mutated in GBM and the reason for this has remained unclear. Unique to IDH3 compared to its family members is that IDH3 is a heterotetramer, composed of four subunits, two α, one β, and one γ subunit. Its main function is as part of the TCA cycle to convert ICT to αKG, like IDH2, but some research has hinted at alternative functions, including one that may involve a nuclear role for IDH3, specifically for the α subunit (IDH3α). My research focuses on confirming nuclear localization of IDH3α and elucidating the role that it plays at the nucleus. Through a non-biased approach, we have identified a novel interactor, cytosolic serine hydroxymethyltransferase (cSHMT), with IDH3α. We determined

that IDH3 α regulates cSHMT activity, promoting thymidylate synthesis at the nuclear lamina. In the absence of IDH3 α expression we observed decreased proliferation, increased sensitivity to the anti-folate chemotherapeutic methotrexate (MTX), and increased flux of folate metabolites through the methionine pathway, leading to an increase in DNA methylation. These effects resulted in decreased tumor growth and increased survival *in vivo*. The epigenetic changes caused a decrease in mRNA for genes related to axonal growth and the Wnt/ β -catenin pathway. Thus, we discovered a novel role for IDH3 α in GBM pathogenesis and in general cellular physiology. Therefore, IDH3 α appears to be a novel metabolic target for future therapies that may improve GBM patient outcomes. (No conflicts of interest to declare.)

203 Manipulating the breast tumor microenvironment with histone deacetylase inhibitors for more robust and durable T cell responses

Tyler McCaw

University of Alabama at Birmingham, Birmingham, USA

Malignant cells harbor an imbalance in histone acetyltransferase and histone deacetylase (HDAC) activity, epigenetically contributing to altered cellular programs. HDAC inhibitors disrupt this balance to impact both cellular transcription and protein function, changing the phenotype of tumor cells as well as responding immune cells, including tumor-infiltrating T cells. We hypothesized that HDAC inhibition could be used to boost anti-tumor T cell responses through inducing expression of immunomodulatory proteins on tumor cells as well as directly altering the transcriptional programs of tumor-specific T cells. To test this, we treated two murine breast cancer models, TS/A and 4T1, with HDAC inhibitors representing class I specificity, entinostat, or pan-specificity, panobinostat, *in vitro* and *in vivo*. Culture of tumor cells with either inhibitor increased surface expression of molecules involved in T cell recognition and stimulation, including MHCI, MHCII, CD74, 41BB, CD40, and ICOSL as well as the T cell chemoattractant CXCL10. Treating tumor-bearing mice with HDAC inhibitor resulted in a significant reduction in tumor growth that was absolutely dependent on adaptive immunity. Using depleting antibodies, we next showed that IFN γ and CD8 T cells, but not CD4 T cells or B cells, are necessary for the anti-tumor effects of entinostat. Interestingly, tumor infiltration of CD4 T cells was reduced following treatment and their effector functions were largely unchanged. However, CD8 T cell infiltration was dramatically increased, as was their production of IFN γ , TNF α , and granzyme B even at later time points. This upregulation of effector function was paralleled by a significant increase in the transcription factor T-bet, while Eomes actually decreased over time, trends opposite those seen in CD8 T cells from vehicle treated tumors and that would suggest entinostat treatment can imprint T cells with a transcriptional program less susceptible to exhaustion. Strikingly, we also found that simply adjusting the timing of entinostat dosing relative to T cell activation could abolish anti-tumor effects or lead to rejection in nearly 50% of mice. These effects corresponded with a significant shift in the responding T cell repertoire. Collectively, our data suggests that HDAC inhibition has important effects on both tumor cells and T cells; specifically, altering tumor cell gene expression leads to a repolarization of the tumor microenvironment more favorable to anti-tumor immunity and reprogramming transcriptional profiles of activated T cells improves effector functions and reduces susceptibility to exhaustion. Thus, appropriately timed administration of HDAC inhibitors may synergistically potentiate current tumor immunotherapies, especially adoptive cellular transfer and T cell reinvigoration strategies.

204 Compositional Data Analysis with sleuth-ALR: implications for reinterpreting RNA-Seq data

Warren McGee

Northwestern University, Chicago, USA

Molecular probing *Seq techniques (e.g. RNA-Seq) generate “compositional” datasets, where the number of fragments sequenced is not directly proportional to the total RNA in the cell population, but rather directly proportional to other experimental factors. Thus, the dataset carries only relative information constrained by the arbitrary dataset size, even though absolute copy numbers are often of interest. Unless external information is added (e.g. spike-ins), or unless there is no change to the overall composition (i.e. only a few features change), then conclusions drawn from the relative information can be misleading. Critically, many datasets do not have external information available and have contexts where many features are expected to change (e.g. cancer cells versus control cells; knockout of a transcription factor).

We propose a new approach that combines an “additive logratio (ALR) transformation” from compositional data analysis with the strengths of the current pipeline using the R package sleuth, which we call sleuth-ALR. ALR transformation is analogous to the normalization with a reference gene used in qPCR. Simulations demonstrated sleuth-ALR performs just as well as previous methods when only a few changes occur but outperforms previous methods when many changes dramatically shift the composition. This approach was used to re-analyze several RNA-Seq datasets studying the RNA-Binding Protein FUS. Normalizing the data using ALR and GAPDH, the reference gene used by the FUS field, led to dramatically different patterns of genes detected as differentially expressed. Implications for understanding FUS biology and applying sleuth-ALR to other biological problems will be discussed. Sleuth-ALR can be found on github: <https://www.github.com/warrenmcg/sleuthALR>.

205 Lower axon density in residual temporal white matter is related to semantic paraphasia prevalence

Emilie T. McKinnon

Medical University of South Carolina, Charleston, USA

Introduction: Wallerian degeneration after ischemic stroke is a recognized phenomenon, although, the importance of residual white matter (WM) integrity in aphasia remains poorly understood. Diffusion MRI (dMRI) is ideally suited to probe WM integrity non-invasively, admitting, traditional dMRI results can be hard to interpret as they characterize underlying general physical processes and not tissue-specific microstructural properties. Biophysical models, a simplification of complex biological systems, are necessary to overcome this drawback. In this study, we use the white matter tract integrity model (WMTI), which provides a physically meaningful interpretation to diffusional kurtosis images (DKI). Specifically, we focused on the modeling parameter labeled axonal water fraction (AWF), describing the amount of water in the axons relative to the total amount of water (axonal + extracellular space). We hypothesize that Wallerian degeneration results in a decreased AWF, caused by the diminished axon count. Additionally, we probe regional differences in AWF and their relationship to the number of semantic paraphasias made during the Philadelphia naming test (PNT).

Methods: Twenty-four subjects (age=5711y; 75%male; MRI time post-stroke=2832m; WAB-AQ=5323; semantic paraphasias=1511%) with chronic post-stroke aphasia underwent the PNT and MRI imaging. Structural images (T1 and T2) and DKI (b=0, 1000, 2000 s/mm²) were acquired. Diffusional Kurtosis Estimator was used

to estimate diffusion and kurtosis tensors, from which AWF was calculated using in-house software. A probabilistic WM mask was created using the clinical toolbox in SPM12. The WM mask and the JHU WM atlas were warped into native diffusion space using the non-linear deformation field calculated by the clinical toolbox. The following regions of interest (ROI) were defined for both ipsi- and contralateral sides: whole-hemisphere WM, temporal lobe WM (defined by the inferior longitudinal fasciculus) and parietal lobe WM (defined by the superior longitudinal fasciculus). The ROIs were created as such to exclude lesioned white matter. Simple correlations and t-tests were performed to study AWF behavior. Additional partial correlations were run to control for lesion size.

Results: Average AWF is significantly lower throughout the whole left-hemisphere, the left temporal and the left parietal lobes ($p < 0.05$; $r = 0.05$, $p > 0.05$). Controlling for lesion size further strengthened the correlation between temporal lobe AWF and semantic paraphasia prevalence ($r = 0.53$, $p < 0.001$). **Conclusion:** Biophysical models such as the WMTI are promising techniques to study WM integrity since they provide us with physically meaningful and interpretable parameters. Our results suggest widespread left hemisphere axonal degeneration, as quantified by AWF. Importantly, AWF shows regional specificity, as a reduction in temporal lobe axon density is reflected by an increase in the number of semantic paraphasias. These results possibly reflect the wide-spread process of Wallerian degeneration occurring after ischemic incidents.

206 CD301b/MGL2⁺ mononuclear phagocytes orchestrate autoimmune cardiac valve inflammation and fibrosis

Lee Meier

University of Minnesota, Minneapolis, USA

Background: Cardiac valve disease is common and affects the mitral valve (MV) most frequently. Despite its prevalence, relatively little is known about its cellular and molecular pathogenesis. Herein, we dissect the mechanisms by which autoimmune MV inflammation and fibrosis are initiated *in vivo*.

Methods: K/B.g7 mice develop fully-penetrant MV disease (MVD) in the setting of systemic autoantibody-associated autoimmune disease. We used complementary approaches including histological staining, *in vivo* monoclonal antibody blockade, constitutive and conditional gene deletion, bone marrow (BM) chimeric mice, diphtheria-toxin mediated cell ablation, multi-parameter flow cytometry, multiplex immunofluorescence (IF), and image analysis to study the cellular and molecular mediators of MVD in this model. Valve samples taken from patients with rheumatic heart disease (RHD) were used to correlate our findings with human pathology.

Results: Through characterization of the immune cell milieu in inflamed K/B.g7 MVs, we determined that CD301b/MGL2⁺ mononuclear phagocytes (MNP) are required for MVD progression in K/B.g7 mice and depend on fractalkine (CX3CL1) receptor (CX3CR1) signaling. Furthermore, we identified analogous cells in human RHD valves. In K/B.g7 mice, the valve-infiltrating CD301b/MGL2⁺ MNPs express tissue-reparative molecules such as arginase-1 (Arg-1) and resistin-like molecule alpha (RELM-α). Depletion of CD301b/MGL2⁺ cells protects mice from valve pathology. Spleen tyrosine kinase (Syk) signaling downstream of IgG-recognizing Fc receptors on CD301b/MGL2⁺ MNPs in MV promotes tumor necrosis factor (TNF) and interleukin-6 (IL-6) production and both are required for MVD. TNF acts through TNF receptor 1 (TNFR1) expressed on valve-resident cells to promote MVD through upregulation of vascular cell adhesion molecule-1 (VCAM-1) expression. Correspondingly, we show that very late antigen-4 (VLA-4) expression by circulating

CX3CR1-expressing MNPs is also necessary for MVD.

Conclusions: Here, we defined the *in vivo* mechanism by which circulating autoantibodies activate a CD301⁺ phagocyte-mediated immune response to initiate MV inflammation. Our studies uncovered multiple targets for therapeutic intervention that could readily be translated to a clinical setting.

207 Erosive rheumatoid arthritis is associated with a limited B cell receptor gene segment repertoire

Kofi A. Mensah

Yale School of Medicine, New Haven, USA

There is normally a diverse repertoire of B cell receptors (BCRs) generated via random recombination of variable, diversity, and joining (V(D)J) gene segments on the immunoglobulin heavy chain (IgH) and kappa (κ) or lambda (λ) light chain genes. In some rheumatoid arthritis (RA) patients, there is a skewed BCR κ light chain repertoire with under-representation of upstream Vk gene segments (found toward the 5' region of the BCR κ gene locus) and downstream Jk gene segments (found in the 3' region). Whether this BCR phenotype relates to erosive joint disease in RA is unclear.

A cross-sectional analysis was performed on peripheral blood B cells obtained from 36 consecutively enrolled, seropositive, RA patients. BCR Vk and Jk gene segment expression were determined using PCR assays. Patients were grouped according to extent of Vk and Jk gene segment usage, and we examined the association between gene segment usage and the presence of joint erosions. Flow cytometry and gene expression assays were used to further characterize B cells to determine differences that may imply a mechanism for an association to erosive disease.

Diversity in expression of the ~40 Vk and 5 Jk gene segments allowed for subgrouping of RA patients. The expression of upstream Vk and downstream Jk gene segments was significantly correlated in RA patients ($r = 0.66$, $P < 0.01$) but not in healthy donors (HD) ($r = 0.05$, $P = 0.88$). In a subgroup of RA patients, B cells were characterized by decreased upstream Vk and downstream Jk gene segment expression. This indicates limited use of the full BCR κ gene repertoire; hence, we designated these patients as BCR.ltd. Among BCR.ltd patients, 70% had erosive disease compared to 28% of non-BCR.ltd patients ($P < 0.05$). Additionally, the non-BCR.ltd subgroup contained 81% of all patients *without* erosions ($P < 0.05$). There were no significant differences in age, disease duration, autoantibody titers, or treatment between BCR.ltd and non-BCR.ltd patients. We found a significantly increased frequency of atypical CD21^{-low} B cells in the BCR.ltd subgroup [mean (SEM) = 9.1% (1.7%)] compared to non-BCR.ltd patients [mean (SEM) = 1.8% (0.4%), $P < 0.01$] and HD [mean (SEM) = 0.8% (0.1%), $P < 0.01$]. CD21^{-low} B cells have been shown to express elevated levels of RANKL which stimulates bone-eroding osteoclast formation. CD21^{-low} B cells showed increased levels of *TNFR2* and decreased *IL4R* compared to conventional CD21⁺ mature naïve B cells ($P < 0.01$). This indicates increased ability of CD21^{-low} B cells to respond to TNF-α, which promotes RANKL expression, over IL-4, which inhibits RANKL expression.

Limited expression of the full BCR κ light chain repertoire is associated with an elevated frequency of CD21^{-low} B cells and increased prevalence of erosive RA. Identifying patients with the BCR.ltd phenotype has implications for prognosis and early treatment to prevent irreversible joint destruction.

208 Microvascular Pathology In Peripheral Artery Disease

Constance J. Mietus

University of Nebraska Medical Center, Omaha, USA

Background: Peripheral Artery Disease (PAD) is caused by atherosclerotic narrowing of arteries supplying the legs. PAD induced myopathy is characterized by myofiber degeneration and produces functional limitations. Furthermore, work from our laboratory (Ha *et al.* J Transl Med 2016) has established a progressive fibrosis in the affected calf muscles of patients with PAD. Qualitative histological review suggests systematic pathological changes in the microvasculature of PAD muscle, in association with advancing fibrosis. In this study, we tested the hypothesis that microvessel architecture, collagen profiles, and tissue density systematically change with advancing disease and are consistent with advancing microvascular pathology.

Methods and Results: Calf muscle biopsies of PAD patients at Fontaine Stage II (n=15) and IV (n=16), and controls (n=15) were labeled with Wheat Germ Agglutinin (WGA) and antibodies specific for Collagen-I and Collagen-IV. Images were acquired with a wide-field fluorescence microscope and processed with AutoQuant @ deconvolution software and Image Pro Plus @ software. Collagen-IV label was used to measure thickness of the basement membrane (BM) and lumen diameter of approximately 50-200 microvessels (5-12µm total diameter) per biopsy specimen with a custom MatLab program. Regions of interest were generated around microvessels and Collagen-I density (area weighted mean fluorescence intensity) was measured. WGA label was used to measure total tissue area and microvessel density was calculated as a ratio of number of microvessels per total tissue area sampled. Means and 95% confidence intervals were determined for each measurement. Significant differences were determined with one-way ANOVA and *post hoc* pairwise comparisons using Student's T Test with Bonferroni correction. Correlations were determined by linear regression analysis. Thickness of the BM was greater in Stage-II patients (1.58 µm) compared controls (1.42 µm) (p<0.043) and in Stage-IV (1.75 µm) compared to Stage-II patients (p<0.021). Microvascular lumen diameter was increased (p<0.001) in Stage-IV patients (3.97 µm) compared to control (3.25 µm) and Stage-II patients (3.29 µm). BM thickness correlated positively with microvascular lumen diameter (R²= 0.513, p<0.001). Microvascular density was increased in PAD patients compared to controls (p<0.001) and in Stage-IV patients compared to Stage-II (p=0.025). Collagen-I deposition around the microvasculature was greater in Stage-IV patients compared to Stage-II patients (p=0.040). Peri-microvascular Collagen-I deposition correlated positively with microvascular lumen diameter (R²= 0.162, p=0.006).

Conclusions: Increases in microvessel density and lumen diameter in PAD muscle represent advancing microvascular disease since they occurred in association with increased perivascular deposition of Collagen-I and BM thickening. Loss or dysfunction of microvascular pericytes has been shown to produce microvascular lumen hyperdilation and altered collagen composition of the BM. Thus, pericyte loss may produce the changes observed and will be evaluated in future studies.

209 Examining the merits of engaged department cohorts: Where to begin and how to proceed?

Gloria Mileva

Grand Valley State University, Allendale, USA

I hope to explore the conditions under which engaged department initiatives (EDIs) are effective starting points for fostering collaborative, scaffolded, and sustained civic engagement across one's institutions. Given that departments are an integral unit of power within the current infrastructures of higher education, some leading scholars argue that they are one of the best starting points for shifting from expert-driven, "one-off" community-based projects to collaborative and sustainable engagement opportunities that span programs of study. Building upon this research, I will share lessons learned from two initiatives beginning in the spring of 2015.

These initiatives encompass ten engaged departments across three institutions of higher education (a large, public; a small private; and a local community college) in Grand Rapids, MI. Findings emerge from a systemic action research approach and harness mixed methods, including traditional surveys, interviews, and comparison analyses of reporting documents. Initial findings indicate cohorts—when intentionally supported by a number of other structures (like civic action plans, committed administrative and faculty leadership, etc.)—can be a particularly effective mechanism for generating institutional capacity. Cohorts can generate on-campus leadership in addition to fostering a community of reflective practice essential for providing support, fostering accountability, and expanding narrow disciplinary frameworks. In addition, they have the potential to catalyze more pervasive and sustained institutional change. For instance, the implementation of successive cohorts over time and across the campus can nurture transdisciplinary collaboration and generate pathways towards institution-wide change.

Designed to facilitate discussion relevant to each participants' work, this poster will highlight critical challenges across departments and institutions along with key recommendations for shifting academic culture and structures towards an environment that inspires and sustains collaborative engagement.

210 Characterizing the Effects of TiO₂ Nanotubes on the Vascular Response to Inflammatory Cytokines in In-Stent Restenosis

Anvita Mishra

California Institute of Technology, Pasadena, USA

Cardiovascular diseases are the leading cause of death globally, estimated to cost over \$320 billion in annual healthcare costs in 2017 alone. Many cases of cardiovascular diseases are treated with percutaneous coronary intervention (PCI); however, nearly 40% of these patients suffer from restenosis within a year of treatment.

Restenosis is characterized by arterial wall remodeling and neointimal hyperplasia or the uncontrolled proliferation of vascular smooth muscle cells and endothelial cells after injury. Previous research in the Desai lab has shown that nanostructured TiO₂ stent surfaces can lower the rate of restenosis. However, the mechanism of attenuation in the experimental model of Human Coronary Artery Endothelial Cells (HCAEC) and Human Coronary Artery Smooth Muscle Cells (HCASMC) is not yet understood. We believe that inflammatory cytokines such as Tumor Necrosis Factor α (TNFα) and Platelet-Derived Growth Factor (PDGF) may play an important role in mediating vascular restenosis. In this project, we developed a model of vascular inflammation by comparing the vascular response to various cytokines with quantitative PCR. Ongoing studies are using this model to understand the potential protective effects of nanostructured TiO₂ surfaces against restenosis.

211 Ultrasound Oncotripsy: Targeting Cancer Cells Selectively Via Resonant Harmonic Excitation

David R. Mittelstein
Caltech, Pasadena, USA

Therapeutic ultrasound is a promising non-invasive method to ablate tumors. Clinical trials demonstrate that high intensity focused ultrasound (HIFU) can improve clinical outcomes in prostate, breast, liver, pancreas, bone, and brain tumors. However, HIFU uses thermal ablation or acoustic cavitation to destroy tissue in a target area and as such is largely non-specific. Safely implementing HIFU is an involved procedure that demands costly MRI tumor tracking to prevent off-target ablation and still may induce collateral damage.

An emerging field of research in low intensity focused ultrasound (LIFU) may allow for more targeted ultrasound therapy. Pulsed ultrasound at 2 does not cause heating or cavitation, but can induce bioeffects through a mechanism that is currently not well understood. At Caltech, a cross-disciplinary collaboration investigates the inherent cellular effect of LIFU. We have developed a computational model that predicts that ultrasound pulsing patterns at target frequencies can induce resonant oscillation in the membranes of target cells. "Ultrasound oncotripsy" involves applying these waveforms to lyse cancer cells without affecting healthy cells. We have experimentally validated that this technique can effect selective cell targeting with in vitro and in vivo leukemia / lymphoma models and used high-speed imaging to quantify cell membrane deformation and verify the ultrasound oncotripsy mechanism.

Ultrasound oncotripsy theoretically does not require tumor tracking or the enforcement of therapeutic margins. By taking advantage of its cancer-cell selective mechanism, an oncotripsy system can administer therapy to an entire organ and only disrupt the invading cancer cells. This provides clinicians with a powerful and novel technique to locally administer targeted cancer therapy without harming healthy tissue. Cancers with tissues that differ in mechanical properties of stiffness or structure from surrounding healthy tissue may be candidates for oncotripsy.

Preliminary studies suggest that oncotripsy is effective at targeting cancer cells in suspension, as tested in hematological malignancies such as leukemia or lymphoma. A higher impact application of this capability is eliminating circulating tumor cells, cancer cells that have hematogenously spread from primary tumor sites. An oncotripsy system focusing over a major vein could disrupt circulating tumor cells before they metastasize.

Many therapeutically challenging cancers involve a solid tumor mass with poorly defined borders and invasion into healthy tissue. While HIFU may be unable to safely ablate these tumors, oncotripsy may be specifically suited to targeting these invading cells. For example, the treatment of glioblastoma multiforme (GBM), the most common primary brain tumor in adults, is complicated by the difficulty of establishing effective surgical margins in brain tissue. However, the shear elastic moduli are substantially different between normal brain tissue and glioma tissues. This suggests that oncotripsy may be a noninvasive therapy option for GBM.

212 Characterization of two *E. coli* bacteriophages isolated from the bladder of adult females

Cesar Montelongo Hernandez
Loyola University - Stritch School of Medicine, North Riverside, USA

It is now established that the bladder is not sterile; it contains a resident community of bacteria, which we now know contains an abundance of bacteriophages. Bacteriophages (phages) are abundant in nature and interact with bacteria in a complex manner. Phages can alter microbial population dynamics by lysing bacteria, conferring traits via horizontal gene transfer, and protecting hosts against infection from other phages. Our group has identified prophage sequences in the genomes of phylogenetically diverse bladder bacteria, and isolated seven *Escherichia coli* phages from the bladders of adult women with urinary incontinence. In terms of host range and propagation ability, we have begun to characterize two of these phages: Greed and Lust. In terms of its genome, Lust is similar to other phages isolated from the bladder (Envy, Gluttony, Pride, Sloth), and both the Greed and Lust genomes resemble those of phages identified in cattle slurry. To assess host range for Greed and Lust, we utilized a spot titration assay, which was also used to screen for phage resistant mutant bacteria. To assess phage propagation in *E. coli* strains, we used a full plate titration assay. Greed and Lust share little sequence identity, apart from 15 small genetic segments ranging from 10 to 28 base pairs long. Yet, they share a similar host range as it relates to strains of *E. coli* isolated from the bladders of women with and without urinary symptoms. Of forty bladder isolates screened, only three (UMB0149, UMB7542, UMB7513) were susceptible to both Greed and Lust. Although *E. coli* strains UMB7542 and UMB7513 were isolated from patients with a urinary tract infection (UTI), we have found no evidence that Lust or Greed can lyse uropathogenic *E. coli* (UPEC) CFT073, NU14, or UT189; the titers of Lust incubated with these UPEC strains indicate that the phage does not propagate in these strains. In addition, Greed and Lust appear to not infect bacteria species other than *E. coli*. We isolated *E. coli* K12 strains resistant to Greed and Lust. Of note is that *E. coli* K12 resistance to Lust does not confer resistance to lysis by Greed. Taken together, these preliminary findings indicate that while Greed and Lust do not share sequence identity and that their mechanism for resistance may differ, there is a common shared element in terms of the strains that they can infect. In the future, we plan to sequence bladder isolates susceptible to Greed and Lust, in addition to *E. coli* K12 isolates resistant to Greed and Lust infection. We suspect that the genome sequence of these isolates will provide insight regarding the targets used by Lust and Greed for entry into the host.

213 The role of ARID1A in the pathogenesis of nonalcoholic fatty liver disease

Austin B. Moore
University of Texas Southwestern Medical Center, USA

Nonalcoholic fatty liver disease (NAFLD) is a rapidly growing cause of chronic liver damage, cirrhosis, and hepatocellular carcinoma both in the United States and worldwide. The role of epigenetic regulation in the pathogenesis of fatty liver disease is unclear. ARID1A, a DNA-binding component of the SWI/SNF ATP-dependent chromatin remodeling complex, is frequently mutated in HCC and contributes to nucleosome repositioning and access by transcriptional regulators. We hypothesized that chromatin remodeling is important for the pathogenesis of fatty liver disease. We analyzed previously existing human gene expression datasets and found that ARID1A expression is suppressed in the liver tissues of patients with nonalcoholic

steatohepatitis (NASH), a more progressive form of NAFLD that involves liver inflammation and damage.

The functional impact of this suppression was examined in mice with Cre-mediated liver-specific deletion of Arid1a (Arid1a LKO), which develop age-dependent fatty liver disease as measured via the NAFLD activity score (NAS). These Arid1a LKO mice exhibit a phenotype marked by increased liver weight, elevated cholesterol, and increased markers of liver damage. They are also more susceptible to high fat diet induced liver steatosis and inflammation. RNA-sequencing analysis of Arid1a-deficient liver tissue revealed upregulation of lipogenesis genes, such as Srebf1 and Fasn, and downregulation of fatty acid oxidation genes, including Acs1. Chromatin immunoprecipitation sequencing (ChIP-seq) studies corroborated these results, demonstrating direct binding of Arid1a to the promoters of differentially regulated genes involved in lipid handling and fatty acid metabolism.

To better study the later stages of fatty liver disease progression, we combined adenoviral Cas9-mediated Pten deletion with our Arid1a LKO model, which synergistically drove fatty liver development. Inhibition of lipogenesis using CAT-2003, a potent SREBP inhibitor, showed improvements in markers of fatty liver disease progression in this Arid1a/Pten double knockout model. Collectively, our data show that ARID1A plays a role in the epigenetic regulation of hepatic lipid homeostasis, and its suppression contributes to fatty liver pathogenesis.

214 The development and utilization of exosome driven polarization of PD-L1+ gamma delta T cells in cancer

Samantha Morrissey

University of Louisville, Louisville, USA

Purpose: Determine if tumor derived exosomes (TDE) can drive cancer progression through polarization of immunosuppressive cell phenotypes capable of restricting $\alpha\beta$ T cell functioning. Preliminary data shows that exosome stimulation differentially upregulates PD-L1 (programmed-death-ligand-1) expression on peritoneal macrophages and lung resident $\gamma\delta$ T cells while also upregulating PD-1 expression on $\alpha\beta$ T cells. Additionally, given the immunosuppressive nature of these cells, we hypothesize that they can restrict proliferation and effector functioning of auto-reactive T cells in a LPR lupus model as a potential new cell based therapy. The ultimate goal of this project is develop new therapies based on the utilization or elimination of tumor derived exosomes for the treatment of autoimmunity or cancer, respectively. **Methods:** TDE were isolated using serial ultracentrifugation from Lewis Lung Carcinoma cells. Exosome stimulated peritoneal macrophages and $\gamma\delta$ T cells were co-cultured with ova-transgenic -I (CD8+) T-cells to assay for suppressive function. Anti-PD-1 antibody was added to the culture to confirm that the PD-1/PDL-1 axis mediates the immune suppression. The effect of TDE on $\gamma\delta$ T cell metabolism was also investigated. Human peripheral blood samples from lung cancer and anti-PD-1 treated lung cancer patients were compared via flow cytometry for $\gamma\delta$ /PD-L1 expression profiling. Lastly, TDE stimulated $\gamma\delta$ T cells were adoptively transferred into δ TCR-/-LPR+ mice to determine their ability to restrict $\alpha\beta$ T cell induced disease pathogenesis. **Results:** The results suggest that TDE play a role in tumor metastasis by polarizing $\gamma\delta$ T cells and macrophages to an immunosuppressive PD-L1+ phenotype capable of restricting $\alpha\beta$ T cell effector functioning. Additionally, these cells display a strong immunosuppressive phenotype capable of restricting $\alpha\beta$ T cell effector functioning in vivo. **Discussion/Conclusion:** TDE could be directly antagonizing the effects of immune checkpoint therapies.

Therefore, future experiments will focus on eliminating exosome secretion by using siRNARab27 inhibition and the small drug compound, cambinol, concurrently with anti-PD-1 or anti-PD-L1 monoclonal antibody in efforts to increase progression free survival for cancer patients. Further investigation as to the role $\gamma\delta$ T cells play in lupus is another main objective of this project.

215 Local action of monocyte chemoattractant protein-1 and osteopontin in aneurysm healing

Kartik Motwani

University of Florida, Gainesville, USA

Background: Asymptomatic cerebral aneurysms occur in up to 5% of adults. In aneurysm therapy, though complication rates are lower for endovascular coiling than for operative clipping, aneurysm recurrence is a limitation of coiling. Recurrence is attributed to recanalization of the aneurysm neck following coil embolization, whereas the goal is to establish durable occlusion from the parent artery. Coiling therapy is limited by lack of mechanistic knowledge regarding aneurysm healing. In previous work in our lab, we have characterized biological molecule-releasing platinum coils to elute inflammatory regulators such as monocyte-chemoattractant protein 1 (MCP-1) in a murine carotid aneurysm model to mediate durable aneurysm healing. In our murine aneurysm model, sustained local elution of monocyte chemoattractant protein-1 (MCP-1) increases tissue ingrowth into the aneurysm sac which requires osteopontin (OPN)-mediated signaling. **Hypothesis:** Local MCP-1 activity is necessary for murine aneurysm healing. OPN mediates healing by reparative (M2) macrophage interaction with lymphocytes and platelets, by CD44 or integrin pathways. **Methods:** Carotid aneurysms are created in wild-type (WT), MCP-1 knockout (KO) or CCR2 KO mice using our established model. MCP-1-eluting, OPN-eluting, or control PLGA-coated platinum coils are implanted into the aneurysm sac. Systemic neutralizing antibody is applied to inhibit MCP-1 or OPN pathways. Cytokine levels of OPN-coiled aneurysm lysate are assayed in early days of aneurysm healing. Coiled aneurysm tissue is measured for percent tissue ingrowth into aneurysm lumen and immunohistochemistry for effector cell populations. **Results:** With MCP-1-coiling, systemic depletion of MCP-1 or CCR2 by neutralization (0.8% or 9.2%) or KO (11% or 4.6%) attenuates luminal ingrowth versus WT (56%, $p < 0.0001$). M2 macrophage-stained area is increased in WT (7.4%) versus MCP-1/CCR2 KO (1.4% or 1.6%) or inhibitor (1.4% or 1.5%) groups. Systemic MCP-1 administration reveals no difference in ingrowth versus vehicle. Cytokine arrays at post-OPN coiling days 1, 3, and 7 reveal upregulation of numerous cytokines including PF4 and IL-17 versus control. **Conclusion:** Local delivery of MCP-1 is critical for murine aneurysm healing. OPN may further activate lymphocyte subsets and platelets to promote aneurysm healing, which merits future study.

216 The LKB1-MITF pathway: dysregulation in melanomagenesis

Nisma Mujahid

Boston University School of Medicine; Massachusetts General Hospital; Cutaneous Biology Research Center, Boston, USA

Background: Upon UV exposure, signals from keratinocytes stimulate melanocytes through melanocortin 1 receptor, leading to downstream activation of the cAMP response element binding protein (CREB) transcription factor and microphthalmia-associated transcription factor (MITF), the master regulator of pigmentation. Although MITF normally functions as an activator of pigment-related genes, if amplified MITF can serve as a melanoma oncogene shown to cooperate with BRAF (V600E) to induce tumorigenic

transformation of melanocytes. Only 10% of melanomas carry an *MITF* amplification emphasizing the need to identify pathways that modulate *MITF* expression. Recent genetic data in mice suggest the presence of a pathway in which CREB-regulated transcription co-activator (CRTC) and salt-inducible kinase 2 (SIK2) regulate *MITF* expression. Liver kinase B1 (LKB1) regulates many cancer-relevant cell phenotypes and is a known SIK inducer. However, the interaction of the LKB1-SIK pathway and *MITF* in melanoma formation is not fully understood.

Methods: Genomic data from 471 skin cutaneous melanoma tumors from The Cancer Genome Atlas Analysis was analyzed using cBioPortal for Cancer Genomics. Normal human melanocytes and 49 melanoma cell lines were profiled for LKB1 expression utilizing western blot analysis. Lenti-viral transduction systems were used to overexpress wild-type LKB1 (WT), kinase defective LKB1 (D194A), and CRTC2-GFP, and small interfering RNA transfection was utilized to knockdown *LKB1*. SIK inhibition was conducted with a previously published small molecule inhibitor of SIK, HG 9-91-01. Quantitative real time polymerase chain reaction (qRT-PCR) and western blot analysis were employed to determine mRNA expression and protein levels, respectively. Cell growth was determined utilizing a cell viability assay.

Results: Collectively, LKB1, SIK, CRTC, and *MITF* are altered in 49% of the 471 skin cutaneous melanomas from The Cancer Genome Atlas (TCGA) dataset. Reduced LKB1 protein levels were observed in majority of melanoma cell lines evaluated compared to normal human melanocytes. Wild-type *LKB1* overexpression inhibits CRTC2-GFP nuclear localization, and knockdown of *LKB1* increases nuclear import of CRTC2-GFP. Overexpression of LKB1 (WT) suppresses *MITF* expression in LKB1-deficient G361 melanoma cells and A2058 melanoma cells, but no change in *MITF* mRNA expression is seen when kinase defective LKB1 (D194A) is overexpressed. *LKB1* knockdown increases *MITF* expression in WM88 melanoma cells. A salt-inducible kinase inhibitor rescues *MITF* expression after LKB1 overexpression in LKB1-deficient melanoma cells. Rescue of LKB1 (WT) but not LKB1 (D194A) in G361 melanoma cells suppresses cell proliferation.

Conclusion: Overall, our findings establish LKB1 as a negative regulator of the CRTC-CREB-*MITF* pathway through activation of SIK, an axis altered in almost half of TCGA skin cutaneous melanoma samples, and demonstrate how this pathway could potentially play a critical role in as a tumor suppressor in melanoma oncogenesis and may offer new targets for cancer therapy.

217 ROR γ inverse agonists suppress the NLRP3 inflammasome

Meghan Murray

Saint Louis University School of Medicine, Saint Louis, USA

The retinoic acid receptor-related orphan nuclear receptor gamma (ROR γ) is a ligand-dependent transcription factor known to upregulate pro-inflammatory gene expression in multiple lineages of adaptive and innate immune cells. ROR γ has been shown to regulate adaptive immunity (role in Th17 differentiation), but its role in innate immune cells is poorly understood. The NLRP3 inflammasome is a component of the innate immune system that processes IL-1 β and IL-18 into mature cytokines. Over-activation of the NLRP3 inflammasome is known to contribute to the progression of many immune and metabolic diseases. In the lab, we developed several synthetic ligands to ROR γ , and we have shown their efficiency in metabolic and inflammatory diseases. This study investigates the role of ROR γ in NLRP3 activation both in vivo and in vitro. We

hypothesize that inhibition of ROR γ activity using synthetic ligands can regulate the NLRP3 inflammasome and have a potential therapeutic benefit for NLRP3 dependent diseases.

Using an in vitro model of macrophage polarization and bio-molecular techniques, we demonstrated that suppressing ROR γ with synthetic inverse agonists attenuates both NLRP3 and IL-1 β gene expression and suppresses the release of mature IL-1 β . Previous studies demonstrate that the NLRP3/IL-1 β pathway is significantly upregulated in mouse models of LPS induced sepsis and fulminant hepatitis. In vivo results show that ROR γ inhibition reduced plasma IL-1 β as well as IL-1 β production by peritoneal macrophages in an LPS induced sepsis. Also, ROR γ inverse agonists reduced mortality rate in an LPS/D-galactosamine induced fulminant hepatitis mouse model. Together, these findings demonstrate the feasibility of targeting ROR γ to suppress the NLRP3/IL-1 β axis both in vitro and in vivo.

In conclusion, inhibition of ROR γ via synthetic ligands could be a new therapeutic approach in treating NLRP3 associated diseases.

218 Repetitive Transcranial Magnetic Stimulation for the Treatment of Fibromyalgia

Nilson N. Mendes Neto

Extension Center, University of California, Davis/School of Medicine, UnP, Natal - RN, Brazil

INTRODUCTION: Recurrent Transcranial Magnetic Stimulation (rTMS) is a noninvasive neuromodulation technique that has been used to treat patients with fibromyalgia (FM). This study aimed to evaluate the efficacy and safety of rTMS as a treatment for FM in a center for diagnosis and treatment of pain.

METHODS: From January 2015 to May 2017, 17 patients with FM were enrolled in an open-label uncontrolled clinical trial. To be included in this study, patients should have received rTMS in the left prefrontal cortex. The sessions were performed in a series of 3 to 5 consecutive days with maximum break of 2 days between the series. A minimum of 10 sessions was required. Parameters used: frequency (10Hz), cycles of 10 stimuli with pause of 20 seconds between them. 20 minutes was the length of each session. Motor threshold was adjusted according to the acceptance of patients. Variables such as side effects, pain, depressive symptoms, insomnia, fatigue, quality of life and side effects were assessed after each session.

RESULTS: Among the 17 patients, 88.2% were women. Mean sample age of 55.7 years (ranging from 31-81 years). 41.2% reported significant improvement of pain after 3rd rTMS session. Improvement of depressive symptoms was observed after 3rd sessions in 50% of patients. Improvement of insomnia and fatigue was reported after 3rd sessions in 52.9% in 35.3% of patients, respectively. Increased quality of life was seen in 47.1% of patients after the 3rd session. Three patients reported mild and transient symptoms such as tinnitus and headache.

CONCLUSION: In our experience, rTMS had a significant influence on the reduction of diffuse pain in patients with FM. In addition, it showed to be a good option for rapid relief of symptomatology since most patients reported relief of symptoms after third session. It was well tolerated with minimal adverse effects. Therefore, it showed to be a safe technique. Additional studies are needed to determine optimal protocols for the use of rTMS in the treatment of FM.

219 Clinical data correlations to algorithmic surgical skill assessment metrics during robotic assisted surgery

Daniel Naftalovich

California Institute of Technology, Pasadena, USA

Surgical technical skill and efficiency are studied in the context of robotic assisted surgery using algorithmic computation of surgical skill and safety features from surgeon motion data during oncological surgeries performed with the da Vinci Surgical System. Surgical robots can serve as a rich source of data for motion, skill, and efficiency data, but this has been limited to the setting of virtual simulators and laboratory robots. Recent progress and industry collaborations now enable study of surgeon motion data from clinical cases, as well as corresponding clinical information, from which metrics for safety, skill, and efficiency can be computed akin to the simulator and laboratory environments. The ongoing pilot study at the City of Hope Comprehensive Cancer Center is presented, in which surgeon motion and robot kinematic data are analyzed for prostatectomies, nephrectomies, gastrectomies, and hepatectomies.

220 A Functional Signature Ontology (FUSION) screen detects an AMPK inhibitor with selective toxicity toward human colon tumor cells

Beth Neilsen

University of Nebraska Medical Center, Omaha, USA

AMPK is a serine threonine kinase composed of a heterotrimer of a catalytic, kinase-containing α and regulatory β , and γ subunits; however, the specific contributions of individual subunit isoforms to its function and activity are unknown and likely contribute to the inconsistent and context-specific role of AMPK in cancer. In a panel of colon cancer cell lines, individual AMPK subunit expression and requirement for survival varies. AMPK α 1, AMPK γ 1, and AMPK β 1 expression was relatively consistent across colon cancer cell lines and was comparable to immortalized, non-transformed human colon epithelial cells (HCECs) expression. However, the expression of AMPK α 2 was variable between cancer cell lines with the highest expression being demonstrated in the SW480 and SW620 cancer cells and moderate expression being demonstrated in the HCECs as well as the HCT116 cancer cells. Even though AMPK γ 1 is consistently expressed, depletion of the γ 1 subunit of AMPK is toxic to HCT116 colon cancer cells, but less so to SW480 colon cancer cells. On the other hand, depletion of AMPK α 1, which is also consistently expressed, does not induce cell death in any of the colon cancer cell lines tested. RNAi-mediated depletion of the other kinase subunit, AMPK α 2, induces cell death in SW480 and HCT116 colon cancer cells, two cell lines expressing high and moderate levels of AMPK α 2 respectively. These data suggest colon cancer cells have variable requirements for specific AMPK subunit isoforms, which may be indicative of isoform-specific roles for AMPK activity and function.

Colon cancer cells are largely susceptible to decreased AMPK kinase activity, but vary in their dependence for a given AMPK subunit. These data suggest that AMPK kinase inhibition may be a useful component of future therapeutic strategies. Therefore, Functional Signature Ontology (FUSION) was used to screen a natural product library to identify compounds that were inhibitors of AMPK to test its potential for detecting small molecules with preferential toxicity toward human colon tumor cells. FUSION identified 5'-hydroxystaurosporine, which competitively inhibits AMPK kinase activity. Human colon cancer cell lines are notably more sensitive to 5'-hydroxystaurosporine than are non-transformed human colon epithelial cells, but demonstrates variable toxicity across cancer cell lines. This could be a consequence of increased AMPK a subunit

expression. This study demonstrates the potential efficacy of AMPK inhibition as a cancer therapeutic and serves as proof-of-concept for unbiased FUSION-based detection of small molecule inhibitors of therapeutic targets. These results highlight the potential for FUSION to identify novel compounds for cancer therapy development.

222 Investigating context-dependent integration potential of postnatally born interneurons

Gabriel F. Neves

Duke University School of Medicine, USA

Understanding the principles guiding neuron integration into neural circuits have important implications for functional recovery post-injury. Firing action potentials (AP) is a central characteristic of all neurons, quintessential for circuit-level computation. Despite our mechanistic understanding of how APs are generated, how newborn adult neurons develop abilities to fire APs remains unknown. This is likely a key step to successfully transplant neurons as a therapy. The Ankyrin proteins organize voltage-gated ion channels necessary for AP generation in neurons. Their roles have not been studied during adult born interneuron integration. Using adult neurogenesis in the rodent subventricular zone (SVZ) as a model for understanding neuronal integration into functional circuitry, we combined innovations in mouse genetics, microscopy, and electrophysiology to characterize Ank3 expression and function during olfactory bulb (OB) interneurons maturation. To determine developmental Ank3 expression by OB interneurons, we generated a novel DCX-CreERtm transgenic driver line that specifically targets newborn neurons migrating from the adult SVZ to the OB enabling us to age these interneurons. Using this strategy, we were able to characterize Ank3's developmental expression in OB interneurons finding Ank3 upregulating during the initial phase of neuronal integration. Electrophysiological recordings showed that Ank3 upregulation paralleled the interneurons' ability to fire APs. Using the DCX-CreERtm transgenic driver crossed to a Ank3^{flox} allele, tamoxifen-induced Ank3 deletion resulted in decreased dendritic complexity, as well as reduced AP firing frequencies and amplitudes. Strikingly, 4 weeks following tamoxifen-induction, Ank3-deletion resulted in significantly fewer integrated interneurons compared to control littermates, revealing Ank3 as a critical regulator of neuronal integration into adult neural circuits. Together, our data demonstrated that Ank3 upregulation during interneuron integration in the adult brain is required for proper AP generation, promoting interneuron survival.

223 Motor dysfunction and skeletal muscles atrophy in rats with spinal cord injury

Bich Tram Nguyen

Cleveland Clinic Lerner Research Institute, Brooklyn, USA

Spinal cord injury (SCI) is a traumatic condition to any level of the spinal cord that causes impaired neurological function with associated deficits in the musculoskeletal system and can lead to permanent disability. This study is to test the hypothesis that the motor dysfunction and skeletal muscle atrophy is correlated with the severity of SCI. We used two different SCI models including thoracic 8 (T8) level complete injury or T8 incomplete injury in adult rats. The complete SCI was created by a surgical scissor to transect spinal cord. The incomplete SCI was created by the computer-controlled impactor to generate a contusive injury. The rats were observed for 3 months after SCI. Within the 3 months, the locomotor patterns were assessed using the Basso, Beattie, and Bresnahan (BBB) scale. Analyses showed more significant deficit in the transection animals while compared to the contusive injury group. Both SCI groups were also shown the significant decrease of motor function while compared

to the spinal-intact animals. At the end of 3 months, the animals were perfused with 4% paraformaldehyde. The soleus and tibialis anterior were harvested for muscle analysis process including cryostat tissue sectioning and hematoxylin & eosin staining. The cross-sectional areas (CSA) of both hindlimb muscles were photographed and measured in the computer. Similar to the motor function, both SCI groups showed the significant decrease of CSA when compared to spinal-intact animals. The transection group showed significant further reduction of CSA when compared to contusion group. This further validates the correlation analyses between BBB score and muscle mass. These findings suggest the spared neural tissue after SCI contributing to the preservation of motor function and skeletal muscular mass due to the severity of SCI.

224 Bionanosensors for *in vivo* monitoring of cancer therapeutics

Freddy T. Nguyen

Massachusetts Institute of Technology, Cambridge, USA

Brain tumors are the most common form of pediatric solid tumors affecting ~20% of all pediatric cancers. Pediatric gliomas make up approximately 8-12% of pediatric central nervous system tumors. High grade gliomas are highly aggressive and malignant tumors with 5-year survival rates between 15 to 35%. Current management follows a multipronged approach that include surgery, radiation, and chemotherapy. Surgery is used for tumor debulking and followed by radiation and chemotherapy. Current chemotherapeutics include temozolomide, bevacizumab, lomustine, cyclophosphamide, and platinum complexes. There is a pressing need for a platform to provide precision chemotherapy screening to increase survival rates, reduce adverse effects, and lower overall costs. Current standard of care utilizes imaging to assess tumor response to therapeutic interventions and to monitor for cancer recurrence. Endogenous H_2O_2 and NO are involved in numerous signaling pathways that contribute to the initiation, progression, metastasis, and regression of cancer but its exact roles are not fully understood. Being able to measure in real-time and *in vivo*, the concentrations of NO and H_2O_2 during tumor initiation, progression, and regression will be crucial to better understand their dual roles in cancer metabolism and response to chemotherapeutics. We recently developed a series of nIR fluorescent probes for NO and H_2O_2 using single-walled carbon nanotubes (SWNT) that have been demonstrated *in vitro* with no evidence of photobleaching, and *in vivo* with no decrease in sensor performance or signs of inflammation over 400+ days. The nIR emission allows for deeper tissue penetration. We also present novel bionanosensors that have been developed for some of the major chemotherapeutic drugs in brain cancers (5-Amino-4-imidazolecarboxamide (AIC), an inactive byproduct of degradation of temozolomide; irinotecan; cisplatin; and lomustine). During degradation of 50 μ M TMZ, DNA-SWNT show a 50% fluorescence increase with no significant wavelength shift and most sensitive to concentrations between 5 and 500 μ M. Molecules similar in structure to AIC were also tested, showing no significant fluorescence signal change confirming the high specificity achieved using corona phase molecular recognition technique to design our SWNT based bionanosensors. The irinotecan bionanosensor showed a two-step mechanism, with strong initial fluorescence decrease followed by a significant red-shift. The bionanosensor for cisplatin and lomustine showed significant 20% fluorescence quenching responses. With this dynamic and real-time information, physicians and patients will be able to quickly know more about the local delivery and diffusion of chemotherapeutics in the complex heterogeneous tumor microenvironment and the tumor molecular response in a matter of

hours or days as opposed to the weeks or months currently needed to see measurable size changes on CT or MRI.

225 A novel role of phosphatidylinositol-5-phosphate, 4-kinases (PI5P4Ks) at the synapse and in excitotoxicity

Evan Noch

Weill Cornell Medicine, New York, USA

The phosphoinositide kinases, along with their corresponding phosphatases and phospholipases, regulate key functions of the phosphoinositide family of lipids in cells. These functions include proliferation and migration, metabolic adaptation to growth acceleration, and survival in the setting of genotoxic stress. The type 1 phosphatidylinositol-4-phosphate 5-kinases (PI4P5Ks), which catalyze the formation of PI-4,5- P_2 (PIP2), are critical to diverse cellular functions. Recently, the type 2 phosphatidylinositol 5-phosphate 4-kinases α and β (PI5P4K α and β), which catalyze the formation of PIP2 by phosphorylating the 4 position of phosphatidylinositol 5-phosphate (PI5P), have been shown to be upregulated in breast cancer and are essential for tumorigenesis in the absence of p53, possibly through the regulation of autophagy. Though the expression and function of these kinases have been explored in a host of human cancers, few studies have examined their role in the brain. In the brain, the majority of PIP2 is created through phosphorylation of PI4P by the type I PIP kinase gamma isoform. However, the potential role of the type II PIP kinases in synaptic PIP2 function and neurotransmission has not been explored. We first explored the expression patterns of PI5P4K α and PI5P4K β in normal mouse brain through immunohistochemistry and electron microscopy. We focused our work on mouse hippocampus given the potential involvement of the type II PIP kinases in oxidative stress and excitotoxicity as may pertain to a seizure model. We report that PI5P4K α and PI5P4K β are differentially expressed throughout mouse hippocampus. Using electron microscopy, we demonstrate expression of both isoforms in axon terminals and dendritic spines, indicating a potential novel role in PIP2 formation at the synapse. In addition, we find high levels of expression of both PI5P4K α and PI5P4K β in astrocytes, indicating a potential role for these kinases in glial function. To explore the functional impact of PIP4K2 expression in neurotransmission, we utilized a kainic acid model of excitotoxicity in mice. We show that mice deficient in PIP4K2B and with astrocyte-specific knockout of PIP4K2A exhibit delayed and less severe seizures than their wild-type counterparts. RNAseq analysis in whole brains from these GFAP-PIP4K2A-/-;PIP4K2B-/- animals demonstrates globally reduced synaptic and excitatory signaling, at least partly due to changes in endosomal trafficking pathways. This work explores the expression of the type II PIP kinases in the brain and may indicate a novel role in neurotransmission and in excitotoxicity. Further experiments will explore the mechanism of PIP4K2 involvement in neurotransmission and synaptic vesicle trafficking.

226 Vemurafenib inhibits ILEI by repressing its transcriptional activator Upstream Stimulatory Factor-1

Ken Noguchi

Medical University of South Carolina, Charleston, USA

Interleukin-like EMT Inducer (ILEI, FAM3C) is a secreted factor that contributes to the epithelial-to-mesenchymal transition (EMT), a cell biological process that confers metastatic properties to a tumor cell. We previously described the role of ILEI in melanoma phenotype switching. Herein, we describe the role of USF-1 as a transcriptional activator of ILEI. The BRAF inhibitor vemurafenib decreases ILEI protein and mRNA expression. ILEI promoter and 3'-UTR luciferase

reporter constructs were used to show that vemurafenib treatment reduces ILEI promoter activity, but not 3'-UTR activity. Successive 5' deletions on the ILEI promoter reporter highlighted a proximal E-box (CACGTG) 160 bp upstream of the transcriptional start site that contributes to vemurafenib-responsive ILEI promoter activity. The E-box binding transcription factor upstream stimulatory factor-1 (USF-1) binds to this E-box in a vemurafenib and sequence-dependent manner. Finally, we show that overexpression of USF-1 blocks the vemurafenib-mediated inhibition of ILEI expression. Mechanistically, vemurafenib inhibits ILEI expression by repressing its transcriptional activator USF-1.

227 Changes in Brain Leukocyte Populations Instigate Alterations in Cognitive and Sensorimotor Behaviors of Septic Male Mice

Divine Nwafor

West Virginia University, Morgantown, USA

Sepsis is a debilitating systemic inflammatory process that is often concomitant with an infectious etiology. Although much focus in sepsis has been on peripheral organ insults, cognitive decline and sepsis associated encephalopathy (SAE) appear to be important factors precipitating mortality in sepsis patients. In fact, many patients who survive sepsis are burdened with neuropsychiatric symptoms of memory loss, delirium, mood disorders and long term cognitive impairment. The mechanism through which sepsis exacerbates brain dysfunction is unclear. In this study, we looked at differences in immune cell populations of male mice subjected to a surgical cecal ligation and puncture (CLP), an experimental model of sepsis, versus their sham counterparts. We hypothesized that CLP mice would exhibit increased leukocyte extravasation across the blood-brain barrier (BBB) and show altered behavioral outcomes compared to controls. Following sepsis initiation, both CLP and sham mice were followed for 7 days. Sickness behavior in these mice was assessed with a murine modified sepsis severity scale (MMSS) derived from previous studies. The 7-day period was also accompanied with a series of behavioral assays to assess spatial learning and memory, cognition, depression, thermal nociception and locomotion. Perfused brains were harvested on Day 7 for isolation of leukocytes and quantification by flow cytometry. Immune cell populations of interest included: microglia (CD45^{lo}/CD11b⁺/CD11c^{+/-}), infiltrating monocyte (CD45^{high}/CD11b⁺/Ly6G⁻/Ly6C⁺), CNS macrophage (CD45^{low}/CD11b⁺/CD11c⁻), neutrophil (CD45^{hi}/Ly6G⁺), dendritic cells (CD45^{hi}/CD11b⁺/11c⁺), B cell (CD19⁺), cytotoxic T cells (CD45^{hi}/CD8⁺) and T helper cells (CD45^{hi}/CD4⁺) with emphasis on T regulatory cell populations (CD25⁺, Foxp3⁺). Taken together, we hope to elucidate a functional understanding of the immune system's role in neuroimmune responses and mechanisms that contribute to long term cognitive impairment in sepsis patients.

228 Neuronal IL-4R α and JAK1 signaling critically mediate chronic itch

Landon K. Oetjen

Washington University School of Medicine, St. Louis, USA

Rationale: Atopic dermatitis (AD) is a chronic inflammatory skin disorder with itch as its most debilitating symptom. Blockade of the type 2 cytokines IL-4 and IL-13 with dupilumab, an anti-IL-4R α antibody, has demonstrated unprecedented efficacy in treating AD including rapid improvements of itch. However, how disrupting type 2 cytokine signaling improves itch remains unknown. Given the remarkable effects of IL-4R α blockade on itch, we hypothesized that, in addition to their known proinflammatory functions, IL-4 and IL-13

directly stimulate sensory neurons to mediate chronic itch.

Methods: We investigated the contributions of neuronal IL-4 and IL-13 signaling to chronic itch using sensory neuron-specific genetic deletion of type 2 cytokine signaling components and pharmacologic blockade with JAK inhibitors in a mouse model of AD. We also performed observational studies to explore the anti-itch properties of JAK inhibitors in patients.

Results: We found that IL-4 and IL-13 directly activate itch-sensory neurons in mice. Strikingly, we observed that IL-4 also activates human sensory neurons, suggesting that neuronal type 2 cytokine signaling promotes itch across species. Using conditional deletion of IL-4R α from sensory neurons, we discovered that neuronal IL-4R α critically mediates AD-associated itch. Additionally, we found that type 2 cytokine responses in neurons were dependent on JAK1, and disruption of neuronal JAK1 signaling reduced chronic itch. Finally, in translational studies, we found that JAK inhibitors markedly improved itch symptoms in chronic itch patients.

Conclusions: The classical immune signaling molecules IL-4R α and JAK1 represent new targets within the sensory nervous system to treat itch in AD and other chronic itch disorders.

229 Reprogramming Pluripotent Stem Cells toward Totipotency

Sanders Oh

Northwestern University, Chicago, USA

Totipotent cells have the highest developmental potential and can only be created by nuclear transfer into oocytes. Identities of maternal factors that can induce this reprogramming remain a mystery. In this report, we demonstrate induction of totipotency on mouse embryonic stem cells by introducing six factors, Hist1h2aa, H3f3b, H1foo, p-Npm2, Zscan4d, and Ubtfl1. We observed dose-dependent increases in the MuERV-L endogenous retrovirus expression, typically seen in totipotent 2-cell stage blastomere, and adding p150 siRNA and trichostatin A further increased the expression. These cells, which we designated iTLCs (induced totipotent-like cells), had upregulation of totipotent genes but downregulation of pluripotent and differentiation genes, suggesting a distinct shift towards the totipotent state. Furthermore, iTLCs displayed unusually large nuclei, a characteristic of zygotic genome activation (ZGA). Also, iTLCs showed telomere lengthening and were able to be cultured in totipotent condition. Meanwhile, iTLCs did not show malignant transformations as indicated by normal karyotypes, inability to grow in nutrient-deprived condition, and sensitivity to contact inhibition. iTLCs demonstrated expanded cell fate potential by differentiating into all three distinct lineages of the pre-implantation embryo and expressed markers for both embryonic and extraembryonic lineages. RNAseq data showed remarkable similarities between iTLCs and totipotent cells. Early ZGA genes were strongly upregulated in iTLCs, indicating active totipotent state. When reprogrammed with factors only for an extended period, we observed cells resembling various stages of embryogenesis. These data suggest that pluripotent stem cells can be reprogrammed toward totipotent state without the need of oocytes and raise the tantalizing possibility of creating totipotent cells.

230 Type 2 Diabetes and Cardiometabolic Risk Associated with Increase in DNA Methylation of FKBP5

Robin Ortiz

Johns Hopkins University School of Medicine, Baltimore, USA

It has been hypothesized that early life stress may burden the hypothalamic-pituitary-adrenal (HPA) axis leading to associated epigenetics changes that may influence cardiometabolic, cancer, and neurodegenerative disease risk later in life. Subclinical hypercortisolism and HPA axis dysfunction are specifically associated with type 2 diabetes, cardiovascular disease, and metabolic dysfunction, however, further research in this area has been hindered by lack of a chronic total cortisol (glucocorticoid) exposure measure. Intronic epigenetic methylation of the gene for FK506 binding protein 51 kD (FKBP5), a co-chaperone of the glucocorticoid receptor, has been implicated as a potential indicator of chronic cortisol exposure. Our overall objective in this study was to determine the association of percent methylation of FKBP5 with glycosylated hemoglobin (HbA1c), low-density lipoprotein cholesterol (LDL), waist circumference, and body mass index (BMI), in a sample of 65 individuals with type 2 diabetes mellitus. The Johns Hopkins Institutional Review Board approved this study and the authors had no conflicts of interest. Data was collected during clinic visits using standardized demographics questionnaires and calibrated devices to measure participants' weight, waist circumference, height, and blood pressure. Blood samples were collected and analyzed by Johns Hopkins Clinical Core Laboratory for HbA1c and lipid panels and DNA was extracted from the blood and stored at -20°C. Two sets of bisulfite polymerase chain reaction (PCR) primers were designed to target each of two regions (flanking a glucocorticoid response element) in the second intron of the human FKBP5 gene. Percent DNA methylation at each of the targeted cytosine guanine dinucleotide sites (CpGs) was determined by bisulfite pyrosequencing. Analyses were conducted by multivariable linear regression including age, sex, and race as covariates. We observed that greater percent methylation of the FKBP5 intron 2 at one CpG dinucleotide region (CpG9) was significantly associated with higher HbA1c ($b=0.535$, $p=0.003$) and LDL ($b=0.344$, $p=0.037$) and a second CpG dinucleotide region (CpG7) was significantly associated with higher BMI and waist circumference ($b=0.516$, $p=0.001$; $b=0.403$, $p=0.006$, respectively). In a secondary analysis, it was observed that having a history of more invasive cardiovascular procedures was associated with greater percent methylation at CpG9 when adjusting for LDL ($b=0.344$, $p=0.033$). Greater percent methylation at CpG7 was inversely associated with more days a week completing more than 30 minutes of physical activity even when controlling for waist circumference ($b= -0.390$, $p=0.011$). In conclusion, FKBP5 methylation may be a marker of higher metabolic risk in type 2 diabetes, possibly secondary to higher exposure to cortisol. Further work should aim to assess the longitudinal association of FKBP5 with cardiovascular disease and glycemic outcomes in type 2 diabetes as a first step in understanding potential preventive and treatment related interventions targeting the HPA axis.

231 Nanomechanics of a tip-link protein from the cochlea

Aaron B. Oswald

Weill Cornell Medical College, USA

Sound transduction occurs in cochlear hair cells when deflection of hair bundles opens mechanically sensitive ion channels. Each hair bundle comprises 100-200 stiff, cylindrical projections called stereocilia, whose distal ends are connected by tip links, filamentous biopolymers consisting of dimers of protocadherin 15 (PCDH15) and cadherin 23 (CDH23). Numerous pathogenic mutations affecting both proteins are associated with Usher Syndrome and nonsyndromic deafness in humans. The sensitivity and dynamic range of mammalian hearing require a certain amount of elasticity in a hypothetical mechanical element, the "gating spring," that transmits tension to the transduction channels. Although tip links are candidates to be gating springs, molecular-dynamics simulations of fragments of PCDH15 and CDH23 suggest that tip links are far too stiff for this purpose. Even though the mechanical properties of full-length tip-link proteins and their dimers remain unknown, other structures are therefore believed to dominate gating-spring elasticity.

We hypothesize that the mechanical properties of tip links play a key role in the elasticity of gating springs, and that some of the pathogenic mutations in tip-link proteins perturb tip-link elasticity. To test these hypotheses, we characterize the mechanics of individual PCDH15 molecules by confining the proteins between a glass substrate and a polystyrene bead 1 μm in diameter. By holding the bead in an optical trap, we subject the protein to tensions as great as 40 pN. Tethered by PCDH15, the bead explores a range of positions in response to thermal forces. After measuring the position of the bead over time, we use the position distribution to infer the force-extension relation and energy landscape of PCDH15. Measurements at a Ca^{2+} concentration typical of cochlear endolymph demonstrate the unfolding of individual cadherin domains under physiologically relevant forces. By acting as an entropic spring, the resulting unstructured peptide chain displays a greatly reduced stiffness. When loud sounds put hair cells at risk of damage, tip-link elongation and the ensuing reduction in stiffness might offer physiological protection against acoustic trauma.

232 Measles pseudotyped vectors for improved gene delivery to hematopoietic stem cells

Stosh Ozog

The Scripps Research Institute, La Jolla, USA

Pseudotyping lentiviral vectors (LVs) with alternate viral envelopes significantly widens the range of targetable cell types for transduction. Vesicular stomatitis virus glycoprotein (VSV-G) pseudotyped LVs are the standard for human hematopoietic stem and progenitor cells (HSPCs) gene delivery. However, VSV-G pseudotyped LVs inefficiently transduce long-term repopulating stem cells. Our group has proposed that this low efficiency is due to a block in pH-triggered vector escape from the endosome and that vectors with alternate entry mechanisms may be able to avoid this block.

LVs pseudotyped with the Edmonston vaccine strain measles virus hemagglutinin (H) and fusion (F) glycoproteins have shown enhanced ability to transduce resting lymphocytes and monocyte-derived dendritic cells. Edmonston strain hemagglutinin recognizes the ubiquitously expressed CD46 protein, unlike wild-type virus strains that utilize CD150 or Nectin-4.

Herein, we show that H/F LVs have up to 3-fold enhanced capability to transduce HSPCs as compared to VSV-G LVs at an equivalent multiplicity of infection (MOI) (mean %EGFP =10% vs. 35%

respectively at MOI 1). This improved efficiency may arise from the use of an alternate, pH-independent entry mechanism, as VSV-G enhancing small molecules such as rapamycin and PGE2 did not improve H/F LV transduction.

However, low titers during vector production limit widespread H/F LV applicability. We show that CD46 expression on H/F transfected HEK 293T cells is sufficient to induce adjacent cell membrane fusion, resulting in multinucleate syncytia and cell death prior to peak vector production in cell supernatant.

Consequently, we pursued the CRISPR/Cas9 mediated knockout of CD46 in HEK 293T cells (CD46 KO). H/F LVs produced in CD46 KO cells produced 2-fold higher titer vector compared to H/F LVs produced in wild type HEK 293Ts. CD46 KO HEK 293Ts also demonstrated no syncytia formation and continued cell viability throughout vector production.

When matched for MOI, H/F LVs generated in CD46 KO cells resulted in approximately 2-fold higher transduction in HSPCs, compared to vector produced in wild type HEK 293Ts (mean %EGFP =29% vs. 62% respectively at MOI 1). Confocal microscopy analysis of HSPCs transduced with H/F LV showed improved vector loading compared to VSV-G LV, with limited colocalization to early endosomal antigen-1 (EEA1) positive vesicles, further indicating an alternate entry mechanism.

Since vector production and quality are major sources of cost and variability in clinical trials of gene therapy, we reason that the use of CD46 KO packaging cells may lower the cost and improve the efficiency of generating H/F LVs.

233 Senescent cell clearance in diet-induced obese mice decreases adipose tissue macrophage burden

Allyson Palmer

Mayo Clinic College of Medicine, Rochester, USA

Background. Senescent cells accumulate in adipose tissue of obese mice and humans and may contribute to the development of insulin resistance. Obesity is also associated with accumulation of immune cells, including macrophages and activated CD4+ lymphocytes, in adipose tissue, however the priming stimulus for this immune cell infiltration remains elusive. It remains unclear what effect senescent cells have on macrophage burden in adipose tissue, or what impact strategies to target senescent cells have on adipose tissue macrophage infiltration in obesity. **Objectives.** We aimed to: 1) investigate the relationship between senescent cell burden and adipose tissue macrophages, 2) determine the impact of senescent cell clearance on adipose tissue macrophage burden, and 3) elucidate the role of senescent cells in macrophage infiltration into adipose tissue. **Methods.** For these studies, we used two genetic mouse models in which p16-positive senescent cells can be eliminated: p16-3MR mice, in which a p16Ink4a-promoter sequence drives expression of a trimodal reporter-killer fusion protein, allowing senescent cell killing by ganciclovir, and INK-ATTAC mice, in which a p16Ink4a-promoter sequence drives expression of a vFKBpcaspase-8-FLAG fusion protein that can be activated by AP20187, a vFKBP dimerizer, to cause senescent cell apoptosis. Obesity was induced either by diet or genetically using leptin receptor knockout (db/db) mice. **Results and Conclusions.** F4/80+ macrophage abundance positively correlated with senescent cell burden as measured by transgene expression in diet-induced obese mice. Following senescent cell clearance with ganciclovir from obese p16-3MR mice, expression of the macrophage marker F4/80 in intra-abdominal adipose tissue (IAT) was reduced and crown-like structures were

decreased. Eliminating senescent cells also reduced plasma levels of the macrophage-attracting chemokines MCP-1 and MIP-1 β as well as macrophage colony stimulating factor (M-CSF). By CyTOF, p16Ink4a+ preadipocytes were decreased in DIO-INKATTAC mice 4 days after AP20187 treatment, while macrophages had not yet decreased. In addition, monocytes from donor mice injected into obese INK-ATTAC;db/db mice 4 days after AP20187 treatment exhibited decreased migration into IAT compared to vehicle-treated INKATTAC;db/db mice. Taken together, our results indicate that senescent cells can cause macrophage migration into adipose tissue in obesity, and targeting senescent cells prevents and reduces the adipose tissue macrophage infiltration characteristic of obesity. **Support:** This work was supported by NIH grants AG13925 (J.L.K.), AG041122 (J.L.K.), AG31736 (Project 4: J.L.K.), AG044396 (J.L.K.), AG46061 (A.K.P.), the Connor Group (J.L.K.), the Glenn (J.L.K.), Ted Nash Long Life (J.L.K.), and Noaber Foundations (J.L.K.).

234 A FACS-based CRISPR screen for host determinants of Chlamydia trachomatis invasion reveals the multiple roles of COPI during infection

Joseph S. Park

Harvard Medical School, USA

Chlamydia trachomatis, an obligate intracellular bacterium, is a major cause of human genital and ocular infections worldwide. The pathogen is not easily genetically tractable and the advent of CRISPR editing in human cells enables a new approach for investigating how this pathogen interacts with host. Using a fluorescence-activation cell sorting (FACS) approach, we undertook an unbiased genome-wide screen in a CRISPR-edited genome-wide library of HT29 human epithelial cells that were infected with fluorescently labelled *C. trachomatis*. Enrichment of mutants that were resistant to invasion and deep sequencing of their sgRNAs led to identification of multiple hits in the COPI vesicular trafficking pathway. In siRNA-transfected or temperature-sensitive mammalian cell lines, COPI depletion led to a significant reduction in bacterial attachment. This was caused by a decrease in cell surface heparan sulfate, the receptor for *C. trachomatis* binding. Acute inactivation of COPI trafficking via golgicide A treatment, which spared heparan sulfate, unmasked a defect in pathogen Type III secretion and consequent internalization. Furthermore, internalized bacteria were closely associated with COPI-labelled structures in microscopy. Together, these findings reveal the diverse roles of COPI during the early steps of *C. trachomatis* invasion into host cells and demonstrate the utility of FACS-based CRISPR screening in studying the mechanisms of entry of intracellular pathogens.

235 Mayaro viral replication kinetics and *in vitro* cytopathogenicity in human dermal fibroblast

Aum Patel

University of Florida, Gainesville, USA

Mayaro virus (genus *Alphavirus*, family *Togaviridae*) is an emerging arthropod-borne virus transmitted by *Haemagogus* mosquitoes in sylvatic regions of Central and South America. Similar to chikungunya virus, Mayaro virus (MAYV) infection leads to fevers, maculopapular rash and arthralgia. Many aspects of its transmission and pathogenicity remain unknown in human cells. Since the virus is injected into the skin by mosquitoes, cells residing in the skin are of particular interest in understanding early infection and antiviral immune responses. Here, we examine viral replication kinetics and cytopathogenicity of MAYV in human dermal fibroblasts, as well as humoral immune responses. Intracellular MAYV infection was visualized by immunofluorescence microscopy, and further

quantified by flow cytometry. IF staining revealed that 74% of cells stained positive for intracellular antigen at 24 hours, and 88% staining positive at 72 hours using an MOI of 1. By flow cytometry, 49% of cells stained positive for viral antigen at 20 hours post infection at MOI of 0.1. Upon viral infection of fibroblasts, virus replication was assessed every 6 hours for 72 hours, and extracellular viral titers were quantified by plaque assay in Vero cells. These assays demonstrated that peak levels of extracellular virus release occurred at 20 hours with a multiplicity of infection (MOI) of 1, at which time titers reached 3.7×10^6 pfu/ml. Cytopathic effect (CPE) in fibroblasts was observed at varying time points (0 to 72 hours post infection). CPE was clearly observable with crystal violet staining, resulting in 78% reduction in adhered cells at 72 hours (MOI=1). Using fibroblasts as target cells, we then conducted antibody-dependent cell cytotoxicity assays with MAYV positive human sera. This assay revealed no clear trends compared to media controls. Taken together, these findings advance our understanding of initial Mayaro viral infection in a critical cell type, the human dermal fibroblast.

236 Investigating role of anti-tau antibodies in blocking tau seeding and spreading in vitro and in vivo

Tirth Patel

Washington University School of Medicine, St. Louis, USA

Alzheimer's disease is characterized by two main neuropathological hallmarks: extracellular plaques of amyloid-beta protein and largely intracellular tangles of tau protein. The microtubule associated protein tau is soluble protein, predominantly expressed in axons. It is thought to play a role in axonal trafficking by binding and stabilizing microtubules. Under normal physiological conditions tau is a soluble monomer that is released in the interstitial space by neurons. In diseased state tau loses this solubility, detaches from microtubules, migrates to the somatodendritic compartment and forms insoluble aggregates. Aside from its role in AD, tau is also involved in several other neurodegenerative disorders collectively called tauopathies, such as progressive supranuclearpalsy (PSP), corticobasal degeneration (CBD), frontotemporal dementia, and argyrophilic gran disease (AGD). Recent work in the field seems to suggest that after an initial trigger event, tau pathology spreads to different regions of the brain in a stereotypical pattern, much like a prion protein would. Under this 'prion hypothesis' after an initial trigger, misfolded forms of tau spread through different brain regions by seeding previously normal forms causing them to misfold as well.

Since propagation of tau appears to be critical to pathogenesis of tauopathies, tau spreading is an attractive therapeutic target. Previous work in the lab has shown that treatment with anti-tau antibodies is effective at reducing tau pathology, improving brain atrophy and behavior in the P301S tau transgenic mouse model. It remains to be seen if specifically blocking spread of tau prior to onset and establishment of pathology can also work as a viable therapeutic approach.

Here we describe: 1) Development of an inducible spread model, a young P301S animal where the only pathology present is due to spread of tau, 2) Efficacy of various anti-tau antibodies at blocking seeding in vitro (using the well-established FRET based seeding assay), and 3) Preliminary results investigating effectiveness of these antibodies in blocking tau spreading in vivo.

237 Myocardin related transcription factor (MRTF) constitutively active and dominant negative line analysis

Praveen Paudel

University of New Mexico, Albuquerque, USA

MRTFs, a family of conserved transcriptional co-activators, are expressed in cardiac and smooth muscles where they regulate cell differentiation via transactivation of differentiation marker genes. As important mediators in muscle differentiation, MRTFs have been implicated in fruit fly (*Drosophila melanogaster*) flight muscle development, and appear to have an essential role in early muscle cell progenitor development. However, the mechanism through which MRTF is regulating muscle development is not yet understood. Therefore, I have obtained and characterized the phenotypes of transgenic *Drosophila* lines that cause MRTF to be always "on" (constitutively active) or always "off" (dominant negative). I used the UAS-Gal4 system to overexpress these transgenes specifically in adult muscle progenitor cells through a 1151-Gal4 driver. The functional flight test showed that the transgenic flies have a weaker flight. Moreover, I cryosectioned and fluorescent immunostained these flies, and analyzed the specific muscle disruptions through confocal imaging. The dominant negative MRTF appears to transform indirect flight muscles, a fibrillar muscle, to a structure more similar to the jump muscle, a tubular muscle type. Similar to *Drosophila*, the vertebrate muscle system comprises several types of muscle fibers, indicating that MRTF may have an important conserved role in muscle fiber differentiation not only in *Drosophila*, but also in vertebrates. Therefore, this project leads to a better understanding of the role of MRTF in early muscle development.

238 Matters of Mucus: Mucociliary Physiology in a Bleomycin-Induced Pulmonary Fibrosis Ferret

Jacelyn Peabody

University of Alabama at Birmingham, Birmingham, USA

Introduction: Idiopathic pulmonary fibrosis (IPF) is a progressive fibrotic lung disease with median-survival ranging from 3-5 years after diagnosis. The greatest risk factor for developing IPF is a gain-of-function promoter variant in the mucin *MUC5B*; however, the role of *MUC5B* in IPF pathogenesis is unknown. Unlike rodent IPF models, ferrets airways contain submucosal glands, the major source of *MUC5B* in humans. We are developing a novel bleomycin-induced pulmonary fibrosis ferret model to evaluate the hypothesis that mucociliary physiology may alter pro-fibrotic mechanisms.

Methods: A single-dose of bleomycin-sulfate solution (2.5-5U/kg) or saline-vehicle was administered intratracheally via microaerosolization to normal ferrets. Fibrosis was assessed with μ CT scans, histology, and second harmonic imaging. Functional microanatomy of the airway epithelium including airway surface morphology, ciliary beating (CBF), and mucociliary transport (MCT) were assessed *ex-vivo* using micro-optical coherence tomography (μ OCT). *Muc5B* expression was assessed with immunohistochemistry.

Results: All ferrets (N=16) survived to euthanasia at 3 or 6 weeks post-bleomycin administration. μ CT scans demonstrated evidence of patchy airway-centric and peripheral ground glass opacities that was worse in the dependent lung, evident at 2 weeks, and persistent through 6 weeks. Threshold-based volumetric μ CT analysis revealed that bleomycin-treated lungs showed 38.2% fibrosis and a significant increase from baseline compared to controls (mean increase $18.1 \pm 2.2\%$ bleomycin compared to $-0.8 \pm 0.8\%$ control, $P < 0.001$). Histopathological analysis revealed airway centric inflammatory infiltrates, patchy severe interstitial fibrosis with cystic remodeling and

epithelialization, airway remodeling, diffuse alveolar damage, type II pneumocyte hyperplasia, and pleural thickening. Second harmonic imaging revealed dose-dependent fibrosis with 3.35 ± 0.1 and 5.41 ± 0.57 mean intensity for 2.5U/kg and 5U/kg bleomycin ferrets, respectively ($P < 0.05$). Masson's trichrome staining revealed distinct regions of fibroblasts and collagen matrix, resembling fibroblastic foci observed in humans. Proximal and distal airways had goblet cell hyperplasia with increased Muc5b staining. Immunohistochemistry for Muc5b was also observed in cystic areas of metaplastic epithelialization. Evaluation of mucociliary transport by μ OCT (N=4/group) following carbachol stimulation showed decreased MCT in bleomycin-treated main-stem bronchi (0.2 ± 0.1 mm/min) compared to controls (3.4 ± 2.0 mm/min, $P = 0.10$). Bleomycin treated ferrets also had reduced CBF in the main-stem bronchi (8.8 ± 0.3 Hz, $P = 0.057$) prior to carbachol compared to controls (10.7 ± 0.6 Hz, respectively).

Conclusions: Bleomycin treatment induced pulmonary fibrosis in ferrets, with inflammation, fibrotic lesions, and remodeling changes analogous to IPF in humans. Contemporaneous analysis of fibrosis development and the mucociliary transport apparatus suggests a strong relationship and indicates that the altered airway surface microenvironment may affect the pathogenesis of fibrosis.

239 Canonical Wnt-associated extracellular matrix in adrenocortical carcinoma

Morgan Penny

University of Michigan and Sidney Kimmel Medical College, Whitehall, USA

Adrenocortical carcinoma (ACC) is a rare and often aggressive cancer that affects 1-2 people per million in the United States annually. Genomic alterations activating canonical Wnt signaling occur in approximately 40% of ACCs and are associated with poor prognosis. However, the biological consequences of constitutive canonical Wnt activation in ACC are poorly understood. To better characterize the transcriptional programs that are engaged in ACC, we performed independent component analysis on The Cancer Genome Atlas ACC transcriptome dataset to identify components of coordinately expressed genes. One of the components identified was significantly enriched for Wnt signaling ($p = 0.001$) and was strongly associated with somatic *CTNNB1* (β -catenin) mutations ($p = 2.276 \times 10^{-7}$). Interestingly, this Wnt-enriched component also showed enrichment for extracellular matrix (ECM)-receptor interaction ($p = 0.00139$), including (but not restricted to) expression of *COL11A1*, *LAMC3*, and *ITGA2*, suggesting that Wnt signaling is regulating cell-ECM interactions and ECM composition in ACC. To follow up on this observation, we performed immunohistochemical staining on tissue microarrays (TMAs) containing 104 ACC samples. We observed a strong correlation of *COL11A1* expression in ACCs with nuclear β -catenin localization ($p = 0.0088$), suggesting *COL11A1* expression may be regulated by canonical Wnt signaling. To determine whether ECM and ECM-receptor genes are regulated by canonical Wnt activity, the H295R human ACC cell line, harboring an activating *CTNNB1* mutation, was used. Cells were treated with PKF115-584, an inhibitor of canonical Wnt signaling that disrupts β -catenin interaction with TCF/LEF transcription factors. PKF115-584 treatment significantly reduced expression of *COL11A1*, *LAMC3*, and *ITGA2* in H295R cells ($p < 0.05$), consistent with our hypothesis that canonical Wnt signaling regulates expression of ECM components in ACC. Following PKF115-584 treatment, H295R cell viability decreased, indicating that canonical Wnt activity may regulate cell survival in ACC. Taken together, these results suggest that canonical Wnt activity in ACC contributes to expression of ECM proteins that

promote cancer cell survival. Future studies will employ genetic approaches to manipulate canonical Wnt signaling, investigating the effect of canonical Wnt activity on the ACC cell transcriptome, and characterizing the contribution of extracellular proteins to ACC phenotypes.

240 Chromatin folding with DFRAC

Alan Perez-Rathke

University of Illinois at Chicago, Chicago, USA

Deciphering the detailed mechanisms governing gene regulation often requires 3-D reconstruction of the chromatin fold. Chromosome conformation capture techniques such as Hi-C provide insight into the chromatin folding state but only give averaged spatial information in the form of 2-D contact heat maps. Using these techniques alone, it is not possible to answer questions such as: the existence of functional cellular sub-populations, the contact probabilities among multiple (> 2) interacting loci, the causal folding relationships among the spatially interacting genomic regions, or the identification of driver interactions governing the folding state. We present DFRAC (Dirichlet FRActal ChromaTin), a Bayesian method utilizing models of physical chromatin folding to offer probabilistic answers to these questions. We demonstrate our method on a TAD locus within the K562 Hi-C data set of Rao et al.

241 Functional analysis of human cardiac sarcomere missense mutations

Anthony M. Pettinato

UConn Health and The Jackson Laboratory for Genomic Medicine, New Britain, USA

Cardiomyopathies are diseases of the myocardium that produce abnormal cardiac structure and function. The two major forms are dilated cardiomyopathy (DCM) and hypertrophic cardiomyopathy (HCM), which have estimated prevalences of 1:250 and 1:500, respectively. Both DCM and HCM have a strong genetic basis and are significant causes of sudden cardiac death (SCD) and heart failure (HF), a condition that affects 5 million people in the U.S. and has a 5-year mortality of 50% (similar to cancer). Missense mutations in thick (*MYH7* and *MYBPC3*) and thin (*TNNT2*) myofilaments are common genetic causes of HCM and DCM, but genetic heterogeneity, variants-of-unknown-significance (VUS), and small sample sizes make it difficult to predict pathogenicity and assess risk of HF and SCD. Our objective is to understand the functional meaning and pathogenicity of all missense mutations in the sarcomere by using lentivirus to deliver missense variants to knockout human iPS-derived cardiomyocytes (iPS-CMs), which will then be analyzed in our cardiac power and energy utilization assays.

As proof of feasibility of our approach, we are first focusing on *MYH7*, which encodes myosin heavy chain beta (MHC- β), the molecular motor of human cardiac muscle. Missense mutations in *MYH7* account for one-third of HCM mutations and are also associated with DCM. We generated a homozygous *MYH7* knockout iPSC line (*MYH7*^{-/-}) using CRISPR/Cas9 to introduce a deletion that leads to nonsense-mediated mRNA decay of *MYH7* transcripts. Following confirmation that *MYH7*^{-/-} iPSC-CMs express no MHC- β , we generated cardiac tissues from *MYH7*^{-/-} iPSC-CMs and wildtype (*MYH7*^{+/+}) controls to determine impact on force generation. In parallel to dramatic reductions in sarcomere content, *MYH7*^{-/-} cardiac tissues generate negligible force, confirming that *MYH7* is necessary for normal sarcomere structure and function. Towards reestablishing sarcomere content and function in a scalable method, we delivered wildtype *MYH7* via lentiviral vector into *MYH7*^{-/-} iPSC-CMs. This

method restored sarcomere structure and power in *MYH7*^{-/-} iPSC-CMs, as cardiac tissues generated from these *MYH7* transgene (*MYH7*^{tg}) iPSC-CMs generated normal force, indistinguishable from cardiac tissues generated from *MYH7*^{+/+} iPSC-CMs. We will further characterize our model using molecular signatures, such as B-type natriuretic peptide (*NPPB*; induced by mechanical strain), telethonin (*TCAP*; marker of sarcomere assembly), and mitochondrial content, which we will use to define wildtype and gold standard HCM/DCM mutations, with the subsequent aim of extending this approach to screen all missense variants.

While *MYH7* serves as proof of concept, we will extend our efforts to test all sarcomere genes that can be delivered by lentivirus and contain missense variants, such as cardiac myosin light chains, tropomyosin, and troponin, with knockout iPSC lines currently in development.

242 Low fat diet alters the microbiome and improves quality of life in patients with ulcerative colitis: results of a pilot, cross-over design study

Matthew C. Phillips
University of Miami, Miami, USA

A diet high in animal meat and fat has been linked to an increased risk for ulcerative colitis (UC) and high meat intake increases the likelihood of UC flares. Despite these correlations, there has never been a controlled, prospective study to investigate the contribution of dietary fat to inflammation and the quality of life in patients with UC. In this pilot, cross-over design study, patients with UC were randomized and given two, 4 week, isocaloric dietary interventions with a 2 week wash out between diets: a low fat diet (LFD), containing 10% total calories from fat, and a standard American diet (SAD), containing 35-40% total calories from fat. Patients were provided daily, catered food to ensure standardization of the diets. Patients had to be in remission or only mildly active and have had a flare within the past 18 months. To assess improvement in quality of life (QoL), patients completed the Inflammatory Bowel Disease Questionnaire (IBDQ) before and after each diet. Biochemical markers of inflammation were measured in the stool and serum and stool was collected for microbiome analysis. Eight patients completed both dietary interventions. Patients experienced a significant increase ($p=0.01$) in their QoL, as measured by the IBDQ, while on the LFD as compared to the SAD. Results were consistent regardless of the initial diet. Patients on LFD had significant changes in the composition of their microbiome including a significant increase in the relative abundance of Bacteroidetes ($p>0.05$). Changes in the microbiome also correlated with patient's IBDQ and with serum levels of CRP, IL-6, and IL-1b. Our data indicate that a LFD improves the QoL of patients with quiescent or mild UC and this improvement is correlated with changes in the microbiome. The LFD also increased the abundance of bacteria traditionally associated with a healthy microbiome. This simple dietary intervention would provide clinicians an informed recommendations to improve the QoL their patients.

243 Delineating the mechanisms underlying oncogenic transcription in ALKF1174L/MYCN neuroblastoma

Monica M. Pomaville
Dana-Farber Cancer Institute, USA

Neuroblastoma, a malignancy of the developing sympathetic nervous system, is the most common extracranial solid tumor in children and has a survival rate of <50% in high-risk patients. One of the most influential determinants of poor prognosis in children with neuroblastoma is amplification of the transcription factor MYCN, found

in approximately 20% of tumors. Because small-molecule inhibition of MYCN has not been clinically achieved, recent investigations have focused on the identification of critical targets that modulate MYCN. In a disease with few recurrent somatic mutations, a gain-of-function mutation, a phenylalanine to leucine substitution at codon 1174, exists in a gene encoding the cell surface receptor tyrosine kinase ALK. Interestingly, the ALKF1174L mutant is preferentially associated with MYCN amplification and accounts for a subset of patients with a particularly poor clinical outcome. In vivo studies have shown that concomitant expression of MYCN and ALKF1174L in neural crest cells leads to development of neuroblastoma with earlier onset, higher penetrance, and enhanced lethality compared to tumors in mice with isolated MYCN amplification. Mice bearing tumors with MYCN amplification and ALKF1174L show a distinct transcriptional profile compared to those with isolated MYCN amplification, suggesting a positive cooperative effect between the two. However, we do not have a clear understanding of the contribution of ALKF1174L in altering gene expression.

The goal of this study is to understand the mechanism(s) underlying the ability of ALKF1174L to affect oncogenic transcription of MYCN. To investigate this, I performed shRNA-mediated knockdown of ALK in cell lines expressing ALKF1174L or wild-type (WT) ALK together with and without amplified MYCN. Depletion of oncogenic ALKF1174L resulted in a decrease in MYCN protein levels, while knockdown of WT ALK showed no discernible change in MYCN protein expression, supporting a role for the mutant receptor but not its WT counterpart, in regulating the expression of oncogenic MYCN. By examining the genome-wide changes caused by inducible overexpression and deletion of ALKF1174L in isogenic cell line pairs with and without MYCN amplification, we hope to better characterize this oncogenic relationship and potentially identify therapeutically targetable nodes in high-risk neuroblastoma.

244 Histological Analysis of the Effects of Pulsed Focused Ultrasound in the Brain

Farhan M. Qureshi
University of Miami, Miami, USA

MRI-guided pulsed Focused Ultrasound (pFUS) is a non-invasive, non-destructive therapy with numerous applications. We have previously shown that pFUS coupled with intravenous microbubbles (MB) is an effective method of transiently disrupting the blood brain barrier (BBB). In the current study, we use histological analysis to visualize and quantify the effects of pFUS in the brain.

Female Sprague-Dawley rats ($n = 9$) were treated with pFUS at 9 focal points in the anterior portion of the left hemisphere of the brain. A pFUS transducer was used to apply 0.3 MPa acoustic pressure in 10 ms bursts. 200 μ l of Optison™ MB were administered intravenously 30 seconds pre-treatment. Gd-enhanced T1-weighted images were obtained with a 3.0 T MRI for pre-treatment planning, and to assess successful BBB opening post-treatment.

Brains were collected and fixed with 4% paraformaldehyde at 1, 6, and 24 hours post treatment, and either embedded in paraffin or frozen blocks for IHC. 10 μ m slices were collected from the anterior portion of the brain and analyzed using IHC.

Quantitation of GFAP stain shows significant astrocytosis at 6 and 24hrs post treatment. Iba1 stain showed significant microgliosis at 1 and 6hrs. Expression of ICAM in the treated area increased linearly with time, and a significant increase is seen at 6 and 24hrs. The opposite held true for apoptotic cells seen through TUNEL staining; the number of apoptotic cells decreased with time, having significant

differences at 1 and 6hrs post pFUS treatment. The presence of astrocytosis and microgliosis along with increased apoptosis indicate that pFUS may cause inflammatory responses similar to those seen in ischemia and traumatic brain injury. Further studies of the long-term implications of these results must be done in order to differentiate between the acute and chronic effects of pFUS and MB in the brain.

247 Inflammatory Ly6Chigh monocytes and their conversion to M2 macrophages drive atherosclerosis regression in mice

Karishma Rahman

NYU School of Medicine, New York, USA

Progressing atherosclerotic plaques are characterized by inflammatory M1 macrophages (M ϕ). We have shown that reversal of dyslipidemia induces plaque regression characterized by significant M ϕ loss and anti-inflammatory (M2) M ϕ enrichment. To now determine the origin of these M2 M ϕ s, aortic arches from hyperlipidemic Apolipoprotein E (Apoe) $-/-$ mice (baseline) were transplanted into normolipidemic C-C chemokine receptor type 2 (Ccr2) $-/-$ (receptor for Ly6chigh M ϕ recruitment), Ccr5 $-/-$ (receptor for Ly6clow M ϕ recruitment), Wild type (WT) (control regression) and Apoe $-/-$ (progression) mice. Plaques from WT and Ccr5 $-/-$ recipient mice had approximately a 50% reduction in total Cluster of Differentiation 68 (CD68)+ M ϕ area and a greater than 4-fold increase in M2 M ϕ (Arginase-1 or Mannose Receptor+) area ($p < 0.001$) compared to corresponding results in baseline and progression groups. In contrast, plaques from Ccr2 $-/-$ mice had minimal changes in total M ϕ or M2 M ϕ area compared to baseline and progression groups. To confirm that the CCR2 deficiency affected circulating monocyte recruitment, we transplanted arches from hyperlipidemic Apoe $-/-$ CD45.1 mice into recipient WT, Ccr2 $-/-$, or Ccr5 $-/-$ mice on CD45.2 backgrounds. Plaques from WT and Ccr5 $-/-$ mice had 2-fold more CD45.2+ recipient cells as % total CD45+ cells compared to Ccr2 $-/-$ mice ($p < 0.05$). Furthermore, in WT recipient mice, approximately 80% of Mannose Receptor+ (M2) M ϕ s were CD45.2+. To determine whether these newly recruited monocyte-derived M2 M ϕ s are required for regression and whether their polarization is regulated by the M2 canonical signal transducer and activator of transcription 6 (STAT6) signaling pathway, arches from hyperlipidemic Apoe $-/-$ mice were transplanted into normolipidemic Stat6 $-/-$ mice, which showed no significant reduction in total M ϕ or M2 M ϕ area compared to the progression group despite similar levels of monocyte recruitment as WT mice. Collectively, our studies indicate that recruitment of inflammation-prone Ly6chigh monocytes into plaques and their differentiation into M2 M ϕ via the STAT6 pathway drive atherosclerosis regression in mice.

248 ONC201 and its analogues sensitize breast cancer cells to tumor necrosis factor-related apoptosis-inducing ligand through death receptor 5 upregulation

Marie D. Ralff

Lewis Katz School of Medicine at Temple University, Philadelphia, USA

ONC201 is a potent inducer of cancer cell death through the tumor necrosis factor related apoptosis inducing ligand (TRAIL) pathway. The compound is being tested clinically against a range of solid tumors and hematological malignancies. ONC201 and its structural analogs comprise a novel class known as the imipridones. We found that both triple negative and non-triple negative breast cancer cells are sensitive to ONC201. This was initially surprising, as the majority of breast cancer cells are resistant to TRAIL. In TRAIL-sensitive cells, ONC201 induced cell death in a TRAIL-dependent

manner. In TRAIL-resistant cells, the effects of ONC201 are not pro-apoptotic but are rather anti-proliferative. Here we further investigate the effects of ONC201 and its more potent analogues in TRAIL-resistant breast cancers. ONC201 has been previously shown to induce transcriptional upregulation of TRAIL receptor death receptor 5 (DR5). A known mechanism of TRAIL resistance in breast cancer is low cell surface DR5 expression. We hypothesized that pre-treatment with ONC201 would upregulate DR5 and lead to TRAIL sensitization in resistant cells. Our results show that ONC201, ONC212, and ONC213 treatment upregulates DR5 and sensitizes TRAIL-resistant breast cancer cells to the pro-apoptotic effects of TRAIL. Caspase-8 and PARP are cleaved when cells are treated with the combination of imipridone and TRAIL, but not when treated with either compound alone. Annexin-V PI staining and quantitation of subG₁ DNA content via flow cytometry further confirmed these results. Knockdown of DR5 abrogated TRAIL sensitization by imipridone compounds. Natural killer (NK) cells are known to use TRAIL to kill targets like tumor cells. We hypothesized that pre-treatment of tumor cells with imipridone compounds would increase their killing by NK cells, and this was demonstrated experimentally. We are currently investigating the importance of the TRAIL pathway and DR5 upregulation by imipridone compounds in this sensitization to NK cell induced apoptosis. These results describe a novel mechanism by which imipridone compounds sensitize breast cancer cells to the effects of apoptosis inducing ligand TRAIL. They also provide preclinical rationale for the testing of imipridones against breast cancers in the clinic.

Conflicts Wafik El-Deiry, MD/PhD is a founder and shareholder in Oncoceutics, Inc. This is the company developing the imipridone compounds clinically.

249 Small molecule allosteric modulators of the β 2-adrenergic receptor

Paula K. Rambarat

Duke University, USA

The β -adrenergic receptors (β AR) are a subfamily of G-protein coupled receptors (GPCR) implicated in the pathophysiology of cardiovascular and pulmonary diseases. Drugs that bind to the highly conserved, orthosteric hormone binding site of the β ARs are a mainstay of treatment for conditions like asthma and heart failure. However, the use of such orthosteric drugs is often limited by off-target side effects. For instance, antagonists for the cardiac-predominant β 1AR are often contraindicated in patients with asthma, as binding to β 2ARs in the lung causes undesirable bronchoconstriction. Likewise, the use of β 2AR agonists in asthma is limited by adverse effects like tachycardia. Targeting allosteric sites, which are topographically and evolutionarily distinct from the orthosteric one, has potential to yield more highly specific, efficacious medications. Allosteric drugs exert their effects by modulating the activity of orthosteric ligands. Negative allosteric modulators (NAMs) diminish the activity of orthosteric agonists, whereas positive allosteric modulators (PAMs) enhance agonist function.

Here, we present our isolation and characterization of the first PAM for the β 2AR, Compound-6, and compare its properties with our recently reported β 2AR NAM, Compound-15. These compounds were discovered through affinity-based, in vitro screening of highly diverse DNA-encoded small molecule libraries (DELs) against the purified human- β 2AR. Of note, compound-15 was isolated by screening DELs against the unliganded β 2AR, whereas compound-6 was obtained by screening against β 2AR bound to a high-affinity agonist. Both compounds have low micromolar affinity for the β 2AR

and display diametrically opposed allosteric activity in radioligand binding studies. As expected for a NAM, compound-15 decreases β 2AR affinity for orthosteric agonists, whereas the PAM, compound-6, enhances agonist affinity for the receptor. Both compounds also show unbiased allosteric modulation of β 2AR-mediated signaling in cellular assays measuring cAMP production and β -arrestin recruitment downstream of the activated receptor. Compound-15 decreases the responsiveness, and therefore efficacy, of orthosteric agonists, while compound-6 increases agonist activity at the β 2AR. Importantly, both modulators are highly specific for the β 2AR, as their ability to modulate agonist function at the closely related β 1AR is greatly diminished. Interestingly, compound-15 binds to the canonical, intracellular transducer binding site of the β 2AR thereby sterically blocking transducer function, whereas compound-6 potentiates transducer function, suggesting a different binding site on the receptor. Additionally, using structurally modified analogs of each compound, we define the respective chemical groups that are key to their biological activity.

Overall, our studies outline a generally applicable, proof-of-concept strategy to isolate conformationally-specific, small molecule GPCR ligands with unique functional profiles such as compound-6 and 15. It will be of interest to test these compounds in animal disease models to further determine their potential utility as therapeutics. In addition, comparative analyses of their atomic level interactions with the β 2AR will offer further mechanistic insights into GPCR allostery.

250 Germline BARD1 mutations predispose to neuroblastoma through defective DNA double-strand break repair

Michael P. Randall

Perelman School of Medicine, University of Pennsylvania, USA

Neuroblastoma, an embryonal malignancy of the autonomic nervous system and the most common cancer diagnosed during the first year of life, is a complex genetic disease. While a genome-wide association study (GWAS) has identified several neuroblastoma predisposition loci, each individual SNP association has a relatively low effect size. By contrast, rare germline variants may have a larger effect size and contribute more significantly to malignant transformation. Our sequencing of neuroblastoma patients' germline DNA has revealed significant enrichment for putative loss-of-function mutations in the BRCA1-associated RING domain 1 (BARD1) gene (7/766, 0.9%, $p < 0.001$). Notably, no tumors showed loss of heterozygosity of the wild type (WT) allele. BARD1 heterodimerizes with BRCA1 and promotes its stability and subcellular localization; the BRCA1-BARD1 complex is essential for homology-directed repair (HDR) of DNA double-strand breaks (DSB). We hypothesized that germline BARD1 variants contribute to malignant transformation via dysregulation of HDR and ensuing genomic instability.

We first used a biochemical approach to evaluate the impact of BARD1 variants on the formation and function of the BARD1-BRCA1 heterodimer. Five BARD1 germline variants (p.R112*, p.R150*, p.E287fs, p.Q564*, and p.R641*) were prioritized for study here. These variants were characterized for BARD1-BRCA1 heterodimerization after co-transfection with BRCA1 cDNA into HEK293T. Co-immunoprecipitation demonstrated that all but one truncated BARD1 protein (p.R112*) maintained the ability to bind BRCA1, though only p.E287fs stabilized BRCA1 comparably to WT BARD1, as measured by persistence following cycloheximide treatment. Immunofluorescence and immunoblotting after nuclear fractionation showed that three variants with truncations within or near the BRCA1-binding RING finger domain caused aberrant

BRCA1 localization to the cytoplasm. We next introduced the E287fs variant into the IMR-5 neuroblastoma cell line as a monoallelic knock-in via CRISPR/Cas9 (IMR-5 BARD1WT/E287fs). Successful knock-in was confirmed using Sanger sequencing. BARD1WT/E287fs IMR-5 cells assembled significantly fewer RAD51 foci after UV irradiation than WT IMR-5 cells (38% vs. 12% of nuclei with ≥ 3 foci; $p < 0.001$), suggesting reduced capacity for DNA DSB repair. Moreover, IMR-5 BARD1WT/E287fs cells were sixfold more sensitive to poly (ADP-ribose) polymerase (PARP) inhibition with olaparib relative to WT IMR-5 cells (IC50 of 860 vs. 5400 nM).

Taken together, these data suggest that BARD1 germline mutations predispose to neuroblastoma by disrupting the stability and localization of BRCA1. The resultant dysregulation of DNA DSB repair and increased sensitivity to PARP inhibition may provide a therapeutic opportunity. Efforts are ongoing to engineer additional heterozygous BARD1 variant knock-ins, and to further characterize these variants' effects on BARD1-BRCA1 heterodimerization and DNA DSB repair.

251 HDAC1 and PKA inhibitor combination therapy for targeted chemotherapy resistant FLT3-IDT+ Acute Myeloid Leukemia.

Guillermo O. Rangel Rivera

Medical University of South Carolina, Charleston, USA

Acute Myeloid Leukemia (AML) is a malignant proliferation of myeloid precursors in the bone marrow with an overall survival rate of 40-50% in young patients, however acquired mutations can pose challenges to treatment. An activating internal tandem duplication (ITD) in Fms-like tyrosine kinase 3 (FLT3) present in 30% of cases is associated with worsened proliferation, survival and differentiation by constitutive activity of its downstream signaling targets. FLT3-IDT+ targeted therapy with Crenolanib has proven successful, however chemotherapy resistance rapidly develops. It is known that AML suppress *CERS1* via histone deacetylase 1 (HDAC1), blocking expression of Ceramide Synthase 1 (CerS1) which plays an important role in mediating lethal mitophagy. We propose that targeting downstream effectors of the FLT3 signaling pathway such as HDAC1 and PKA alone or in combination would be effective in Crenolanib resistant cell line models of AML. Crenolanib resistant (CR) and a Crenolanib Sensitive (CS) cell lines were developed and treated with PKA inhibitor H-89 or HDAC1 inhibitor MS-275 alone or in combination. H-89 treatment of CR-AML cells (ED50= 27.67 μ M) decreased viability with similar potency as CS-AML cells (ED50= 28.89 μ M), while MS-275 treatment of CR-AML cells (ED50= 49.04 μ M) was less potent compared to CS-AML cells (ED50= 25.57 μ M). Autophagy was assessed by confocal microscopy, which indicated autophagosome punctae in the H-89+MS-275 combination treatment of CR cells but to a lesser extent in the CS cells. Isobologram analysis of combination therapy in CS and CR AML cells showed additive effects, but not synergistic effects. Proximity ligation assays showed increased PKA and HDAC1 interaction in CR AML cells (7.3 fold) compared to CS AML cells (2.2 fold) as measured by confocal microscopy. Upon treatment of CR-AML cells and CS-AML cells with H-89 this interaction was abrogated in resistant cells (3.4 fold). These results suggested an important role for PKA and HDAC1 in mediating increased viability in crenolanib resistant cells. PKA and HDAC1 may be viable targets for Crenolanib resistant AML cells.

Conflicts of interest: None

252 Toward high throughput immune infiltrate analysis from H&E stained images

Rishi Rawat

University of Southern California, Los Angeles, USA

Our appreciation of the immune system in breast cancer is rapidly evolving. New methods to quantify the composition and spatial distribution of the immune infiltrate from pathology images are urgently needed to develop better strategies to activate the anti-tumor immune response. Existing methods to quantify the immune infiltrate are tedious (manual counting) or rely on immunohistochemistry (IHC) staining to identify immune cells. While significant efforts are underway to develop machine learning tools to categorize cells based on morphologic features in hematoxylin and eosin (H&E) stained histopathology images, all approaches are limited by the scarcity of large, annotated ground truth training sets. In this work, we propose a new approach, leveraging “style-transfer” algorithms from the computer vision community to generate large quantities of training data from IHC stains. Using style transfer, we generate synthetic H&E images from IHC stains for immune markers, such as CD45, CD8 and CD4. The generated images have pixel-perfect ground truth provided by IHC, and do not need manual labeling. We investigate the impact of training on increasing numbers of synthesized images and validate our algorithms on an independent test set annotated by a pathologist (n=100 patients, 3064 identified lymphocytes). Our baseline classifier achieves a 83% accuracy, compared to the pathologist ground truth. This work provides a novel, tractable, and efficient way to train data-hungry algorithms to identify multiple cell types from H&E stained images.

This work is supported by a grant from the Breast Cancer Research Foundation (BCRF-17-002)

253 Saturated fatty acids impair organellar trafficking in dorsal root ganglion (DRG) sensory neurons

Erin Reasoner

Grand Valley State University, Allendale, USA

Diabetic Peripheral Neuropathy is a common complication of diabetes, characterized by a distal to proximal loss of sensation in the limbs. In type 2 diabetics, progressive nerve damage is associated with elevated levels of triglycerides. Long-chain fatty acid (FA) precursors of triglycerides impair axonal transport of mitochondria in primary sensory DRG neurons, however, the molecular source of this impairment is unknown. In this study, we sought to determine whether hyperlipidemia specifically impairs mitochondrial transport or induces a global alteration in trafficking of all organelles. To accomplish this, we compared mitochondrial and synaptic vesicle trafficking in DRG neurons. We treated primary cultures of DRG neurons from adult mice with physiological concentrations of saturated and unsaturated FA ranging from 31 μ M to 250 μ M. Both mitochondria and synaptic vesicles showed a significant and dose-dependent decrease in percent motility. Mitochondria and synaptic vesicles also showed a trending decrease in retrograde and anterograde velocities. Interestingly, bidirectional transport of both organelles was not altered. Overall, our data indicated that hyperlipidemic concentrations of saturated FAs may cause universal trafficking dysfunction through the inhibition of organellar transport in DRG neurons.

254 The role of calcineurin in normal myelination and neuropathy

Chelsey Reed

Hunter James Kelly Research Institute, SUNY at Buffalo, Buffalo, USA

Charcot Marie Tooth disease (CMT) is the most common inherited neuromuscular disorder. CMT presents as slowly progressive weakness beginning in the distal limbs usually in the first two decades of life. There is no treatment and for those with severe disease CMT can be disabling. Mutations in numerous genes have been associated with CMT, including mutations in P0, the most abundant protein in myelin. In the S63del CMT1B mouse, the folding of P0 is disrupted and causes a toxic gain of function. The accumulation of P0 in the endoplasmic reticulum (ER) leads to the unfolded protein response (UPR) and a demyelinating phenotype. Surprisingly, Schwann cell specific ablation of *Perk*, encoding a kinase activated to relieve ER stress (PERK), improves myelination in S63del mice. This improvement despite persistent ER stress led us to consider if PERK was interfering with a pathway outside of the UPR involved in myelination. We have hypothesized that calcineurin, a newly identified PERK substrate and promyelinating signal, is over activated as a result of active PERK and ER stress. Increased activation of calcineurin in S63del results in a chronic gain of function of NFATc4, an important promyelinating signal. Aberrant myelination in other neuropathies has been associated with gain of function of promyelinating signals. Using Schwann cell specific ablation of *Perk* (S63del/*Perk*^{SCKO}) or *calcineurin* (S63del/*CnB*^{SCKO}) in S63del mice we will study the promyelinating calcineurin pathway in normal development and disease, as well as how PERK may be perturbing this pathway when activated by the UPR. By better understanding the pathogenesis of S63del we have the potential to identify new therapeutic targets for Charcot Marie Tooth disease.

255 Quantum Chemical Protein Engineering: Development of a Long-Acting Insulin Analog via Enhanced Aromatic-Aromatic Interactions

Nischay Rege

Case Western Reserve University, Cleveland, USA

The development of improved long-acting (basal) insulin analogs represents a clinical need for treating Type I and Type II Diabetes Mellitus. Insulin is stored in the secretory granules of pancreatic β -cells as zinc-coordinated hexamers; stabilization of these hexamers in pharmaceutical formulations has been a strategy for conferring basal action to insulin analogs. A major feature contributing to the stability of the insulin hexamer is a network of aromatic amino acids that form a series of edge-to-face (ETF) aromatic-aromatic interactions across a critical interface within the hexamer. Semi-classical simulations of aromatic-aromatic interactions at this interface suggested that substitution of residue TyrB26, a central residue in the aromatic network, by Trp would preserve native structure while enhancing hexamer stability. The crystal structure of a TrpB26-insulin analog was observed to be essentially identical to that of wild-type insulin. Further, spectroscopic studies demonstrated a 150-fold increase in the in vitro lifetime of the variant hexamer. Functional studies in diabetic rats indeed revealed prolonged action following subcutaneous injection. Thus exploiting a general feature of protein structure and stability, our results exemplify a mechanism-based approach to the optimization of a therapeutic protein assembly.

256 Immune regulation of cartilage tumors

Spencer M. Richardson

St. Jude Children's Research Hospital, USA

Osteochondromas are the most common type of benign bone tumor caused by neoplastic outgrowths of cartilage and bone. Although these tumors are benign, osteochondromas cause severe pain, deformity, and constriction of tendons and neurovascular structures. Individuals can develop multiple osteochondromas in a condition called multiple hereditary exostoses (MHE). MHE is linked to heterozygous mutations in the genes encoding exostosin glycosyltransferase 1 (EXT1) or 2 (EXT2). Although most MHE patients bear mutations in either EXT1 or EXT2, studies in both mice and humans indicate that heterozygous EXT mutations are not sufficient to cause disease. Mice with a heterozygous deletion of *Ext1* model the loss-of-function EXT1 mutations observed in MHE patients, however these mice show very limited penetrance of osteochondromas. Thus, it is not understood how a loss of function of one EXT allele causes such severe disease. We previously demonstrated that the immune system impacts the formation and severity of osteochondromas in a mouse model of multiple osteochondromas caused by genetic deletion of *Erk1* and *Erk2* in CD4+ cells. This was surprising as no immune regulator of osteochondroma growth had been described. Thus, we hypothesize that EXT mutations render individuals susceptible to osteochondromas, but that additional "hits" mediated by inflammation and the immune system are necessary for tumor formation and growth.

To test whether activation of the immune system impacts the incidence and severity of osteochondromas, we stimulated the innate immune system in two different mouse models of multiple osteochondromas; heterozygous *Ext1* (*Ext1*^{+/-}) mice and mice deficient in *Erk1* and *Erk2* in CD4+ cells (*Erk* double knockout [DKOCD4]). The innate immune system was activated by giving the mice various adjuvants including polyinosinic-polycytidylic acid, complete Freund's adjuvant, and bacterial lipopolysaccharide at weekly intervals starting at three weeks of age. We found that the incidence of osteochondroma formation was accelerated after sequential treatment with multiple adjuvants. Histological analysis of the affected bones demonstrated an increase in severity of osteochondromas in mice treated with adjuvants compared to littermate controls. These data indicate that stimulation of the innate immune system can impact osteochondroma growth. Importantly, we show that *Ext1*^{+/-} mice develop larger and more numerous tumors following innate stimulation, which supports our hypothesis that the immune system can serve as an additional "hit" resulting in tumors. The immune system may also contribute to the wide spectrum and severity of tumors observed in MHE patients. These data reveal a novel role for the immune system in development of osteochondromas.

257 Characterizing the role of fibronectin splice variants in glioblastoma

Jonathan W. Rick

University of California San Francisco, USA

Glioblastoma (GBM) is an aggressive primary brain cancer with a dismal overall survival of under two years from diagnosis. A defining feature of these tumors is their invasiveness, which enables escape from surgical resection and drives inevitable recurrence, with over 90% of recurrences occurring within 2 cm from the original tumor. Work to identify mediators of invasion and target them has thus far yielded little progress. This knowledge gap could be explained by the fact that studies focused on cancer cells themselves are unable to capture GBM for what is really is, an organ with complex

dynamic interplay between tumor cells and their microenvironment. Consequently, we are interested in studying the milieu surrounding GBM tumors to identify factors that permit invasion. One suspect is EDA expressing fibronectin, a splice variant that has been associated with other malignancies. In other cancers, EDA is thought to play a role in invasion and in making the tumor microenvironment more susceptible to growth. In work completed under the fellowship to date, I have demonstrated that EDA fibronectin is expressed in GBM and have also shown that this expression is particularly elevated in periventricular tumor locations. In areas rich with EDA expression, this protein appears to form scaffolds that may serve a role for angiogenesis, haptotaxis and/or macrophage polarization. We have also identified that cancer associated fibroblasts (CAFs) in GBM preferentially accumulate in periventricular tumor locations, where they are the cellular source of EDA fibronectin. Ongoing work seeks to elucidate the roles that EDA fibronectin plays in pro-tumoral invasiveness and macrophage polarization and, in so doing, identify a potential therapeutic target.

258 Characterization of the inflammatory infiltrate in primed mycobacterial uveitis

Kevin I. Rolnick

University of Washington, USA

Uveitis is the fifth leading cause of blindness in the U.S., however our understanding of its immunologic pathophysiology is only nascent. To develop novel treatments for this set of diseases and to understand the ramifications of uveitis associated with viral vector mediated gene therapy for retinal degeneration, a more robust understanding of the inflammatory sequence in uveitis is required. Both innate and adaptive immunity are implicated in uveitis. Recently, an animal model incorporating innate and adaptive immunity, primed mycobacterial uveitis (PMU), was developed. This study aims to describe in detail the immune responses associated with PMU. Further, we aim to determine if aqueous samples represent the inflammatory response that occurs throughout the entire eye in PMU, as this could potentially serve as a diagnostic approach for uveitis.

To generate uveitis in C57BL/6J mice, mycobacterial H37Ra antigen was delivered subcutaneously one week prior to unilateral intravitreal injection of the same antigen (n=5). Inflammation was confirmed via vitreoretinal and anterior chamber optical coherence tomography at day 1 post-intravitreal injection (D1). At D1, cell suspensions were generated from inflamed eye aqueous ("Ia" sample), inflamed eye vitreous and choroid ("Ivc" sample), as well as from fellow eye aqueous, vitreous, and choroid ("FE" sample). Flow cytometry was performed to identify ocular cells and leukocytes as well as lymphocytic and granulocytic lineages.

Isolated cells were first gated to identify CD45+ leukocytes. The vast majority of CD45+ cells in Ia as well as Ivc were granulocytic (CD3-, CD19-, NK1.1-) with neutrophils (Ly6g+) representing >90% of these cells in Ia and Ivc. Of CD45+/CD3+ cells, a minority were CD8+ (17.2%, 16.4%, and 22.4% in Ia, IVC, and FE, respectively). A larger proportion of CD3+ T cells and CD19+ B cells were observed in Ivc than Ia (CD3+: 0.72% in Ia, 1.50% in Ivc; CD19+: 0% in Ia, 0.27% in IVC). A significant population of plasmacytoid dendritic cells (CD45+/CD11^{high}/CD11^{low}) was found in both Ia and Ivc (0.25% and 1.81% of CD45+/CD3-/CD19-/NK1.1- cells, respectively).

These findings illustrate the complex manifestations of intravitreal mycobacterial exposure. Both the anterior and posterior eye experience a granulocyte-predominant response at D1 following H37ra exposure. Further, the inflammatory infiltrate in the anterior chamber is distinct from that found in the vitreous and choroid, thus a

“anterior chamber tap” diagnostic tool may not be adequate to inform of the inflammatory response throughout the eye. These findings will guide future studies utilizing the PMU model. Our forthcoming PMU experiments will focus on elucidation of the immune response following intravitreal H37Ra exposure with and without systemic priming to understand the specific effects of priming on adaptive immune system activation.

259 Enucleation in induced red blood cells: a platform for autologous cell therapy and in vitro modeling of sickle cell anemia

Tolulope O. Rosanwo
Boston Children's Hospital, USA

Human induced pluripotent stem cells (hiPSCs) hold tremendous promise for disease modeling and the development of novel therapeutic treatments for sickle cell anemia (SCA). hiPSCs can theoretically produce all cell types including induced red blood cells (iRBCs). Sickle cell patients could benefit from autologous, engineered red blood cells as these patients have rare blood types, are frequently allo-sensitized to blood products, and at risk of iron overload from recurrent transfusions. However, in vitro modeling of SCA as well as iRBC production from hiPSCs has been hampered by their inability to differentiate into terminally-mature, enucleated, beta globin-expressing red blood cells. Here, we describe strategies to improve in vitro production of iRBCs. We generated hiPSCs from sickle cell patients with hemoglobin SS disease seen at our hematology clinic at Boston Children's Hospital. Using a cocktail of transcription factors that promote self-renewal and multipotency expressed under the control of a doxycycline-regulated promoter (ERG, HOXA9, RORA, SOX4, MYB), we generated conditionally immortalized hematopoietic progenitors that serve as a renewable source of robust erythroid cells in vitro. Erythroid progenitors differentiated from these lines underwent globin-switching once transfused into immunodeficient mice, with a 27% induction of beta globin expression. An in vitro protocol incorporating human plasma can be used to produce 30-40% beta-globin-expressing cells. 10-50% of generated iRBCs are also enucleated. Preliminary iRBC analysis reveals nearly 36% of the enucleated population to be RNA negative erythrocytes and 64% RNA positive reticulocytes. With an expandable source of erythroid progenitors capable of producing mature red cells, we hope to assess the feasibility of this platform for autologous cell therapies. In future studies, we anticipate the improvement of the sickling model via a robust induction of beta-globin expression. The generation of hiPSC-derived SCA models will be critical in broadening the current understanding of the molecular mechanisms of this disease, and the development of improved pharmacological treatments for the treatment of SCA.

260 A novel antibody-based diagnostic test for rapid differentiation of Zika and dengue seropositivity

Brandon C. Rosen
University of Miami Miller School of Medicine, Miami, USA

The emergence of Zika virus (ZIKV) in the Western hemisphere in 2015 precipitated a global health crisis, and hundreds of thousands of individuals have been infected to date. The high degree of concern surrounding ZIKV resulted from its implication as the etiologic agent of microcephaly and other severe congenital abnormalities in the neonates of women infected while pregnant. Future prevention of ZIKV-induced birth defects will require accurate diagnostic testing to inform prospective parents of their ZIKV serostatus prior to conception. However, the high degree of cross-reactivity exhibited by

antibodies (Abs) against ZIKV and the closely-related dengue virus (DENV) poses a significant diagnostic challenge. The current method for differentiation of ZIKV and DENV exposure, the plaque reduction neutralization test (PRNT), is an expensive, laborious, and time-consuming assay requiring sophisticated laboratory infrastructure. In this study, we sought to develop a novel immunological diagnostic test capable of differentiating ZIKV and DENV seropositivity rapidly, reproducibly, and inexpensively. We hypothesized that Abs recognizing epitopes specific to the ZIKV envelope would be produced by individuals infected with ZIKV, but not DENV, and that these Abs would serve as a marker of prior ZIKV exposure. To detect these ZIKV-specific Abs in human plasma, we developed an Ab competition ELISA in which the ability of plasma-borne Abs to block binding of a purified, labeled ZIKV-specific Ab to whole virus is assessed. We found that the plasma of ZIKV-exposed individuals blocked binding of the labeled ZIKV-specific Ab to ZIKV, whereas the plasma of DENV-exposed individuals did not. Furthermore, the assay accurately predicted the ZIKV exposure status of 20/21 (95%) blinded plasma samples from Flavivirus-exposed patients in Brazil. The assay also accurately predicted the ZIKV seronegativity of Flavivirus-naïve individuals in the U.S. (15/15) and Brazil (5/5) and in individuals who had received yellow fever vaccinations (4/4). Collectively, these results indicate that this Ab competition assay is highly specific for ZIKV and can accurately differentiate exposure to ZIKV and other Flaviviruses. Importantly, these findings suggest that an Ab competition-based diagnostic method could provide a promising approach for the eventual development of a point-of-care ZIKV diagnostic.

Competing Interests: Authors DMM, EGK, and DIW are inventors on a patent application related to the ZIKV-specific Abs described in this study.

261 Aging enhances the deleterious role of neutrophils in ischemic stroke

Meaghan A. Roy-O'Reilly
University of Texas Health Sciences Center at Houston, Houston, USA

Background: Ischemic stroke is a leading cause of mortality and disability worldwide. Neutrophils exacerbate brain injury via the release of toxic products, particularly reactive oxygen species (ROS). Clinical trials of anti-inflammatory therapies for ischemic stroke have been unsuccessful, due to poor drug specificity and inadequate pre-clinical modeling. Most importantly, age represents the greatest non-modifiable risk factor for ischemic stroke incidence, and is a strong predictor of poor functional outcome. However, little is known regarding the effect of age on neutrophil-driven tissue damage. We hypothesized that age enhances pro-inflammatory neutrophil functions, driving damage and poor outcomes after ischemic stroke, and that neutrophil depletion after ischemic stroke would preferentially benefit aged animals.

Methods: Using biological samples and clinical information from stroke patients, we examined the associations between neutrophil gene expression, age and poor outcome after stroke. A mouse model was then used to determine the organ distribution, brain infiltration and inflammatory phenotype of neutrophils in young (3 month) and aged (22 month) mice at baseline and following ischemic stroke. Flow cytometry was used to measure neutrophil ROS production after *ex vivo* and *in vivo* challenge. Neutrophil-specific anti-Ly6G was used to deplete neutrophils after ischemic stroke, followed by assessment of functional outcomes.

Results: In stroke patients, neutrophil counts were significantly upregulated ($p < 0.0001$) 24 hours after stroke compared to controls. RNA-sequencing demonstrated that older stroke patients had greater upregulation of genes involved in neutrophil degranulation compared to younger stroke patients. In mice, flow cytometry showed that aged mice had higher proportions of neutrophils at baseline across multiple organs, and that stroke-induced neutrophilia was exacerbated in aged animals ($p < 0.0001$). After stroke, aged animals were seen to experience poorer outcomes than young animals. Infiltrating neutrophils in the stroke-damaged brains of aged animals had significantly higher intracellular ROS levels compared to those in young animals. Similarly, *ex vivo* stimulation of naive neutrophils showed a more sensitive and robust production of ROS in aged neutrophils. Depletion of neutrophils with anti-Ly6G after stroke conferred no benefit in young males, but a significant improvement in gross neurological deficits, sensorimotor function and strength was seen in aged animals treated with anti-Ly6G.

Conclusions: This work demonstrates that age enhances stroke pathophysiology and neutrophil degranulation in stroke patients. Additionally, aged animals were found to have exacerbated neutrophil ROS production in the brain after stroke, a phenomenon that was also seen in *ex vivo* experiments, suggesting an intrinsic age-related change in neutrophil biology. Aged animals had significantly poorer outcomes after stroke and neutrophil depletion was specifically protective in aged animals, illustrating the importance of testing potential therapeutics in aged animals and suggesting a promising role for neutrophil-targeted therapies in the future treatment of ischemic stroke.

262 Alterations in the gastric landscape and effects on *Helicobacter pylori* pathogenesis

Jose B. Saenz

Washington University School of Medicine, St. Louis, USA

Infection with *Helicobacter pylori* (Hp) remains the most significant risk factor for the development of gastric adenocarcinoma. The sequence of events leading to gastric dysplasia begins with the gradual loss of acid-secreting parietal cells, followed by the expansion of pre-neoplastic changes in the setting of chronic inflammation. The early mucosal response to oxyntic atrophy includes a reorganization of the gastric unit, characterized initially by an increased proliferation of gastric progenitor cells and the reprogramming of post-mitotic chief cells at the base of the gastric gland into a proliferating population of metaplastic cells. This pattern of metaplasia is normally a transient alteration in the gastric landscape to facilitate subsequent restoration of normal architecture. In some cases, however, restoration is blocked, and the lesion progresses to gastric dysplasia in the setting of chronic inflammation. While it is known that Hp steadily establishes its gastric niche in a relatively hostile environment, it remains unclear how Hp adapts to changes in the gastric metaplastic landscape.

We hypothesized that Hp interacts differently with metaplastic gastric epithelium and that this could explain Hp's ability to expand its niche within the stomach. Hp adhesion to gastric epithelium is largely mediated by the binding of two of its adhesins, BabA and SabA, to host Lewis B (Le^b) and sialylated Lewis X (sLe^x) antigens, respectively, epitopes expressed as terminal residues on gastric mucins. Using a murine model for acutely and reversibly inducing metaplasia, we find that the onset of metaplasia results in an expansion of sLe^x expression along the length of the gastric unit axis. Hp is able to penetrate deep within metaplastic glands *in vivo*, while it is largely restricted to the surface epithelium of uninjured glands. This phenotype could be reproduced using a newly developed *in situ*

bacterial adherence assay relying on Hp adherence to thick sections of fixed gastric tissue from uninjured and metaplastic stomachs. In addition, penetration of Hp deep within metaplastic glands *in situ* could be blocked by pre-treating the fixed sections of metaplastic gastric tissue with neuraminidase, which cleaves exposed sialic acid residues.

Following recovery from injury, the sLe^x expression pattern reverts to that of uninjured tissue. Accordingly, Hp is unable to penetrate deep within glands that have recovered from injury, suggesting that Hp's binding is mediated in part by reversible changes in sLe^x expression. Finally, consistent with the *in situ* findings, Hp is able to expand its topographic distribution *in vivo* by more effectively colonizing the gastric corpus of mouse stomachs undergoing metaplasia compared to uninjured stomachs, implying that Hp has a tropism for metaplastic gastric epithelium. Taken together, our data illustrate a potential mechanism by which Hp expands its niche and interacts with metaplastic gastric epithelium.

263 Centromere driven gene regulation in prostate cancer

Anjan Saha

University of Michigan, Ann Arbor, USA

The centromere is an essential component of the cellular machinery required for the faithful segregation of chromosomes during mitosis, a process that is significantly dysregulated in cancer. The centromere H3 histone variant CENPA serves as the epigenetic marker for the centromere. CENPA overexpression has been identified in numerous malignancies, yet the functional consequences of its overexpression remain elusive. We hypothesize that centromeres represent a functionally important molecular signature that can drive gene regulation in prostate cancer. We confirm overexpression of CENPA in several malignancies through cancer vs. normal analysis within a compendium of 10,848 poly(A)⁺ RNA-sequencing (RNA-seq) libraries containing primary cancer tissue, normal tissue, and cancer cell lines. Further analysis restricted to the prostate tissue type cohort demonstrated an association between increased disease severity and higher CENPA expression. RNA-seq findings were further validated via tissue microarray (TMA). Overexpression of CENPA mRNA within the prostate cancer tissue type cohort is tightly associated with proliferation and mitosis gene expression signatures, demonstrating CENPA involvement with processes important for cell division. Functional interrogation through RNAi based depletion of CENPA results in reduced proliferation of LnCaP, DU145 and 22rv1 by inhibiting progress through the cell cycle. Furthermore, CENPA targeted chromatin immunoprecipitation followed by sequencing (ChIP-seq) reveals numerous ectopic binding sites for CENPA. CENPA binding has a predilection towards proximal regions of gene bodies, as revealed by annotation association inquiries. In view of the above, we show CENPA is indeed overexpressed in prostate cancer and that its expression is necessary for proliferation of prostate cancer cell lines. Furthermore, cell lines overexpressing CENPA exhibit novel CENPA-binding characteristics that suggest a functional role for CENPA in gene regulation. Future studies include xenograft transplantation of CENPA-depleted cell lines, transcriptomic assessment of CENPA-depleted cell lines, and CRISPR-based evaluation of specific CENPA binding sites.

264 Alterations in estrogen metabolism in pulmonary arterial hypertension: Aromatase expression in pulmonary arterial endothelial cells.

Sandeep Sahay

Houston Methodist Hospital, Houston, USA

The role of estrogen in vascular disease in general and in pulmonary arterial hypertension (PAH) specifically is contradictory. PAH affects females more commonly than males. In animal models of pulmonary hypertension, estrogen increases nitric oxide and prostacyclin production and decreases endothelin-1, resulting in beneficial vascular effects. In contrast, a comparison of BMPR2 mutation carriers from families with familial PAH demonstrated that relative increases in a proangiogenic estrogen metabolite (16-OHE1) was highly associated with disease (PAH) expression. Elevated estrogens and estrogen metabolites have been reported in males with PAH compared to matched males absent cardiovascular disease. Patients awaiting liver transplant have a high incidence of feminization features and PAH (portopulmonary hypertension [POPH]). Aromatase (CYP19A1) catalyzes the production of estrogen from testosterone and androgen, and has been identified in the lungs of patients with COPD (in pulmonary alveolar macrophages) and is upregulated in pulmonary vascular smooth muscle cells in animal models of PH. Whether the lungs are a source of estrogen production or a site of estrogen receptor activation in PAH is unknown.

We hypothesize that alterations in estrogen levels, estrogen metabolic byproducts, intrapulmonary estrogen receptors and/or aromatase activity in the lung and/or the liver contribute to PAH.

Historical lung and liver specimens from autopsy or at organ explant (lung or liver transplant) underwent aromatase staining as our first steps to address this hypothesis. Immunohistochemical (IHC) aromatase staining on deparaffinized tissues was undertaken on 2 autopsied lungs with POPH, and 7 explanted cirrhotic livers. Controls were normal lung and liver and standard placental tissue positive and negative staining controls using primary antibodies for Aromatase (1:700: NB10-1596, Novus Biologicals, Littleton, CO). Secondary antibodies were incubated with the tissue slides (HRP antiRabbit IgG and anti-Mouse IgG, vVector Laboratories, ready to use) and the tissue was counterstained with hematoxylin. Slides were graded for presence, absence and staining intensity for aromatase by two pathologists blinded to the PH status of the patients. Immunohistochemical staining for aromatase in the pulmonary arterial endothelial cells of two POPH patients was demonstrated with no staining in normal lung tissue. Immunohistochemical aromatase staining was strongly positive in cirrhotic patients with and without PH but absent in normal liver. This is preliminary evidence for altered intrapulmonary estrogen metabolism in PAH specifically increased aromatase expression in the pulmonary arterial endothelial cells. Further evaluation in all PAH patients undergoing autopsy or explant is ongoing.

265 Different properties of training-induced visual recovery in sub-acute versus chronic occipital stroke patients

Elizabeth L. Saionz

University of Rochester, Rochester, USA

Stroke damage to primary visual cortex (V1) in adult humans causes cortical blindness (CB). We have previously shown that visual discrimination training in chronic (>6 months) stroke patients decreases the deficit, but recovered vision remains impaired. Evidence in sensorimotor stroke suggests that earlier intervention promotes greater recovery. Here, we asked if visual discrimination

training initiated sub-acutely (<3 months) after V1 stroke enhances improvement in CB. Ten sub-acute and 12 chronic CB patients trained with a global direction discrimination and integration task in their blind field. Three additional sub-acute were tested but not trained, serving as controls. Initial discrimination performance was at chance (baseline normalized direction range [NDR] thresholds=100% for all subjects). After daily home training for 3 months, sub-acute attained normal NDR thresholds ($30 \pm 14\%$) at trained locations much faster than chronics (sub-acute: 11 ± 14 sessions; chronics: 99 ± 65 sessions; $t(20)=4.18$, $p<0.001$). Moreover, unlike chronics, whose recovery never transferred deeper into the blind field, trained sub-acute exhibited transfer of recovery up to 10 degrees deeper into the blind field than trained locations. Untrained sub-acute had no spontaneous improvement in NDR, though all sub-acute improved similarly on clinical Humphrey perimetry (luminance detection). Thus, discrimination training initiated in sub-acute CBs generates faster, more spatially distributed discrimination improvements than identical training in chronic CBs. While luminance detection perimetry improved in both trained and untrained sub-acute, only trained subjects recovered discrimination performance. In summary, without an intact V1, luminance detection may improve spontaneously during the sub-acute period, but deliberate training is required to recover visual discrimination abilities.

266 Perfect Skeletal Muscle Regeneration After Repeated Injury in the African Spiny Mouse (*Acomys*)

Aaron Gabriel W. Sandoval

University of Florida, Lakeland, USA

Regeneration is the perfect regrowth and repair of damaged tissue. In most adult mammals, the body replaces damaged tissue with a disorganized collagen matrix, better known as a scar. It is believed that the scarring response is antagonistic to the regenerative process. Thus, studying animals that are able to heal scar-free will provide insight into the mechanisms underlying regeneration. The African spiny mouse (*Acomys*) is the only known mammal in the world that is capable of scar-free skin regeneration as an adult. In the laboratory, we are using the normal lab mouse (*Mus*) as a non-regenerating control to analyze the true extent of *Acomys*'s regenerative abilities. After an ear punch wound, *Acomys* fully regenerated hair follicles, adipocytes, cartilage, sebaceous glands, and, most notably, skeletal muscle. To further study *Acomys*' skeletal muscle regeneration abilities, we focused on the tibialis anterior, a leg muscle also found in humans. The muscles of both *Acomys* and *Mus* were injected with cardiotoxin, a snake venom-derivative, to induce a wounding response. The healing muscles were harvested at 2, 4, 6, 8, and 16 days post-injection. The muscles were embedded in OCT medium, sectioned and mounted on slides. Subsequent immunohistochemistry with a collagen I antibody showed that both *Mus* and *Acomys* recovered from the single injection. It took approximately 11 days for the *Mus* muscle to fully recover; however, the *Acomys* muscle fully regenerated more quickly in just 8 days. Furthermore, immunohistochemistry with a collagen XII antibody showed significant scarring in the *Mus* connective tissue, whereas no scarring took place in *Acomys*. RT-qPCR analysis of muscles showed decreased levels of NF- κ B and TGF- β 1 gene expression in *Acomys* compared to *Mus*, signifying lower levels of inflammation and fibrosis. In order to study regeneration in response to repeated injury, we then injected a novel cohort of mice. After the initial injection, the mice were given 3 weeks to heal after which they were again injected. This was repeated for a total of 5 injection-healing cycles. Amazingly, *Acomys* was still able to regenerate its muscle perfectly after repeated insult. However, *Mus* showed an extremely

intriguing result: adipocytes had accumulated within the muscle. Immunohistochemistry with a perilipin antibody confirmed that fat cells were indeed present throughout the *Mus* muscle yet absent in the *Acomys* muscle. Although initially surprising, the abundance of fat cells throughout the *Mus* muscle after repeated injections is reminiscent of Duchenne muscular dystrophy during which human muscle cells are replaced by fat cells. Since *Acomys* averted this dystrophy-like phenotype, continued study of the African spiny mouse will help us to better understand ways to treat and prevent this debilitating disease. Truly, there is much to learn about the keys to scar-free tissue regeneration from this phenomenal model organism.

267 The Application of Medicare Data for Musculoskeletal Research in the United States: A Systematic Review

Tiana Sarsour

University of Toledo, Sylvania, USA

Musculoskeletal disorders hinder the human body's movement via their negative effects upon the musculoskeletal system, which consists of multiple components such as muscles, tendons, ligaments, and nerves, to name a few. These disorders can lead to many problems, including carpal tunnel syndrome, tendonitis, and epicondylitis. The consequences of these conditions affect the lives of aging adults, the direct and indirect costs of their care, and the use of different healthcare services. By utilizing the PubMed and Medline databases as sources for peer-reviewed manuscripts published between 1990 and 2015, the study aimed to examine literature on all musculoskeletal surgical outcomes which used Medicare Claims data in the United States in order to assess the reliability and usefulness of such claims data. Each study, of those observed, reported the primary use of Medicare claims data, involved musculoskeletal surgery, and was an original peer-reviewed study. By using the Newcastle Ottawa Assessment Scale, the study assessed the quality of each article. Surgical procedures, specific aims, evaluated outcomes, strengths, and weaknesses were all extracted from each individual study for analysis. Of the articles searched, 119 met the study's inclusion criteria, which focused upon various outcome measures such as epidemiology and treatment variation, cost of care, hospital-level analyses, health outcomes, validity and accuracy of Medicare claims data, disparities in healthcare, and policy evaluation. From the results obtained, it is concluded that Medicare claims data provide a unique way for researchers to study nationally representative patient population longitudinally. However, the results found a significant limitation in the usage of claims data; specifically, this limitation involves the lack of medical granularity on defining the severity of a given condition. Transition to the tenth revision of the International Statistical Classification of Diseases and Related Health Problems, ICD-10, will help eliminate some of these limitations.

268 Zebrafish Model of Human SLC26A4 Deafness

Ashley J. Scott

Mayo Clinic, Rochester, USA

Two out of every thousand newborns are born deaf or hard of hearing. Sixty percent of hearing loss has an identifiable genetic cause with disease causing variants in *SLC26A4* being among the most common. Pathogenic variants in *SLC26A4* cause bilateral sensorineural hearing loss, temporal bone abnormalities, and occasionally thyroid goiter, known as Pendred syndrome. Pendrin, the protein product of *SLC26A4*, is a solute carrier. Pendrin is expressed in the inner ear, thyroid, and kidney. In the inner ear, Pendrin modulates the transport of bicarbonate and chloride, allowing bicarbonate to leave the supporting cells of the inner ear and chloride to enter. This helps maintain a relatively neutral pH environment in the inner ear. It is

not known how the abnormal *SLC26A4* protein products modulate hearing loss and contribute to temporal bone abnormalities. The goal of this study was to model *SLC26A4* associated hearing loss in zebrafish and elucidate a mechanism responsible for hearing loss in patients with pathogenic variants in *SLC26A4*. To model the human condition, *slc26a4* mutations in zebrafish were generated via transcription activator like effector nucleases (TALENs) at the site of the most common *SLC26A4* pathogenic variants. We obtained a 23bp deletion mutation in exon 10 of *slc26a4*. We hypothesized that fish with biallelic *slc26a4* mutations would closely recapitulate the human phenotype and have significant hearing loss and structural ear malformations. To test for deafness in zebrafish, we developed a hearing assessment which exposes larval or adult fish to specific sound stimuli while recording startle responses. To quantitatively study the *slc26a4* mutant ear phenotype, we took measurements of the posterior and anterior otolith area and the ear area using bright field microscopy. Results indicate that homozygous larvae tested at 5 days post fertilization, the day of hearing onset in zebrafish, have hearing similar to wildtype. However, adult fish with two copies of mutated *slc26a4* have frequency specific reduced responses at 400 Hz, 80db. These results indicate that *slc26a4* mutants may have progressive frequency specific hearing loss. Bright field imaging and measurement analysis showed that *slc26a4* homozygous mutant larvae have significantly smaller standardized posterior otolith areas, anterior otolith areas, and ear areas on average compared to wildtype at 5dpf. This closely matches the human phenotype, as humans with *SLC26A4* pathogenic variants may have progressive hearing loss and temporal bone abnormalities.

269 Thin Filament Dysregulation as a Mechanism for Diastolic Dysfunction in Hypertrophic Cardiomyopathy: Computational and Experimental Investigation of TPM1 E192K Mutation in Patient-Derived Engineered Heart Tissue

Lorenzo R. Sewanan

Yale University, New Haven, USA

Missense mutations to alpha-tropomyosin (TPM1) are implicated in the development of hypertrophic cardiomyopathy (HCM). Linking HCM to mutation-induced molecular changes is challenging but critical for improved diagnosis and treatment. A young patient diagnosed with HCM after presenting with severe left ventricular hypertrophy, type II diastolic dysfunction, left atrium dilation, and moderate interstitial fibrosis (via CMR LGE) was genetically tested and found to have a sarcomeric TPM1 E192K variant. In order to understand the impact of this specific TPM1 mutant on muscle function and resulting pathophysiology leading to HCM, we have used multiscale modeling and experiments at the molecular, myofilament, and tissue levels. In order to model the impact of the mutation, we derived measures of TPM1 stiffness from molecular dynamics simulations of mutant and wild-type protein and used a novel Markov Monte-Carlo model of the regulated thin filament to translate the molecular alteration of the TPM1 flexibility into the effect on regulation of muscle contraction. We found that thin filament dysregulation altered actomyosin contraction leading to increase diastolic cross-bridge binding and reduce ability of thin filament to transition to the blocked state. Our model further predicted that these molecular changes would lead to increased systolic and diastolic twitch force production in intact muscle. In order to understand whether these mechanisms would lead to contractile dysfunction in the context of human tissue, we generated induced pluripotent stem cell cardiomyocytes (iPSC-CMs) from the TPM1 E192K-positive HCM patient. Engineered heart tissues (EHTs) were created from patient iPSC-CMs and cultured for 16 days under electrical pacing. Contractile characterization of EHTs

revealed that the peak force generated by mutant EHTs was several times higher than two independent sets of non-mutant control EHTs. Contraction kinetics were also changed, exhibiting significantly slower time to peak and relaxation time. Furthermore, the stiffness of the mutant EHTs during diastole significantly increased. Altogether, experimental observations and modeling indicate that E192K leads to lower TM stiffness and a consequent inability of the actin filament to inhibit myosin-based force production. We posit that this multiscale, multi-modal approach may be generally useful for predicting and understanding pathogenicity of TPM1 variants in cardiomyopathy.

270 Understanding the molecular function of RBFOX and determining the role in congenital heart disease

Harsh N. Shah

Harvard Medical School, USA

Congenital heart disease (CHD) accounts for nearly one-third of all major congenital anomalies and affects approximately 40,000 births per year in the United States. Although critical breakthroughs in cardiovascular diagnostics and surgery have led to increased survival rates in newborns with CHD, the etiologies of most CHDs remain largely unknown. Progress on this front has been recently achieved with the advent of whole exome sequencing where both inherited and de novo mutations were identified in newborns that segregate with CHDs. Although these mutations are likely to be causative for disease, this hypothesis has yet to be tested. Moreover, because the majority of loci discovered have not been previously linked to cardiovascular development, their mechanisms of action are elusive. One locus identified by the whole exome approach encodes RBFOX2, an evolutionarily conserved RNA binding protein of unknown function. During my internship in the Burns Lab at Massachusetts General Hospital/Harvard Medical School, I will uncover the molecular and cellular mechanisms underlying the cardiovascular phenotypes I observe in a new genetic zebrafish model of RbFox-mediated CHD.

The zebrafish genome contains three RBFOX paralogs including RBFOX1, RBFOX1-like, and RBFOX2. Using whole mount in situ hybridization, we only observed RBFOX1-like and RBFOX2 transcripts in the zebrafish heart. Based on their expression patterns, we generated new zebrafish strains that harbor small deletions in RBFOX1-like and RBFOX2 by CRISPR-Cas9 genome editing to learn whether they play a required role in heart development or function. Compared to single mutants that develop grossly normal hearts during embryogenesis, double mutant embryos show severe cardiac edema indicative of cardiovascular abnormalities. Heart beat monitoring revealed a significantly decreased rate of ventricular. Moreover, sarcomere structure appears highly disorganized in RBFOX double mutant ventricular cardiomyocytes. Together, these data demonstrate that RBFOX is required for normal heart function during embryogenesis.

In the coming months, I plan to more deeply characterize the RBFOX cardiac phenotype. Specifically, I will assess heart function by analyzing fractional shortening, calcium transients, and action potential duration and heart structure by counting cardiomyocyte numbers and by measuring cardiomyocyte cell size with the goal of uncovering the primary cellular mechanism underlying the observed cardiac failure. Concurrently, I plan to compare the transcriptomes of control to double mutant embryos by deep sequencing analysis to gain insight into potential molecular mechanisms underlying the heart failure phenotype. Ultimately, my research will demonstrate that mutations in RBFOX are causative for cardiovascular phenotypes in zebrafish and uncover the mechanisms by which RBFOX regulates heart development and function.

271 Creation of a robust genetically engineered mouse model of IDH-mutant glioma

Diana D. Shi

Dana-Farber Cancer Institute, USA

Glioblastoma (GBM) is the most common and aggressive form of brain tumor. Secondary GBMs are a subset of GBMs that progress from a low-grade or anaplastic astrocytoma, and display a high prevalence (70-90%) of mutations in the gene isocitrate dehydrogenase (IDH). 1. The ability to study IDH1 mutations in vivo has been hampered, however, by a lack of faithful mouse models. The goal of this project is to create a genetically engineered mouse model (GEMM) of IDH1-mutant glioma by introducing the most common glioma-associated IDH1 mutation (encoding the IDH1R132H oncoprotein) into mouse brain cells in vivo concomitantly with other driver mutations that frequently co-occur in IDH1-mutant gliomas.

Data from low-grade glioma patients compiled by The Cancer Genome Atlas (TCGA) show that IDH1 mutations often co-occur with activating PIK3R1 or PIK3CA mutations, together with loss of function mutations in TP53 and ATRX. We first investigated the cooperativity between IDH1 and PIK3R1 mutations in a human astrocytic cell line immortalized via ectopic expression of telomerase (hTERT), which phenocopies inactivating mutations in ATRX, as well as E6 and E7, which inactivate p53 and Rb, respectively. Lines expressing either IDH1 or PIK3R1 mutants exhibited significantly increased colony size and number in soft agar assays compared to the empty vector-expressing line, and these phenotypes were enhanced further in cells expressing both mutants together. Furthermore, intracranial injection of these cell into immunodeficient mice demonstrated significantly increased tumor incidence and aggressiveness in mice injected with cells expressing both oncogenes relative to either oncogene alone.

We used this knowledge to develop our strategy for generating an IDH1-mutant GEMM. We constructed an adeno-associated virus (AAV) encoding Cre-recombinase and sgRNAs targeting murine isoforms of ATRX, TP53, and RB1. This virus was intracranially injected into four different engineered mouse strains [designated: (1) LSL-Cas9; (2) LSL-Cas9; LSL-PIK3CAH1047R (3) LSL-Cas9; LSL-IDH1R132H; (4) LSL-Cas9; LSL-IDH1R132H; LSL-PIK3CAH1047R], where the indicated genes were placed downstream of a loxP-stop-loxP (LSL) cassette. These mice have been monitored for tumor initiation with serial MRIs. One of the first mice injected developed a needle track osteosarcoma, and validated the in vivo efficacy of our sgRNAs and Cre activation efficiency. We then re-engineered our AAV so that Cre was controlled by a tissue-specific glial fibrillary acidic protein (GFAP) promoter and injected it into the four engineered mouse strains. At 3 months post-injection, 3 out of 10 LSL-Cas9; LSL-IDH1R132H; LSL-PIK3CAH1047R mice demonstrated intraparenchymal enhancement on MRI suspicious of developing GBMs. Furthermore, 0 out of 8 double-mutant mice (LSL-Cas9; LSL-PIK3CAH1047R) showed evidence of tumor formation on MRI at this same time point, suggesting that mutant IDH1 is acting as a driver in our model. We anticipate that our IDH1-mutant mice will develop tumors that recapitulate the histopathological, metabolic, and epigenetic changes seen in human IDH1-mutant gliomas.

272 EphA2 receptor tyrosine kinase regulates programmed death ligand 2 expression in tumor cells and inhibits immune infiltration

Eileen Shiuan

Vanderbilt University, Nashville, USA

Given the success of both targeted and immunotherapies in cancer, there is increasing utility for identifying targeted agents that also promote anti-tumor immunity. EphA2 is a receptor tyrosine kinase that contributes to tumor growth and metastasis in various cancer types and plays a role in inflammatory processes. Previous work in our lab demonstrates EphA2 is a viable target for non-small cell lung cancer (NSCLC) and breast cancer. Here, we examine how EphA2 affects immune checkpoint protein interactions, including programmed death-ligands (PD-Ls), and immune response in the tumor microenvironment.

Our preliminary studies suggest EphA2 regulates the expression of PD-L2 but not PD-L1 in human lung and breast cell lines. To investigate this, we induced PD-L2 expression *in vitro* via cytokines, overexpressed or knocked down EphA2, and measured PD ligand expression by flow cytometry. To evaluate the mechanism by which EphA2 affected PD-L2 expression, we curated the ENCODE database to identify transcription factor (TF) binding sites near the PD-L2 promoter and validated individual TF candidates with knockdown experiments. To study *in vivo* effects, we generated an EphA2-overexpressing murine NSCLC cell line from a primary mouse lung tumor. Both subcutaneous and tail vein injected lung tumor models were used to assess the impact of EphA2 overexpression on tumor burden and survival, as well as immune infiltration by flow cytometry.

In human bronchial and mammary epithelial cells, PD-L2 was induced by IFN γ and, to a lesser extent, TNF α and IL-4, and knockdown of EphA2 decreased surface expression of PD-L2. TF binding sites for Myc and p65, among others, were found in the PD-L2 promoter region. Because our lab has previously shown that Myc and YAP are downstream effectors of EphA2, we pursued these TFs for validation studies, which are ongoing. In contrast to human epithelial cells, murine counterparts do not express PD-L2, even after IFN γ stimulation. While the EphA2-overexpressing murine NSCLC cell line did not display proliferative advantage over control cells *in vitro*, they developed larger tumors and had worse survival in both tumor models. Analysis of lung tumor immune infiltrate revealed decreased NK and T cells in the EphA2-overexpressing tumors.

Our studies suggest EphA2 upregulates PD-L2 in cancer cells and inhibits tumor infiltration of key lymphocytic populations. Ongoing investigations are determining the mechanisms behind these findings. Despite PD-L2's known role in immune tolerance, its impact on the tumor microenvironment is understudied compared to PD-L1. Thus, elucidation of EphA2's role in regulating PD-1 and PD-L2 interactions and immune recruitment will further our understanding of PD-1 and PD-L biology and mechanisms of immune evasion, as well as provide additional rationale for targeting EphA2 in cancer.

273 Lymphatic bile acids play an important role in modulating enhanced insulin sensitivity following Roux-en-Y gastric bypass

Ornella E. Simo

Vanderbilt University Medical Center, USA

Bariatric surgery is the most effective and durable treatment for obesity as well as Type 2 diabetes, though the mechanisms underlying its effectiveness remain to be fully elucidated. Roux en Y Gastric Bypass (RYGB) is the most effective and most widely

used bariatric procedure. We previously demonstrated (Nat. Comm, 2015) that bile diversion to the ileum (GB-IL) has identical metabolic effects to RYGB in rodent models of obesity. We showed that the metabolic improvements, particularly the enhanced insulin sensitivity, are associated with circulating bile acids (BAs). In this study we hypothesize that BAs increase incretin responses. We fed C57BL6 mice a high fat diet for 12 weeks, following which the mice were subjected to either bile diversion from the gall bladder to the ileum (GB-IL), or RYGB vs. sham (controls); additionally, each mouse was fitted with a chronic cannula into the mesenteric lymphatics. Four weeks following surgery, and after an overnight fast, lymph samples were collected on hourly basis before (2 h) and after (4 h) nutrient mixed meal bolus (Ensure®). GB-IL and RYGB mice had significant weight loss and reduced food intake during the first week postop. At 4 weeks post-surgery, body fat composition was significantly lower in RYGB and GB-IL and had significantly lower blood glucose levels. Lymph content of triglycerides and phospholipids were remarkably higher in RYGB and GB-IL mice. Plasma BA levels in RYGB and GB-IL were 2-fold and 10-fold higher following controls; lymphatic BAs mirrored the changes in plasma BAs. Plasma GLP-1 levels were undetectable in both groups, but lymphatic incretin levels (GLP-1 and GIP) were significantly higher in GB-IL and RYGB mice. However, only GB-IL mice had significantly higher lymphatic levels of C-peptide compared to other study groups. These results suggest a differential effect of BAs on pancreatic insulin and C-peptide secretion, which may be responsible for a significant component of the improved insulin sensitivity following bariatric surgery.

274 Differential Rna Editing Across *Trypanosoma Brucei* Life-Cycle Stages Reveals Underlying Mechanisms Of Editing Coordination

Rachel M. Simpson

Department of Microbiology and Immunology, University at Buffalo Jacobs School of Medicine and Biomedical Sciences, Buffalo, USA

The order *kinetoplastea* contains multiple human pathogens, including *Trypanosoma brucei* the causative agent of Human African Trypanosomiasis, *Trypanosoma cruzi* of Chaga's disease, and *Leishmania* species responsible for various forms of leishmaniasis. Uridine insertion/deletion RNA editing is an essential and complex process in kinetoplastids whereby mitochondrial mRNAs are modified by specific insertion and deletion of uridines throughout the length of the transcript. Editing generates functional open reading frames that encode mitochondrial respiratory proteins. The unique and essential nature of this process to the parasite makes the mitochondrial RNA editing system an excellent potential drug target. Numerous enzymatic and non-enzymatic factors are required for RNA editing. Additionally, editing is directed by small non-coding guide RNAs (gRNAs) which act as templates for the editing process. Multiple gRNAs are required for complete editing of the majority of transcripts and interactions between the gRNAs and the pre and partially edited mRNAs appear precisely coordinated by mechanisms that are yet unclear. Editing occurs in all lifecycle stages of *T. brucei* and some transcripts appear to have differentially regulated editing and expression levels between the procyclic (insect) stage and the bloodstream (mammalian) stage. The underlying mechanisms for differences observed between lifecycle stages have remained opaque given the limitations of conventional methods to examine the intermediate, partially-edited sequence populations. To overcome this limitation, we developed a novel bioinformatic platform, the Trypanosome RNA Editing Alignment Tool (TREAT), which allows us to examine whole populations of partially edited sequences using

high throughput sequencing (HTS). Using HTS/TREAT, we examine transcripts known to be differentially modified between lifecycle stages in both the procyclic and bloodstream forms of *T. brucei*. We interrogate differences in the order of editing modifications and the mechanisms by which editing progresses between the two lifecycle stages to uncover common and distinct mechanisms responsible for regulating RNA editing in *T. brucei*.

275 GATA2 in normal endometrium and GATA6 in endometriosis are associated with genome-wide H3K27ac histone modification and active transcription of genes essential for tissue phenotypes

Christia Angela M. Sison

Northwestern University Feinberg School of Medicine, Chicago, USA

Endometriosis is a complex inflammatory disease that affects 5-10% of reproductive-age women. The mechanism through which normal intrauterine endometrial cells (NoEM) transform into ectopic endometriotic cells (OSIS) remains unknown. Previous studies from our lab pinpointed the GATA family of transcription factors as key regulators of uterine physiology and pathology. GATA2 regulates key genes necessary for decidualization and GATA6 induces markers of endometriosis. We hypothesize that GATA2 and GATA6 in NoEM and OSIS, respectively, are mechanistically associated with the histone modification H3K27ac that causes active transcription of genes essential for tissue phenotypes.

Both normal intrauterine endometrial and ovarian endometriotic tissues were collected from patients undergoing uterine surgery at Northwestern Memorial Prentice Women's Hospital. We digested the tissue and isolated NoEM and OSIS for primary stromal cell cultures. We used these two groups (n=3 per group) for chromatin immunoprecipitation followed by sequencing (ChIP-Seq) using antibodies against GATA2, GATA6, and H3K27ac. We also utilized RNA-seq to assess differential mRNA expression between NoEM and OSIS.

We found that genome-wide GATA2 binding to DNA is increased in NoEM compared with OSIS, while GATA6 binding is dominant in OSIS versus NoEM. A large number of genes are co-bound by GATA2 in NoEM, GATA6 in OSIS, and H3K27ac in both (n=5,097). Gene ontology was conducted on the overlap of these genes, indicating biological processes significant to their state in the endometrium or endometriosis. In NoEM, genes involved in the regulation of developmental process, cell migration, and cell motility are modulated by GATA2 and H3K27ac. In OSIS, genes involved in mesenchymal cell differentiation, blood vessel development, and positive regulation of cell migration are regulated by GATA6 and H3K27ac. Genes found to be upregulated in OSIS versus NoEM coincide significantly with genes bound by both GATA6 and H3K27ac, demonstrating GATA6 function in marking genes for active transcription in OSIS.

This study uncovers a potential role of GATA2 and GATA6 in the modification of histone marks and active gene transcription in endometrial or endometriotic tissue. GATA2 binds to genes essential for the physiological phenotype in NoEM while GATA6 binds to genes responsible for pathological processes relevant to OSIS. These genes are marked by H3K27ac, indicative of active transcription at both promoters and enhancers, suggesting a role for GATA2 and GATA6 modifying histone marks in these tissues. Upregulation of gene transcription is confirmed by RNA-Seq data, indicating a likely mechanism causing active transcription of genes relevant for each phenotype.

276 Degradable and non-degradable polymeric chloroquine: altering the pharmacokinetics of chloroquine for translational improvements in the treatment of cancer and Inflammatory bowel disease

Richard Sleightholm

University of Nebraska Medical Center, Omaha, USA

Background: Hydroxychloroquine (HCQ) has been used for nearly 70 years for the treatment and prevention of malaria, as well as in the management of autoimmune diseases like rheumatoid arthritis and inflammatory bowel disease (IBD). However, chronic administration can lead to toxicities like retinopathy. Recently, HCQ has been investigated as a sensitizing agent in cancer with radiation and/or chemotherapy. *In vitro* HCQ works well, but translates poorly to *in vivo* cancer models. The pharmacokinetic (PK) profile of HCQ may explain the discrepancy in efficacy between cellular and animal studies. We have previously reported our work on two different polymeric drug analogs of hydroxychloroquine modified using hydroxyethyl starch (CQ-HES) and hydroxypropyl methacrylamide (CQ-HPMA). The biodegradability of CQ-HES makes it suitable for intravenous (i.v.) use, while the stability of CQ-HPMA makes it ideal for oral administration and localized effects in the GI tract.

Methods: The PK profiles of CQ-HES and CQ-HPMA were assessed after single i.v. or oral administration, respectively, and compared to free HCQ administration. HCQ and metabolite levels in blood and tissue were analyzed using extraction and hydrolysis coupled methods to determine free versus polymeric HCQ levels. The anticancer effects of i.v. administered CQ-HES were analyzed in an orthotopic model of pancreatic cancer using Colo357 cells. The anti-inflammatory properties of orally administered CQ-HPMA were assessed in a *C. rodentium*-induced model of IBD in mice.

Results: CQ-HES demonstrated an extended half-life of 17 hours compared to 12 hours with free HCQ in blood (p<0.01). Liver tissue levels of HCQ were substantially higher at 72 hours with CQ-HES administration, 747 versus 27 ng/mg tissue (p<0.001), while liver metabolite levels were drastically reduced with CQ-HES, 46% and 23% lower at 6 and 24 hours, respectively (p<0.01). Moreover, primary tumor growth was substantially reduced in mice receiving CQ-HES (p<0.001) and displayed no observable liver metastasis versus ~50% in the control groups (p<0.05). With oral administration of CQ-HPMA, nearly all HCQ was retained in the colon and persisted in the polymeric form. HCQ and CQ-HPMA similarly reduced inflammatory cytokine levels and apoptosis in crypt cells. However, CQ-HPMA more readily reduced macrophage infiltration and demonstrated better overall pathologic resolution of colitis (p<0.05).

Conclusion: CQ-HES improves circulating levels of HCQ translating to reduced tumor growth and metastasis when given i.v. Conversely, non-degradable CQ-HPMA is almost solely retained in the colon when given orally and may reduce inflammation in IBD while circumventing the toxicities of chronic HCQ therapy. Thus, polymeric HCQ analogs retain the biological activity of HCQ, but because of their ability to alter the PK profile of HCQ, they can produce more favorable outcomes and increased therapeutic indexes. In conclusion, creating polymeric drug formulations represent an underutilized method to improve current drug formulations.

277 Animal Model of Human Ankyrin-B Syndrome Exhibits Adrenergic-Mediated Arrhythmias

Ellen Lubbers

The Ohio State University, Columbus, USA

Ankyrin-B (AnkB) is a spectrin-associated cytoskeletal protein that plays a critical role in anchoring the Na⁺/Ca²⁺ exchanger (NCX), the Na⁺/K⁺ ATPase, and the inositol triphosphate receptor at the transverse tubules and sarcoplasmic reticulum in cardiomyocytes. Additionally, loss-of-function mutations in AnkB cause various arrhythmia phenotypes including long QT (LQTS4), sinus bradycardia, ventricular fibrillation, catecholaminergic polymorphic ventricular tachycardia, and atrial fibrillation. Past work has identified an AnkB variant L1622I, which has been associated with human arrhythmia. Patients harboring this variant present with a long QT interval, ventricular tachycardia, and ventricular fibrillation. In this study, we investigated the cellular phenotypes of a knock-in mouse model carrying the L1622I AnkB variant. To determine the role of the L1622I variant in AnkB, cardiomyocytes were isolated from adult L1622I mice. Previous studies have shown prolongation of the late phase of the action potential and frequent early afterdepolarizations (EADs) and spontaneous activity when treated with 1μM isoproterenol (ISO). We hypothesized that these arrhythmogenic substrates were due an exacerbation of calcium overload caused by loss of proper localization of NCX. However, immunofluorescence staining of isolated cardiomyocytes showed reduced, but correctly localized NCX in L1622I mice. While small, this reduction may be sufficient to produce arrhythmia, as telemetered ECG recordings revealed arrhythmia in mice dosed with epinephrine (2mg/kg). In conclusion, reduced NCX displayed in L1622I mice provide a potential basis for the stress induced arrhythmias of patients harboring this AnkB variant.

278 Combining Key Residues of the Russian and U.S. Live Attenuated Influenza Virus' for a More Attenuated Vaccine

Andrew Smith

University of Rochester, Rochester, USA

Seasonal influenza infects 50 million people every year in the United States, leading to the hospitalization of between 50,000 and 200,000, and the death of between 2,000 and 49,000 people a year. While formerly efficacious as a vaccine the Live Attenuated Influenza Virus (LAIV) based on the cold passaged A/AnnArbor/6/60 strain that was licensed for use in the United States is no longer recommended for use due to a sudden decline in sub-type specific efficacy, which is currently not well understood. However, the LAIV based on the cold passaged A/Leningrad/134/17/57 is still in use as a seasonal vaccine in multiple countries around the world. When previously in use, the U.S. LAIV was found during multiple sequential influenza seasons to have superior efficacy in children as compared to the inactivated influenza vaccine. During its use in the U.S. LAIV was not recommended for children under two years of age due to wheezing. This wheezing is due to LAIV replicating at high enough levels in young children to be mildly pathogenic. Investigations into alterations of attenuation and safety of LAIV in a mouse model were previously impossible due to the limited replication of both LAIVs in mice. To solve this problem, our lab developed a mouse-model virus that permits investigations of alterations in attenuation and safety of LAIVs in mice, in addition to efficacy, by making the amino-acid substitutions responsible for the temperature sensitive (ts) and attenuated (att) phenotypes of LAIV in the mouse adapted virus, A/Puerto Rico/8/1934. In this study, we use this model virus to show that using various combinations of the previously identified residues responsible for the ts and att phenotypes of both Ann Arbor

and Leningrad strain LAIVs, we can generate LAIVs with a range of replication phenotypes that could potentially expand the range of ages in which LAIVs can be safely used.

279 Weakly and semi-supervised deep learning for immunohistochemistry feature representation in tissue microarrays with generative adversarial networks

Andrew M. Sohn

Perelman School of Medicine, University of Pennsylvania, USA

Histopathology is still considered to be the gold standard in the diagnoses of many cancers. Recently, there have been two major developments that are poised to change the face of pathology at the center of clinical diagnosis: (1) digital pathology, and (2) molecular profiling technologies. The emergence of digital pathology allows for the introduction of automated image analysis to pathology, which can greatly aid a pathologist's workflow and offer new quantitative tools that are otherwise laboriously prohibitive. Molecular technologies offer complementary information probed at a resolution that is not accessible by tissue morphology and phenotype analyses. While we are presently in the era of 'omics', histological images still provide important features that are unavailable from molecular profiling/omics data, such as the spatial context of the tumor microenvironment.

The 50,000-foot view of our work is an attempt to extract phenotypic features from tissue microarrays (TMAs) and correlate with genetic features. To extract phenotypic features, we use techniques from semi-supervised deep learning, and more specifically, generative adversarial networks (GANs). Very briefly GANs are a class of generative models (as opposed to discriminative models) that can perform representation learning on unlabeled data by imitating a real data distribution via transforming noise variables into synthetic data within target domain. Using GANs, we perform data augmentation and image-to-image translation/image style transfer (among IHC stains) as proxies for representation learning as well as disentangled representation learning. Once a robust deep learning model has been trained, we will search for a common feature space for the phenotypic and genetic features, followed by clustering analyses to observe whether any phenotypic and genetic features correlate with one another.

We perform our analyses on a dataset of BRCA1 and BRCA2 germline mutation-associated breast and ovarian tumors. The dataset consists of TMAs with twenty different immunohistochemistry stains (stromal and immune) and genetic profiles generated from exome sequencing. This dataset has been generated and compiled from patients seen at the Hospital of the University of Pennsylvania.

280 CaCO₃ nanoparticles modulate the tumor microenvironment pH and subsequently inhibit growth and metastasis

Avik Som

Washington University in St. Louis, Houston, USA

Models on tumor extracellular pH (pHe) demonstrate a significant relationship between tumor invasiveness, chemotherapy resistance and the increased production of acid in the extracellular environment most tumors. Very few groups have attempted to modulate this pH microenvironment for therapeutic purposes via nanoparticles. The therapeutic potential of modulating the pH has been realized recently through the demonstration of metastasis inhibition from the systemic administration of oral sodium bicarbonate, but is not practical. A nanoparticle delivery of this base may allow similar therapeutic results with significantly lower doses and thereby significantly lower degrees of toxicity. We have been able to demonstrate the synthesis

and stabilization of nano-CaCO₃ particles in water via the use of an albumin based solution. In addition, we demonstrate the particle's ability for modulating pH *in vivo* and the subsequent inhibition of growth and metastasis.

281 A systematic approach to identify proteins that interact with the aryl hydrocarbon receptor *in vivo*

Jaclyn Souder

University of Alabama at Birmingham, Houston, USA

The aryl hydrocarbon receptor (AHR) is a ligand-dependent transcription factor that is involved in multiple developmental processes including hematopoiesis and cardiac development. One hypothesis is that AHR recruits cofactors in a ligand- and tissue-specific manner to elicit biological effects, yet this has not been confirmed *in vivo*. This hypothesis could be tested by analyzing AHR cofactor recruitment in specific tissues following treatment with AHR ligands. Zebrafish embryos provide an attractive model to test this hypothesis due to the ease of chemical exposure and genetic manipulation, and conservation of AHR signaling. We used CRISPR-Cas9 to generate knock-in zebrafish lines with epitope-tagged AHR2 (the zebrafish paralogue of AHR) to reliably and efficiently isolate AHR2 and its bound proteins *in vivo*. In addition, we generated a loss-of-function AHR2 mutant line (AHR2^{-/-}) that demonstrates ragged-fin and protruding jaw phenotypes in adulthood, allowing us to determine if our knock-in lines retain normal AHR2 function. In parallel, we created 1) a single epitope AHR2-V5 line with a 14 peptide V5 tag inserted in the *ahr2* gene, 2) a double epitope AHR2-SA-V5 line with a modified streptavidin Strep II (SA) + V5 insertion, and 3) a triple epitope AHR2-FSV line with a FLAG + SA + V5 insertion. Beginning with the AHR2-V5 line, we first derived homozygous AHR2-V5 embryos, then confirmed epitope utility by immunoprecipitation of the AHR2-V5 protein in pooled embryos via both western blot and mass spectrometry. We next confirmed that epitope insertion did not affect normal protein function in embryos and adults, by treating homozygous embryos with TCDD, which causes AHR2-dependent cardiotoxicity in embryos, and comparing AHR2-V5 adults with AHR2^{-/-} mutant adults. AHR2^{-/-} embryos do not respond to TCDD treatment, while AHR2-V5 embryos demonstrate cardiotoxicity equivalent to wildtype embryos, confirming normal protein function in AHR2-V5 embryos. Further, AHR2-V5 homozygote adults are phenotypically normal, in contrast to AHR2^{-/-} adults, confirming normal protein function in AHR2-V5 adults. Future studies will utilize AHR2-V5 embryos in a mass spectrometry-based assay to identify tissue- or ligand-specific cofactor recruitment by AHR2 and potentially discover novel interacting proteins of AHR2. We will also confirm the functional utility of our other knock-in lines using this systematic approach.

282 Evaluation and prevention of heart disease using three fatty acids from postprandial pythons

Kelsey M. Spaur

University of Colorado School of Medicine, USA

Extreme environments drive species to develop novel adaptations, which have been a source of scientific innovation for years. For the Burmese python, its environmental pressure is infrequent feeding. Following a meal weighing up to its body weight, multiple organs undergo significant growth to accommodate a 40-fold increase in metabolic rate. Regarding the heart, the Leinwand lab showed that this hypertrophy is physiologic rather than pathologic by several criteria including a signature of gene expression changes that were distinct from those of pathological hypertrophic growth. Most notable of the genes activated by serum from post-fed pythons was the water

and glycerol transporter aquaporin 7 (AQP7). From post-fed python plasma, they identified a combination of three fatty acids (FAs) that replicated cardiac hypertrophy when administered subcutaneously to pythons and mice and when applied to cultured neonatal rat ventricular myocytes (NRVMs). The FAs were: 40 mM myristic (C14:0), 100 mM palmitic (C16:0), and 7.5 mM palmitoleic (C16:1).

In this study, we evaluated the capacity for the FAs to prevent or reduce negative cardiac changes due to pathologic stimuli. This hypothesis was first tested using FAs dissolved in dimethyl sulfoxide (DMSO) and NRVMs. Administering FAs to NRVMs prior to the pathologic hypertrophic stimulus, phenylephrine (PE), blunted the hypertrophic effect of PE compared to DMSO controls after 48 hours of total treatment. We also applied FAs to NRVMs following PE for 48 hours and still saw a significant increase in AQP7 expression relative to DMSO controls. This induction of AQP7 and the reduction of pathologic hypertrophy in the presence of a pathologic stimulus suggests that the FAs can exert a dominant effect. These *in-vitro* findings led us to investigate *in-vivo*. Due to variability seen using DMSO-FAs mini-pumps, we investigated oral gavage as an alternate route of administration. Several recent papers have shown efficacy of FAs via oral gavage for other purposes. The FAs were suspended in corn oil and administered to two cohorts of mice for four weeks. The groups were either six or ten weeks of age at the beginning of the experiment. We did not see cardiac hypertrophy in either group, but the six week group did show significant up-regulation of α -MyHC, which is an indication of a physiologic effect. Although oral gavage does not cause a robust enough response to be utilized for future experiments, this finding indicates there was some effect. We recently conjugated the FAs to bovine serum albumin (BSA). Our next step is to test BSA-FAs on NRVMs to ensure they induce the hypertrophy we have seen with DMSO-FAs. If successful, we will perform mini-pump experiments in mice. Our ultimate goal is to administer FAs *in-vivo* prior to or following a pathologic stimulus such as PE or trans-aortic constriction.

283 The role of neural stem cell-derived extracellular vesicles as a therapeutic in a porcine middle cerebral artery occlusion model of stroke.

Samantha E. Spellicy

Medical College of Georgia and the University of Georgia, Athens, USA

Stroke annually claims over 6 million lives worldwide and is the 3rd leading cause of death for adults in the United States. Currently, there is only one FDA-approved small molecule therapy for ischemic stroke, tissue plasminogen activator (tPA). Extracellular vesicles (EVs), or cell-derived nanoparticles, have been shown to be involved in a range of normal physiological processes as well as tissue repair, stem cell maintenance, and immune surveillance. We propose to use neural stem cell-derived extracellular vesicles (NSCEVs), as a potential novel neuroprotective therapeutic to limit gait and behavioral impairments following middle cerebral artery occlusion (MCAO) in a porcine stroke model.

EVs were first isolated by ultrafiltration from the spent media of neural stem cells. We then performed various *in vitro* assays, such as mass spectroscopy and Spatial Light Interference Microscopy (SLIM), for the characterization and visualization of these NSCEVs. For this study, we used 16 castrated male landrace pigs which were divided into either NSCEV or sham treatment groups. Following MCAO, pigs were IV-administered NSCEVs or PBS solution, respectively, at 2, 14, and 24 hours. Longitudinal gait and behavioral tests were conducted over 84 days post-MCAO to evaluate functional recovery.

Magnetic resonance imaging (MRI) was conducted at 1 and 84 days post-MCAO.

Characterization of NSCEVs through mass spectroscopy revealed they contained 17/18 of the most commonly reported EV markers. SLIM imaging studies revealed efficient and robust uptake and internalization of NSCEVs by mesenchymal stem cells (MSCs). MRI conducted on Day 1 post-MCAO demonstrated that NSCEV treatment eliminated intracranial hemorrhage (ICH) following ischemic lesion (0/7 NSCEV treated vs. 7/8 sham group). In addition, NSCEV treatment resulted in decreased midline shift, as well a significant ($p < 0.01$) decrease in cerebral infarct volume and edema when compared to sham pigs. Through functional testing at 1-week post-MCAO, NSCEV-treated pigs showed limited changes in measured open field and gait parameters, while control pigs had a statistically significant ($p < 0.01$) decrease in velocity and distance traveled during open field testing, as well as in cadence, stride length, and relative pressure measured during gait testing. At 12 weeks post-MCAO, NSCEV-treated pigs had significant ($p > 0.01$) increases in velocity and distance traveled from their pre-MCAO open field testing, while sham pigs did not.

In this study, we demonstrated for the first time that intravenous treatment of NSCEVs in a porcine large animal ischemic stroke model can robustly prevent critical structural changes in the brain, limiting functional gait and behavioral deficits and promoting recovery.

284 HLA-E-expressing “universal” pluripotent stem cells as a source of retinal pigment epithelium to treat age-related macular degeneration

Marta Stevanovic

University of Southern California, USA

Identifying a suitable stem cell source for retinal pigmented epithelium (RPE) has been a challenge in treating dry age-related macular degeneration (AMD). Using human embryonic stem cells (hESC), which express polymorphic human leukocyte antigens (HLA), may cause immune rejection. Creating induced pluripotent stem cells from a patient's own tissue is costly and time-consuming. A solution may be to use “universal stem cells” (Ucells), which do not express polymorphic HLA proteins. We differentiated Ucells into RPE and tested the phenotype and function of RPE derived from U3 (lack HLA class I expression), U37 (lack HLA class I and II expression), and the controls U1 and H9 in vitro. We will inject U1-, U3-, and U37-RPE cell suspensions into the subretinal space of pigmented athymic nude-RCS rats with RPE dysfunction to test the ability of Ucell-RPE to rescue photoreceptor function in vivo.

Quantitative PCR (Q-PCR) was used to analyze RPE gene expression and test for genes of contaminating cell types. Morphology and epithelial polarity were assessed using light microscopy and immunohistochemistry. Differentiation efficiency was examined by flow cytometry using the Pmel17 antibody, which labels pigmented cells. Loss of Oct4, a pluripotency marker, was also determined by flow cytometry. Ucell-RPE function was analyzed by measuring secretion of the growth factor PEDF using ELISA assays and also by measuring the ability of Ucell-RPE to carry out phagocytosis of bovine photoreceptor outer segments. For all in vitro studies, hESC-derived (H9) RPE was a positive control. For the in vivo study, immunocytochemistry of retinal tissue will be performed 1 and 3 months after injections. Photoreceptor nuclei in the outer nuclear layer will be quantified and rod/cone ratios will be determined. Phagocytic capability of the Ucell-RPE will be examined by staining tissue sections for rhodopsin and quantifying phagosomes. For all in vivo experiments, U1-RPE will be used as a positive control and

sham surgery as a negative control.

Ucell and H9-RPE showed similar expression of RPE-specific genes, including visual cycle genes (RPE65, CRLBP), RPE membrane channel and transporter genes (BEST1), and pigment and melanin biosynthesis genes (TYRP1, tyrosinase, and MITF). The Pmel17 gene was expressed in 86.12 ± 0.9248 % of U1-, 84.65 ± 1.392 % of U3-, and 88.67 ± 1.506 % of H9-RPE. There was no significant difference between U3- and U1-RPE (Mann-Whitney test, two-tailed, $p = 0.4$) or U3- and H9-RPE (Mann-Whitney test, two-tailed, $p = 0.1$) Pmel17 expression. Ucell-RPE morphology and phagocytosis ability were also similar to those of H9-RPE.

Our results in vitro show that Ucell-RPE is similar in form and function to H9-RPE (in vivo results pending). RPE from Ucells is a novel approach to bypass immune-mediated graft rejection without using immunosuppression. Using Ucells as progenitors may be also be applicable to transplantation of other cell types.

285 Exploring substrate promiscuity toward a novel method of sortase-mediated bioorthogonal protein labeling

Erica M. Storm

Stanford University School of Medicine, USA

Sortases are bacterial transpeptidases with wide applications for post-translational covalent modification of proteins. Sortase A is highly specific for its LPXTG peptide recognition motif which it incorporates to any substrate with a terminal oligoglycine moiety. Recent engineering of sortase A has improved its catalytic activity, but its utility for in vivo labeling remains limited by the lack of cell permeable and commercial available oligoglycine peptide probes. Thus, there remains a need for a versatile bioorthogonal method of site-specific protein labeling in living cells.

We present a two-step, sortase-based approach to in vivo protein labeling using an intermediate azide tag. First, we demonstrated that an engineered sortase A variant (termed 7M) exhibits promiscuous activity with an array of primary amines including 3-azido-1-propanamine (Azp) and propargylglycine, with incorporation rates of up to 80-100%. By using sortase A 7M to enzymatically label proteins with Azp, we showed that fluorescent probes could then be added through click chemistry via the azide tag. We have demonstrated this strategy both in vitro and in vivo using an Escherichia coli expression system. Application of 25 mM Azp to E. coli cultures coexpressing sortase A 7M and an LPTEG-tagged GFP variant, followed by incubation with a Cy3-dibenzocyclooctyne (DBCO) modified dye yielded complete conversion to the labeled protein conjugates.

To demonstrate the versatility of our sortase bioconjugation system, we sought to optimize the sortase labeling reaction in mammalian cells. Sortase A 7M was successfully expressed at low levels in adherent HEK293 cells, but not in suspension HEK293 cultures. Conversely, suspension HEK cultures displayed 800-fold lower sensitivity to Azp concentrations than adherent HEK cells. Thus, engineering of sortase A for selective Azp activity is essential not only to expand the toolbox of sortase variants but to reduce concentrations of Azp substrate to sustainable levels for mammalian culture.

Towards this end, a yeast-display library of 160,000 sortase A 7M variants was generated through saturation mutagenesis of four residues within the predicted oligoglycine pocket of sortase A. In order to quantify the bioconjugation reaction of yeast-displayed sortase variants, we developed a simplified dual-protein expression vector, termed pCL. Our construct utilizes both termini of the α -agglutinin mating protein (Aga2p) subunit to facilitate internal conjugation of the LPETG recognition motif by co-displayed sortase A. Induction of

the pCL yeast library in the presence of Azp was followed by copper-free click reaction with biotin-DBCO and conjugation detected by staining with PE-labeled avidin. Fluorescence activated cell sorting (FACS) will be used to select enzyme variants for sequencing and additional kinetic characterization. Identifying sortase variants with improved Azp functionality will further demonstrate the versatility of our pCL display system and facilitate biorthogonal site-specific protein labeling in mammalian cells.

286 Krüppel-like factor 2 regulates an extracellular matrix remodeling transcriptional network in macrophages

David R. Sweet

Case Western Reserve University and University Hospitals Cleveland Medical Center, Cleveland, USA

Fibrosis, the result of unrestrained wound healing processes, affects nearly every organ system and significantly contributes to mortality in the United States. With advancing age, chronic noxious insults result in cellular damage with compensatory tissue remodeling. Macrophages are central orchestrators of physiological and pathological tissue remodeling, secreting a multitude of proteases, growth factors, and chemokines that result in cellular proliferation, matrix deposition, and angiogenesis. Modulating the macrophage response to tissue damage, therefore, represents a potential therapeutic avenue for diseases of aberrant ECM remodeling. Previous work in our group has identified Krüppel-like factor 2 (KLF2) as a tonic repressor of macrophage activation, serving as a “transcriptional brake” that resists inflammation. While the loss of myeloid KLF2 results in robust inflammatory activation and inflammatory disease *in vivo*, the effects of sustained overexpression of myeloid KLF2 are unknown. High throughput RNA sequencing analysis on macrophages deficient in KLF2 indicates substantial downregulation of genes critical to ECM remodeling, providing the basis of our hypothesis that KLF2 governs macrophage ability to remodel matrix during physiological and pathological processes. To determine if KLF2 expression is critical in acute ECM remodeling, we performed a cutaneous wound healing assay in mice with myeloid specific deletion (K2KO) or overexpression (K2Tg) of KLF2. We observed substantial impairment in wound healing in K2KO mice while K2Tg mice healed faster than control mice, suggesting that KLF2 promotes beneficial ECM dynamics and regeneration. Given that age is a risk factor for many fibrotic diseases, we sought to explore whether myeloid KLF2 fostered pathological ECM remodeling as well. Indeed, aged K2Tg mice demonstrated enhanced spontaneous fibrosis of multiple organs including kidney, lung, and heart. In addition, the fibrotic change seen in K2Tg hearts contributed to systolic dysfunction as evidenced by echocardiographic features. Mechanistically, macrophages isolated from K2Tg mice exhibit increased transcription of genes associated with ECM remodeling including fibroblast-stimulating growth factors (e.g. *Fgf2*, *Fgf18*, *Hgf*, *Igf1*), matrix metalloproteinases (e.g. *Mmp2*, *Mmp12*, *Mmp13*), angiogenic factors (e.g. *Vegfa*, *Vegfb*, *Vegfd*), and markers of ‘profibrotic’ polarization (e.g. *Arg1*, *Ym1*, *Ccl17*). These data, along with ongoing studies, provide insight into the central role KLF2 plays in coordinating an ECM remodeling transcriptional network. This work will serve as a nidus for future studies in targeted therapies for ECM remodeling processes including wound healing, fibrotic disease, and cancer.

287 Decreased expression of TCF12 transcription factor in glioblastoma stem-like cells results in an increased mesenchymal subtype signature

Rukayat M. Taiwo

Washington University School of Medicine, USA

The basic helix-loop-helix (bHLH) transcription factor, TCF12, has been implicated in precursor cell proliferation during embryogenic neurogenesis and continues to be expressed postnatally in mitotically active regions of the brain. TCF12 has been shown to be preferentially expressed in glioblastoma stem-like cells (GSCs), a key subpopulation of cancer cells thought to underlie tumor therapy resistance and recurrence. But the exact role of TCF12 in gliomagenesis has remained unclear since it has been shown to be both a proto-oncogene and tumor suppressor depending on the cellular context. We therefore investigated the potential role of TCF12 in regulating the biology of GSCs. Using microarray analysis of 24 patient-derived GSCs, we find that TCF12 is highly expressed in proneural GSCs relative to normal human astrocytes, and differentiation of proneural GSCs in culture markedly downregulated TCF12 mRNA. To test the role of TCF12 in GSCs, loss-of-function approaches using both RNA interference and CRISPR-Cas9-mediated knockout demonstrated reduced self-renewal capacity, a key measure of stem-like cell identity, relative to control infection. Conversely, over-expression of TCF12 using a lentiviral approach increased GSC self-renewal capacity. Mechanistically, a mini-screen of candidates known to regulate GSC self-renewal revealed that knock-down of TCF12 led to a decrease in the expression of the bHLH transcription factor, OLIG2, helix-loop-helix protein, ID1. By contrast, over-expression of TCF12 led to increased expression of these markers. Furthermore, bioinformatic analysis of the genomic regions upstream of OLIG2 and ID1 transcription start sites revealed the presence of evolutionarily conserved TCF12 binding sites, implicating these stem-identity genes as potential transcriptional targets of TCF12. Taken together, these findings suggest that TCF12 controls the stem-like identity of proneural GSCs by stimulating expression of transcriptional regulators OLIG2 and ID1. Finally, using OLIG2 and CD44 as markers of proneural and mesenchymal identity respectively, knock down of TCF12 demonstrated decreased OLIG2 expression with a concomitant increase in CD44 expression. These findings suggest that TCF12 is necessary for the maintenance of a proneural stem identity and loss of TCF12 may lead to a switch from proneural to mesenchymal subtype.

288 CK1δ-BRD4 pathway as novel therapeutic target for SHH subtype of medulloblastoma

Sze Kiat Tan

University of Miami Miller School of Medicine, Miami, USA

Background: Medulloblastoma is the most common malignant pediatric brain tumor with variable prognosis due to its clinical and genomic heterogeneity. Despite decades of treatment advances, approximately 40% of children experience tumour recurrence, and 30% will die from this disease. Thus, new drugs and drug combinations need to be developed that effectively treat medulloblastoma. Casein kinase 1δ (CK1δ) is a serine/threonine kinase that controls cell cycle progression, signal transduction and neurogenesis, and we previously reported high levels of CK1δ in mouse models of medulloblastoma. BRD4 is an epigenetic reader protein that controls expression of several oncogenes. We wanted to determine the mechanism through which CK1δ regulates BRD4 activity. We also wanted to assess whether a combination of CK1δ and BRD4 inhibitors could be more effective in decreasing medulloblastoma progression *in vivo*.

Methods: Granule cell progenitors (GCPs), medulloblastoma *Ptch*^{-/-}*P53*^{-/-} mouse cells and *SUFU*^{-/-} mouse embryonic fibroblasts were incubated with the CK1δ inhibitor SR-1277 and the phosphorylation levels of BRD4 were determined by WB and its binding to chromatin by ChIP. *In vitro* phosphorylation studies with human BRD4 purified from *E. coli* were performed. In addition, we tested whether genetic disruption of CK1δ also reduced BRD4 phosphorylation. We combined BRD4 and CK1δ inhibitors (JQ1 and SR-1277, respectively) and analysed Gli1 mRNA expression and EdU incorporation to determine synergistic effects. We deleted CK1δ in GCPs in *Ptch*^{-/-}*P53*^{-/-} mouse models of medulloblastoma by breeding these mice with a Tg(*Atoh1-Cre*);*CK1δ*^{fl/fl} strain. Furthermore, we intracranially transplanted human SHH medulloblastoma TB-14-7196 cells expressing luciferase in mice, to validate the combination therapy.

Results: CK1δ inhibitor treatment and CK1δ knockout reduced BRD4 phosphorylation, suggesting that CK1δ phosphorylates BRD4 and is required for BRD4 recruitment to chromatin. *In vitro* phosphorylation studies with purified human BRD4 and CK1δ confirmed CK1δ-mediated BRD4 phosphorylation and CK1δ is required for BRD4 phosphorylation at serine 492 and 494 *in vivo*. Using loss of function studies in GCPs, both CK1δ and BET inhibition reduced BRD4 association with Gli1 promoter, thereby reducing Gli1 mRNA levels. Furthermore, SR-1277 suppressed SHH signaling downstream of *SUFU* of medulloblastoma cells, *in vitro* and *in vivo*. We also found synergy by combining these compounds *in vitro* and in reducing tumor burden in the *in vivo* model with intracranial allografts.

Conclusion: Together, our studies validate the CK1δ-BRD4 pathway as a novel target in medulloblastoma. The significance of our work is underscored by the possibility that simultaneous CK1δ-BRD4 inhibition could overcome the resistance observed with BRD4 inhibitors and we are the first group to demonstrate that CK1δ acts downstream of SHH signalling in SHH-driven medulloblastoma. Since CK1δ inhibition could decrease BRD4 phosphorylation and signaling via the WNT pathway, it is feasible that combinatorial therapy may reduce BET resistance and enhance therapeutic benefits to patients.

289 Intrahepatic CD206⁺ macrophages contribute to inflammation in advanced viral-related liver disease

Alfonso Tan Garcia
Duke-NUS Medical School, singapore, Singapore

Liver inflammation is central to the progression of chronic viral hepatitis to cirrhosis and hepatocellular carcinoma. Monocytes and macrophages (CD14⁺ myeloid cells) are increasingly recognised as protagonists of chronic viral-related liver inflammation but their functional characterisation and relation to inflammation in human livers is still poorly understood. We aim to better define the mechanisms by which intrahepatic CD14⁺ myeloid cells contribute to chronic viral-related liver inflammation. Detailed phenotypic, molecular and functional characterisation of intrahepatic CD14⁺ myeloid cells from healthy donors and patients with viral-related liver cirrhosis (HBV, HBV/HDV or HCV) was performed. Unsupervised analysis of multi-parametric data revealed that chronic viral-related liver inflammation was associated with the expansion of activated CD14⁺ myeloid cells within the liver, primarily pro-inflammatory CD14⁺HLA-DR^{hi}CD206⁺ cells, which spontaneously produced TNFα and GM-CSF. These cells were refractory to endotoxin-induced tolerance and displayed robust pro-inflammatory responses to bacterial TLR agonists. Using a humanised mouse model of HBV-induced liver inflammation, we observed a similar accumulation of CD14⁺HLA-DR^{hi}CD206⁺ cells in HBV-infected mice which occurred in a temporal and liver-specific manner. Treatment with oral antibiotics abrogated this intrahepatic

accumulation of CD14⁺HLA-DR^{hi}CD206⁺ cells, indicating an involvement of gut-derived microbial products in liver inflammation. There were significant positive correlations between bacterial product translocation, serum GM-CSF concentration and the intrahepatic frequency of CD14⁺HLA-DR^{hi}CD206⁺ cells. We demonstrated that bacterial products (LPS) increased the expression of CD206 and pro-inflammatory cytokine secretion by CD14⁺ myeloid cells in a GM-CSF-dependent manner and was abolished with anti-GM-CSF neutralising antibodies, suggesting a previously undefined role for GM-CSF in chronic liver inflammation. These findings highlight the importance of the gut-liver axis in chronic viral-related liver inflammation and support the use of gut microbiome-modifying, specific CD206⁺ macrophage-depleting or GM-CSF-neutralising therapies for the management of these patients.

290 The role of cerebellum in Huntington's disease

Alexander V. Tereshchenko
University of Iowa, Iowa City, USA

Huntington's disease (HD) is a fatal neurodegenerative disorder caused by a CAG trinucleotide expansion in the huntingtin (*HTT*) gene. The characteristic neuropathological change associated with HD is striatal atrophy. While MRI studies have shown that striatal volume decreases up to 20 years before the disease onset, patients have no detectable motor symptoms. This suggests that another brain region compensates for failing striatal function. Previous animal tracing studies established that bidirectional connections exist between cerebellum and striatum. The purpose of our study was to assess cerebello-striatal connectivity patterns in a sample of pre-symptomatic HD subjects.

The University of Iowa Kids-HD program enrolls participants 6-25 years of age who have a family history of HD. The subjects were tested for *HTT* gene expansion. All genetic information is used for research purposes only. Subjects with CAG >40 are called gene-expanded (GE) – they are currently pre-symptomatic, but will develop HD as an adult. A total of 64 GE children were studied (mean CAG = 46). GE subjects were compared to a large combined control (CC) group composed of subjects who did not inherit a gene expansion plus the subjects from families with no HD (n = 131, mean CAG = 20). Each participant undergoes an MRI scan, including resting state fMRI. Seed-to-seed connectivity in the cerebello-striatal network was evaluated between groups.

GE subjects had substantially increased resting state functional connectivity between anterior cerebellar lobe and dentate nucleus ($p < 0.05$). Notably, we observed no statistically significant changes in the basal ganglia connectivity of the GE cohort (dorsal caudal putamen to globus pallidus externus to subthalamic nucleus). Finally, higher number of CAG repeats within GE group was associated with stronger connectivity between cerebellar seeds.

The primary pathology of HD extends beyond the striatal changes. Mutant *HTT* may alter not only striatal development, but also the cerebello-striatal connectivity. Cerebello-striatal network directly integrates with indirect pathway in the basal ganglia, which is responsible for suppressing excess movements. Increased cerebellar activity stimulates indirect pathway, inhibiting involuntary movement in pre-symptomatic HD adults. When cerebellar compensation fails, symptoms of chorea emerge. Further study is needed to assess how cerebellar function in HD changes across the entire disease span.

291 Breast cancer anti-estrogen resistance 3 (BCAR3) regulates epithelial homeostasis, cell migration, and tumor growth in colorectal cancer

Joshua Thompson

Vanderbilt University, Nashville, USA

Blood vessel epicardial substance (BVES) is a tight junction-associated protein that regulates epithelial-to-mesenchymal transition (EMT) and functions as a tumor suppressor in colorectal cancer (CRC). Through a yeast two-hybrid screen, BVES was shown to interact with breast cancer anti-estrogen resistance 3 (BCAR3). BCAR3 was originally identified via its upregulation in tamoxifen resistant breast cancer cell lines and functions as an adapter protein, recruiting p130Cas to focal adhesions, and regulating cellular adhesion, migration, and proliferation. We sought to define the role of BCAR3 in colorectal cancer (CRC) and determined which cellular phenotypes were dependent on the BCAR3-p130 interaction.

We began by analyzing the combined Moffitt Cancer Center/Vanderbilt University Medical Center CRC expression array dataset consisting of normal, adenomatous, and 250 tumor samples organized by tumor stage. BCAR3 was downregulated in adenomas ($p = 0.01075$) and further decreased at all CRC stages ($p = 4.527e-07$). Analysis of TCGA RNASeq data confirmed reductions at all stages ($p < 2.2e-16$). In a panel of paired normal and tumor samples, BCAR3 expression was reduced in seven out of eleven samples but was significantly elevated in a subset ($n=3$) of tumors. shRNA knockdown of BCAR3 and Crispr-Cas9 mediated knockout of BCAR3 in HCT116 cells impaired transwell migration. Conversely, in the low BCAR3 expressing MC38 cells, stable lentiviral expression of mouse BCAR3 (mBCAR3) increased transwell migration and invasion through Matrigel coated inserts (34.7 ± 2.0 vs. 106.2 ± 4.5 , $p < 0.0001$ and 4.2 ± 0.4 vs. 7.1 ± 0.7 migrated cells per 20x field, $p = 0.0003$). Metastasis modeling via splenic injection of MC38 cells demonstrated increased micrometastasis in the mBCAR3 expressing line (4.6 ± 3.1 vs. 15.8 ± 3.3 surface micrometastasis in left lateral liver lobe, $p = 0.03$), implicating BCAR3 in colorectal migration and metastasis. Mechanistically, BCAR3 mediated transwell migration is dependent on the BCAR3-p130Cas interaction as BCAR3 addback with a BCAR3-p130 uncoupling mutant abrogates migratory phenotypes in both HCT116 and MC38 cells.

Interestingly, altering BCAR3 expression has minimal effect on proliferation *in vitro*, but subcutaneous allografts of MC38 cells in syngeneic C57BL/6 mice demonstrated a 4-fold increase in tumor volume 10 days post-injection (72.7 ± 7.9 vs. 301.4 ± 40.3 mm³, $p = 0.0012$). cDNA rescue using a guide-RNA resistant BCAR3 construct in HCT116 Crispr KO lines similarly promotes tumor growth. This discordance between *in vivo* and *in vitro* tumor growth may be attributable to circulating growth factors as BCAR3 is known to aid in integrating receptor tyrosine kinase mediated signaling cascades. Accordingly, we show for the first time here that BCAR3 interacts with the hepatocyte growth factor (HGF) receptor, cMET, and can alter cMET phosphorylation. Together, these results implicate BCAR3 in cell migration, tumor growth, and receptor tyrosine kinase signaling in CRC.

292 Hyaluronic Acid-Astrocyte Extracellular Matrix Hydrogels Improve Histological Outcomes following Spinal Cord Injury and Support V2a Interneuron Transplantation

Russell E. Thompson

Washington University in St Louis, St Louis, USA

Background: Every year 17,000 Americans suffer a traumatic spinal cord injury (SCI) that leads to a significant, lifelong healthcare burden due to the limited of regenerative capacity of the adult mammalian spinal cord. This lack of regeneration is due, in part, to a highly organized, predominantly astrocytic glial scar that forms to limit the spread of secondary injury, but also represents a chemical and physical barrier to neuronal growth. Interestingly, it has been observed that astrocytes are also present where axons are able to cross the injury site. This suggests that astrocytes are involved in both the formation of the glial scar and the creation of bridges across the scar and lesion environments. V2a interneurons are glutamatergic, ipsilaterally projecting cells that have been found to be important for local rewiring following SCI, particularly in the phrenic circuit. In this work, we present a novel hyaluronic acid (HA)-astrocyte extracellular matrix (ECM) hydrogel and demonstrate that this hydrogel can be used to deliver V2a interneurons into the injured spinal cord.

Methods: Protoplasmic astrocytes were derived from RW4 mouse embryonic stem cells (mESCs) and the culture plates decellularized. Protoplasmic extracellular matrix (P-ECM) was then scraped from the plate and lyophilized. V2a interneurons were derived from Chx10-PAC CAG-TdTomato mESCs and aggregated for transplant. This cell line produces cultures containing 80% Chx10⁺ cells (V2a Interneurons) following puromycin selection. ECM was reconstituted in 1% HA-methylfuran prior to addition of PEG-bismaleimide crosslinker (3.4 kD) and V2a aggregates. The resulting shear thinning gels were then injected into Long-Evans rats 2 weeks after a T8 dorsal hemisection SCI. Following implantation animals were immune suppressed with cyclosporine-A. Histological recovery was assessed 2 weeks after implantation with staining for Tuj1, GFAP, CS56, and ED-1. The phenotype of the transplanted V2as was determined with the TdTomato, Vglut2, and NeuN.

Results: We found that either P-ECM or V2a interneuron presence increased host axonal growth into a SCI lesion. P-ECM incorporation was also found to reduce astrocyte reactivity surrounding the SCI lesion, and reduce macrophage infiltration into the lesion and surrounding tissue compared to HA alone. The HA hydrogel itself was found to reduce staining for inhibitory proteoglycans in the glial scar compared to a sham implant. By quantifying TdTomato expression, we found that the transplanted V2a interneurons survived in both HA and HA + ECM gels. Furthermore, based on co-localization of TdTomato with β -tubulin, transplanted interneurons extend processes both within the SCI lesion and into the host spinal cord. This work shows that astrocyte ECM maintains bioactivity and improves histological outcomes following SCI. Future work will focus on determining if transplantation of these HA:ECM hydrogels and/or the V2a interneurons results in any behavioral improvements following SCI.

293 Modeling inflammation in heterotopic ossification using human induced-pluripotent stem cells

Amy N. Ton

University of California, San Francisco, USA

Heterotopic ossification (HO) is a debilitating process where bone forms abnormally in soft tissue. This can occur in response to trauma or injury and complicates over 40% of hip replacement surgeries. However, what factors predispose HO formation are largely unknown. To address this, we established an iPS cell model of fibrodysplasia ossificans progressiva (FOP), a congenital disease of HO caused by a gain-of-function mutation in the ACVR1 receptor of the BMP pathway. Given that FOP patients develop HO in response to trauma, sepsis, or immunizations, we sought to understand how the classical ACVR1 R206H mutation may affect acute inflammation. Macrophages and endothelial cells are found in nascent HO lesions and both cell types play critical roles in inflammation of numerous tissues. Our prior clinical studies showed that FOP patients are in a pro-inflammatory state with increased populations of pro-inflammatory monocytes and elevated circulating inflammatory cytokines. In addition, FOP iPS cell-derived endothelial cells (iEC) can secrete increased inflammatory factors when co-cultured with mesenchymal stem cells. Since HO lesions show a massive infiltration of immune cells by histology, we hypothesized that the FOP endothelial cells induce increased chemotaxis of monocytes in response to injury. Because primary tissue specimens are not possible to obtain from FOP patients due to the risk of inducing more HO, we generated macrophages from our iPS cell lines (iMac) using a new highly efficient and reproducible differentiation protocol. iMacs express macrophage lineage markers of CD14 and CD11b, with FOP iMacs having larger populations of CD206-expressing cells than that of CD163. We are currently co-culturing our iMacs with iECs in a transwell model to assess macrophage migration and chemotaxis. These data suggest that FOP iMacs have different immune responses caused by abnormal BMP signaling that may affect cell-cell interactions. This immune activation may predispose FOP patients to the development of HO, and may also be a key regulator of bone formation in non-genetic forms of HO.

294 Biomimicry of the breast cancer microenvironment in a 3D, patient-derived, tissue engineered model

Yoshiko Toyoda

Weill Cornell Medical College, USA

Obesity is a known risk factor for the development and prognosis of breast cancer. Obesity is associated with less response to breast cancer therapy and more aggressive disease. Adipocytes have been identified as a source of exogenous lipids in many cancer cell types, including breast, and provide energy to fuel malignant survival and growth in breast cancer. Autologous fat transfer is an increasingly ubiquitous procedure for breast reconstruction after mastectomy, but the oncologic safety is largely unknown. There is a compelling need to better understand the biology behind the obesity-breast cancer link. We have developed a 3D, patient-derived tissue engineered platform to directly assess the metabolic interactions among cells of the breast cancer tumor microenvironment.

Breast tissue was enzymatically digested to retrieve adipocytes. Polydimethylsiloxane wells were filled with type I collagen encapsulated with stromal cells and adipocytes labeled with the fluorescent lipid dye boron-dipyrromethene (BODIPY) 493/503 and RFP-labeled MDA-MB-231 breast cancer cells on the surface. Cultures of MDA-MB-231 in non-adipocyte containing collagen matrices as well as adipocyte containing constructs without breast

cancer cells served as controls. After 1, 2, 3, and 7 days, constructs were fixed then immunohistochemically stained with Hoescht nuclear stain and Cytokeratin 19. Lipid transfer and breast cancer cell invasion into the collagen bulk were analyzed using laser scanning confocal microscopy and images were processed with Imaris.

The 3D collagen culture platform demonstrated BODIPY-stained mature adipocytes neighbored by stromal cells, akin to the native architecture in human breast tissue. At the interface of the cancer cells with the biomimetic stroma, lipid transfer was observed—breast cancer cells which were close in proximity to the lipid-filled adipocytes demonstrated small, green fluorescent lipid droplets in the cytoplasm. Breast cancer cell invasion into the collagen bulk was assessed via confocal Z stacks on Imaris.

We have established a novel 3D tissue engineered platform to study breast cancer microenvironment, including metabolic interactions between primary human breast adipocytes and breast cancer cells. Transfer of fluorescently-labeled lipids directly from adipocytes to breast cancer cells may induce aberrant metabolism to fuel malignant growth and adaptive survival which may have implications in breast cancer prognosis in patients of different obesities as well as in the setting of autologous fat transfer after oncologic resection.

295 19-gene risk score predicts poor survival in hepatocellular carcinoma patients

Lynn Tran

Medical College of Georgia at Augusta University, Augusta, USA

Hepatocellular carcinoma is the 4th leading cause of cancer-related deaths, and patients have median survival times of 6-20 months. Despite this poor prognosis, there are no clinically available prognostic biomarkers to identify patients with particularly poor survival. We aim to identify putative poor-survival genes using The Cancer Genome Atlas's hepatocellular carcinoma gene expression data. Briefly, univariate Cox proportional hazard models were constructed for 20,530 genes based on individual genes' expression values and overall survival status. Genes with the highest hazard ratio (HR) and significant p-values after application of a genome-wide Bonferroni correction were reduced to a risk score consisting of 19 genes using a supervised generalized linear model (least absolute shrinkage and selection operator regression) network algorithm. Using this 19-gene risk score as a univariate survival prediction model, the hazard ratio is 5.76, with a p-value of 3.22×10^{-15} , demonstrating a significant separation of good survival (low risk score) and poor survival (high risk score) patients. One group of genes we identified is associated with mitosis, cell division, and cell cycle regulation; these genes may play important roles in tumor progression and resistance. We plan to validate this 19-gene risk score in a single-center retrospective analysis of archived patient formalin-fixed paraffin-embedded (FFPE) tissues.

296 Discovery of a Proliferative Gene Signature Predictive of Cancer Patient Survival

Paul Tran

Augusta University, Augusta, USA

We herein analyze data from The Cancer Genome Atlas (TCGA) database to identify patient groups with differential survival characteristics using gene expression data. Our goal is to use molecular data to help stratify patients in terms of survival prognosis and cancer therapy selection. We downloaded TCGA gene expression RNASeq data and clinical data from the University of California Santa Cruz (UCSC) Xena Public Data Hub. We applied a univariate Cox

regression model gene identification approach to identify a list of genes which exhibit a high degree of internal correlation, with poor prognosis patients exhibiting higher expression levels of all genes compared to the better prognosis patient group. The high degree of correlation suggests the expression levels of these genes are controlled by a single upstream pathway. The gene signature is enriched for genes associated with cellular proliferation. Patients from the TCGA dataset whose tumors have a higher gene expression score are more likely to have worse survival prognosis compared to tumors with a lower gene expression score, demonstrated through Kaplan-Meier survival analysis and univariate and multivariate Cox proportional hazard models. This suggests we have identified a co-regulated gene expression network associated with cellular proliferation which predicts overall and recurrence-free survival in many of the cancers in the TCGA dataset. We plan to validate these findings in a single center retrospective analysis of cancer patient formalin-fixed paraffin embedded (FFPE) tissue blocks.

297 Therapeutic Role of Intrapartum PDE-5 Inhibition on Blood Pressure and Renal Injury in Offspring of Preeclamptic Rats

Hannah R. Turbeville

University of Mississippi Medical Center, Brandon, USA

Up to 10% of pregnancies are complicated by preeclampsia. As a result, up to 15 million US citizens today are offspring of preeclamptic pregnancies. Offspring of preeclamptic pregnancies have increased blood pressure (BP) during childhood, and preeclamptic pregnancy can result in small for gestational age babies that are at a heightened risk for chronic kidney disease later in life. The Barker hypothesis proposes that the adverse intrauterine environment created by preeclampsia programs fetal tissues and organs to develop high BP from early childhood. Clinical and experimental studies have demonstrated the ability of various therapies that target the nitric oxide (NO)-cGMP signaling pathway, such as NO donors, to attenuate hypertension. Sildenafil citrate, a phosphodiesterase-5 (PDE-5) inhibitor, prolongs the NO-cGMP signaling cascade and improves the maternal syndrome of preeclampsia; however, determination of optimal timing, effectiveness, and safety during perinatal use have yet to be reported. This project tests the hypothesis that use of a PDE-5 inhibitor during preeclamptic pregnancy improves the long-term BP and renal injury in the offspring. Female Dahl S rats on a 0.3% salt diet, a previously characterized spontaneous model of superimposed preeclampsia, were mated and treated orally with sildenafil (50 mg/kg/day), labetalol (currently used to manage hypertension in preeclamptic patients, 10 mg/kg/day), or vehicle from gestational day 10 to delivery. All dams were returned to control 0.3% salt diet at delivery up through weaning of offspring at four weeks of age. At seven weeks of age, male and female offspring (n=4-7 per group) were acclimated to restraints for four days before tail cuff BP measurement on day five. BP was measured again at 11 weeks of age for analysis of the time-dependent change in systolic BP. Systolic BP increased in Dahl S rats of untreated mothers as expected from week 7 to 11; however, the rise in BP was abolished in offspring from sildenafil treated dams (VEH: +28 mmHg \pm 7; SLD: -7 mmHg \pm 5, p=0.007). This protective effect was not elicited by treatment with labetalol (+13 mmHg \pm 5). At 12 weeks of age, urine was collected for the determination of protein excretion and subsequently kidneys were harvested for measurement of tubulointerstitial scarring. No significant differences in urinary protein excretion were observed in either male or female offspring between groups. Tubulointerstitial scarring was increased in male Dahl S offspring of untreated mothers as compared with offspring of sildenafil treated dams

(Area: VEH: 9 \pm 0.6%; SLD: 5 \pm 0.6%, p=0.006), but no changes were observed in kidney sections from female rats. These data support the hypothesis that use of a PDE-5 inhibitor during preeclamptic pregnancy improves the long-term BP and renal injury in the offspring.

298 The transcriptional response of endothelial cells to statin treatment in vivo

Katherine N. Turnbull

University of Michigan, USA

Statins inhibit hydroxymethylglutaryl-CoA reductase, an enzyme in the cholesterol synthesis pathway, and are widely prescribed for cardiovascular risk reduction. In addition to lowering plasma cholesterol levels, statins have also been proposed to further reduce cardiovascular risk via other pleiotropic anti-inflammatory and pro-angiogenic effects, potentially mediated through the endothelium, though the underlying molecular mechanisms are still largely unknown. Analysis of endothelial cells (ECs) in vivo has been limited due to their extensive heterogeneity across vascular beds as well as their interspersed anatomical distribution. In addition, isolation of ECs from complex tissues and/or expansion in vitro results in rapid phenotypic drift and changes in gene expression programs.

To characterize changes in the EC transcriptome induced by statin treatment, we applied the Translating Ribosome Affinity Purification (TRAP) technique, tagging the ribosomal protein RPL22 with hemagglutinin (HA) in all ECs in the mouse in vivo by crossing a conditional Rpl22-HA allele with a Tek-Cre recombinase transgene. Mice are perfused with cycloheximide at the time of sacrifice, freezing actively translating mRNA within the ribosomal complex. EC ribosomes are then selectively isolated from tissue lysates by immunoselection for the HA tag and the associated mRNA is then purified from this complex. Multiple tissues (brain, heart, kidney, liver, lung and skeletal muscle) were subjected to high throughput RNA sequencing (RNASeq) and EC-enriched transcripts were identified by comparison of the HA-selected mRNA to total tissue mRNA. To study the effects of statin treatment on the endothelium, 3 male mice were treated orally with 1mg/kg body weight atorvastatin daily for one week, and 3 untreated males were used as controls.

RNASeq analysis of control tissues identified a set of pan-EC enriched genes in all tissues evaluated, including the known EC markers Tek, Cdh5, Flt1, and Nos3. Additionally, each tissue exhibited a set of vascular bed-specific EC transcripts, which was most prominent in brain. Gene ontology analysis of identified EC markers showed enrichment for vascular-related biologic processes, including 'vascular development,' 'blood vessel morphogenesis,' and 'angiogenesis.' Though analysis of the statin treated samples is still in progress, preliminary unsupervised hierarchical clustering analysis of the brain samples showed high similarities between transcriptional profiles for the statin-treated and control groups. We are currently validating these findings in other tissues as well as via single-molecule in situ hybridization assays.

In conclusion, we are able to isolate endothelial specific mRNA in vivo and observed distinct heterogeneity between expression profiles of different vascular beds, as well as in response to treatment with atorvastatin.

299 Model-based adaptation of artificial pancreas gains using physiologic noise adjustment calculations

Nichole S. Tyler

Oregon Health and Science University, Portland, USA

Evolutions in the treatment of Type 1 Diabetes (T1D) have led to automated insulin delivery, or artificial pancreas (AP) technologies. However lacking within this treatment framework is a model-based approach that provides adaptive adjustments to basal and bolus dosing recommendations. Here, we propose new strategies of adaptive dosing adjustments to determine precise treatment recommendations for T1D by modeling the physiologic variations surrounding meals and exercise on blood glucose measures.

Continuous Glucose Monitor (CGM) data was obtained from 25 subjects with T1D during a week-long AP study. Meals and exercise events were controlled and repeated on day one and day four of the study. The Simple Oral Glucose Minimal Model (SOGMM) of insulin and glucose kinetics served as the basis of our adaptive approach. First, we used CGM traces from study day one to identify areas of poor glucose control and then analytically solved for subject-specific physiological errors surrounding meal and exercise events using the best unbiased linear estimator (BLUE) method. Second, through simulation we identified optimal AP gain adjustments to prevent hypoglycemia on day one data. We then applied these gain adjustments and analytic physiologic noise to day four data and simulated the blood glucose response. Our adaptive gain adjustments resulted in a 67% decrease in time spent in hypoglycemia, with a corresponding 9% decrease in euglycemia.

This use of clinical data represents a novel platform for model-based AP parameter adaptation for the treatment of Type 1 Diabetes. Future directions include use of BLUE to solve for analytic insulin doses to precisely inform time-varying gain adjustments and implementation of model-based adaptive strategies in simulated patient populations.

300 Genetic elevation of beta-linked N-acetylglucosamine in cardiomyocytes causes heart failure

Priya Umapathi

Johns Hopkins Medical Institutions, Hunt Valley, USA

The pathologic effect of hyperglycemia on cardiomyocytes may involve the excessive post-translational protein modification known as O-GlcNAcylation (OGN). Intriguingly, increased OGN is a feature of myocardial infarction (MI) and heart failure (HF), even in the absence of hyperglycemia. OGN is dependent on metabolism through the hexosamine biosynthesis pathway, which incorporates glucose, amino and fatty acids into production of a rate limiting substrate, UDP-GlcNAc. Ultimately, OGN levels are determined by the net activity of two enzymes: OGT (O-GlcNAc transferase) adds OGN from UDP-GlcNAc, and OGA (O-GlcNAcase) removes OGN. OGN is a highly conserved stress response, and constitutive myocardial-restricted OGT knock out is embryonic lethal, while inducible myocardial OGT knock out contributes to HF, suggesting some OGN is required for myocardial development, and normal heart function. However, it is unknown if excessive OGN contributes directly to myocardial disease and HF. Up until now, the lack of genetic tools to increase OGN in vivo, independent of glucose or pathological stress, has prevented a clear determination of the pathological potential of OGN.

Based on increased OGN after MI and in HF, we hypothesized that excessive OGN can promote HF. We created transgenic mice overexpressing OGT or OGA exclusively in myocardium in order to directly test if OGN can cause HF, independently of hyperglycemia or pathological stress. Our transgenic OGT (Tg OGT) mice have

increased OGN and exhibit severe systolic dysfunction (left ventricular ejection fraction (LVEF) % 24 ± 4 , versus WT at 8 weeks, $p=0.0005$) and increased mortality compared to WT (median survival Tg OGT 24.9 weeks); transgenic OGA (Tg OGA) mice exhibit normal contractility (LVEF% 74 ± 4) compared to WT and no significant mortality. Tg OGT and Tg OGA interbred mice, overexpressing both OGT and OGA in myocardium, had lower levels of OGN and demonstrated marked improvement of systolic function when compared to Tg OGT mice (Tg OGT/OGA LVEF% 68 ± 5.7 versus Tg OGT LVEF% 30 ± 4.7 and WT LVEF% 82 ± 1.8 , all $p = <0.0001$).

Our new, preliminary data show that chronic, myocardial OGT overexpression is maladaptive and sufficient to cause HF, even in the absence of hyperglycemia or injury. Increased OGA expression is well tolerated, and has the ability to prevent cardiomyopathy induced by excessive OGN. Our data identify excessive OGN as an independent HF mechanism, and suggest OGN may contribute to diverse types of HF associated with diabetes and common forms of myocardial injury.

301 Chagas Disease: Understanding Exposure Risk Across a Land Use Gradient in Panama

Erin Allmann Updyke

University of Illinois Urbana-Champaign, Urbana, USA

Chagas disease, a neglected tropical disease affecting millions of people throughout the world, is transmitted by multiple species of triatomine "kissing bug" (Hemiptera: Reduviidae). In Panama, species that transmit the disease are sylvatic (ie: wild-living), and the risk factors that govern human transmission are not well characterized. This study investigates the factors potentially contributing to Chagas disease exposure risk across a human land-use gradient in central Panama. Epidemiological surveys and sixteen months of in-home kissing bug collection were performed in nine communities across three urban to rural land-use gradients. Household surveys explored social and behavioral factors, such as living conditions, education level, socioeconomic status, and knowledge of both kissing bugs and Chagas disease. Reported presence of domestic and wild animals around the home was positively correlated with having seen kissing bugs around the home and with greater average kissing bug capture during the study. Entomological surveys captured five common species of kissing bug across the gradients, with a greater diversity of kissing bug species in more rural areas. Generalized linear models (performed in R with the lme4 package) using a Poisson distribution revealed significantly more kissing bugs captured in semi-urban ($p<0.001$) and rural areas ($p<0.001$) as compared to urban areas. Additionally, the number of domestic animals, including dogs and chickens, that households kept was significantly associated with the kissing bug capture rate ($p<0.02$ and 0.006 , respectively). PCR and qPCR testing has indicated presence of *Trypanosoma cruzi*, causative agent of Chagas disease, in 56% of kissing bugs, with differences across the land use gradient. In rural areas, 62% of kissing bugs were infected with *T. cruzi*, while in semi-urban and urban areas 52-53% were infected, respectively. This has important potential implications for the distribution of risk of Chagas disease transmission across a land use gradient and according to household factors, and a better understanding of these risk factors is integral to successful control efforts.

302 Identity on the West Side of Grand Rapids: A History of Westtown

Kenny Urena-Gonzalez

Grand Valley State University, Wyoming, USA

This paper traces the history of what it means to be a “Westsider,” in Grand Rapids, Michigan. Westtown is a neighborhood with a history and identity distinct from other areas of the city. Drawing on interview and archival data, as well as participant-observation, the paper suggests that Westtown identity is rooted in the neighborhood’s history of immigration, its working-class character, and the impacts of construction projects in the past that served to physically separate Westtown from other parts of the city. With this, the paper explores the history of medicine in this area as well as current findings of it being medically underserved and trends on disease/health disparity of the area. In conclusion, the Westtown of Grand Rapids has been culturally diverse in the past, but recent demographic data suggests that there has been a gentrification of poor Caucasians into the area as the majority group with the introduction of a new group, university students. History shows that the area has been unrepresented in Grand Rapids in most areas, including medicine and integration of medical programs/clinics. Currently there are no clinics in the Westtown and is still underserved medically, with many residents showing health concerns and stating a need for medical assistance.

303 Local white adipose tissue browning in breast cancer is not mediated by direct tumor-adipocyte interactions

Janina A. Vaitkus

Virginia Commonwealth University School of Medicine, Midlothian, USA

The role of adipose tissue in the context of cancer is multifaceted. ‘Browning’ or ‘beiging’ of white adipose tissue (WAT) to thermogenic ‘beige’ or brown-in-white (‘brite’) adipose tissue has been demonstrated in several cancer models; however, the mechanisms underlying this process, and its implications relative to tumor progression and whole-body energy expenditure in the context of cancer, are not fully understood. Breast cancer is contiguous to adipose tissue, and therefore represents an ideal experimental model to assess the interactions between tumor microenvironment and adipose tissue. Our objectives were to characterize the extent of WAT browning in breast cancer and to investigate whether or not it is mediated by direct tumor-adipocyte interactions. We employed immunohistochemistry for key thermogenic and immunologic markers in a mouse transgenic mammary tumor model (B6.FVB-Tg(MMTV-PyVT)634Mul/LelJ) as well as in several human samples of breast ductal carcinoma. We performed a series of *in vitro* experiments using primary and immortalized mouse preadipocytes as well as primary human preadipocytes. Cells were exposed to both co-culture and cancer-conditioned medium from either E0771, MCF-7, or MDA-MB-231 breast cancer cell lines for various timeframes both during and after maturation to white adipocytes. Analyses were carried out for lipid droplet sizes using microscopy, thermogenic gene profiles using real-time qPCR, and protein expression using western blot. Immunohistochemistry experiments demonstrate that uncoupling protein 1 (UCP1), the hallmark of functional thermogenic adipose tissue, is over-expressed at the tumor-adipose interface. Interestingly, UCP1 is expressed in a gradient-like manner, with highest expression most proximal to the tumor and rapidly decreasing moving distally. Lipid droplet size follows a gradient as well, with smaller lipid droplets closest to tumor. We also demonstrate that the expression of interleukin-6 (IL-6), a cytokine involved in many inflammatory processes, is increased at the tumor-adipose interface.

In vitro, we show that after co-culture with or exposure to cancer-conditioned medium, developing or mature white adipocytes have significantly smaller lipid droplets. However, no accompanying increases in UCP1 protein expression or mRNA expression of *Ucp1* and other thermogenic markers such as *Pgc1α* and *Cidea* were observed. Our data indicate that breast cancer promotes localized white adipose tissue browning, not driven by direct cancer-secreted mediators. Instead, the data support the alternative hypothesis that the tumor microenvironment, not the tumor directly, is responsible for WAT browning at the tumor-adipose tissue interface. Future experiments are underway to determine whether the critical cells are stromal or immunologic in nature, to elucidate the signaling pathways by which these changes occur, and to project the impact of this local WAT browning on clinical endpoints including tumor progression, energy expenditure, and cancer-associated cachexia.

304 Breast milk fed infant derived *Propionibacterium* strain UF1 mitigates intestinal inflammation in mice: synthetic biology approaches

Max Van Belkum

University of Florida, Destin, USA

Purpose: Determine whether human breast milk probiotic *Propionibacterium freudenreichii* strain University of Florida 1 (PUF1) has potential as a therapeutic for human intestinal diseases such as necrotizing enterocolitis (NEC.) Mechanistically explain the profound protective effect of PUF1 on murine disease models of human intestinal diseases.

Methods: PUF1, named by our lab after the institution it was discovered in, was identified via 16s rDNA from the feces of human infants fed human breast milk, but could not be found in those fed exclusively infant formula. We then created a series of experiments involving groups of mice gavaged with PUF1 (or genetically engineered variants) or with Phosphate Buffered Saline as a control. We used flow cytometry to analyze the immune function of mice in both groups in steady state and in a variety of disease states including *Listeria monocytogenes ΔactA* (mutation to prevent escape from intestine.) NEC was tested with preterm mice instead of adult mice, reflecting the demographic of humans most affected by NEC.

Results: Flow cytometry of murine tissues showed gavage of PUF1 to have anti-inflammatory effects in steady state, *Listeria monocytogenes ΔactA* (variant localized to intestine), and, in preterm mice, NEC. These anti-inflammatory effects included markedly mitigated inflammation by decreased inflammatory IL-6, increased anti-inflammatory IL-10+ TGF-β + Tregs and IL-10 cytokine, increased TH17 differentiation, decreased inflammatory Th1 differentiation, and drastically increasing survival during NEC in neonatal mice. We used guanidine hydrochloride to isolate the surface layer protein of our bacterium and discovered it had a high affinity for MHC class II. Deletion of the gene, *dlaT*, responsible for producing the surface layer protein via homologous recombination resulted in a loss of anti-inflammatory effect relative to control in disease models and steady state. Transgenic mice lacking the dendritic cell SIGNR1 receptor also did not show the anti-inflammatory results of PUF1 gavage, which we predicted by showing that the PUF1 surface layer protein has a high affinity for SIGNR1 but not other C-type lectin receptors. Hypoxia-induced NEC afflicted preterm mice breastfed by mothers that had been gavaged with PUF1 since pregnancy showed a 90% survival rate and marked reduction of inflammation compared to control, which had a 50% survival rate.

Discussion: These experiments show that, PUF1, isolated from breastfed human infants, markedly improved the immune response

in disease states by facilitating anti-inflammatory and regulatory conditions in mice. We mechanistically linked the probiotic effect to a surface layer protein on our bacterium communicating with a C-type lectin receptor on the surface of the dendritic cell. Future work includes phase 1 clinical trials more detailed basic mechanistic study of the bacterium and genetic engineering of the bacterium to function as an engineered probiotic.

305 A population prevalent and promiscuous Merkel cell polyomavirus CD4 epitope; an ideal therapeutic target for Merkel cell carcinoma?

Natalie Vandeven

University of Washington, Seattle, USA

Merkel cell carcinoma (MCC) is a deadly, skin cancer that is etiologically linked to the Merkel cell polyomavirus (MCPyV) in 80% of cases. Viral oncoproteins are persistently expressed and are required for tumor survival and growth, providing ideal targets for the immune system. Indeed, robust CD8 T cell infiltration into MCC tumors is associated with 100% survival, however, this strong CD8 T cell response is only observed in 4-18% of cases. Lack of CD4 help has been shown to limit the recruitment, survival and function of anti-tumor CD8 T cells in other cancers, however, the role and function of CD4 T cells in the context of MCC remains unknown. Therefore, we sought to study the MCPyV-specific CD4 T cell response through the identification of CD4 epitopes within MCPyV and isolation and characterization of detected MCPyV-specific CD4 T cells. Here we identified a novel MCPyV CD4 epitope, WEDLFCDESLSSPEPPSSSE ('WED') which can be presented by at least three population prevalent HLA class-II alleles, indicating that this epitope is likely relevant in ~80% of virus-positive MCC patients. Furthermore, this epitope lies within the MCPyV Large T-antigen (LT-209-228) encompassing the LxCxE motif. The LxCxE motif is required for T-antigen binding to the tumor suppressor retinoblastoma protein (Rb), one of the main oncogenic mechanisms in MCC. Consequently, expression of the 'WED' epitope is required for tumor growth and persistence, and sequence analysis indicates that this region is highly conserved among MCC tumors. Additionally, we show that 'WED'-specific CD4 T cells are capable of homing to and infiltrating MCC tumors and exhibit strikingly diverse T cell receptor repertoires. Taken together, we have identified a highly conserved and population-prevalent CD4 epitope within MCPyV. These data provide a robust foundation to develop CD4-based cellular therapies and/or a therapeutic cancer vaccine against this deadly skin cancer.

Conflict of Interest: The authors declare no potential conflicts of interest.

306 RSPO2 overexpression in the mouse liver induces tumor formation and progression via the Wnt and Hippo/Yap pathways

German L. Velez Reyes

University of Minnesota, Minneapolis, USA

Recently, we identified *RSPO2* as an oncogene in a subset of human breast, colorectal, peripheral nerve, and liver cancers. *RSPO2* is a member of the R-spondin protein family, which oncogenic activity arises via the Wnt/ β -catenin pathway, important for organ development and regeneration of the liver. We hypothesized that the Hippo/YAP pathway is activated in the liver upon *RSPO2* overexpression given its role in organ development and the Wnt pathway. We overexpressed *RSPO2* in the *Fah*^{-/-} mouse liver and found increased nuclear localization on Yap and activation of Hippo-responsive genes. This suggests that the Hippo pathway is activated

and plays a role in *RSPO2*-overexpressing liver cancers. We then expressed an shRNA targeting mouse *Yap* in the presence of *RSPO2* overexpression to test the role of Yap in *RSPO2*-induced liver cancer. We found that *Yap* depletion in the *RSPO2* overexpressing mice lead to a reduced tumor penetrance.

We then aim to validate our model in human hepatocytes. We found that overexpression of *RSPO2* resulted in increased YAP nuclear localization, colony formation in soft agar, and proliferation. Overall, our results suggest a role for Yap in the initiation and progression of liver cancer and uncovers a novel pathway activated in *RSPO2*-induced malignancies. Currently we are testing Hippo/Yap small molecule inhibitors in preclinical models.

307 Expression of optic fissure closure-associated Zinc Finger Protein 503 (Zfp503/Nlz2) in the developing and postnatal mouse retina

Emile R. Vieta Ferrer

San Juan Bautista School of Medicine, Caguas, Puerto Rico

Eye development begins as an outpouching of the diencephalon, followed by the asymmetric invagination of the optic vesicle and closure of a transient longitudinal opening on the ventral side, called the optic fissure, to form the optic cup. Closure of the fissure gives rise to the normal globular structure of the eye. Failure of this developmental step results in uveal coloboma. We have previously shown that *Zfp503/Nlz2* is important for optic fissure closure in zebrafish and mouse. Mice that are homozygous for the *Zfp503* null allele (*Zfp503* ko) have decreased pigmentation, coloboma, and die perinatally. In this study, our specific aims were to: 1) Evaluate the expression of *Zfp503* in the developing and postnatal mouse eye and 2) to identify the cell types that express *Zfp503* in the adult retina. This was done by immunofluorescence and confocal microscopy.

During embryonic development, at birth, and at postnatal day (P)1, *Zfp503* was expressed in the retinal pigment epithelium (RPE) and in the inner neuroblastic layer of the retina. In the adult mouse, *Zfp503* was expressed in the RPE, the inner nuclear layer (INL), and the ganglion cell layer (GCL). To establish what cell types express *Zfp503*, we performed a series of co-localization studies by immunofluorescence in adult mice using known markers of retinal cell types residing in the INL and GCL. The presence of *Zfp503* in a small number of Brn3a-positive cells in the GCL suggested that *Zfp503* is expressed in a subpopulation of retinal ganglion cells. In addition, cells double-positive for *Zfp503* and *Isl1* in the GCL established *Zfp503* expression in a subset of displaced amacrine cells. Similarly, we observed few cells positive for both *Zfp503* and calretinin in the GCL and INL, which further supported localization of *Zfp503* in amacrine cells. Cells positive for both *Zfp503* and *Lhx2* (a marker of Müller glia and a subset of amacrine cells) were identified in the INL. However, *Zfp503* did not co-localize with calbindin and ChAT, which label horizontal cells and cholinergic amacrine cells, respectively. We thus concluded that *Zfp503*-positive cells likely form part of distinct subsets of amacrine cells and retinal ganglion cells. We finally investigated the histology of the rare *Zfp503* ko mice that we could identify at P0 before death ensued. In these mice, failure of the optic fissure to fuse caused the approaching retinal lips to extend and overlap. In addition, the usually monolayered RPE appeared multilayered and retina-like, giving the appearance of two distinct layers of retina. We posit that *Zfp503* may play very specific functions in sub-types of amacrine and retinal ganglion cells besides its role in optic fissure closure.

308 Inhibition of V-type ATPase in Small Airways Increases Airway Surface Liquid pH

Raul Villacreses

University of Iowa - Department of Internal Medicine, Iowa City, USA

Cystic Fibrosis (CF) is a genetic disorder caused by mutations in the cystic fibrosis transmembrane conductance regulator (CFTR) gene. CFTR encodes an anion channel permeable to both chloride and bicarbonate. In large CF airways, loss of CFTR-mediated bicarbonate secretion and unopposed proton secretion acidifies the airway surface liquid (ASL) and impairs airway host defenses, the secretion of H⁺ is mediated by the non-gastric H⁺/K⁺ ATPase (ATP12A). CF is a disease that starts in the small airways. Therefore, we asked what type of proton pump mediates proton secretion in pigs small airways? and, whether inhibition of proton secretion in the small airways will increase ASL pH, enhance bacterial killing and decrease ASL viscosity?

We investigated the location of ATP12A by immunocytochemistry in small and large airways from pigs, and we compared the expression profile using Affymetrix Gene Chip2, with emphasis on the expression of proton pumps. ATP12A was expressed in large airway epithelia and submucosal glands but not in small airways. Moreover, we found a higher expression (50x) of the vacuolar type H⁺ ATPase (V-ATPase) V0d2 subunit isoform (ATP6V0D2) in small airways epithelia compared to large airways. There was no significant difference in other V-type ATPase subunits.

To investigate the effect of V-ATPase on ASL pH regulation in small airways, we studied the effect of bafilomycin (V-ATPase inhibitor) on ASL pH using with SNARF pH indicator. The ASL pH became more alkaline. Small airways studied without HCO₃⁻, failed to become more acidic when stimulated with cAMP agonist suggesting the ATP12A is absent and the V-ATPase is not regulated by cAMP.

Inhibition of the V-ATPase H⁺ increases the ASL pH in the presence of HCO₃⁻ containing media and HCO₃⁻ free media in the basolateral side in cell cultures in basal and cAMP stimulated conditions. This data suggests that the V-ATPase might play an important role in the ASL pH regulation in small airways.

309 The MSTP training grant renewal is an opportunity for student-directed program evaluation.

Anil Wadhvani

Northwestern University (Feinberg), Chicago, USA

Medical Scientist Training Programs (MSTP) funded by the National Institutes of Health undergo periodic training grant renewal for continued or enhanced support, often triggering top-down review of program policies, milestones, and goals. Direct student input during the renewal is commonly only gathered by external evaluators during a site visit. Unlike other high-stakes external evaluations in medical education, such as reaccreditation, there is no established mechanism for systematically collecting and evaluating student perceptions of their training, program leadership, and learning environment. In our program, student leaders leveraged the training grant renewal and site visit to initiate a multi-faceted review of our program, including periodic open forums, collaboration with leadership during a mock review, and a comprehensive survey of student perceptions. Independent student analysis identified both areas of strength that leadership was able to incorporate into the grant renewal application and areas of weakness that were addressed prior to initiation of external review. The survey was deployed for a second year, and allowing us to measure the effects of leadership decisions.

Moreover, the process served as professional development for program students who will likely participate in similar reviews during the careers. Together, our approach demonstrated the value of partnering with student leaders in program evaluation and yielded a survey tool that easily could be adapted to other institutions.

310 Pancreatic islets in short-duration type 2 diabetes have secretory dysfunction, variable amyloid accumulation, and altered islet-enriched transcription factor expression

John T. Walker

Vanderbilt University, Nashville, USA

Type 2 diabetes (T2D) is characterized by both peripheral insulin resistance and pancreatic islet dysfunction, but islet dysfunction underlies the progressive nature of T2D in patients. Dissecting mechanisms of T2D progression in humans is challenging due to clinical disease heterogeneity and the difficulty of obtaining relevant pancreatic samples. Our group is addressing these limitations by using an integrated approach to functionally and molecularly study the native pancreas and isolated islets from the same human cadaveric donors linked with donor clinical information. To identify early pathologic mechanisms, we have focused on T2D donors with short disease duration (n=10, age 47-66 years, 2-7 years duration, oral medications) and age matched controls. We determined that T2D islets had reduced baseline insulin secretion and blunted response to high glucose, cAMP-evoked stimulation, and KCl-mediated depolarization in islet perfusion assays despite no difference in insulin content compared to control islets. Conversely, T2D islets had increased baseline and stimulated glucagon secretion in response to stimulation by cAMP, epinephrine and KCl. Glucagon content of T2D islets was variable but not different than control islets. Pancreatic sections showed no difference in islet morphology or cellular composition (T2D vs control: 63% β , 28% α , and 9% δ cells vs 62% β , 30% α , and 8% δ cells). Interestingly, T2D pancreata had significant variability in proportion of islets containing amyloid with four T2D donors having amyloid accumulation in >50% of islets while other T2D donor islets had little amyloid deposition (<6% of islets). RNA-sequencing analysis from FACS-purified α and β cells showed reductions in T2D donors compared to controls in several islet-enriched transcription factors known to play crucial roles in maintenance of islet cell identity and function, including NKX2.2 and PAX6. Together, this data suggests that intrinsic defects in T2D α and β cells contribute to islet dysfunction early in the course of T2D and that amyloid accumulation is not a driver of the disease.

311 Toward a single-neuronal basis of social reciprocity within the macaque anterior cingulate cortex

Amy J. Wang

Massachusetts General Hospital, USA

Social dysfunction is a core component of many psychiatric disorders, but its single-neuronal and causal underpinnings remain largely unknown. Reciprocity, a central feature of social interaction, allows individuals in a group to forge alliances towards augmenting individual and mutual fitness. Here, we studied the neuronal correlates of group interaction by obtaining multiple-neuronal recordings in the anterior cingulate cortex (ACC) of rhesus macaques as they performed a structured social task.

We devised a three-agent social task in which three macaques interacted with each other over multiple rounds. The task required the monkeys to sit around a rotary table apparatus; in each trial, one individual would offer a food reward to one of the other two. Throughout sessions, individuals could reciprocate past rewards that had been delivered to them. Based on this design, we could dissociate

core computations associated with interactive behavior: the animal's own decisions, the decisions of others, their social identities, and past interactions. During task performance, we recorded neuronal activity from their ACC using micro-electrode arrays.

The monkeys showed strategic preferences for other individuals, and preferred to reward those who reciprocated. Engaging in this social strategy increased the amount of reward received by a given animal, enhancing individual fitness. Maintaining a mental representation of specific preferred individuals is a prerequisite for acting out strategic social preferences. We discovered a sub-population of neurons encoding such a signal: these neurons tracked the reward received by other group members and displayed differential activity in response to different individuals.

These findings demonstrate a novel sub-population of neurons in the primate ACC that encode information about particular individuals, forming the necessary basis for social reciprocity. These results lay the groundwork for identifying specific, neurobiologically-guided targets for treatment of social behavioral disorders.

312 DTI and R2* reveal distinct limbic structure changes in parkinsonian syndromes

Ernest W. Wang

Penn State College of Medicine, Hummelstown, USA

Previous studies of clinically similar parkinsonian syndromes have used multimodal MRI to examine differences in motor-related structures. However, limbic structure changes have yet to be compared despite neuropsychiatric and histologic evidence of limbic network involvement. The present study investigated limbic structure changes in Parkinson's disease (PD), multiple system atrophy (MSA) and progressive supranuclear palsy (PSP) patients using diffusion tensor imaging (DTI) and the apparent transverse relaxation rate (R2*), which reflect microstructural disruption and iron accumulation, respectively.

Sixty-nine patients (35 PD, 17 MSA and 17 PSP), and 37 age-matched controls were included in the study. DTI measurements of mean diffusivity (MD) and fractional anisotropy (FA), and R2* were obtained from the amygdala, hippocampus and nucleus accumbens. Non-motor clinical scores relevant to limbic involvement were assessed via the Unified Parkinson's Disease Rating Scale – Part I (UPDRS-I), the Hamilton Anxiety Rating Scale (HAM-A) and the Hamilton Depression Rating Scale (HAM-D). MRI measurements were compared among controls and parkinsonian syndromes, and correlated to clinical scores.

Accounting for both age and gender, MD was higher in PSP than in controls and MSA in both the amygdala and hippocampus. In the hippocampus, MD was also higher in PSP than in PD. FA values in the hippocampus were lower in PSP than in controls. R2* was higher in the amygdala in PD than in controls, higher in the hippocampus in MSA than in PD and PSP, and higher in the nucleus accumbens in MSA than in controls. UPDRS-I positively correlated with MD in the hippocampus in both controls and PD, and in the amygdala and nucleus accumbens in PSP. UPDRS-I negatively correlated with FA in the hippocampus in controls and PD, and positively correlated with FA in both the amygdala in MSA and PSP, as well as in the nucleus accumbens in PSP. In the hippocampus, HAM-A negatively correlated with FA in controls, while HAM-D negatively correlated with FA in PD. All were significant after adjusting for multiple comparisons and correlations.

The results suggest that DTI and R2* can capture distinct limbic structure changes in parkinsonian syndromes, and that patterns

of microstructural disruption and iron accumulation differ among them. The nature of the differences and correlations require further investigation, particularly where changes and correlations overlap. Of note are the contrasting UPDRS-I and FA correlations among syndromes. As DTI and R2* are not capable of describing exact microstructural changes, association of measurements with histopathological findings in future studies may help define changes specific to disease. Nevertheless, distinct differences in limbic structures as captured by DTI and R2* may have certain diagnostic value in differentiating between parkinsonian syndromes.

314 Hypoxia-induced translational profiles of embryonic and adult-derived macrophages: implications in cardiac injury and repair responses to ischemia

Nicholas S. Wilcox

Yale University School of Medicine, USA

Myocardial infarction (MI) remains one of the leading causes of mortality. Healing after MI depends on tight regulation of the inflammatory response because cardiomyocytes have a limited ability to regenerate following injury and consequent cell loss. Macrophages are important in both injury and repair responses to MI because they clear necrotic cardiomyocytes, promote angiogenesis and produce cytokines, chemokines and growth factors. The mammalian heart contains at least 2 macrophage subsets. Yolk sac-derived macrophages (YSDMs) establish themselves during embryonic development and undergo self-renewal. In contrast, bone marrow-derived macrophages (BMDMs) primarily originate from circulating monocytes recruited to the heart following an acute perturbation.

Evidence suggests that YSDMs and BMDMs have disparate roles in tissue repair. Data describing differences between these macrophage subsets has been generated largely by total RNA analyses, which do not necessarily correlate with functional gene expression due to dynamic post-transcriptional regulation. For example, the RNA-binding protein HuR promotes active translation by binding to the three prime untranslated region (3'-UTR) of mRNA, while miRNAs cause mRNA degradation or prevent active translation. We hypothesize that following hypoxia *in vitro*, which assimilates ischemia *in vivo*, YSDMs are anti-inflammatory and promote favorable cardiac repair and remodeling, while BMDMs are pro-inflammatory and hinder tissue repair. To test this, we are employing translating ribosome affinity purification (TRAP), a novel translational profiling approach, which when coupled with a transgenic murine model enables the isolation of cell-specific, polysomal mRNA.

We have determined, by quantitative polymerase chain reaction (qPCR), the optimal duration (16 to 20 hours) of hypoxic incubation of murine BMDMs following seven-day culture for induction of an mRNA subset. This includes vascular endothelial growth factor (Vegf), matrix metalloproteinase 9 (Mmp9) and glucose transporter 1 (Glut1). Gene ontology analysis identified a subset of putative hypoxia-inducible mRNA targets of HuR and miRNA regulation, including endoplasmic (Hsp90b1), a molecular chaperone regulating secretory protein processing including toll-like receptors and integrins. Relevantly, Hsp90b1 is necessary for tumor-associated macrophages to drive inflammation. qPCR analysis of polysomal RNA from BMDMs showed enrichment of select transcripts following hypoxia, including Hsp90b1, Vegf and Mmp9. Finally, Mmp9 was enriched in polysomal RNA relative to non-polysomal RNA after hypoxia.

We have employed TRAP to isolate sufficient yields of polysomal RNA from murine BMDMs, derived from HuR wild type or knockout mice after hypoxia or normoxia, for RNA-seq analysis. We have

demonstrated efficient HuR deletion in BMDMs from knockout mice by flow cytometry and western blot. RNA-seq will enable unbiased detection of novel or less abundant transcripts and elucidate HuR-mediated stabilization of polysomal RNA for targets of interest. Similar experiments will establish a comparative translational profile for YSDMs. Results would provide a molecular basis to explain the non-overlapping properties of these macrophage subsets and identify novel therapeutic targets.

316 Clinical, onychoscopic and histopathological features of fingernail and toenail onychopapilloma

Vivian Wong

Brown University, Providence, USA

Background: Onychopapilloma is a benign tumor of the distal nail matrix and proximal nail bed with heterogenous clinical presentations. It poses a diagnostic challenge since it could mimic subungual malignancies and inflammatory conditions. Clinical, onychoscopic and histopathological clues play critical roles in diagnosis.

Objective: We aim to expand our knowledge on onychopapilloma by adding cases of finger and toenail onychopapilloma to the literature.

Methods: We performed a retrospective chart review of onychopapilloma cases collected over ten years, and characterized the clinical, onychoscopic and histopathological features of finger and toenail onychopapilloma at an academic institution.

Results: We obtained thirty-three biopsy-confirmed cases of onychopapilloma, of which 17 histopathological slides were available for review. Onychopapilloma predominantly affects adults, with a median age of 52 at the time of diagnosis. There is a female gender predilection, with a female to male ratio of 2.7:1. The left side is more commonly involved (left: right ratio=1.8:1). The fingers, especially the left thumb (54.5% of all cases), are favored. Two cases of toenail onychopapilloma were found, both involving the halluces. Onychopapilloma could manifest as longitudinal erythronychia, longitudinal leukonychia, chromonychia, and longitudinal melanonychia. Long longitudinal or short splinter hemorrhages may be present. Distal fissuring with V-shaped notch, as well as onycholysis, are other discernable features. The presence of a subungual keratotic mass is an additional distinctive diagnostic clue. Onychoscopy could help pinpoint these aforementioned clinical features. Histopathological features include papillomatosis acanthosis of the distal nail bed, premature keratinization, hyperkeratosis and splinter hemorrhages.

Limitations: This is a retrospective, single institution study involving Caucasian patients only.

Conclusions: Onychopapilloma has polymorphic clinical and morphological features. Onychoscopic and histopathological studies are important to help exclude malignant mimickers. Consider onychopapilloma in the differential diagnoses of a monodactylous tumor of the nail, especially on the left thumb of an adult female.

317 Δ Np63 is essential for maintenance of tracheal basal cells through modulation of super-enhancers.

Sarah Wu

MD Anderson Cancer Center, Houston, USA

The transcription factor p53 is a well characterized tumor suppressor and is commonly mutated gene in many cancers, including lung cancer. A p53 family member, p63, was identified by the Cancer Genome Atlas as highly amplified, but not mutated, in lung squamous cell carcinoma, suggesting p63 and its target genes may be excellent candidates for treating cancers with mutant or deleted p53.

p63 is a master regulator of epithelial development and differentiation

and has a role in stem cell maintenance of multiple epithelial tissues. Cancer may originate from transformed adult stem cells, due to similarities in signaling pathways and self-renewal abilities. p63's role has been difficult to characterize as it has two isoforms with distinct functions, TAp63 and Δ Np63. p63 is expressed in the basal stem cells of the lung, which is thought to be the cell of origin for lung squamous cell carcinoma however, the physiological roles of individual p63 isoforms have not been characterized.

To understand the roles of individual p63 isoforms, we utilized TAp63 and Δ Np63 conditional knock out mice generated by our lab. To specifically target the trachea and lungs for recombination, we used an intubation technique that involves administering adenoviral Cre Recombinase directly into the mouse trachea to induce recombination in the trachea and lungs, with characterization at time points to assess the effect on different stem cell populations by staining with lung stem cell markers.

We found that Δ Np63, not TAp63, is the primary isoform that regulates the maintenance and differentiation of tracheal basal stem cells in the mouse, through regulation of cell identity genes. Mice with knockout of Δ Np63 exhibited initial hyperproliferation and apoptosis of Krt5+ basal cells in the tracheal epithelium followed by epithelial hypoplasia with loss of the basal cell population at a later time point, suggesting Δ Np63 plays a role in maintenance of this progenitor cell population. By isolating the basal cells *in vitro*, we observed that loss of Δ Np63 led to impairment of basal cell sphere formation and terminal differentiation in 3D culture. Through a combination of RNA-seq and ChIP-seq analysis of wild type and Δ Np63 knock out tracheal basal cells, we identified a transcriptional network of genes regulated by Δ Np63, including epithelial development, proliferation, and metabolism. Our ChIP-seq analysis demonstrated a significant percentage of Δ Np63 regulated genes were super-enhancers, suggesting a mechanism for Δ Np63-mediated epigenetic regulation of cell identity genes. Interestingly, Δ Np63 is highly amplified and overexpressed in lung squamous cell carcinoma and our Δ Np63 gene signature was similarly upregulated in the TCGA lung squamous cell carcinoma cohort. Our research provides new insights to the under-characterized p63 gene in lung cancer while investigating a novel regulatory process for progenitor cells of the lung.

318 Using artificial antigen-presenting cells to enhance antigen presentation in the treatment of glioblastoma

Yuanxuan Xia

Johns Hopkins University School of Medicine, USA

Immunotherapy has become a promising tool in the oncologist's armamentarium for treating cancer. Glioblastoma (GBM), however, exhibits an extremely immunosuppressive tumor microenvironment through multiple mechanisms, including upregulation of checkpoint molecules like PD-1, its ligand PD-L1, and the presence of suppressive myeloid cells such as microglia, macrophages and myeloid-derived suppressor cells. To counteract the immunosuppressive milieu in GBM, we have developed a biodegradable microparticle-based system of artificial antigen presenting cells (aAPCs) that can be placed locally within a tumor. As artificial constructs, aAPCs can perform the duties of native APCs without experiencing tumor-induced immunosuppression. Through a mixture of poly(beta-amino ester) (PBAE) and poly(lactic-co-glycolic acid) (PLGA), we generated biodegradable microparticle cores that can be loaded with any combination of immunostimulatory molecules. Normally, APCs activate the immune system by presenting a specific peptide (Signal 1) and a variety of co-stimulatory molecules (Signal 2) to activate T cells and drive an adaptive immune response against the peptide of

interest. Using the well-characterized OT-1 OVA system, we loaded MHC I dimer expressing OVA chicken peptide (Signal 1) and co-stimulatory anti-CD28, anti-OX40, and anti-41BB molecules (Signal 2) onto our microparticle surface. To identify what combination of Signal 2 molecules best stimulates a cytotoxic immune response, we performed co-culture assays with OT-1 CD8 T cells and aAPCs with each permutation of co-stimulatory molecules. Surprisingly, aAPCs loaded with just MHC-OVA generated as great a proliferation response as those aAPCs loaded with both MHC-OVA and co-stimulatory molecules. This suggests that OVA system aAPCs bearing only Signal 1 are sufficient to stimulate a strong response in vitro. Next, to translate this OVA aAPC system into in vivo experiments for GBM therapy, we tested the efficacy of adoptive transfer of OT-1 T cells into mice implanted with OVA-expressing GL261 tumors. To test whether transfer of OT-1 T cells alone eradicates GL261 tumors, we treated mice with escalating doses of OT-1 T cells. Interestingly, no dose of OT-1 T cells significantly improved survival compared to controls. Currently, we are testing the in vivo efficacy of aAPCs in combination with PD-1 blockade in mice harboring OVA-expressing GL261 tumors.

319 Interleukin-36 mediates innate-like release of interferon- γ from costimulated CD8 T cells through integration of mTOR and STAT pathways

Maria M. Xu

UConn Health, New Britain, USA

Interleukin (IL)-36 α , -36 β , and -36 γ are new additions to the proinflammatory family of IL-1 cytokines. Implicated in epithelial inflammation, dysregulation of IL-36 signaling has been linked to autoimmune psoriasis and is the only known genetic "hit" associated with the severe, systemic, and autoinflammatory disorder Generalized Pustular Psoriasis (GPP). While the physiologic significance of IL-36 cytokines is emerging, the signaling mechanisms that scaffold its proinflammatory outputs are largely unknown. Through systems-based gene expression studies in therapeutically costimulated CD8 T cells, our lab discovered that IL-36 Receptor is induced by IL-2 and that IL-36 mediates a T cell receptor (TCR)-independent mechanism of rapid, robust interferon- γ (IFN γ) production. This "innate-like" response synergistically integrates IL-2 with IL-36 signaling and within hours, de novo IFN γ gene expression occurs. Known to be anti-tumorigenic through class II major histocompatibility complex induction and macrophage activation, IFN γ simultaneously potentiates inflammation in diseases like psoriasis and GPP. To uncover pathways involved in IL-36-mediated IFN γ release, RNA-Sequence analysis was performed on therapeutically costimulated CD8 T cells exposed to media, IL-2, IL-36, or the combination of IL-2 and IL-36. This analysis, in combination with in vitro inhibitor studies, flow cytometry analyses, enzyme-linked immunosorbent assays (ELISA), and quantitative real-time polymerase chain reaction (qRT-PCR) assays, identified mechanistic target of rapamycin (mTOR) and signal transducers and activators of transcription (STAT) pathways as critical, yet singly insufficient, mediators of robust IFN γ production. To define intersections of IL-36 signaling with mTOR and STAT pathways, digital gene expression (DGE) profiling will be employed in conjunction with time-coursed pathway-specific inhibition. Given the therapeutic and pathophysiologic significance of T cell-produced IFN γ in cancer, autoimmunity, and autoinflammation, the mechanisms underlying how IL-36 signaling integrates with mTOR and STAT pathways have broad and significant biomedical implications.

320 The effect of vitamin D on Th17-hyperresponsive systemic lupus erythematosus

Erin A. Yamamoto

Case Western Reserve University, USA

Recently, approximately 20% of Systemic Lupus Erythematosus patients of European descent were found to harbor a mutation in ACT1 (rs33980500) which leads to a non-functional ACT1 protein variant (ACT1 D10N). ACT1 is the key downstream signaling molecule for IL-17, a characteristic cytokine for Th17 cells. The Act1 $^{-/-}$ mouse displays a lupus-like phenotype that is initiated by bacterial gut colonization and driven by Th17 cells and corresponding cytokines. Since vitamin D is a known suppressor of Th17 differentiation, and vitamin D deficiency is suspected to contribute to lupus pathology, we hypothesize that vitamin D supplementation will ameliorate the Act1 $^{-/-}$ phenotype. Additionally, we propose that patients with the ACT1 D10N variant will display a Th17 hyperresponsive lupus similar that of the Act1 $^{-/-}$ mouse.

Act1 $^{-/-}$ Th17 cell populations and disease pathology were assessed after 8 weeks of either a vitamin D low (0 IU/g), normal (2 IU/g), or high (10 IU/g) diet. Compared to mice on a normal vitamin D diet, the spleen weights of mice in the low and high vitamin D groups were approximately 1.5 times greater and 0.75 times reduced, respectively. Differences in serum vitamin D levels were apparent as early as 3 weeks. There was a negative correlation between vitamin D and Th17/Treg ratio in splenocytes and peripheral blood mononuclear cells at the last time point available for each mouse. At 3 weeks there was a greater percentage of CD3+CD4-CD8-ROR γ t+ cells in Act1 $^{-/-}$ mice regardless of vitamin D exposure, compared to Act1 $^{+/+}$ receiving a normal amount of vitamin D. There was a trend toward lower percentages of CD3+CD4-CD8-ROR γ t+ cells in mice with higher vitamin D levels.

Forty-five patients were enrolled in the Lupus Registry from August to November 2017. Overall, patients were relatively inactive, and only three patients received SLEDAI (Systemic Lupus Erythematosus Disease Activity Index) scores greater than 10. Patients with the highest levels of IL-17 were clinically mildly inactive. A negative trend between vitamin D and SLEDAI, as well as serum IL-17 and SLEDAI was observed. Interestingly, there was a slight positive trend between serum vitamin D and IL-17. Five of 45 patients were identified as ACT1 D10N carriers. ACT1 D10N carriers did not differ from wild-type patients regarding mean serum vitamin D or IL-17 levels.

Our work with the Act1 $^{-/-}$ mouse suggests that vitamin D supplementation improves the lupus phenotype, possibly by reestablishing a Th17/Treg balance. Additional studies to further characterize these cell subsets in the corresponding ACT1 D10N patients are underway and may reveal a new therapeutic target for this specific patient population.

321 Investigation of molecular mechanisms mediating MAP7 function in axon branching.

Benjamin Yang

Thomas Jefferson University, Philadelphia, USA

Axon branching is a fundamental process of the developing nervous system, and disruptions are implicated in a variety of pathological conditions including epilepsy and autism. Branching has also been shown to occur after nerve injury. Previous work has shown that 1) microtubules (MT) in the axon are reorganized during branching, and 2) that this reorganization is necessary for branching. Since MT organization is regulated by microtubule associated proteins (MAPs), I am interested in the function of MAP7, which was recently identified in the developmental regulation of branching of sensory neurons in the dorsal root ganglion (DRG). MAP7 has several unique features: 1) It is capable of directly recruiting kinesin-1 motor proteins to MTs via its C-domain; 2) It possesses multiple MT binding domains as we have demonstrated that the P-domain can directly bind MTs. Structure-function analysis of MAP7 in neurons reveals that the P-domain is required for branch formation and growth while the C-domain is required for branch growth. In COS cells, expression of MAP7 results in the reorganization of MTs into bundles in an activity that requires the P-domain. The morphology of these normally static bundles can be altered by co-expression with kinesin-1. This could reflect enhanced MT-on-MT sliding as kinesin-1 is recruited to MT by MAP7 as it can both walk along and transport MTs. As MT sliding is thought to be required for axon outgrowth this is a potential mechanism by which MAP7 could regulate branching.

To directly test the role of MAP7 on both MT reorganization and sliding, we have developed *in vitro* assays for bundle formation and sliding. These assays utilize taxol stabilized MT in conjunction with cell extracts containing MAP7 and kinesin. This approach is advantageous as it allows for rigorous titration of MTs, MAPs, and motors as well as examination of MT interactions which are not easily resolved in neurons. Our results show that MAP7 enhances MT bundling and increases the number and velocity of MT sliding events in a dose dependent manner. These results support a model in which MAP7 enhances both the number and length of axon branches via its ability to reorganize MT and enhance MT sliding. In future studies, we will also use these assays to assess the polarity of MAP7 MT bundling and sliding.

Exploring the mechanisms behind axon branching is important not only for our understanding of development but as an unexplored avenue for therapy of conditions like spinal cord injury. Our research supports novel regulatory mechanisms of MAP7 for MT reorganization and sliding in axon branching.

323 Fibroblast growth factor receptor 2 protein is a potential cell surface marker for isolating endometrial tissue stem cells

Bahar D. Yilmaz

Northwestern University Feinberg School of Medicine, Chicago, USA

The endometrium is known to undergo regeneration with each menstrual cycle, and tissue stem cells in the endometrium are the source of this regeneration. Understanding the physiology of endometrial stem cells can help elucidate the pathogenesis of endometrial disease such as endometriosis and can be used to develop novel therapeutic methods for Asherman's syndrome, which is a form of uterine factor infertility defined as intrauterine adhesions usually occurring after curettage. Our lab recently established a

protocol to differentiate human induced pluripotent stem cells (iPSCs) to endometrial stromal cells (our unpublished observations). In this 14-day-protocol, day-8 cells corresponded to the Mullerian duct (MD) since they expressed higher levels of the markers for MD such as paired box gene 2 (PAX2) compared with iPSCs. Comparison of gene expression by RNA-Sequencing (RNA-Seq) as well as quantitative RT-PCR (qPCR) over the course of differentiation revealed increased expression of fibroblast growth factor receptor 2 (FGFR2) gene at day-8 followed by downregulation in day-14 cells that correspond to mature endometrial stromal cells. Another stem cell surface marker ATP-binding cassette sub-family G member 2 (ABCG2), which is expressed in side populations, has been previously demonstrated in endometrial stem cells. Our gene expression analyses showed increased expression of ABCG2 during early stages of differentiation with a robust decline on day-14. Due to its similar expression pattern with ABCG2, we hypothesized that FGFR2 could be a novel tissue stem cell marker for endometrial stromal stem cells. Endometrial stromal cells were dispersed from a hysterectomy specimen after mechanical and enzymatic digestion, and FGFR2(+) and FGFR2(-) cells were isolated from endometrial stromal cells using fluorescence activated cell sorting. FGFR2(+) cells comprise 3.5% of the proliferative stromal cell population. FGFR2(+) cells, when compared with FGFR2(-) cells, have higher mRNA levels of ESR2 (estrogen receptor- β), NANOG, the pluripotency marker, and PAX2, the MD marker. Immunohistochemistry staining of whole endometrial tissue demonstrated FGFR2 expression in the perivascular area both in the functionalis and basalis layers. Other previously detected putative stem cell markers such as ABCG2 and sushi domain containing 2 (SUSD2) were also shown to have a perivascular location. We speculate that somatic stem cells are one of the first cell types that come in contact with circulating estrogen, which stimulates proliferation through direct or paracrine mechanisms. Altogether, our preliminary findings suggest that FGFR2 is a potential novel marker for isolation of endometrial stromal stem cells based on gene expression analyses during the differentiation stages of iPSCs to endometrial stromal cells.

324 Exosome-mediated systemic deliver of NAD⁺ biosynthetic enzyme extends lifespan and delay aging

Mitsukuni Yoshida

Washington University in St.Louis, Clayton, USA

Population aging is a global health issue and its social and economic implication is becoming increasingly apparent. Age-associated declines in tissue NAD⁺ levels and sirtuin activities play critical role in the systemic aging process across many species. Here, we demonstrated that the circulating levels of nicotinamide phosphoribosyltransferase (eNAMPT), the rate-limiting NAD⁺ biosynthetic enzyme, significantly decline with age in mice. Adipose-tissue specific overexpression of NAMPT suppresses age-induced eNAMPT declines and increases tissue NAD⁺ levels in multiple tissues including hypothalamus, pancreas, and retina. In aged mice, eNAMPT upregulation improves physical activity, sleep quality, glucose metabolism, and photoreceptor function, and extends lifespan. These phenotypes are in part mediated by the activation of SIRT1 activity. Fractionation study revealed that plasma eNAMPT in both mice and human are localized to exosome. eNAMPT in isolated exosome is internalized by target cells and is sufficient to modulate NAD⁺ levels in hypothalamic neurons. We identify exosome as an important mode of regulation for systemic NAD⁺ biosynthesis and potential therapeutic targeting against aging.

325 Phyllanthusmins induce apoptosis and reduce tumor burden in high grade serous ovarian cancer by late-stage autophagy inhibition

Alexandria Young

Univeristy of Illinois at Chicago, Chicago, USA

High grade serous ovarian cancer (HGSOC) is a lethal gynecological malignancy with a need for new therapeutics. Many of the most widely used chemotherapeutic drugs are derived from natural products or their semi-synthetic derivatives. We developed potent synthetic analogues of a class of compounds known as the phyllanthusmins, inspired by natural products isolated from *Phyllanthus poilanei* Beille. The most potent analogue, PHY34, had the highest potency in HGSOC cell lines *in vitro* and displayed cytotoxic activity through activation of apoptosis. PHY34 exerts its effects by initially inhibiting autophagy at a late stage in the pathway, involving the disruption of lysosomal function. The autophagy activator, rapamycin, combined with PHY34 eliminated apoptosis, suggesting that autophagy inhibition was required for apoptosis. PHY34 was readily bioavailable through intraperitoneal administration *in vivo* where it significantly inhibited the growth of cancer cell lines in hollow fibers as well as reduced ovarian tumor burden in a xenograft model. We demonstrate that PHY34 acts as a late-stage autophagy inhibitor with nanomolar potency and significant antitumor efficacy as a single-agent against HGSOC *in vivo*. This class of compounds holds promise as a potential, novel chemotherapeutic and demonstrates the effectiveness of targeting the autophagic pathway as a viable strategy for combating the disease.

326 Applying Psychometric Testing to Evaluation of Professionalism in Medical Education

Tyler Zahrl

Saint Louis University, Saint Louis, USA

Introduction: There are two main approaches to medical professionalism: the rationalist approach and the sensemaking approach. Although predominant, the rationalist approach is fraught with practical limitations: vague terminology, competing models, faulty scales, and poor clinical application. The result of this approach is commonly referenced definitions, guidelines, and checklists. The sensemaking approach encourages physicians and researchers to critically reflect on the dynamic environment in which they work. Sensemaking is supported in the literature for mitigating unprofessional behavior among medical researchers. Philosophers, psychologists, and bioethicists have also argued for the importance of reflection in professional development. Accepting the sensemaking approach, this study aims to determine the utility of psychometric testing in medical professionalism training and education by measuring self-reflection.

Methods: The questionnaire developed consisted of four validated and reliable measures: 1) Perceptions of Medical Professionalism (13 items), 2) five subscales from the Actively Open-minded Thinking (AOT) Scale measuring propensity for reflection (33 items), 3) the Cognitive Reflection Test measuring ability for reflection (7 items), and the Marlowe-Crowne Short Form C to control for socially desirable responding (13 items). Demographic items were included as indicated in the literature. With IRB approval, the questionnaire was distributed to 350 third- and fourth-year (clinical) medical students via email through Qualtrics.

Results: 71 questionnaires were completed, yielding a response rate of 20%. There were many significant positives correlations, the most important being between 1) the Perceptions of Medical Professional

scale and the AOT (and three AOT subscales), 2) age (in years) and the AOT (and two subscales), and 3) socially desirable responding and two AOT subscales. Regression analyses showed the AOT could predict perceptions of medical professionalism ($r=.31$, $p=.01$) with certain subscales and items having greater positive correlations.

Discussion: The results show psychometric testing (the AOT) can be informative regarding medical professionalism after controlling for socially desirable responding. This study identified specific AOT items that demonstrate strong positive correlations with perceptions of professionalism. Through the sensemaking approach, further research could identify additional items to incorporate in a new scale to evaluate students' propensity for reflection, which could reduce problems inherent in the predominant rationalist approach.

327 *EptB* pseudogene accumulation contributes to enhanced systemic dissemination and stealth of typhoidal *Salmonella* serovars

Lillian F. Zhang

University of California, Davis, Davis, USA

Salmonella enterica is a highly diverse species of Gram-negative bacteria that can be grouped into typhoidal and non-typhoidal serovars. Non-typhoidal serovars, such as *S. Typhimurium*, cause gastroenteritis and inflammatory diarrhea, whereas typhoidal serovars, such as *S. Typhi*, cause systemic disease with a comparatively decreased inflammatory response. A small percentage of patients infected with *S. Typhi* may become asymptomatic chronic carriers of disease. These individuals serve as reservoirs to transmit infection to others and pose a significant challenge for eradication of typhoid fever. Although *S. Typhi* and *S. Typhimurium* are very closely related organisms, the properties that distinguish the two and contribute to the *S. Typhi* carrier state remain poorly understood. Previously, comparative analysis of *Salmonella* genomes revealed that typhoidal serovars contain a higher number of pseudogenes or disrupted non-functional genes than non-typhoidal serovars, suggesting that differences in pseudogene number could play a role in the differential pathogenesis. One such pseudogene in *S. Typhi* is *eptB*, which codes for a phosphoethanolamine transferase that can specifically modify the outer keto-deoxyoctulosonate (KDO) residue of lipopolysaccharide (LPS). *S. Typhi* possesses a non-functional copy of *eptB*, whereas *S. Typhimurium* possesses a functional copy of *eptB*. Here, we show that loss of *eptB* function in typhoidal serovars may serve as a virulence mechanism that allows *S. Typhi* to evade detection by the immune system, leading to a diminished host inflammatory response and the development of the chronic carrier state. Human intelectin-1 is known to bind to and recognize multiple microbial glycan epitopes, including the KDO of LPS, and may function in detoxification of LPS. Our results demonstrate that LPS isolated from *S. Typhi*, which possesses a non-functional *eptB* pseudogene, is bound by intelectin, whereas *S. Typhimurium* LPS is not bound by intelectin. Furthermore, loss of *EptB* function in *S. Typhimurium* allows binding of intelectin to *S. Typhimurium* LPS. Mice infected with an *eptB* mutant demonstrate increased bacteria load in the Peyer's patches than mice infected with a wild type *S. Typhimurium*. Additionally, mice infected with the *eptB* mutant *S. Typhimurium* exhibit decreased expression of inflammatory cytokines in the spleen compared to mice infected with the wild type *S. Typhimurium*, suggesting that loss of *eptB* function allows a non-typhoidal *Salmonella* serovar to mimic the stealth phenotype of typhoidal serovars. Together, these results suggest that loss of *eptB* function allows intelectin to bind to and detoxify *Salmonella* LPS, leading to decreased systemic inflammation during infection.

These results have broad implications for how pathogens such as *S. Typhimurium* induce systemic shock during infection and may also help to explain a mechanism for how *S. Typhi* is able to evade immune detection and enhance dissemination to systemic sites, leading to the development of the asymptomatic chronic carrier state.

329 Breast cancer cells exploit an orphan RNA to drive metastatic progression

Steven Zhang

University of California, San Francisco, USA

Cancer cells often hijack endogenous regulatory programs to achieve pathological gene expression landscapes. Notable examples of these strategies include somatic mutations, genetic amplifications and deletions, and epigenetic modifications. Additionally, post-transcriptional pathways have also emerged as major regulators of this transformation, including those involving miRNAs, RNA binding proteins, and tRNAs and tRNA fragments. However, a shared characteristic among these strategies is that they rely on existing pathways within the cell. Given that cancer can be viewed as an evolutionary process, there is a distinct possibility that cancer cells are capable of evolving or rewiring new regulatory pathways during disease progression. One possible source for novel pathways is non-coding RNAs, as these molecules can arise due to ectopic activation of RNA polymerases or nucleases while also possessing versatile regulatory capacity. We posited that non-coding RNAs arise in cancer cells as a consequence of tumorigenesis and provide a pool of cancer-specific molecules with regulatory potential. In this study, we performed a systematic search for the emergence of such neo-regulators of gene expression in breast cancer. We performed a systematic search for such cancer-specific RNA species by comparing the small RNA profiles of eight human breast cancer cell lines to human mammary epithelial cells. We identified a pool of small RNAs that whose presence was further associated with breast cancer using data obtained from The Cancer Genome Atlas Data and the small RNA profiles of patient-derived xenograft samples. We subsequently discovered that a functional oncRNA termed T3p, originating from the 3' end of TERC, acts as a broad regulator of gene expression and is a robust promoter of breast cancer metastasis. We found that T3p exerts its pro-metastatic effects by interacting with the RISC complex and increasing the expression of pro-metastatic genes NUPR1 and PANX2. Our findings raise the possibility that further examination of the cancer-specific RNA landscape and investigation into oncRNAs may yield novel strategies in developing diagnostic and therapeutic methods across many cancer types.

330 Strain-dependent activation and inhibition of Human Immunodeficiency Virus-1 entry by a PF-68742 diastereomer

Connie A. Zhao

Dana-Farber Cancer Institute, USA

Human Immunodeficiency Virus-1 (HIV-1) entry into cells is mediated by the envelope (Env) trimer of gp120 and gp41 heterodimers. Sequential binding to the target cell receptors, CD4 and CCR5 or CXCR4, triggers the metastable Env to undergo entry-related conformational changes. PF-68742 was recently identified as a small molecule that inhibits infection of a subset of HIV-1 strains by interfering with an Env function other than receptor binding, with resistance determinants mapping to the gp41 disulfide loop (DSL) and the gp120 C5 region. We investigated the antiviral mechanism of PF-68742.

Recombinant luciferase-expressing HIV-1 pseudotyped by wild-type (WT) or mutant HIV-1 Envs was incubated with increasing

concentrations of PF-68742 and/or other entry inhibitors and/or antibodies. The virus-inhibitor mixture was then added to CD4+ CCR5+, CD4+ CXCR4+, or CD4- CCR5+ target cells, and luciferase activity was measured 48 to 72 hours later.

Of the four PF-68742 diastereomers, only one, MF275, inhibited the infection of CD4+ CCR5+ cells by some HIV-1 strains. Unexpectedly, MF275 activated the infection of CD4- CCR5+ cells by several HIV-1 strains resistant to the compound's inhibitory effects in CD4+ CCR5+ target cells. In both cases, the strain susceptibility profiles were unique from those of other entry inhibitors. Sensitivity to other entry inhibitors in the presence of MF275 indicated that MF275-activated virus entry requires CCR5 binding as well as gp41 heptad repeat formation and exposure. Washout of MF275 prior to addition of the virus mixture to target cells was able to abrogate its inhibitory effect in CD4+ CCR5+ target cells but not its activating effect in CD4- CCR5+ target cells. In contrast to CD4-mimetic compounds, MF275 inhibitory and activating activity did not depend upon availability of the gp120 Phe43 cavity. Mutants with altered Env reactivity or State 1 preference (previously demonstrated to be resistant to CD4-mimetic compounds) remained susceptible to MF275. Conversely, changes in the gp41 DSL and gp120 C5 regions conferred resistance to MF275 but not CD4-mimetic compounds. The half-lives of the onset and decay of the MF275-activated state were different from those of CD4-mimetic compounds. Finally, while MF275 and CD4-mimetic compounds both enhanced susceptibility of some HIV-1 strains to the 17b and 19b antibodies against a CD4-induced (CD4i) epitope and the gp120 V3 loop, respectively, only MF275 enhanced susceptibility to the 4e10 antibody against the gp41 membrane-proximal external region (MPER).

MF275 apparently binds a site on the HIV-1 Env unique from the CD4 binding site and activates a conformational cascade that leads to virus entry. This pathway is parallel to but distinct from that triggered by CD4 and CD4-mimetic compounds. An understanding of the mechanisms of activity of MF275 should assist efforts to optimize its utility.

331 Phosphoglycerate Mutase 2 is a Metabolic Regulator of Myogenic Differentiation

David Zhao

University of Chicago, Deerfield, USA

Myogenesis, the formation of skeletal muscle tissue, is contingent on the proliferation and subsequent differentiation of satellite cell-derived myoblasts into multinucleated myotubes, which eventually yield functionally mature muscle fibers. The shift from proliferating myoblasts to differentiated myotubes is driven by drastic modifications to aggregate metabolic activity, but it is not precisely understood how this important metabolic shift occurs. C2C12 is a mouse murine myogenic cell line that undergoes rapid myoblast proliferation and myotube formation. We sought to determine the metabolic switch that occurs during the shift from proliferation to differentiation. We found that as C2C12 myoblasts differentiate, they exhibit a lower glycolytic rate and increased mitochondrial respiration. Paradoxically, despite a reduction in glycolysis, differentiation induces increased expression of phosphoglycerate mutase 2 (Pgam2), a glycolytic enzyme abundant in skeletal muscle that reversibly catalyzes the eighth step of glycolysis converting 3-phosphoglycerate (3-PG) into 2-phosphoglycerate (2-PG). Pgam2 is concomitantly upregulated with other known myogenic differentiation markers such as transcription factors myogenin (Myog) and myogenic determination protein (MyoD), myosin heavy chain fiber proteins, and creatine kinase (Ckm). Importantly, we found that Pgam2 is required for C2C12 myogenic

differentiation as siRNA knockdown of Pgam2 results in marked decrease in the expression of myogenic differentiation markers. Since Pgam2 catalyzes a bi-directional reaction, it plays a role not only in glycolysis but also in gluconeogenesis. We found that enzymes of gluconeogenesis, including phosphoenolpyruvate carboxykinase 1 (Pck1) and glucose-6-phosphatase (G6PC), are upregulated during myogenic differentiation. In summary, these results suggest Pgam2 is required for myogenic differentiation. Upregulation of Pgam2 and gluconeogenesis enzymes while glycolysis is reduced suggest that Pgam2 may play a role in metabolic reprogramming during myogenic differentiation.

332 ONC201 Inhibits HIV-1 Replication In Human Macrophages Via FOXO3A and TNFSF10

Runze Zhao

University of Nebraska Medical School, omaha, USA

Background: HIV-1 enters the CNS early in the acute stages of infection and remains sheltered in the CNS. The long lived cells in the CNS, including perivascular macrophages and microglia, support productive HIV-1 infection and may contribute to the viral resurgence. Despite effective cART, eradication of HIV from these reservoir cells remains elusive. Transcription factor FOXO3a and TNF superfamily cytokine TNFSF10 are known to targets HIV-1-infected macrophages for apoptosis. ONC201 is a novel and potent small molecule FOXO3a activator capable of inducing TNFSF10. It is orally active, can cross blood-brain barrier, and has shown antitumor effect in clinical trials. We hypothesize that targeting FOXO3a through ONC201 will induce TNFSF10 and subsequently suppress HIV-1 in its CNS reservoir.

Methods: Primary human monocyte-derived macrophages, microglia, and macrophage-tropic HIV-1_{ADA} were used to study the antiviral activity of ONC201. Viral replication and integration were monitored by HIV-1 reverse transcriptase activity, p24 levels, and two step Alu-based nested PCR. For *in vivo* studies, HIV-1-infected macrophages were intracranially injected into the basal ganglia of NOD/scid-IL-2Rgcnull mice. Mice were intraperitoneally injected daily with ONC201 or DMSO for 6 days before the collection of brain tissues. Brain HIV-1 p24 levels were determined by Western blot and immunohistochemistry. Soluble TNFSF10 receptor and siRNAs for FOXO3a were used to block TNFSF10 and FOXO3a, respectively. Statistical analysis was performed using the one-way ANOVA with Tukey's multiple comparison test. $P < 0.05$ was considered as significant.

Results: ONC201 dose-dependently decreased HIV-1 replication and integrated DNA in infected macrophages and microglia. The levels of HIV-1 replication in the infected cells were negatively correlated with ONC201-induced FOXO3a activation and TNFSF10 expression. Blocking TNFSF10 or knockdown of FOXO3a with siRNA reversed ONC201-mediated HIV-1 suppression. In mouse brains xenotransplanted with HIV-1-infected macrophages, ONC201 treatment significantly reduced the levels of HIV-1 p24 compared with those of the mice that treated with DMSO.

Conclusions: ONC201 inhibits HIV-1 replication via FOXO3a activation and TNFSF10 induction in infected human macrophages, microglia *in vitro*, and in mouse brains xenotransplanted with human macrophages. Therefore, ONC201 can be a promising drug candidate to combat persistent HIV-1 infection in the CNS.

333 Chemotherapy augments recombinant oncolytic poliovirus efficacy for treatment of glioblastoma

Justin Zhuo

Duke University Medical Center, USA

Glioblastoma (GBM), the most common primary malignant brain tumor in adults, is a highly lethal cancer with nearly all patients experiencing tumor recurrence after standard of care surgery, radiation, and chemotherapy. Thus, novel therapeutic strategies are urgently mandated. PVSRIPO is a highly-attenuated, recombinant polio:rhinovirus chimera that has demonstrated promising and robust clinical and radiographic responses in phase I clinical trials for recurrent GBM. PVSRIPO causes direct tumor cytotoxicity via binding to the CD155 poliovirus receptor expressed in GBM and virtually all solid neoplasms. Eliciting type I interferon signals in antigen presenting cells leads to robust innate and adaptive antitumor immunity. An unexpected discovery during the phase I trial was the achievement of complete and durable responses in patients who were treated with single-dose chemotherapy months after tumor progression following PVSRIPO infusion. This led to the initiation of an ongoing phase II trial comparing the efficacy of PVSRIPO and single-dose chemotherapy to PVSRIPO alone.

The goal of this study is to elucidate the therapeutic mechanisms of combined PVSRIPO and single-dose lymphodepletive chemotherapy using syngeneic mouse tumor models. We hypothesize that post-PVSRIPO lymphodepletive chemotherapy elicits an 'immunologic reset' that unmasks antitumor immune responses initially generated by PVSRIPO. To test this hypothesis, mice were implanted subcutaneously on the right flank with CT2A murine glioma cells transduced with human CD155. After one week, PVSRIPO was injected intratumorally, with intraperitoneal temozolomide administration occurring the following week. Tumor caliper measurement data and survival analyses demonstrate that combination treatment decreases tumor growth and increases overall survival compared to either treatment alone. Furthermore, early flow cytometry analyses of intratumoral lymphocyte populations suggest that chemotherapy administration following PVSRIPO treatment may induce memory T cell and regulatory T cell infiltration of the tumor. Ongoing experiments utilizing temozolomide-resistant cell lines will serve to better highlight the role of chemotherapy in restoring antitumor immunity by minimizing its ability to cause direct tumor cytotoxicity. This study has important implications not only for guiding future GBM treatments, but also for the potential inclusion of chemotherapy in other immunotherapeutic approaches.



ORAL PRESENTATIONS & POSTER ABSTRACTS AUTHOR INDEX



APSA
American Physician Scientists Association

www.jointmeeting.org

ORAL PRESENTATIONS & POSTER ABSTRACTS AUTHOR INDEX

APSA Trainee Oral Presentations Index

AUTHOR	PAGE
Berry, Kayla	1 25
Smestad, John	2 25

Poster Abstracts Author Index

AUTHOR	POSTER	PAGE	AUTHOR	POSTER	PAGE	AUTHOR	POSTER	PAGE
A			Brent, Jonathan	26	34	Chung, Shang-Lin	52	43
Abecassis, Zachary A.	1	26	Briggs, Neima	27	34	Coomer, Charles	53	43
Adelaja, Adewunmi	2	26	Brinkley, Garrett	28	34	Corkrum, Michelle	54	43
Al Dhaybi, Omar	3	26	Briscoe, Jessica B.	29	35	Coves-Datson, Evelyn	55	44
Alcoreza, Oscar B.	4	27	Brooke, Dewey	30	35	Culley, Miranda	56	44
Alinger, Joshua	5	27	Buchanan, Kelly L.	31	35	D		
Almiron Bonnin, Damian	6	27	Bungart, Brittani	32	36	Dardick, Joseph M.	57	45
Aloi, Joseph	7	28	C			desJardins-Park, Heather E.	58	45
Amalraj, Sarah K.	8	28	Casaos, Joshua	33	36	Dhillon-Jhattu, Sangeet	59	46
Ameri, Amir H.	9	28	Chandra, Ankush	34	36	Dhingra, Anshul	60	46
Anandappa, Annabelle J.	10	28	Chang, Hsiang-Chun	35	37	Dong, Michael	61	46
Arao, Bianca	11	29	Chang, Leslie L.	36	37	Dues, Dylan	62	46
Ariagno, Sydney N.	12	29	Chaunzwa, Tafadzwa	37	37	E		
Awah, C. Edmond	13	30	Chen, Cynthia	38	38	Erickson, Hanna	63	47
B			Chen, Jasper R.	39	38	Essegian, Derek	64	47
Bacon, Nickolas	14	30	Chen, QiLiang	40	38	Essuman, Kow	65	47
Banerjee, Abhik	15	30	Chen, Stella X.	41	39	Eustace, Nicholas	66	48
Basta, Ameer	16	30	Cheng, Anna M.	42	39	F		
Bayanjargal, Ariunaa	17	31	Cho, Bennet S.	43	39	Fan, Aaron	67	48
Berger, Evan	18	31	Cho, Janice	44	40	Fan, Liyan	68	48
Bern, Michael	19	31	Choksi, Yash	45	40	Farmer, Brandon	69	49
Bhansali, Rahul S.	20	32	Choudhury, Songita	46	40	Farrar, Jared	70	49
Binns, Thomas C.	21	32	Christensen, Paul	47	41	Fatima, Noor	71	49
Biro, Daniel	22	32	Chu, Simon N.	48	41	Fedorova, Olga	72	50
Blayney, Alan	23	32	Chung, Jennifer	49	42	Fine, Rebecca L.	73	50
Bolick, Nicole	24	33	Chung, Michael	50	42	Fischer, David	75	51
Bramah-Lawani, Mariam	25	33	Chung, Michelle J.	51	42			

POSTER ABSTRACTS AUTHOR INDEX

AUTHOR	POSTER	PAGE
Flores, Alyssa M.	76	51
Flores, Guillermo	77	51
Fong, Jerry	78	52
Frantzeskakis, Alexia	79	52
Frantzeskakis, Melina	80	52
Friedland, Scott	81	53
Friedlander, Mollie	82	53

G

Gaillard, Jonathan R.	83	53
Gallo, Mary	84	54
Gallo, Ryan	85	54
Galvan, Adri M.	86	55
Garber, Charise	87	55
Garfinkel, Amanda	88	55
Garg, Anupam	89	56
Gezer, Aysegul	90	56
Giantini Larsen, Alexandra M.	91	56
Gil, Nelson	92	57
Gillis-Buck, Eva M.	93	57
Gomez-Nguyen, Adrian	95	58
Gotian, Ruth	96	58
Grajales-Reyes, Jose	97	58
Grassmeyer, Justin	98	59
Green Haney, Meghan	99	59
Grigorova, Yulia	100	59
Groopman, Emily	101	60
Grunblatt, Eli	102	60
Guan, Mary L.	103	61
Gupta, Aditi	105	61
Guru, Pardeep	106	61

H

Habimana-Griffin, LeMoyne	107	62
Hagood, Madeleine	108	62

AUTHOR	POSTER	PAGE
Harasymiw, Lauren	111	62
Hardy, Laura	112	62
Harvey, Lloyd	113	63
Hasenoehrl, Erik	114	63
He, Chao	115	63
Helfand, Benjamin	116	64
Herrera, Jonathan	117	64
Herring, Brendon	118	64
Heymann, Gabriel	119	65
Hill, Kelly	120	65
Hines, Marcus	121	65
Hockemeyer, Kate	122	65
Hodara, Emmanuelle	123	66
Hon, Win	124	66
Hsieh, Justin	125	66
Hsieh, Paishiun	126	67
Hsu, Isabel	127	67
Hu, Jennifer C. W.	128	67
Hung, Putzer	129	68
Huynh, Tien-Phat	130	68
Hwang, Charles	131	68

I

Imperiale, Thomas	132	69
Inniss, Donovan	133	69
Irons, Eric	134	69
Islam, Bianca	135	70
Istvanic, Filip	136	70
Itoh, Christopher Y.	137	71

J

Jackson, Christopher B.	138	71
Jackson, Hudin N.	139	71
Jackson, Joshua	140	72
Jacob, Anjali	141	72

AUTHOR	POSTER	PAGE
Javidi-Sharifi, Nathalie	142	72
Jean-Baptiste, Samuel	143	73
Johnson, Martin	144	73
Joshi, Sunil	145	73
Jubbal, Sandeep	146	74

K

Karginov, Timofey	147	74
Kaw, Kaveeta	148	74
Kawanishi, Kunio	149	75
Khanolkar, Aaruni	150	75
Kim, Ellis	151	76
Kim, Uriel	152	76
Kim, Yong Hoon	153	76
Kindsfather, Audrey J.	154	77
King, Liam	155	77
Klement, John	156	77
Kochanek, Malgorzata	157	78
Kozek, Krystian	158	78
Kozek, Lindsay	159	79
Kramer, Daniel	160	79
Kress, Benjamin T.	162	79
Krueger, Laura	163	80
Kulbe, Jacqueline	165	80
Kwek, Swee Sen	166	81

L

Ladha, Feria	167	81
Law, Brandon M.	168	81
Lee, Stephanie	170	81
Lemieux, Mackenzie	171	82
Leonard, Daniel	172	82
Leonardo, Trevor	173	83
Lerman-Sinkoff, Dov	174	83
Lever, Jeremie	175	83

POSTER ABSTRACTS AUTHOR INDEX

AUTHOR	POSTER	PAGE
Levin, Solomon N.	176	84
Levy, Rachel	177	84
Li, Lucy	178	84
Li, Selena S.	179	85
Li, Songjun	180	85
Li, Stephen	181	85
Li, Yuping D.	183	85
Lieng, Monica	184	86
Lim, Aaron	185	86
Lin, Hsin-Pin	186	87
Lin, Yen-Nan	187	87
Liu, Connor J.	188	87
Liu, Shimeng	189	87
Locy, Morgan	190	88
Lownik, Joseph	191	88
Lynch, Evan	192	89

M

MacDuffie, Emily C.	193	89
Maia, Jessika T. da S.	194	89
Maiden, Michael	195	90
Marre, Emily A.	196	90
Martin, Anna R.	197	90
Martini, Michael	198	91
Masri, Mohamad Fadhli	199	91
Matasic, Daniel	200	91
Maurano, Megan	201	92
May, Jasmine	202	92
McCaw, Tyler	203	93
McGee, Warren	204	93
McKinnon, Emilie	205	93
Meier, Lee	206	94
Mensah, Kofi	207	94
Mietus, Constance	208	95
Mileva, Gloria	209	95

AUTHOR	POSTER	PAGE
Mishra, Anvita	210	95
Mittelstein, David	211	96
Montelongo Hernandez, Cesar	212	96
Moore, Austin B.	213	96
Morrissey, Samantha	214	97
Motwani, Kartik	215	97
Mujahid, Nisma	216	97
Murray, Meghan	217	98

N

N. Mendes Neto, Nilson	218	98
Naftalovich, Daniel	219	99
Neilsen, Beth	220	99
Neves, Gabriel F.	222	99
Nguyen, Bich Tram	223	99
Nguyen, Freddy	224	100
Noch, Evan	225	100
Noguchi, Ken	226	100
Nwafor, Divine	227	101

O

Oetjen, Landon	228	101
Oh, Sanders	229	101
Ortiz, Robin	230	102
Oswald, Aaron B.	231	102
Ozog, Stosh	232	102

P

Palmer, Allyson	233	103
Park, Joseph S.	234	103
Patel, Aum	235	103
Patel, Tirth	236	104
Paudel, Praveen	237	104
Peabody, Jacelyn	238	104
Penny, Morgan	239	105
Perez-Rathke, Alan	240	105

AUTHOR	POSTER	PAGE
Pettinato, Anthony	241	105
Phillips, Matthew	242	106
Pomaville, Monica M.	243	106

Q

Qureshi, Farhan	244	106
-----------------	-----	-----

R

Rahman, Karishma	247	107
Ralff, Marie	248	107
Rambarat, Paula K.	249	107
Randall, Michael P.	250	108
Rangel Rivera, Guillermo	251	108
Rawat, Rishi	252	109
Reasoner, Erin	253	109
Reed, Chelsey	254	109
Rege, Nischay	255	109
Richardson, Spencer M.	256	110
Rick, Jonathan W.	257	110
Rolnick, Kevin I.	258	110
Rosanwo, Tolulope O.	259	111
Rosen, Brandon	260	111
Roy-O'Reilly, Meaghan	261	111

S

Saenz, Jose	262	112
Saha, Anjan	263	112
Sahay, Sandeep	264	113
Saionz, Elizabeth	265	113
Sandoval, Aaron Gabriel	266	113
Sarsour, Tiana	267	114
Scott, Ashley	268	114
Sewanam, Lorenzo	269	114
Shah, Harsh N.	270	115
Shi, Diana D.	271	115
Shiuan, Eileen	272	116

POSTER ABSTRACTS AUTHOR INDEX

AUTHOR	POSTER	PAGE
Simo, Ornella E.	273	116
Simpson, Rachel	274	116
Sison, Christia Angela	275	117
Sleightholm, Richard	276	117
Lubbers, Ellen	277	118
Smith, Andrew	278	118
Sohn, Andrew M.	279	118
Som, Avik	280	118
Souder, Jaclyn	281	119
Spaur, Kelsey M.	282	119
Spellicy, Samantha	283	119
Stevanovic, Marta	284	120
Storm, Erica M.	285	120
Sweet, David	286	121

T

Taiwo, Rukayat M.	287	121
Tan, Sze Kiat	288	121
Tan Garcia, Alfonso	289	122
Tereshchenko, Alexander	290	122
Thompson, Joshua	291	123
Thompson, Russell	292	123
Ton, Amy N.	293	124
Toyoda, Yoshiko	294	124

AUTHOR	POSTER	PAGE
Tran, Lynn	295	124
Tran, Paul	296	124
Turbeville, Hannah	297	125
Turnbull, Katherine N.	298	125
Tyler, Nichole	299	126

U

Umapathi, Priya	300	126
Updyke, Erin	301	126
Urena-Gonzalez, Kenny	302	127

V

Vaitkus, Janina	303	127
Van Belkum, Max	304	127
Vandeven, Natalie	305	128
Velez Reyes, German	306	128
Vieta Ferrer, Emile	307	128
Villacreses, Raul	308	129

W

Wadhvani, Anil	309	129
Walker, John	310	129
Wang, Amy J.	311	129
Wang, Ernest	312	130

AUTHOR	POSTER	PAGE
Wilcox, Nicholas S.	314	130
Wong, Vivian	316	131
Wu, Sarah	317	131

X

Xia, Yuanxuan	318	131
Xu, Maria	319	132

Y

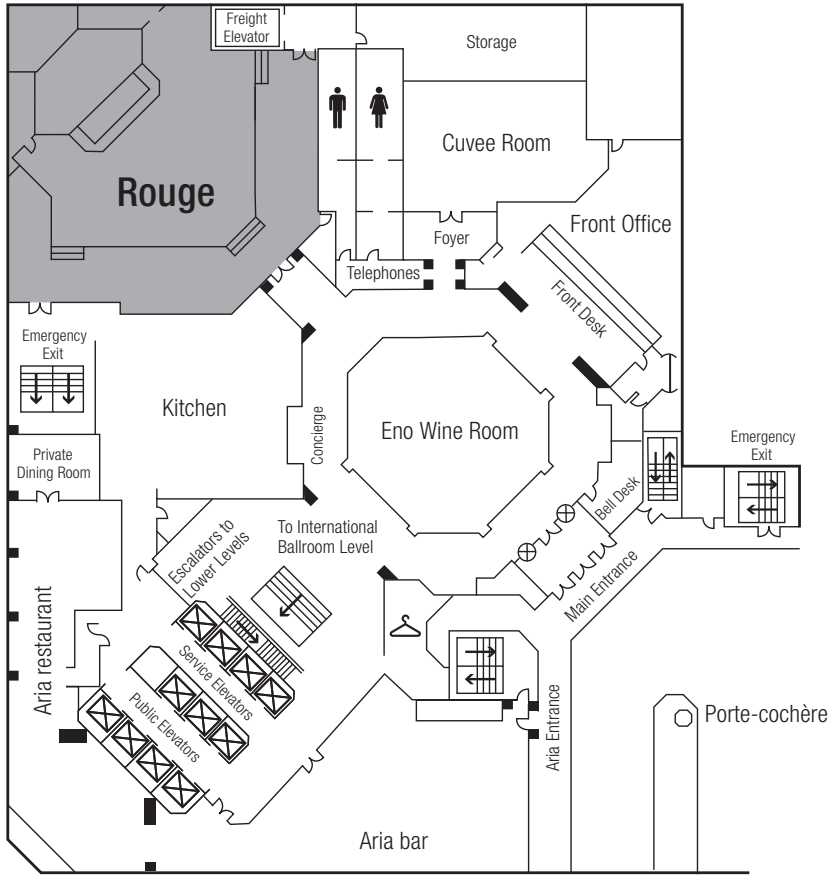
Yamamoto, Erin A.	320	132
Yang, Benjamin	321	133
Yilmaz, Bahar	323	133
Yoshida, Mitsukuni	324	133
Young, Alexandria	325	134

Z

Zahrli, Tyler	326	134
Zhang, Lillian	327	134
Zhang, Steven	329	135
Zhao, Connie A.	330	135
Zhao, David	331	135
Zhao, Runze	332	136
Zhuo, Justin	333	136

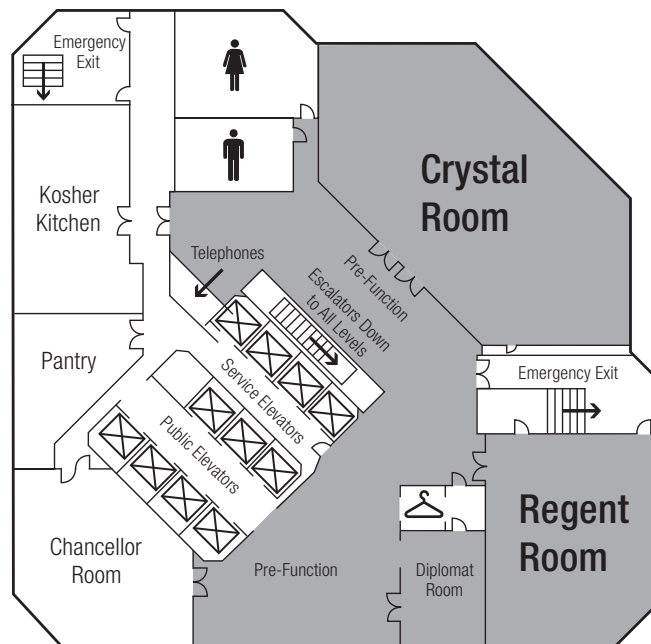


HOTEL FLOOR PLANS

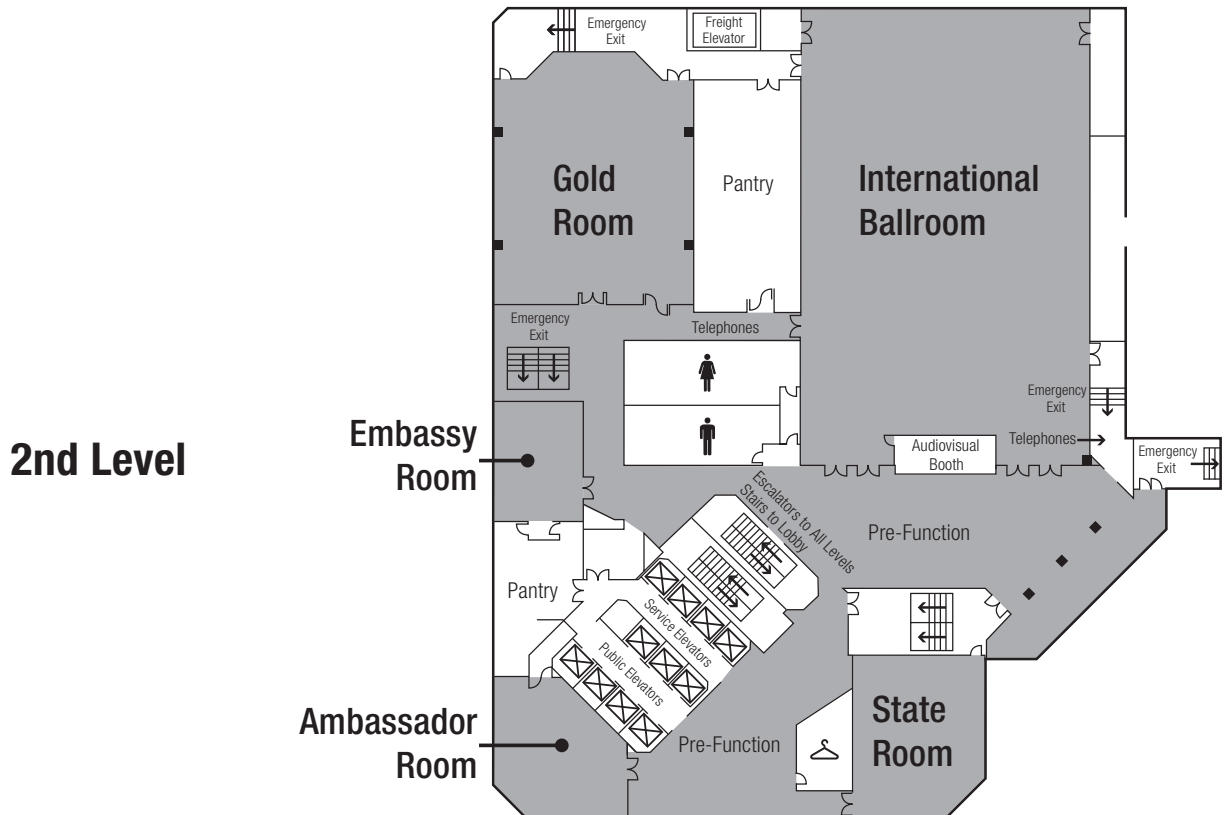
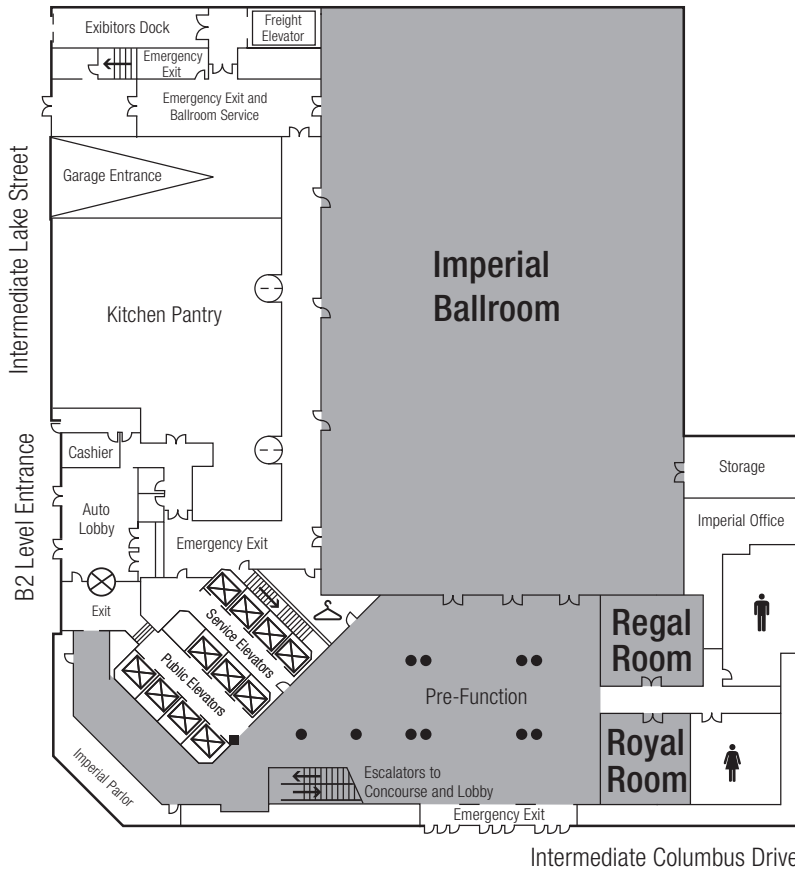


**Lobby Level
1st Level**

3rd Level



HOTEL FLOOR PLANS



JOINT MEETING SPONSORS

PLATINUM

BURROUGHS
WELLCOME
FUND 

GOLD / ACADEMIC BENEFACTOR



National Institute of
General Medical Sciences

SILVER / ACADEMIC SPONSOR



THE HARRINGTON PROJECT
FOR DISCOVERY & DEVELOPMENT

Harrington Discovery Institute
University Hospitals | Cleveland Ohio



ACADEMIC FRIEND



University of Pittsburgh

BRONZE



Special Thanks to This Year's Generous Supporters

SAVE THE DATE

The next few annual meetings have been scheduled, so be sure to mark your calendars.

AAP/ASCI/APSA JOINT MEETING

THE PREMIER ANNUAL MEETING FOR PHYSICIAN-SCIENTISTS



APSA
American Physician Scientists Association

*Join us next year for three days of presentations, lectures,
and networking opportunities with colleagues.*

April 5-7, 2019

2020 – April 3-5

2021 – April 9-11

at the Fairmont Chicago Millennium Park | Chicago | Illinois



www.jointmeeting.org